Australian School of Petroleum and Energy Resources
Faculty of Engineering, Computer & Mathematical Sciences
The University of Adelaide

THE UNIVERSITY
of ADELAIDE

A thesis submitted for the degree of Doctor of Philosophy (PhD)

December, 2020

Analytical Models for Managing and Predicting the Performance of Mature Waterflooded Reservoirs

Daniel I. O'Reilly

B. Eng., Petroleum Engineer

Supervisors: Assoc. Prof. Manouchehr Haghighi,
Dr. Matthew A. Flett and
Dr. Mohammad Sayyafzadeh.

In memory of my dad, who spurred my interest in engineering and hydrology and who left the world too early

Contents

List of Tables

List of Figures

Abstract

In this thesis, new mathematical models are developed for oil production and water injection wells operating in mature fields. In waterflooded reservoirs, production and injection wells should be monitored throughout field life to maximise recovery. This includes interpretation of pressure and flow rate data from wells. Effective management of mature fields results in balanced voidage replacement and the identification of damaged or underperforming wells for remediation.

The motivation for this work originates from the author's experiences working on the mature Windalia waterflooded field on Barrow Island, Australia. While assets like this possess a wealth of production data, methods of direct analysis are often unavailable. Often mature fields are neglected in modern research, but managing these reservoirs is still crucially important for oil & gas operating companies. Application of state-of-the-art methods should not be ignored.

For oil wells undergoing artificial lift, which are common in mature operations, mathematical models are derived for the case of cyclic or intermittent production. Using these models, it is possible to calculate Productivity Index and other reservoir properties from production data in cyclic wells. The transient flow regime is considered along with boundary dominated flow (steady or pseudo steady state cases). In the transient case, the superposition of linearised solutions is used to mimic the operation of well pump controllers. In the boundary dominated case, steady state harmonic theory is applied to solve the problem in a novel way. Type curves are presented to assist with interpretation of field data from Pump Off Controllers. Field case studies are presented; in some cases, the theory identified production wells that were later stimulated by a workover rig.

For water injectors, the classical Pressure Fall Off transient analysis technique is reviewed and applied in its original format on Barrow Island. Yet there are cases when this simple approach is invalid when interpreting shut-in pressure data. Temperature effects when injecting cold-water into a reservoir are scarcely considered in the literature, with regards to effects inside the well itself. A case of this nature was observed in the field, and new theory developed to account for the heating period during a shut-in where cold water in the well equalises with the surrounding formation temperature. The theory combines the transient pressure from a composite reservoir with transient temperature changes during flowing and shut-in periods. The effect on recorded downhole pressure is considerable in some cases.

Finally, the method of Rate Transient Analysis (RTA) is extended to include delayed water injection at the outer boundary. In current practice, this effect is not considered when interpreting long term flow rate data from oil wells. In the proposed method, increased production is observed some time after water injection commences. Type curves are generated from analytical solutions derived in the Laplace domain. In addition to reservoir parameters obtained using RTA, the method allows characterisation

of waterflood support in terms of effective injection rate and boundary condition (constant-pressure or constant-rate injection). The technique is validated using reservoir simulation and applied to field cases.

Statement of Originality

I certify that this work contains no material which has been accepted for the award of any other degree or diploma in my name, in any university or other tertiary institution and, to the best of my knowledge and belief, contains no material previously published or written by another person, except where due reference has been made in the text. In addition, I certify that no part of this work will, in the future, be used in a submission in my name, for any other degree or diploma in any university or other tertiary institution without the prior approval of the University of Adelaide and where applicable, any partner institution responsible for the joint-award of this degree.

I acknowledge that copyright of published works contained within this thesis resides with the copyright holder(s) of those works.

I also give permission for the digital version of my thesis to be made available on the web, via the University's digital research repository, the Library Search and also through web search engines, unless permission has been granted by the University to restrict access for a period of time.

I acknowledge the support I have received for my research through the provision of an Australian Government Research Training Program Scholarship.

Daniel I. O'Reilly 14-Dec-2020

Acknowledgements

The first person I would like to thank in this project is **Assoc. Prof. Manouchehr Haghighi** (Manny), for believing in me at the start and helping out every step of the way. Manny has been the perfect supervisor for me and allowed me to develop my ideas while providing the support I needed. Next, I would like to thank my co-supervisors **Dr. Matthew Flett** and **Dr. Mohammad Sayyafzadeh**. Matt and I live close to each other in Perth, so we've spent a good few times at local coffee shops. I thank Matt for his encouragement and light hearted approach, supporting me when things weren't going smoothly. Mohammad's attention to detail improved my work significantly and he taught me many lessons about academic research. My supervisors all motivated and challenged me, and I am grateful to have worked with them during these 5 years. I would also like to acknowledge Dr. Alireza Salmachi for helpful discussions in the beginning of my project and our occasional chats when I visited the University.

Completing this project by distance while I live and work in Perth has been challenging but I have been helped along the way by many of the kind staff at the Australian School of Petroleum. The Postgraduate Coordinators have been very accommodating of me. In Adelaide, my close friends Dr. Aaron Gaekwad and Dr. Brendan Drew would provide me with a place to stay during my University visits. Staying with them, drinking coffee and playing computer games was part of the fun.

I also want to thank several of my colleagues at Chevron Australia. The co-authors on some of the chapters were a pleasure to work with and inducted me into the Barrow Island way of life: Ash Hunt, Ewen Sze, Kate Nelligan, Guan Ng and Brad Hopcroft. Stationed on the island, many of the field technicians also helped immensely when it came to field history and execution of surveillance activities. While there are too many names to mention, Johan Henrick and Ross Fenwick were particularly helpful. Over the years, some of my other colleagues in the office, Zhi Xia, Josh Beinke and Boniface Yee have also given me several ideas and acted as sounding boards for some of the concepts in these papers.

I owe a huge thanks to my supervisors at Chevron Australia who have supported me in one way or another over the years: **Bree Goff**, Chidi Amudo, Soubhagya Das, Gary Reedy, Nancy Lyche, Graham Harris, Malcolm West, Stephen Rennie and Dr. Andrew House. Bree's support during the first few years of my research was fantastic and she helped me jump through many hoops of internal approval. I also thank **Chevron Australia Pty Ltd** and its management for allowing me to use the company field data and work on these world class assets.

Finally, thank you to my **mum** and **my partner** for supporting me and tolerating my "ups and downs" during the project.

Thesis by Publication

Published Journal Papers

1. **O'Reilly, D.I.**, Haghighi, M., Flett, M.A. and Sayyafzadeh, M. 2016. Pressure and Rate Transient Analysis of Artificially Lifted Drawdown Tests Using Cyclic Pump Off Controllers. *Journal of Petroleum Science and Engineering*. **139**: 240-253.

2. **O'Reilly, D.I.**, Hopcroft, B.S., Nelligan, K.A., Ng, G.K., Goff, B.H. and Haghighi, M. 2018. A Lean Sigma Approach to Well Stimulation on Barrow Island, Australia. *SPE Production & Operations*. **33**(02): 393-408. SPE-182323-PA.

3. **O'Reilly, D.I.**, Haghighi, M., Flett, M.A. and Sayyafzadeh, M. 2019. Productivity Determination for Cyclic Production Using Steady State Harmonic Theory – Application to Artificial Lift Wells. *Journal of Petroleum Science and Engineering*. **172**: 787-805.

4. **O'Reilly, D.I.**, Haghighi, M., Flett, M.A. and Sayyafzadeh, M. 2021. Pressure-Transient Analysis for Cold-Water Injection into a Reservoir Coupled with Wellbore-Transient-Temperature Effects. *SPE Production & Operations*. **36**(01): 197–215. SPE-186306-PA.

5. **O'Reilly, D.I.**, Haghighi, M., Sayyafzadeh, M. and Flett, M.A. 2021. Analytical Rate-Transient Analysis and Production Performance of Waterflooded Fields With Delayed Injection Support. *SPE Reservoir Evaluation & Engineering*. Preprint. SPE-205371-PA.

International Conference Proceedings

6. **O'Reilly, D.I.**, Hunt, A.J., Sze, E.S., Hopcroft, B.S., Goff, B.H. and Haghighi, M. 2016. Increasing Water Injection Efficiency in the Mature Windalia Oil Field, NW Australia, Through Improved Reservoir Surveillance and Operations. Presented at the SPE Asia Pacific Oil & Gas Conference and Exhibition held in Perth, Australia, 25-27 October. SPE-182339-MS.

1 Contextual Statement

Significance of the project. Some of the world's most prolific oil fields are, in terms of field discovery, some of the oldest. Secondary and tertiary recovery methods effectively increase the recovery factor of reservoirs and allow for an increased duration of field operation. At some point during field life, the operation is classified as "mature." At this point in time, it is recognised that the overall production economics may be less favourable than when oil extraction rates were higher during initial field development. An emphasis is placed on managing costs and careful optimisation of production to ensure extended field life. The engineering analysis of reservoir surveillance data can support this.

Several definitions of what constitutes a mature field exist (Babadagli 2006; Parshall 2012), but this delineation is not important for this work. For simplicity it will be assumed that a field is classified as mature when oil production reaches 50% of its original plateau rate. For those operations not undergoing secondary recovery (e.g. waterflood), this may be rapid. In 2011, it was estimated that two-thirds of global daily oil production was attributed to mature fields (IHS Cambridge Energy Research Associates 2011). Mature fields represent a strong reserves base for operating companies. With the recent lack of global exploration and development during 2019–2020, it is possible that this proportion will grow.

In this project an analogue search has been conducted to identify some of the larger fields globally that will be applicable to the new theory. A list of noteworthy mature fields appears in Table 1, with references providing further information on each. This table contains a sample of the world's oldest onshore oil developments that are currently active and undergoing waterflood recovery. Waterflooding is the normal course of action for mature fields where reservoir pressure has declined to the extent where primary production is no longer economic. The oil fields in the table are directly applicable to this thesis. It is important to point out the range in oil production from these developments – from an estimated 800 BOPD in Borislav (Ukraine) to over 4,000,000 BOPD in the giant Ghawar field (Saudi Arabia). Where data are available, it is apparent that mature fields utilise a large number of production and injection wells. The Barrow Island oilfield, from which several field studies appear in this thesis, has been written in bold for context. Several other fields from Table 1 are also analysed in chapters using publicly available field data.

Some of the fields in Table 1 have also progressed to the third stage of recovery, Enhanced Oil Recovery (EOR). The work in this thesis may still have application to the fields in this tertiary stage of recovery.

In spite of the varying production rates between these mature waterflood fields, there is commonality in how the wells must be managed and surveyed periodically. The purpose of this practice is to investigate reservoir performance, identify the key performance parameters and predict their evolution

and identify barriers to meeting or exceeding forecasted production performance, providing methods to mitigate impacts as necessary (Kikani 2012).

Some of the factors that differentiate mature waterflooded fields from other fields are:

- The operation of a large number of production and injection wells,
- Application of artificial lift methods to production wells due to natural production decline,
- Presence of older and less reliable technology (e.g. lack of downhole monitoring equipment or less reliable well metering),
- Use of reservoir stimulation methods to remediate ageing wells or exploit rock properties, and
- A high water cut at oil production wells.

All of these factors will be explored in the chapters in this thesis.

Mature oilfields remain a key component of many operating companies' portfolios. The operation of these fields by companies is well documented. In the following paragraphs, some attention is given to some of the recent industry progress in the area. Later in the literature review, specific mathematical methods will be reviewed that are important for the theoretical work undertaken in this project.

The use of new analytical methods in mature fields poses a unique opportunity; since some fields were developed 50-100 years ago, they were studied using techniques only available at that time. This point is noted by Mohahegh et al. (2005), where so-called intelligent production analysis methods have been applied to mature wells producing from oil fields in Oklahoma, US. Similarly, Murray et al. (2006) provide details on an industry-wide effort to upgrade the hardware and software technologies used in mature fields. The oil industry has termed this the "Smart Field" approach, and there is a promise that more production can be delivered using new technologies. Ruslan (2015) discusses how, given a portfolio of available technology and production enhancement opportunities for mature fields, companies can select the highest ranked opportunities to apply to their assets.

Many international operating companies initiate various projects under themes of rejuvenation, optimisation and unlocking potential in their mature fields (Fedriando et al. 2019; Tiwari et al. 2015; Golovatskiy et al. 2015). Operators see these old fields as valuable assets that must be maintained, both in the physical and reservoir management sense. In some cases, reviewing the available data from their mature reservoirs can also help guide new infill drilling opportunities (Al-Amri et al. 2010; Martino et al. 2012; Varela-Pineda et al. 2014).

It is noted by Hirschfeldt et al. (2017) that well-by-well (producer and injector) review meetings at operating companies assist with identifying production opportunities, making diagnoses and proposing particular action plans to maximise oil production. While the approach is definitely powerful, it may

be difficult to achieve for mature fields with hundreds or thousands of operational wells. Furthermore, the data reviewed in these sessions are often basic and do not include in-depth analysis. The methods proposed in this thesis could be incorporated into field reviews to provide additional depth.

These examples show that there is an active interest from international operating companies in maintaining and investing in their mature assets. In many articles, it is recognised that new technologies are beneficial for mature fields. This provides motivation for the new theory developed in this thesis.

The focus of this thesis is reservoir surveillance for mature fields. There are research gaps in this area. One problem is that the acquisition of conventional pressure transient data is an expensive exercise for operating companies. These data are normally obtained by shutting in the well after production or injection, incurring lost time and revenue, and installing temporary electronic equipment and shut-in valves to record the pressure signal. On mature oil assets, the economic pressure is greater and there is little desire to perform this type surveillance. Conversely, there is a quantity of unused and available production data that are overlooked by engineers. This is due to a lack of mathematical methods or software available to interpret the data easily. This information represents an analysis opportunity.

Scope of the work. This research primarily focuses on reservoir surveillance in mature fields and the impact it can have on maintaining or increasing oil production. The main objectives are:

- Planning and reinstating a field-wide reservoir surveillance programme on the Windalia field, a mature operating waterflood in Western Australia (Chapter 3)
- Development of new theory for artificial lift oil well Productivity Index calculation (transient and steady state production cases). Application of theory to select wells requiring reservoir stimulation treatment. (Chapters 4, 5 and 6)
- Extension of existing theory for water injector pressure falloff analysis to include wellbore temperature effects (Chapter 7)
- Derivation of a new analytical model to predict long-term type curve performance of oil wells undergoing water injection at the outer boundary at any time during field life (Chapter 8)

Table 1: A global selection of onshore mature reservoirs undergoing waterflood (current data taken at year end 2020)

Field Name	Operator Companies	Country	Date of First Production	Current Production Rate - Oil BOPD	Current Water-Cut	Well Count Producers	Well Count Water Injectors	Reference
Bradford (PA)	Numerous	USA	1871	1,223		25,000		Buckwalter (1949)
Coalinga	Chevron	USA	1900	9,947	91.9	6,000		De Francisco et al. (1995)
Midway-Sunset	Aera Energy, Chevron	USA	1900	34,059	90.8	25,000		Guo et al. (1997)
Borislav	Unknown	Ukraine	1904	800		1,675		Popadyuk et al. (2006)
Lost Hills	Chevron	USA	1910		93.4			Minner et al. (2002)
South Belridge	Aera Energy	USA	1911	29,600	94.1	5,704	619	Allan and Lalicata (2012)
Salt Creek	Occidental	USA	1911		98.8			Bargas et al. (1992)
Okha	Rosneft	Russia	1922	6,223		1,882		Meyerhoff (1981)
McElroy	Chevron	USA	1926	7,735				Lemen et al. (1990)
Oregon Basin	Marathon	USA	1927	1,758	99.3			Dershowitz et al. (2002)
Rantau	Pertamina	Indonesia	1930	2,440	73.3	550		Simamora and Ardianto (2011)
El Tordillo	Tecpetrol	Argentina	1932	16,857	93.4			Muruaga et al. (2001)
Ishimbay	Bashneft	Russia	1932	224	88.0	622		Maksimova (1987)
Kirkuk	KAR, North Oil Company	Iraq	1934	120,000				Al-Naqib et al. (1971)
Means	ExxonMobil	USA	1934	5,552		720		Barbe (1971)
Dukhan	Qatar Petroleum	Qatar	1940	335,000				Vera et al. (2009)
Abqaiq	Saudi Aramco	Saudi Arabia	1946	360,557				Grover (1993)
Greater Burgan	KOC	Kuwait	1946	115,632	10.8			Al-Naqi et al. (2009)
Boscan	Petroboscan	Venezuela	1948	103,000		601		Swanson et al. (1993)
Spraberry Trend	Pioneer	USA	1949	108,823	73.5			Putra et al. (1999)
Ghawar	Saudi Aramco	Saudi Arabia	1951	4,043,478		1,996	738	Bayona (1993)
Minas	Chevron	Indonesia	1952	84,000	98.7	1,300	300	Hendih et al. (2002)
Wafra	Chevron, KOC	Kuwait-Saudi Arabia	1956	88,985	68.5	161	44	Rubin (2011)
Duri	Chevron	Indonesia	1958	189,400	72.0			Gael et al. (1995)
Barrow Island	**Chevron**	**Australia**	**1966**	**3,872**	**93.0**	**472**	**230**	**O'Reilly et al. (2016)**
Samotlor	TNK-BP	Russia	1969	619,000	94.0	13,400	4,500	Krasnevsky et al. (2008)
Varegan	Gazprom	Russia	1974	49,538	87.0	1,175	327	Ulmishek (2003)
Prudhoe Bay	BP	USA	1977	338,843	77.6	2,500		Brady et al. (2004)

1.1 Thesis Structure

This is a PhD thesis by publication and the chapters have been organised in this manner. The work comprises one conference paper and five published peer reviewed journal papers. The structure of these chapters will now be outlined. The forthcoming discussion relates to the original work of this thesis, commencing after the literature review.

The *first chapter* in this research serves as a general overview of the Australian mature Windalia waterflooded field, located on Barrow Island. This reservoir appeared in Table 1. Apart from serving as an introduction to mature onshore fields, this chapter is a case study of how surveillance practices were improved on the asset during the 2014–2016 period. The mathematical methods and field practices discussed in this paper are well established, but their application on the asset was new at the time. It is an example of the industrial application of proven analysis methods. It is shown that water injection and oil production were increased and stabilised respectively, as a result of improved engineering practices and field operations.

The *second and third chapters* contain new novel mathematical methods developed to monitor production wells in mature oil fields. As discussed earlier, reservoir surveillance is considered a critical part of maintaining or improving oil production. Assessing the productivity of oil wells helps identify those that are impaired (e.g. mechanical skin or reservoir depletion) and require remediation (e.g. reservoir stimulation or increased injection support respectively). It has been mentioned that mature fields often contain a high number of production and/or injection wells, and the quality of performance data may be mediocre. Performing a rapid assessment on which wells are underperforming, under the constraint of scarce data with a large number of wells, is the objective in these chapters. The second chapter proposes analysis during the transient period of production drawdown, while the third chapter investigates the steady or pseudo-steady period.

Applying new theory to industry cases is an important step towards validation. To this end, the *fourth chapter* works towards applying the theory of the prior chapters to the Windalia reservoir (for the transient drawdown case). Additionally, a general method is given for reservoir stimulation candidate selection, given a large group of wells in a field. The integration of many sources of data, in addition to the new theory, is discussed in this chapter. The utilisation of Lean practices is shown to assist when executing the stimulation activities. The ultimate goal of this work is the improvement of oil production from selected wells. This outcome is shown in the case study.

In the *fifth chapter*, surveillance of water injector wells is discussed. Water injection is a vital part of recovery in mature assets. The method of pressure falloff analysis allows for interpretation of well and reservoir properties after the well is shut in following a period of injection. In the chapter, a new analytical method is derived to incorporate thermal effects on wellbore fluids during injection and

shut-in. During falloff surveys, it is possible that heat conduction into the well from the surrounding rock can interfere with the expected pressure signal from the deeper reservoir. The objective of this chapter is to correct for this effect and proceed with the calculations of injection performance.

Finally, the *sixth chapter* assesses the production performance of oil fields as a combined production and injection problem. A new mathematical method is derived for the rate transient analysis (RTA) of an oil production well that experiences water injection support at some point in its life. This method is a logical development on the original Fetkovich (1980) method of decline curve analysis. The novel aspect is the diagnosis of effective water injection support at a particular producer, along with inferring the nature of the boundary condition imposed at the injector (e.g. constant-pressure or constant-rate injection).

Specifically, this research focuses on onshore mature waterfloods, which tend to be older developments compared to offshore. Since chapters 3–5 focus on sucker rod pumps, the application is mainly to onshore fields, as this artificial lift technique is seldom used offshore. The application of artificial lift itself also usually implies a mature development, as reservoir pressure has declined and natural production diminished. Some of the chapters (e.g. 6 and 7) apply to a waterflood in any environment.

1.2 Relation Between Publications and This Thesis

In this thesis, a separate chapter has been allocated for each publication. The overarching theme in this research is the analysis of production and injection wells in mature water drive fields. All publications are listed in Table 2. Part of the work involves the development of new mathematical theory, while other parts are devoted to the industrial application of the developed theory.

In the paper "Increasing Water Injection Efficiency in the Mature Windalia Oil Field, NW Australia, Through Improved Reservoir Surveillance", some context is given to the overall project and its application to an active Australian field. This is a beneficial overview for readers and does not contain new analytical theory, but rather applies existing surveillance theory to a new case study. The application of existing theory (Lee et al. 2003; Kamal 2009; Kikani 2012) is shown to yield benefit for total water injection and oil production. Specifically, injector falloff analysis is used on hundreds of wells to map reservoir properties pressure across the field. Nonetheless, there is an opportunity to explore new analysis techniques with other unused data available in this case study.

It is difficult for oil operating companies to shut in production wells to perform pressure transient analysis in the same vein as water injectors. Lost oil production during these surveys may not be recovered in a timely manner when the well is restarted. Furthermore, it is uncommon for downhole pressure instruments to be available in mature fields. Therefore, in the paper "Pressure and Rate Transient Analysis of Artificially Lifted Drawdown Tests Using Cyclic Pump Off Controllers", efforts

are made to analyse the problem of transient production drawdown analysis of oil wells without any downhole gauges. Productivity index is the parameter of interest. It is understood that artificially lifted wells, which are pervasive in mature fields, operate in a cyclic manner and this is accounted for in the derivations. In the paper, analysis methods are also given for wells with downhole instruments available. After the transient period of production is complete, the steady or pseudo-steady flow regime starts. Analysis of the productivity of wells operating in a cyclic fashion in this flow regime is outlined in the paper "Productivity Determination for Cyclic Production Using Steady State Harmonic Theory – Application to Artificial Lift Wells". These papers form a complete focus on oil well productivity in mature fields. Field examples from the open literature are considered in each paper.

Drawing attention back to the Barrow Island asset and the Windalia reservoir, the paper "A Lean Sigma Approach to Well Stimulation on Barrow Island, Australia" shows an integrated approach to selecting wells for reservoir stimulation. The aforementioned production analysis techniques are applied along with other available field information to determine the wells most likely to benefit from stimulation. Well acidisation, where hundreds of barrels of hydrochloric acid are injected downhole, was performed on three wells on Barrow Island. The success of this method is shown in the article and is supported by the theory developed in this research. This paper is partly considered as an industrial application of the theory developed in the previous paragraph.

In the paper "Pressure-Transient Analysis for Cold-Water Injection into a Reservoir Coupled with Wellbore-Transient-Temperature Effects", attention is paid to more careful modelling of reservoir and thermal wellbore effects. This new theory is considered as an extension of the classical falloff interpretation techniques that were applied in the first chapter. A new set of field data from Australia are shown in this paper where the effect of changing temperature inside the wellbore on bottomhole pressure is large relative to the transient reservoir falloff signature. Application of the theory allows the separation of wellbore-density effects from the reservoir pressure transient response. If the new interpretation techniques were not applied to the field data, reservoir and well properties derived from pressure transient analysis alone would be incorrect and possibly lead to poor decisions.

The paper "Analytical Rate-Transient Analysis and Production Performance of Waterflooded Fields with Delayed Injection Support" is the last chapter in this thesis and represents a holistic view of the reservoir system. In this work, the variable of interest is the oil production rate at a particular well, supported by water injection at the outer boundary. Reservoir simulation studies are performed to validate the new theory for multiphase flow in porous media, using an open source reservoir simulator. Analysis is performed on production data in the literature taken from 7 separate fields globally. It is shown that many field cases fit the type curves developed in the paper, with new insights given regarding the strength of injection support and the nature of the outer boundary

Table 2: Publications included in this thesis

Paper	Chapter	Article Title	Status
1	3	Increasing Water Injection Efficiency in the Mature Windalia Oil Field, NW Australia, Through Improved Reservoir Surveillance and Operations	Published conference paper
2	4	Pressure and Rate Transient Analysis of Artificially Lifted Drawdown Tests Using Cyclic Pump Off Controllers	Published journal paper
3	5	Productivity Determination for Cyclic Production Using Steady State Harmonic Theory – Application to Artificial Lift Wells	Published journal paper
4	6	A Lean Sigma Approach to Well Stimulation on Barrow Island, Australia	Published journal paper
5	7	Pressure-Transient Analysis for Cold-Water Injection into a Reservoir Coupled with Wellbore-Transient-Temperature Effects	Published journal paper
6	8	Analytical Rate-Transient Analysis and Production Performance of Waterflooded Fields with Delayed Injection Support	Published journal paper

condition.

The 6 above-mentioned conference and journal articles demonstrate an investigation into the steady and unsteady multiphase flow of fluids in a mature reservoir that has been undertaken in this project. These articles form a complete body of work encompassing several years of research and will be of use to scientists and engineers studying the nature of production from mature waterflooded reservoirs.

1.3 References

Al-Amri, B.A., Al Bulushi, N.I., Al-Busaidi, R. et al. 2010. Identifying the Remaining Opportunities in a Mature Field – A Case Study. Presented at the Abu Dhabi International Petroleum Exhibition & Conference, Abu Dhabi, UAE. 1-4 Nov. SPE-138202-MS.

Al-Naqi, M., Al-Kandari, I., Al-Qattan, M., A/Rahman, B., Bou-Mikael, S., and Gazi, N.H. 2009. Lessons learned from the first water flood pilot project in a clastic reservoir in the Greater Burgan Field in Kuwait. SPE Middle East Oil & Gas Show and Conference, Bahrain. SPE-120427-MS.

Al-Naqib, F.M., Al-Debouni, R.M., Al-Irhayim, T.A., and Morris, D.M. 1971. Water drive performance of the fractured Kirkuk Field of northern Iraq. 46th Annual Meeting, Society of Petroleum Engineers of the American Institute of Mining, Metallurgical and Petroleum Engineers, New Orleans. SPE-3437-MS.

Allan, M.E., and Lalicata, J.J. 2012. The Belridge giant oil field - 100 years of history and a look to a bright future AAPG Search and Discovery Article, no. 20124.

Babadagli, T. 2006. Development of mature oil fields – A review. *J Petrol Sci Eng.* **57**(3-4): 221-246.

Barbe, J.A. 1971. Evaluation and modification of the Means (San Andres) Unit waterflood. Journal of Petroleum Technology. **23**(12):1421-1427 SPE-3301-PA.

Bargas, C.L., Montgomery, H.D., Sharp, D.H., and Vosika, J.L. 1992. Immiscible CO2 process for the Salt Creek Field. *SPE Reservoir Engineering.* **7**(04): 397-402. SPE-21577-PA.

Bayona, H.J. 1993. A review of well injectivity performance in Saudi Arabia's Ghawar Field seawater injection program. SPE Middle East Oil Show & Conference, Bahrain. SPE-25531-MS.

Brady, J.L., Ferguson, J.F., Seibert, J.E., Chen, T., Hare, J.L., Aiken, C.V.L., Klopping, F.J., and Brown, J.M. 2004. Surface-gravity monitoring of the gas cap water injection project, Prudhoe Bay, Alaska. *SPE Reservoir Evaluation and Engineering.* **7**(01):59-67. SPE-87662-PA.

Buckwalter, J.F. 1949. Water flooding The Bradford field-1949. *Appalachian Geological Society Bulletin*, **1**:287-296.

DeFrancisco, S.T., Sanford, S.J., and Hong, K.C. 1995. Utilizing WASP and hot waterflood to maximize the value of a thermally mature steam drive in the West Coalinga Field. Proceedings of the Western Regional Meeting, Bakersfield, CA. SPE-29665-MS.

Dershowitz, W., Shuttle, D., and Parney, R. 2002. Improved oil sweep through discrete fracture network modeling of gel injections in the South Oregon Basin Field, Wyoming. SPE/DOE Improved Oil Recovery Symposium, Tulsa. SPE-75162-MS.

Fedriando, F., Pambudi, A.R., Rolanda, D.S. et al. 2019. New Perspective to Unlock Opportunities in Mature Field: Sanga-Sanga Block, Indonesia. Presented at the SPE/IATMI Asia Pacific Oil & Gas Conference and Exhibition held in Bali, Indonesia, 29-31 Oct. SPE-196417-MS.

Gael, B.T., Gross, S.J., and McNaboe, G.J. 1995. Development planning and reservoir management in the Duri steam flood. SPE Western Regional Meeting, Bakersfield, CA. SPE-29668-MS.

Golovatskiy, Y., Petrashov, O., Syrtlanov, V. et al. 2015. Huge Mature Fields Rejuvenation. Presented at the SPE Annual Caspian Technical Conference & Exhibition held in Baku, Azerbaijan, 4-6 Nov. SPE-177334-MS.

Grover, G.A., Jr. 1993. Abqaiq Hajifa reservoir: Geologic attributes controlling hydrocarbon production and water injection. SPE Middle East Technical Conference, Bahrain, SPE-25607-MS.

Guo, D.S., Smith, M.E., and Tucker, K.E. 1997. The use of pulsed-neutron capture logs for reservoir management in the Midway-Sunset Field. *SPE Formation Evaluation.* **12**(02):109-119. SPE-25807-PA.

Hendih, A.R., Imran, R., and Williams, L.L. 2002. Investigation for mature Minas waterflood optimization. Proceedings SPE Asia Pacific Oil & Gas Conference & Exhibition, Melbourne. SPE-77924-MS.

Hirschfeldt, C.M., Bertomeu, F.D. and Lobato-Barradas, G. 2017. Practical Management in Mature Field Operations. Presented at the SPE Latin America and Caribbean Mature Fields Symposium

held in Salvador, Bahia, Brazil, 15-16 Mar. SPE-184937-MS.

IHS 2011. Mature Oil Fields – Unleashing the Potential. IHS Cambridge Energy Research.

Kamal, M. 2009. *Transient Well Testing.* Society of Petroleum Engineers Monograph Series, Vol. 23. Richardson, TX.

Kikani, J. 2012. *Reservoir Surveillance.* Society of Petroleum Engineers. Richardson, TX.

Krasnevsky, Yu. S., Gorobets, E.A., Kundin, A.S., and Podrezenko, Yu.V. 2008. Optimum well patterns and well paths selection in formation AV11-2 (Ryabchik) during Ust-Vakhskaya area of Samotlor Field development. SPE Russian Oil & Gas Technical Conference and Exhibition, Moscow. SPE 117384-MS.

Lee, J., Rollins, J.B. and Spivey, J.P. 2003. *Pressure Transient Testing.* SPE Textbook Series Vol 9. Richardson, TX.

Lemen, M.A., Burlas, T.C., and Roe, L.M. 1990. Waterflood pattern realignment at the McElroy Field - Section 205 case history. SPE Permian Basin oil and gas recovery conference, Midland. SPE-20120-MS.

Maksimova, S.P. 1987. (English translation 1989), *Oil and gas fields of the USSR.* JPRS-UEA-89-026-L.

Martino, L., Iuliano, A., Ucan, S. et al. 2012. Reviewing Mature Fields – A Case History. Presented at the SPE Latin American and Caribbean Petroleum Engineering Conference, Mexico City, Mexico, 16-18 Apr. SPE-152715-MS.

Meyerhoff, A.A. 1981. *The oil and gas potential of the Soviet Far East.* Scientific Press. Beaconsfield.

Minner, W.A., Wright, C.A., Stanley, G.R., de Pater, C.J., Gorham, T.L., Eckerfield, L.D., and Hejl, K.A. 2002. Waterflood and production-induced stress changes dramatically affect hydraulic fracture behaviour in Lost Hills infill wells. SPE Annual Technical Conference, San Antonio, SPE-77536-MS.

Mohaghegh, S.D., Gaskari, R. and Jalali, J. 2005. New Method for Production Data Analysis to Identify New Opportunities in Mature Fields: Methodology and Application. Presented at the SPE Eastern Regional Meeting held in Morgantown, WV, 14-16 Sept. SPE-98010-MS.

Murray, R., Edwards, C., Gibbons, K. et al. 2006. Making Our Mature Fields Smarter – An Industrywide Position Paper From the 2005 SPE Forum. Presented at the SPE Intelligent Energy Conference and Exhibition held in Amsterdam, The Netherlands, 11-13 Apr. SPE-100024-MS.

Muruaga, E., Antunez, E., Nogaret, C., and Stancel, S. 2001. Integrated reservoir study in El Tordillo Field. SPE Latin American and Caribbean Petroleum Engineering Conference, Buenos Aires. SPE-69688-MS.

O'Reilly, D.I., Hunt, A.J., Sze, E.S., Hopcroft, B.S., Goff, B.H. and Haghighi, M. 2016. Increasing Water Injection Efficiency in the Mature Windalia Oil Field, NW Australia, Through Improved Reservoir Surveillance and Operations. SPE Asia Pacific Oil & Gas Conference and Exhibition, 25-27 Oct, Perth. SPE-182339-MS.

Parshall, J. 2012. Mature Fields Hold Big Expansion Opportunity. *Journal of Petroleum Technology.* **64**(10): 52-58.

Popadyuk, I., Vul, M., Ladyzhensky, G., and Shpak, P. 2006. The petroleum geology of the Ukrainian Carpathian Foredeep, in Golonka J. and F. J. Picha, *The Carpathians and their foreland: Geology and hydrocarbon resources: AAPG Memoir*, **84**:443-454.

Putra, E., and Schechter, D.S. 1999. Reservoir simulation of waterflood pilot in naturally fractured Spraberry Trend. SPE Asia Pacific Oil and Gas Conference and Exhibition, Jakarta. SPE-54336-MS.

Rubin, E. 2011. Full field modeling of Wafra First Eocene reservoir 56-year production history. SPE Heavy Oil Conference and Exhibition, Kuwait City. SPE-50575-MS.

Ruslan, M. 2015. Production Excellence Opportunities Portfolio Management System: Key in Mature Field Rehabilitation. Presented at the SPE/IATMI Asia Pacific Oil & Gas Conference and Exhibition, held in Nusa Dua, Bali, 20-22 Oct. SPE-176057-MS.

Simamora, J.H., and Ardianto, R.N. 2011. Integrating subsurface, well and surface data as a plan

for waterflood project in Rantau Field. SPE Projects and Facilities Challenges Conference, Doha. SPE-142269-MS

Swanson, D.C., Jaimes, J., Valdez, C., Pirela, B., Puche, F., Rojas, D., and Moya, E. 1993. The Boscán Field - Venezuela's giant stratigraphic trap with a complex history. *AAPG Bulletin.* **77**:350-351.

Tiwari, A., Sharma, N.M., Manickavasagam, C. et al. 2015. Production Optimisation in Mature Fields. Presented at the SPE Oil and Gas India Conference and Exhibition held in Mumbai, India, 24-26 Nov. SPE-178090-MS.

Ulmishek, G.F. 2003. Petroleum Geology and Resources of the West Siberian Basin, Russia. *U.S. Geological Survey Bulletin.* 2201-G.

Varela-Pineda, A., Hutheli, A.H. and Mutairi, S.M. 2014. Development of Mature Fields Using Reservoir Opportunity Index: A Case Study from a Saudi Field. Presented at the SPE Saudi Arabia Section Annual Technical Symposium and Exhibition held in Al-Khobar, Saudi Arabia, 21-24 Apr. SPE-172231-MS.

Vera, L.B., Ariffin, T., Trabelsi, A., Al-Qarshubi, I., and Al-Ansi, H.A. 2009. Assessing fluid migration and quantifying remaining oil saturation in a mature carbonate reservoir: Dukhan Arab D. International Petroleum Technology Conference, Doha. IPTC-13503-MS.

2 Literature Review

2.1 Introduction

The scope of this research includes new analytical solutions to fluid flow problems that occur in mature oil reservoirs undergoing waterflood. Several problems of transient fluid flow are studied, along with some in the boundary dominated regime, which occurs when the drainage radius extends to the outer boundary. The thesis combines transient pressure diffusion with multiphase (oil and water) fluid flow in the reservoir rock. Therefore, this literature review considers aspects of each effect.

A common theme with fundamental reservoir surveillance research is that the operational scenarios assumed when deriving analytical solutions are idealistic in nature. One historical example is the line source solution to transient flow (Theis 1935), later extended to include the additional factor of wellbore storage (van Everdingen and Hurst 1949), which can occur when the well is shut-in at the surface instead of downhole. Operationally, it is not always possible to shut wells with a valve positioned near to the reservoir interval. Hence, this effect was incorporated into mathematical models at a later date by the authors.

In newly developed fields or during reservoir appraisal, it is often possible to gather surveillance data honouring the conditions of the ideal analytical reservoir solutions; money can be spent on careful well intervention work or apparatus to acquire high quality data. Mature assets are less likely to have money spent on data acquisition. These fields, however, have large amounts of data collected over their operating life, but the data are not directly compatible with idealistic solutions available in the literature. For example, fluid saturations in the reservoir and boundary conditions applied at wells may change considerably over the time periods considered. The following review will highlight the underpinning analytical work that can be extended to the more complicated operational cases that are common in mature fields.

This literature review is structured as follows. Firstly (in Section 2.2), a broad mathematical account is given for the two-phase flow of oil and water through a reservoir, in terms of the governing partial differential equations and some fundamental solutions. Next, in Section 2.3, oil production wells will be specifically discussed for both transient and boundary dominated flow. Investigation is undertaken for wells undergoing the cyclic flow condition. In Section 2.4, the focus will turn to water injection wells, which are considered a crucial part of recovery in waterflooded fields. Section 2.5 will then include a review on the topic of production decline curves and their study in the literature. The review will focus on existing decline curve techniques, how they may be extended to include the waterflood event, and cover some alternative methods of production analysis. Each section will highlight research gaps and these will be summarised completely in Section 2.6.

The main conclusion of this literature review is that several practical problems specific to fluid

flow in mature fields have received minimal attention over time. There is an opportunity to utilise more of the commonly available field data if new analytical solutions are found.

2.2 Mathematical Preliminaries

In this section, an introduction to the governing equations is given for the flow of two phases through reservoir rock. The equations apply to work covered in all forthcoming chapters. In a waterflood production system, the reservoir is penetrated by both injection and production wells, which are considered as sources and sinks in the reservoir domain.

A two-phase system of oil and water flow considering compressibility effects is considered. In the absence of gravity and capillary pressure between phases, flow is governed by the following system of two nonlinear partial differential equations in cylindrical coordinates:

$$\frac{1}{r}\frac{\partial}{\partial r}\left(r\frac{k_o}{\mu_o B_o}\frac{\partial p}{\partial r}\right) = \phi\frac{\partial}{\partial t}\left(\frac{S_o}{B_o}\right) \tag{1}$$

$$\frac{1}{r}\frac{\partial}{\partial r}\left(r\frac{k_w}{\mu_w B_w}\frac{\partial p}{\partial r}\right) = \phi\frac{\partial}{\partial t}\left(\frac{S_w}{B_w}\right) \tag{2}$$

with pressure p, radius r, permeability k, viscosity μ, formation volume factor B, porosity ϕ, time t and fluid saturation S. The subscripts o and w denote oil and water phases respectively. It is assumed that the pore space is filled with oil and water, i.e.:

$$S_o + S_w = 1 \tag{3}$$

No mass transfer occurs between phases in this formulation. Equations 1 and 2 are nonlinear second order partial differential equations. The equations are developed from mass conservation of each phase and applying Darcy's law for laminar flow in the rock. Obtaining analytical solutions to these equations is difficult due to the inherent nonlinearity of the terms; several parameters are functions of saturation or pressure – e.g. $k_w(S_w)$, $\mu_w(p)$ and $B_w(p)$. Nevertheless, under some simplifying assumptions, it is possible to derive fully analytical solutions for transient flow in a waterflood. Perrine (1956) and Martin (1959) proposed that, under small saturation gradients, Equations 1 and 2 can be approximated by:

$$\frac{1}{r}\frac{\partial}{\partial r}\left(r\frac{\partial p}{\partial r}\right) = \frac{\phi c_t}{\lambda_t}\frac{\partial p}{\partial t} \tag{4}$$

Here, the total mobility of the reservoir fluid/rock system is defined as:

$$\lambda_t = \frac{k_o}{\mu_o} + \frac{k_w}{\mu_w} = \lambda_o + \lambda_w \tag{5}$$

and the total compressibility is defined as:

$$c_t = S_o c_o + S_w c_w + c_f \tag{6}$$

where S_o and c_o are oil saturation and compressibility respectively, S_w and c_w are water saturation and compressibility respectively, and c_f is the formation compressibility. If mobility and compressibility are constant in Equation 4, the differential equation is linear. The linearisation allows analytical solutions to be obtained.

While being simple, Equation (4) is also practically applicable to many pressure and rate transient tests. For example, for certain multiphase flow conditions it permits use of the well known Theis (1935) solution for the problem of transient pressure response in an unbounded formation under constant-rate drawdown:

$$p_w(t) = p_i + \frac{q_t B \mu}{4\pi k h}\left[\mathrm{E_i}\left(\frac{-\phi \mu c_t r_w^2}{4kt}\right) - 2S\right] \tag{7}$$

Here, q_t is the total flow rate (oil + water) and $\mathrm{E_i}(x)$ is the exponential integral function. The mechanical skin factor, S, is defined as:

$$S = \frac{2\pi k h \Delta p_s}{q_t \mu} \tag{8}$$

In the skin equation, Δp_s denotes the steady state pressure loss across the near-wellbore mechanically damaged skin region. For values of the term, $4kt/(\phi \mu c_t r_w^2) > 100$ (Matthews and Russell 1967), Equation 7 can be approximated as:

$$p_w(t) = p_i + \frac{q_t B \mu}{4\pi k h}\left[\ln\left(\frac{e^\gamma \phi \mu c_t r_w^2}{4kt}\right) - 2S\right] \tag{9}$$

where γ is Euler's constant ($\gamma = 0.577216...$). Equation 9 is used extensively in pressure transient test analysis to calculate reservoir properties using the semilog chart interpretation method. As mentioned, this equation represents the pressure response during the infinite acting flow period. Other solutions are also available that incorporate reservoir outer boundaries (van Everdingen and Hurst 1949; Matthews and Russell 1967).

Since Equation 4 is a linearisation of Equations 1 and 2, the application of many existing well testing equations to multiphase flow conditions is permitted. This is an important point that will be

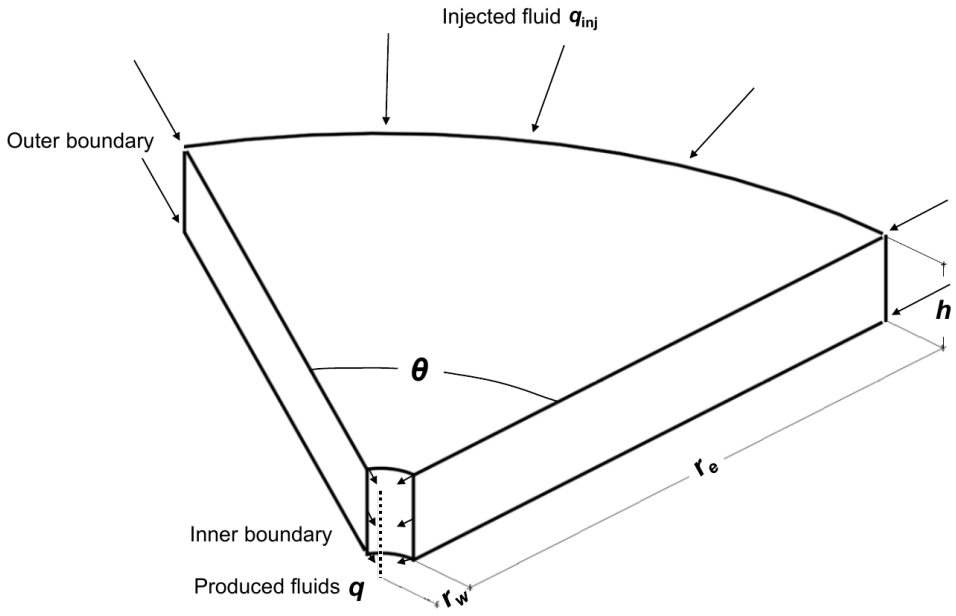

Figure 1: Schematic of radial mathematical model for a mature reservoir undergoing waterflood injection at the outer boundary

utilised heavily in this thesis.

A schematic of a radial reservoir system under two-phase flow is shown in Figure 1 (assuming $\theta = 360\,\text{deg}$). In this diagram, a single production well drains fluids at radius r_w from a finite reservoir of radius r_e. The reservoir thickness is denoted h. It can be assumed that injected water is evenly distributed across the outer boundary. A fluid saturation gradient will exist across the reservoir for water injection into an oil formation. For this setup, it is possible to obtain full analytical solutions for the pressure response of unsteady flow in the reservoir. This will be explored in later chapters.

A short discussion on the limitations of the equations will now be given. The application of the differential equations expressed by Equations 1 and 2 in transient well testing is widespread. In order to obtain analytical solutions, the equations necessarily ignore gravity effects and capillary pressure. These phenomena usually occur over timescales much larger than that over which transient pressure diffusion occurs. This is the case in conventional sandstone reservoirs, which are the topic of this thesis. For the case of longer term production (e.g. for boundary-dominated decline curve analysis), capillary pressure effects may or may not be important in conventional reservoirs. For rock-fluid systems exhibiting large interfacial tension, wettability towards a particular phase, or for particularly tight sands, there may be a large capillary pressure difference. During a waterflood, this results in the 'smearing' of what would otherwise be a sharp, discontinuous flood front. Naturally fractured reservoirs are also frequently dominated by capillary pressure effects over long term production. In these cases, it may be necessary for Equations 1 and 2 to incorporate the capillary pressure difference, at least for the long term production period. These cases are not considered in the present research.

2.3 Oil Production Wells

The treatment of production wells on mature assets with cyclic flow conditions will now be discussed. The overall objective is to calculate productivity index for a well with oscillating production flow rate. This problem can be practically applied to artificial lift wells since they are frequently stopped and started during normal operation. For this discussion, injectors are treated only as simple boundary conditions, or are ignored altogether. This literature review relates to Chapters 4, 5 and 6 in the thesis. In those chapters, an account is given for productivity and property determination in wells undergoing artificial lift.

Oil wells producing with beam pumps consist of a downhole positive displacement pump driven by a surface prime mover. Often, the engine or electric motor at the surface is only capable of operating at a single speed. Options such as gearing and stroke length allow the pump flow rate to be adjusted to some extent, but it is difficult to exactly match the inflow from the reservoir exactly to the speed of the pump. Due to this, it is normal to operate the pumps at a rate higher than reservoir inflow, and stop the pump from producing periodically (Takacs 2015). The pumps are controlled by pump-off-controllers (POCs). These devices are discussed by Acton (1981), Eckel et al. (1995) and McCoy et al. (1999).

POCs can be configured in several different ways. In the most basic case, the technician is able to manually define a separate producing and shut-in duration. For example, the beam pump may be operated for 16 hours each day. This simple case is often used by small operating companies or individual well owners at remote locations where power and communications to well sites are unavailable. In a more advanced case, a tensile load measuring device placed on the sucker rod is connected to the POC and production only permitted when adequate inflow into the well is detected. This installation often improves the oil production rate, because average operating BHP (bottom hole pressure) over the day is reduced compared to the previous scenario. A lower BHP results in additional production from the reservoir sand. For example, a field pilot of POCs by Eckel et al. (1995) in the mature Lost Hills waterflood (also included in Table 1) reports an 11% oil production increase after installation. Lower pump failure rates are also noted.

More recently, the Variable Speed Drive (VSD) has been introduced to continuously alter the speed of beam pump operation, so the controller theoretically never needs to stop the pump, instead adjusting speed as required (Takacs 2015). These devices are comparatively expensive but allow additional control.

Acton (1981) discusses a case study of POC implementation in the Midway Sunset oil field, undergoing steam flood and cyclic steam production. Several benefits are discussed. One problem that beam pumps often face in cyclic steam operations is the variable production before and after a steam

stimulation treatment. Manually matching the pump speed after a treatment is difficult, because the rate may peak and quickly decline, and afterwards the pump may operate too fast, resulting in dry pumping and fluid pound. This may damage the pump. This issue also applies to waterfloods with variable injection support over time. The benefit with a POC is that production is only permitted when adequate inflow is detected (via load on the rods). This automatically maximises oil production and lowers the risk of mechanical failure.

It is worth noting that other types of artificial lift, e.g. plunger lift or gas lift, may also operate in a periodic fashion (Chacin et al. 1994). This is done due to the flow regime inside the well; the well should be stopped prior to liquid loading occurring (Huff III 1988; Brill and Mukherjee 1999). Liquid loading begins when the superficial gas velocity in the well is below a critical value and the liquid buildup may prevent the well from being restarted easily after shut down.

Calculating the productivity of reservoirs when production starts and stops many times per day is not as simple as the constant-production case. For the idealised case of constant-production in the transient pressure drawdown case, the Theis (1935) or van Everdingen and Hurst (1949) equations can be used to calculate reservoir properties (Equation 7). This transient drawdown condition may occur when a well is returned to production after a prolonged period offline, e.g. for maintenance or a workover. For the case of constant-pressure in the well and subsequent transient production, van Everdingen and Hurst (1949) present equations that can be used to calculate reservoir properties, later extended by Ehlig-Economides (1979) and Ehlig-Economides and Ramey (1985). The constant-pressure drawdown transient case is described by the following solution for production rate at the well in an infinite reservoir:

$$\overline{q}_t(u) = \frac{2\pi kh(p_i - p_w)}{B\mu} \frac{K_1(\sqrt{u})}{\sqrt{u}\left[K_0(\sqrt{u}) + S\sqrt{u}K_1(\sqrt{u})\right]} \tag{10}$$

The overbar ($^-$) here denotes the Laplace integral transform, and $K_n(u)$ is the modified Bessel function of the second kind. This solution for transient production is contrasted against the constant-rate drawdown solutions given earlier in Section 2.2. The constant-pressure production case is not as straightforward to invert into the real domain as the constant-rate case given in Equation 7 (Ehlig-Economides 1979), and is thus left in this form. The Laplace transform $\bar{f}(u)$ of the function $f(t)$ is defined as:

$$\bar{f}(u) = \mathcal{L}\{f(t_D)\} = \int_{0^+}^{\infty} f(t_D) e^{-ut_D} dt_D \tag{11}$$

Note that for transient problems in porous media, $t_D = kt/\phi\mu c_t r_w^2$.

Application of the Laplace transform to problems of flow in porous media is useful for cases of

transient flow (van Everdingen and Hurst 1949). When analytical inversions into the time domain are not available, it is possible to employ numerical inversion techniques. For this purpose, the majority of work in this thesis uses the Stehfest (1970) algorithm. This algorithm is popular in the pressure transient analysis literature. It is reliable for the inversion of functions that are smooth in the time domain and do not contain discontinuities. When flow rate discontinuities are present, the method of superposition should be applied to inverted functions in the time domain.

Nevertheless, the case of intermittent production has not been studied as closely as the fixed boundary condition cases. Obtaining direct solutions is understandably more difficult.

The problem of a constant-rate drawdown test is displayed in Figure 2(a). The artificial lift problem at hand is shown in Figure 2(b). The transient decline in bottomhole pressure is observed to be an accumulation of many start-stop cycles. As discussed, the producing duration of each cycle depends on how the well is operated. The case shown in Figure 2(b) is the simple case of a timer-based POC controller, where the producing and shut-in time are constant values set in the controller (Eckel et al. 1995; McCoy et al. 1999). This creates a production situation that, over long term and on an average basis, resembles the *constant-rate drawdown case* (Equation 7).

Advances in production optimisation methods during the 1980s and 1990s led to POC devices that improved oil production rates in beam pump wells (Takacs 2015). An example is the load cell device attached to the polished rod of the beam pump, which sends continuous measurements to the POC. The controller stops production at the well when a limiting load is reached at the wellhead. This load is related to a minimum value of bottomhole pressure in the well and essentially stops the well producing in a "dry" condition. Overall, this situation shares similarities with the *constant-pressure drawdown case* (Equation 10), though it is not exactly the same due to its intermittent nature. Corrections are needed to account for the differences. Aside from the present thesis, the author is not aware of significant studies in this area.

Several authors have considered flow in a reservoir where production from the well is cyclic. Gasbarri et al. (1997) have modelled the inflow of wells undergoing intermittent production using numerical reservoir simulation, but did not approach the problem analytically. A finite difference simulator was used instead. Spivey et al. (1993) studied the problem of periodic production curtailment analytically, focusing on gas wells (not artificial lift) with a specific ratio of producing time only. Using a fixed ratio of production to shut-in time is known to be suboptimal in beam pump wells. Their study was not general and did not consider more complicated production schedules programmed into POCs. It appears that this detailed problem has not been studied in the literature for the transient drawdown of wells with oscillating production. This is a research gap for the transient production case.

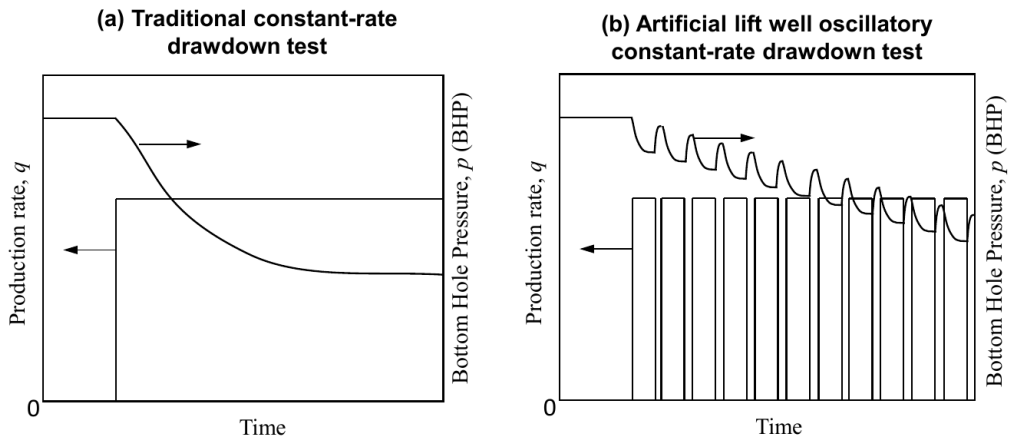

Figure 2: Comparison between: (a) the traditional drawdown test and (b) a drawdown test occurring with artificial lift production wells

The extension of existing methods to account for variable production in artificial lift wells can be accounted for by using the principle of superposition, though this has not yet been studied in the literature. Superposition may be used with the solutions of linear or linearised partial differential equations to create new solutions that are combinations of those with different boundary conditions. For the case under consideration, the pressure response of a well with multiple, discrete changes in flow rate is represented by the following superposition equation (Lee et al. 2003; Kuchuk et al. 2010):

$$p_w = \sum_{i=1}^{n} (q_i - q_{i-1}) p_u(t_i - t_{i-1}) \tag{12}$$

In Equation 12, p_w represents the pressure response at the well due to the varying flow schedule, q_i the flow rate over period i (ranging from 1 to n periods) and $p_u(t)$ denotes the unit step ($q = 1$) constant-rate solution (e.g. Theis' (1935) solution). This equation is already applied frequently in well test analysis when the flow rate varies prior to an analysis period. It is expected that it is also suitable for application to transient production at artificial lift wells operated by a POC controller. This will be investigated in this thesis.

The separate case of steady, stabilised production will now be discussed. Once reservoir boundary effects are felt at a production well, the transient drawdown period ceases and a stabilised period begins. This phenomenon also occurs over a long time period with cyclic production wells. A Productivity Index (P.I.) value may be calculated from the well during this period, but adjustments are still necessary for the cyclic flow condition. One novel way of solving this problem is to apply some of the concepts used in pressure transient pulse testing, namely the theory of harmonic solutions to reservoir inflow (Hollaender et al. 2002; Cardiff and Barrash 2014). Harmonic pulse testing is usually used to calculate reservoir properties between an active and observation well, and consists of either

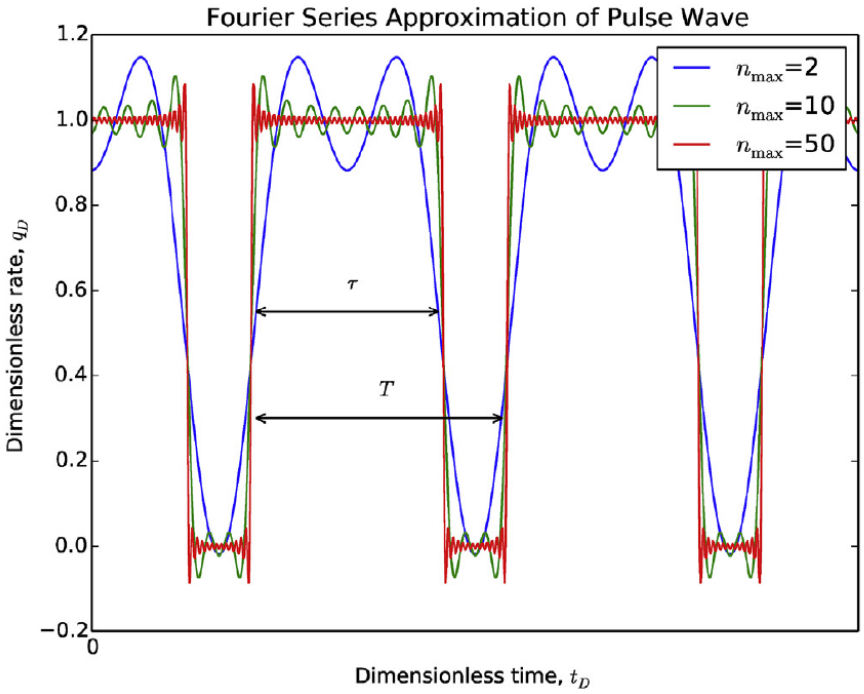

Figure 3: Fourier series approximation of the pulse wave used to model cyclic POC wells in the boundary dominated cases

sinusoidal, square wave or other production rates (Kuo 1972; Fokker and Verga 2011; Fokker et al. 2012; Ahn 2012). Analytical solutions for cyclic flow rate variation are available that incorporate wellbore storage and skin effects (Rosa 1991; Rosa and Horne 1997), however these have only been applied to pulse testing between wells. The theory is also valid for long term stabilised production at artificial lift wells and this does not appear to be studied in the literature until now.

In Figure 3, a graph of production rate vs. time is shown for a well undergoing cyclic operation. The production rate follows a pulse wave shape. The period of each cycle is marked as T, with the producing time τ. It is possible for this pulse wave to be approximated by a finite Fourier series as below:

$$q(t) = q_0 \left[\frac{\tau}{T} + \sum_{n=1}^{n_{\max}} \frac{2}{n\pi} \sin\left(\frac{\pi n \tau}{T}\right) \cos\left(\frac{2\pi n}{T} t\right) \right] \tag{13}$$

In the approximation to the pulse wave, the series is summed to a total of $n_{\max}$ terms. Using Equation 13, the pressure response at an oscillating well can be determined by adding together individual solutions to the constant-rate and harmonic parts of the problem, i.e.:

$$p_w = p_{w,\text{const}} + \sum_{n=1}^{n_{\max}} p_{w,\omega_n}(t) \tag{14}$$

Solutions to the boundary dominated constant-rate production problem are readily available. For example, the steady-state case is given as (Lee et al. 2003):

$$p_{w,\text{const}} = p_e - \frac{q_t B\mu}{2\pi kh}\left[\ln\left(\frac{r_e}{r_w}\right) + S\right] \tag{15}$$

where pressure is held at p_e at the external reservoir radius r_e. Pressure solutions to the harmonic part of Equation 14 are also available in other references (Rosa and Horne 1997; Ahn 2012), though they are usually for the infinite acting reservoir case. For example, the pressure response of pure sinusoidal production in an infinite reservoir is given as (Rosa 1991):

$$\overline{p}_w = \frac{q_t B\mu}{2\pi kh}.\frac{\omega_D K_0(\sqrt{u})}{\omega_D^2 + u^2} \tag{16}$$

for dimensionless angular frequency $\omega_D = \phi\mu c_t r_w^2 \omega/k$. In our case, the motivation is to study long term production, so adaptation of the solutions will be required to reflect boundary dominated flow.

There is also a distinct analogy between pulse testing and cyclic artificial lift wells that is understudied. The majority of work in pulse testing research focuses on the observation well and inference of reservoir properties in-between. Only recently, some researchers have also studied transient analysis of pulse testing at the oscillating well (Fokker et al., 2017; 2018). There is worth in applying the existing solutions at the production well itself, to infer its Productivity Index. In this way it is possible to understand productivity indices of some wells that may previously not have been considered – e.g. artificial lift wells that are opened and closed based on a timer or bottomhole pressure. It is not accurate to assume that said wells are producing at constant pressure and hence methods are needed to correct for the cyclic operation. The classic P.I. equations assume constant, stabilised BHP. At the oscillating well itself, wellbore storage and skin may be very important (Ogbe et al., 1987). This work is considered an extension of pulse testing theory, which will be applied to a production well undergoing long term, boundary dominated production.

2.4 Water Injection Wells

Monitoring injection well performance is also a crucial part of waterflood reservoir management. One method to obtain reservoir properties near the injector is the transient pressure falloff (PFO) survey. This literature review will apply to Chapter 7 of this thesis. The transient problem of water injection into an oil reservoir is a two-phase flow problem that presents analytical difficulties. Nonetheless, many researchers have studied these conditions and analytical solutions are available for the inverse problem of reservoir characterisation. Verigin's (1952) approach is one of the first analytical solutions available to the transient problem. The solution assumes the piston-like displacement of one fluid by another, and can be applied to the problem of waterflood injection. Over time, the problem has been studied and extended by other authors using various methods (Hazebroek et al. 1958; Kazemi

et al. 1972; Abbaszadeh and Kamal 1990). Noteworthy is the extension of the problem to include saturation gradients that occur when fluid displacement is not piston-like behind the shock front. The pressure transient response during shut-in is also considered. These later studies assume that the position of the front and description of saturation gradients is given by the Buckley and Leverett (1942) theory. This approximation is allowed for the case of water injection because of water's relatively low compressibility (Kamal 2009). In essence, the saturation profile inside the reservoir is decoupled from the transient pressure diffusion problem.

Nonisothermal effects (caused by cold water injection) are considered by Benson et al. (1986), Bratvold (1989) and Bratvold and Horne (1990). Multilayered reservoir effects are considered by Abbaszadeh (1991) and other heterogeneities by Banerjee et al. (1998). Ramakrishnan and Kuchuk (1993) study the impact of a variable rate history on the falloff response. More recently, Levitan (2003) proposed a more accurate approach to the problem of variable rate history. All of these discussed approaches have been analytical. Several of the studies solved the displacement problem by accurately including the moving front in the analytical solution, while others (e.g. Ramakrishnan and Kuchuk 1993) approximated the front movements using a quasi-stationary approach. By using this approximation, it is possible to also incorporate wellbore storage and superposition of flow rates in an easier way. Earlier texts often use the Boltzmann transform with the injection well taken as a line sink; this method of solution does not allow the inclusion of wellbore storage (Bratvold and Horne 1990).

Habte and Onur (2014) recently discussed a semi-analytical method to solving the multiphase problem which, in theory, can include many additional nonlinear effects. Their method also uses the quasi-stationary approximation, but solves the problem numerically using spatial finite differences. The time domain is solved analytically using the Laplace integral transform. One apparent benefit to this method is the computational speed improvement compared to earlier analytical solutions.

It is clear that an extensive effort has been made to study the transient pressure response of the reservoir during water injection. However, the majority of authors work on problems assuming that wellbore effects do not occur, or that they follow the simplified wellbore storage model (Bratvold 1989). Very little analysis has been done on the effects of wellbore heating and cooling on the pressure signal. For development wells, it is possible that these effects could be significant, due to the location of the permanent downhole gauge (PDHG) (not positioned directly at sandface), and the lack of a downhole shutin valve. The ideal completion design for obtaining a PFO test is shown in Figure 4(a). In this test, minimal wellbore effects occur due to the installation of a down hole shut-in valve. Unfortunately for most development wells, the completion in Figure 4(b) is what occurs in practice, and the well can only be shut-in using a surface valve. After cold water is injected, the water inside the well heats up

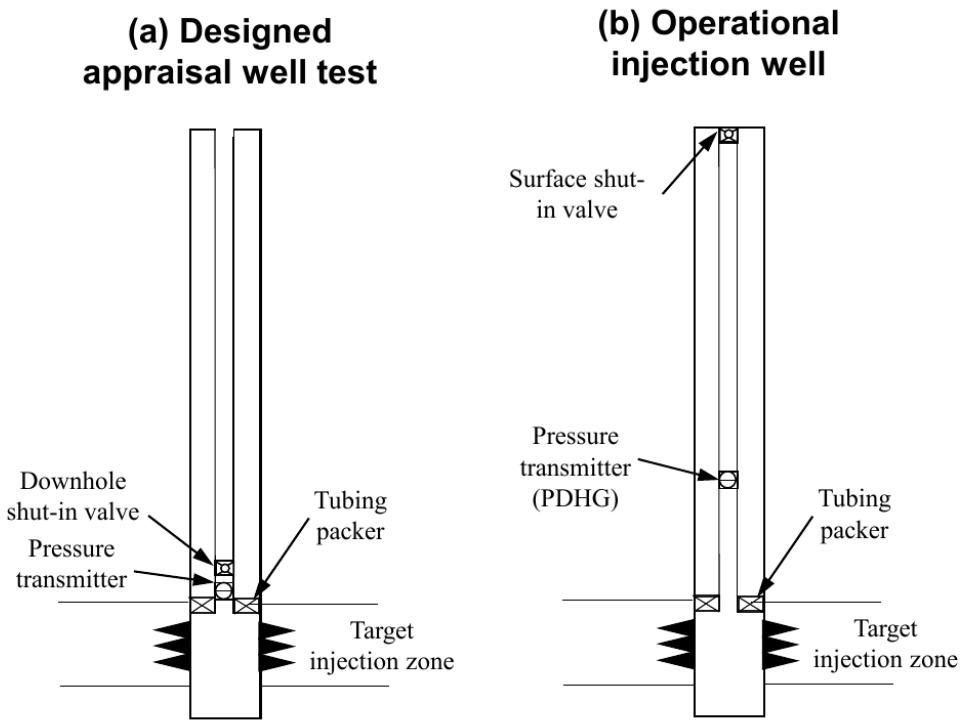

Figure 4: Water injector well schematic for: (a) A designed well test, and (b) normal operation of the well with a PDHG installed

and this interferes with the pressure signal at the transmitter. The impact of this must be considered as it combines with the pressure transient response of the reservoir.

The opportunity for research appears to be the coupled effects of wellbore fluid storage, well temperature changes and the pressure transient response of the reservoir following cold water injection. This problem has been observed by the present author in field cases.

Prior to incorporating wellbore effects, a reservoir model must be selected for use. The analytical models described earlier are accurate for the water injection problem but often difficult to combine with wellbore afterflow effects. One pragmatic alternative is to use the radial composite reservoir model, with the inner and outer regions representing flooded and unflooded zones respectively. This represents the problem in a stationary sense. According to Ambastha (1989), the solution for the two-region composite model is, adjusted for an injection case:

$$\overline{p}_w(u) = p_i + \frac{wB\mu}{2\pi kh}\left[C_1 I_0(\sqrt{u}) + C_2 K_0(\sqrt{u})\right] \tag{17}$$

where w represents the water injection rate. No wellbore skin is included in this solution, but it is able to incorporated later using convolution. The constants C_1 and C_2 are determined by solving the following matrix equation:

$$\begin{bmatrix} \alpha_{11} & \alpha_{11} & 0 \\ \alpha_{21} & \alpha_{22} & \alpha_{23} \\ \alpha_{31} & \alpha_{32} & \alpha_{33} \end{bmatrix} \begin{bmatrix} C_1 \\ C_2 \\ C_2 \end{bmatrix} = \begin{bmatrix} 1/u \\ 0 \\ 0 \end{bmatrix} \tag{18}$$

For a case without wellbore effects and zero skin at the interface between regions, the coefficients are defined as follows for the infinite acting outer-boundary case:

$$\begin{aligned} &\alpha_{11} = -\sqrt{u}I_1(\sqrt{u}),\ \alpha_{12} = \sqrt{u}K_1(\sqrt{u}), \\ &\alpha_{21} = I_0(R_D\sqrt{u}),\ \alpha_{22} = K_0(R_D\sqrt{u}),\ \alpha_{23} = -K_0(R_D\sqrt{u\eta}), \\ &\alpha_{31} = M\sqrt{u}I_1(R_D\sqrt{u}),\ \alpha_{32} = -M\sqrt{u}K_1(R_D\sqrt{u}),\ \alpha_{33} = \sqrt{u\eta}K_1(R_D\sqrt{u\eta}). \end{aligned} \tag{19}$$

Here, $R_D = r_f/r_w$ represents the dimensionless radius of the flooded region, η is the diffusivity ratio and M is the mobility ratio between flooded and unflooded regions. $I_n(u)$ is the modified Bessel function of the first kind. These equations provide a starting reservoir model for the inclusion of complex wellbore effects. While the model is not as accurate as other discussed earlier in this literature review, e.g. those with a moving flood front, for the problem of pressure falloff during a shut-in period, it is relatively accurate since the front is approximately stationary. The wellbore effects will now be discussed in more detail.

For a water injector without heat transfer inside the well, the first effect to consider is the fluid storage effect that occurs due to the volume inside the well. The capacity of a well to accept fluid is related to the compressibility of the fluid already in the well (if the fluid already occupies the entire well volume) or the density of the fluid (if there is a liquid-gas interface inside the well). Both of these phenomena are described by a wellbore storage coefficient, C. van Everdingen & Hurst (1949) related the flow rate at surface, $q(t)$, to the sand face flow, q_{sf} as follows:

$$q_{sf}(t) = q(t) + C\frac{dp_w(t)}{dt} \tag{20}$$

This equation provides a framework for incorporating storage inside the well with the effect of reservoir diffusivity, via p_w. With regards to water injection wells, the wellbore storage effect for a constant value of C has been fully considered by other authors (e.g. Bratvold 1989). The primary issue is that C may not be constant in cases where the thermal expansion of well fluid forces water into the reservoir during heating.

In many cases it is not acceptable to neglect heat transfer inside the well, which occurs in addition to the discussed storage effect. Discussion of this problem for water injectors is limited in the literature, yet the author has witnessed field cases where its effect has been significant.

Ramey (1962) provided analytical solutions to wellbore heating and cooling problems due to heat

transfer from convection and conduction to the overburden rock. Other researchers have extended this work to more complicated well conditions, including oil and gas wells (Hasan et al. 1997; Hagoort 2004; Hasan et al. 2005; Spindler et al. 2011). It is possible to apply these results to the transient PFO problem. During continuous water injection, the analytical solution below describes fluid temperature inside the well, as a function of depth z and time t (Hasan et al. 2005):

$$T_f(z,t) = T_{ei}(z) + \frac{1-e^{-at}}{L_R}(e^{-zL_R} - 1)g_G \tag{21}$$

In this equation, $T_f(z,t)$ represents the fluid temperature, T_{ei} the temperature of the earth at an undisturbed location far from the well, and g_G is the geothermal temperature gradient. The parameters a and L_R control heat transfer into the well.

For a shut-in after injection, heating of a cold body of water inside the well can be described by the following equation, as a function of depth z and time t (Hasan et al. 2005):

$$T_f(z,t) = [T_{fo}(z) - T_{ei}(z)]e^{-a't} + T_{ei}(z) \tag{22}$$

with T_{fo} the fluid temperature at the instant of shut in. The parameter a' controls the heat transfer to the well from the earth during this shut in period. Since the well is shut in during a PFO survey, the heat transfer occurs during a relatively static condition. Equation 22 represents heating of a static control volume of fluid.

As yet, no authors have studied the interaction of Equation 22 with the other pressure transient solutions during the falloff period (e.g. Equations 17–20). It is worth discussing why this is relevant. The analytical solutions for water injection into an oil reservoir have been developed for practical use with field pressure data, with the end goal of determining reservoir properties and the location of the flood front. The flood front location is determined by matching the subtle changes in the pressure trace and its derivative during the middle time of the falloff response. Field cases showing this are available in Abbaszadeh and Kamal (1989). It is likely that these well tests were planned with precision and hence used downhole shut-in devices; this is an expensive exercise. Referring to Figure 4, the more likely outcome for mature fields is shown in the schematic of an operational injection well. In this case, the full effects of wellbore storage and heat transfer into the well are felt at the PDHG. Determination of the front location inside the reservoir must now occur after the correction of physical effects happening inside the well itself. This area needs attention.

Part of the problem can be approached in the same way that Fair (1981) analysed the phenomenon of wellbore phase redistribution for oil wells, although the results will obviously be different. This aspect accounts for backflow into the reservoir that may occur during a shut-in due to temperature

changes in the well. The methods of Brill and Mukherjee (1999) should also be used to incorporate any pressure losses inside the wellbore itself. Relating to this, a practical discussion on the effect of PDHG placement for wells is given by Kabir and Hasan (1998), but their work does not include the water injector PFO case. This highlights another research gap.

2.5 Full Reservoir System – Production and Injection Wells

The last problem to be considered in this thesis involves a fully combined transient and boundary dominated production model to predict rate performance in a waterflooded oil production well. This reservoir characterisation method is distinct from the pressure transient techniques studied in other parts of the thesis. Rather than focusing on a pressure signal, the long term flow rate performance of a well is used to infer reservoir properties. Historically, this has been referred to as "decline curve analysis". The following review relates to Chapter 8 in this thesis.

The previous sections review reservoir surveillance in the local vicinity of production or injection wells. Surveillance data in these cases can be used to assess well performance, and to some extent provide an estimate of a waterflood front location. In order to analyse data from the entire reservoir over a longer period, however, a method is required that accurately combined production and injection wells. Thakur (1991) refers to this type of activity as "Reservoir Characterisation and Performance Monitoring" in contrast to "Well Monitoring." Reservoir performance monitoring will be the focus of this discussion.

Previously, Arps (1945) developed some of the earliest methods to mathematically characterise oil well production rate decline. An important application of this theory is forecasting future oil production and calculating oil reserves. In the work, empirical decline equations were presented based on experience with production data from American oil fields. The equations were categorised into the exponential, hyperbolic and harmonic decline types. It is important to note that these equations were given on an empirical basis. Furthermore, the theory neglected the initial transient production decline period.

The general equation for the Arps (1945) oil production decline is:

$$q(t) = \frac{q_i}{(1 + bD_i t)^{1/b}} \tag{23}$$

for initial production rate q_i, initial decline rate D_i and exponent b. For $b = 0$, Equation 23 becomes the exponential decline equation, and for $b = 1$, the decline is classified as harmonic. In between, $0 < b < 1$, the decline is defined as hyperbolic. While this equation was developed empirically, it is known theoretically that exponential decline occurs in the pure depletion case in a bounded reservoir (Ehlig-Economides 1979; Lee et al. 2003). Therefore, in the exponential case, there is a theoretical

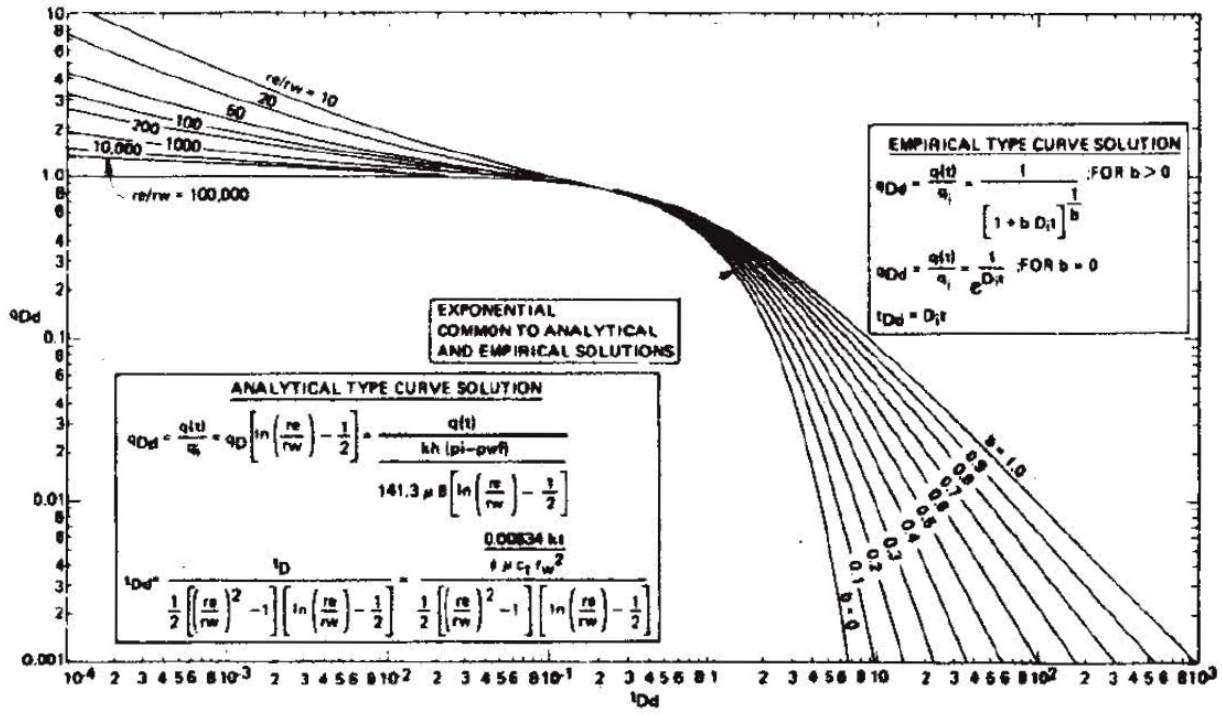

Figure 5: Production decline type curves from Fetkovich (1980)

basis. Exponential decline is given by the following equation, developed from Equation 23 with $b = 0$ and based on constant decline D:

$$q(t) = q_i e^{-Dt} \tag{24}$$

The quality of production data and instrumentation has improved immensely since original decline curve analysis was conceived. This results in the resolution of other flow regimes and effects visible in the production data. Recognising this, Fetkovich (1980) extended Arps' (1945) work by creating a type curve including both transient and boundary dominated effects. This chart is reproduced in Figure 5. By plotting field production data on this chart, it is possible to determine three reservoir properties – e.g. reservoir radius r_e, permeability k and mechanical skin S (providing that the other required reservoir properties are known). Using the chart leads to an assessment of both well and reservoir performance.

In the Fetkovich type curve, the transient rate decline is plotted in the graph separately to the boundary dominated portion. The transient decline arises from the constant well pressure solution in an infinite reservoir, given earlier as Equation 10. The boundary dominated curves are given separately by Equation 23. A range of decline exponents from $b = 0$ to 1 are included in the chart as multiple "stems". Special dimensionless groups are used on the log-log chart to collapse the curves onto a single scale. These groups are termed the "dimensionless decline groups" and are defined as:

$$q_{Dd} = q_D \left(\ln r_{eD} - \frac{1}{2} \right) \tag{25}$$

for production rate, and as follows for time:

$$t_{Dd} = \frac{2t_D}{(r_{eD}^2 - 1)(\ln r_{eD} - \frac{1}{2})} \tag{26}$$

where q_D and t_D are the dimensionless groups commonly used in the pressure transient literature (see Lee et al. 2003). The dimensionless outer radius is the important correlating parameter in this chart and is defined as $r_{eD} = r_e/r_w$. These dimensionless decline groups have excellent utility, even when extending the case to include water injection effects.

The Fetkovich (1980) type curves do not directly include the effects of water injection on an oil production well. The curves only account for declining liquid production, but with water injection it is expected that at least some of the production rate should be restored at some time in the well's production rate history. This can be observed in field cases and represents a current research gap. Doublet and Blasingame (1995) began addressing the theory of delayed water injection into a bounded reservoir for production decline curves, however their theory was incomplete and suffered some analytical and numerical artefacts. In this thesis, their work will be modified and extended to create precise curves similar to the Fetkovich (1980) curves, but including the effects of delayed water injection. After an initial period of production decline, it is possible to incorporate the delayed injection through application of the superposition principle. Apparently this method has not been studied in the literature until now.

The method of decline curve analysis (otherwise known as Rate Transient Analysis) remains popular today. It is a method used for forecasting remaining reserves and production rates from hydrocarbon wells. The area still receives attention in the research literature (Sun 2015; Jongkittinarukorn et al. 2020). Multiphase aspects continue to be studied over time (Raghavan 1989; Turki et al. 1989; Raghavan 2009; Uzun et al. 2016) and it is expected that this is an important consideration for the waterflood case. The aforementioned studies consider multiphase flow for fields undergoing primary depletion and thus do not incorporate the effect of a waterflood. It is possible to use methods similar to these papers, and the Martin (1959) and Perrine (1956) approaches, to model the effects of simultaneous water and oil flow in decline curve analysis.

For long-time stabilised flow, the Buckley and Leverett (1942) solutions to water-oil immiscible displacement are also useful for matching with production data. The Buckley-Leverett frontal advance equation is given as:

$$r \left.\frac{dr}{dt}\right|_{S_w} = \frac{q_{\text{inj}}}{2\pi\phi h} \left.\frac{df_w}{dS_w}\right|_{S_w} \tag{27}$$

where q_{inj} is the water injection rate and $f_w = q_w/q_t$ the water fractional flow. Integrating, it is possible to determine the relationship between saturation and time at a particular radius:

$$t(S_w) = \frac{\pi\phi h}{q_{\text{inj}} f'_w(S_w)}(r_e^2 - r^2) \tag{28}$$

Note that the method does not include transient pressure diffusion effects inside the reservoir, hence it is used later in time during steady-state flow. Usually, analysis is done on long term data to predict or match fractional flow performance data. In the present thesis, the modified waterflood Fetkovich type curves will be supplemented with the Buckley-Leverett oil-water fractional flow effect. This method then includes transient and boundary dominated effects of injection as well as late-life two phase flow.

More recent methods for matching the water cut at oil production wells have been proposed by Baker et al. (2003) and Yang (2009). The methods focus on liquid injection, production and corresponding water cut, forecasting how they will change over time. Again, these methods do not consider the transient periods of flow from the oil well. As part of the research in this thesis, a complete analytical model will be developed for the case of transient and stabilised production analysis of an oil well under delayed water injection at the outer boundary; basic multiphase aspects will be considered as part of this new model.

There are also similarities between modeling waterflooding and aquifer pressure support in reservoirs. Many mathematical solutions are available to model aquifer support (van Everdingen and Hurst 1949; Carter and Tracy 1960; Fetkovich 1971; Izgec and Kabir 2010). One option available in RTA is the composite (two-zone) model of subsurface to account for the reservoir and a large attached aquifer in the outer zone (e.g the. Ambastha (1989) model applied to RTA). This method allows external influx into the reservoir from the aquifer. Unfortunately these aquifer models do not perfectly describe the situation occurring during a waterflood. Since oil wells are often developed years before waterflood operations commence, there is a period of extensive decline prior to the commencement of any form of pressure support. Aquifer models in RTA analysis (including the composite model) are usually connected to the reservoir since the beginning of depletion and this can pose problems interpreting data from waterflooded fields where pressure support did not commence until later. The model proposed in this thesis resolves this by allowing injection to commence later in field life.

Alternative Production Analysis Methods

Several alternative methods are available for the analysis of production data in waterflooded fields.

These techniques can be broadly categorised as numerical, semi-analytical or analytical/empirical. They are discussed here purely as alternatives to the RTA technique and are not utilised in this thesis, apart from benchmarking and comparison.

In the last 15 years, Capacitance Resistance Modelling (CRM) has gained popularity for fields with many production and injection wells (Liang et al. 2007; de Holanda et al. 2018). This method is classified as analytical/empirical. Several related methods have also emerged (e.g. Sayyafzadeh et al. 2011). CRM is a rapid tool that can consider the effect of hundreds or thousands of wells, however it does not include the transient flow period. This is a benefit of the Rate Transient Analysis technique. The fact that CRM does not model transient flow is a result of its chosen governing differential equation used to model flow:

$$q_j(t) = \sum_{i=1}^{n} \Lambda_{ij} I_i - \tau_j \frac{dq_j}{dt} \tag{29}$$

Here, q_j is the liquid flow rate at production well j, I_i is the injection rate of injector i, Λ_{ij} is the fraction of injector i's water supporting producer j, and τ_j is the time constant for the production well. This differential equation assumes that a production well is placed in a zero-dimensional control volume, and therefore transient effects are neglected. At least one dimension in space is required to incorporate pressure transience due to compressible flow. In the absence of injection, the solution to Equation 29 is the exponential decline equation (Equation 24). The pressure response in CRM is always boundary dominated. This is contrasted with the governing equation used for the majority of work in this thesis, Equation 4, which is one-dimensional in terms of radius, r.

It is also worth discussing the use of reservoir simulation for performance monitoring and forecasting in mature waterfloods. Reservoir simulation is a numerical computing method where the governing nonlinear partial differential equations are solved using space and time discretisation (Aziz and Settari 1979). The method is beneficial for complicated geological features (e.g. heterogeneity or faulting), when non-linear physical processes occur (e.g. chemical or thermal flooding) or when the normal means of linearising the governing differential equations are invalidated (e.g. large pressure or saturation gradients inside the reservoir). Nowadays, many commercial and open source reservoir simulators are available for use.

Examples are available in the literature where reservoir simulation is applied to mature field waterfloods. For example, Galas et al. (1994) used simulation to assess the outcome of new infill wells in the mature Weyburn waterflooded unit. History matching of 30 years' production data was undertaken before commencing future forecasting. Afterwards, parametric studies allow assessment of new horizontal well performance. The impact of permeability uncertainty, well length/skin and well location on ultimate recovery were studied. Based on their findings, three horizontal oil wells were

drilled.

A separate study was given for the South Belridge diatomite waterflood by Yang and Urdaneta (2017). Their work focused on the special case where injected water breaks through prematurely at production wells. Through a history matching process and some analytical work, they were able to reconcile reservoir models with actual field data. The final simulation model was used to forecast oil production into the future.

An alternative to full numerical reservoir simulation is the semi-analytical method of streamline simulation. This method solves for pressure diffusion numerically on a discretised grid, while the transport of phases is calculated analytically along streamlines. Normally, streamline simulation assumes incompressible fluid flow. There are several practical benefits for waterflood simulation when using streamlines over conventional finite difference reservoir simulation. Since streamlines start at an injector and terminate at a producer, it is possible to ascertain how much support a producer is receiving from a particular injector. Due to the geometry of streamlines, it is also possible to determine drainage zones around wells easily. Visualisation of the streamlines is quite informative for analysts studying the flow around wells. Thiele and Batycky (2006) have used this type of model to improve reservoir management of a waterflood field through the use of calculated injector efficiency values. The Injector Efficiency is similar to the parameters used in the CRM method, however CRM relies on matching actual production data for the values to be meaningful.

Reservoir simulation technology is important for solving a variety of reservoir problems; however, it is most powerful when making decision for new projects, e.g. greenfield developments, or infill drilling campaigns. It is also useful for complicated or special cases of reservoir physics. While numerical simulation is highly flexible and can solve a larger variety of problems, there are several practical challenges when compared to analytical methods like RTA. Setting up models to run on a computer is time consuming process and matching vast amounts of production data is complicated. This is why its power is often reserved for new developments requiring large amounts of capital expenditure. Often, simpler cases of production forecasting and well performance assessment can be tackled using decline curves or RTA. When it comes to calculating oil and gas reserves, the simplicity of these analytical methods allows for greater transparency and auditability by regulators (Cronquist 2001). These reasons may explain why decline curve analysis remains popular.

Over the last decade, the application of artificial intelligence and machine learning to history matching and subsequent forecasting has been growing. This method is a mostly empirical science and does not rely on first principles physics methods, instead using trained computing systems to reproduce observed data. For example, Deng and Pan (2020) use machine learning to match waterflood well pressure and water cut performance after water breakthrough has occurred. It is possible to use

these matched models to optimise parts of the field where water is injected, in order to maximise oil production.

While the artificial intelligence area is emerging and showing promise for reservoir engineering, the advantage of physics-based methods is that they provide an explanation and physical meaning to oil field performance. Analytical models can also be used in the absence of field data.

2.6 Summary and Research Gaps

This literature review highlights several research gaps in the area of reservoir surveillance for mature fields. Several problems specific to mature waterflooded fields have not yet been studied analytically in the literature.

While constant-rate and constant-pressure transient analysis cases are well covered in the literature, the case of cyclic production in an infinite reservoir is scarcely covered. Solving this problem analytically would allow for reservoir property determination from frequently available field operating data in mature fields. This has the benefit of performing analysis on wells that are currently online and producing, rather than shutting in wells for analysis and foregoing oil production. It is a research gap in the case of transient drawdown production. Furthermore, the available solutions for boundary dominated (or stabilised) production do not consider cyclic production. A new way to study this problem is to apply the harmonic theory frequently applied in the pulse testing literature to stabilised artificial lift wells.

With regards to water injection wells, pressure transient surveys incorporating temperature effects inside the well are not considered extensively in the literature. In mature fields, it is unlikely that water injector PFO surveys will be planned using specialised downhole shut-in equipment. Due to this, it is not appropriate to use existing multiphase pressure falloff covered by research such as Abbaszadeh and Kamal (1989), Bratvold and Horne (1990) or Levitan (2003), in a standalone way. The effects of wellbore storage and temperature changes inside the well must also be considered, which will be undertaken in this research.

Finally, while rate transient analysis is a well known technique for use with fields undergoing primary depletion, details are lacking on its extension to the case of water injection support. The Fetkovich (1980) approach to analysing production data has proven successful over time, yet it does not include a mechanism to interpret production changes over time owing to water injection later in field life. This extension presents an opportunity to characterise the effective water support at a producer, utilising commonly available production flow rate history. While numerical methods can be applied to this problem, they are not as practical for engineers to apply or directly applicable to oil reserves bookings.

2.7 References

Abbaszadeh, M. 1991. Two-Phase Transient Testing of Water Injection Wells in Layered Reservoirs. Presented at the ATCE Conference held in Dallas, TX, Oct 6-9. SPE-22680-MS.

Abbaszadeh, M. and Kamal, M. 1989. Pressure-Transient Testing of Water-Injection Wells. *SPE Res Eng* **4**(1): 115-124. SPE-16744-PA.

Acton, J.F. 1981. Pump-off Controller Application for Midway-Sunset Cyclic Steam Operations. SPE California Regional Meeting, 25-27 Mar, Bakersfield, CA. SPE-9915-MS.

Agarwal, R.G. 1970. An Investigation of Wellbore Storage and Skin Effect in Unsteady Liquid Flow: I. Analytical Treatment. Presented at the SPE 44th Annual Fall Meeting, Denver, CO, Sep 28-Oct 1. SPE-2466-MS.

Ahn, S. 2012. *Pressure Pulse Testing in Heterogeneous Reservoirs.* PhD thesis. Stanford University.

Ambastha, K.A. 1989. *Pressure Transient Analysis for Composite Systems.* Technical Report DOE/BC/14126-11, Stanford University, Stanford, CA.

Arps, J.J. 1945. Analysis of Decline Curves. *Trans AIME.* **160**: 228-247. SPE-945228-G.

Aziz, K. and Settari, A. 1979. *Petroleum Reservoir Simulation.* Applied Science Publishers, Ltd. London.

Baker, R.O., Anderson, T. and Sandhu, K. 2003. Using Decline Curves to Forecast Waterflooded Reservoirs: Fundamentals and Field Cases. Presented at the Petroleum Society's Canadian International Petroleum Conference, Calgary, Alberta.

Banerjee, R., Thompson, L.G. and Reynolds, A.C. 1998. Injection/Falloff Testing in Heterogeneous Reservoirs. *SPE Reservoir Evaluation & Engineering.* **1**(06): 519-527. SPE-52670-PA.

Benson, S.M. and Bodvarsson, G.S. 1986. Nonisothermal Effects During Injection and Falloff Tests. *SPE Formation Evaluation.* **1**(01):53-63. SPE-11137-PA.

Bratvold, R. B. and Horne, R. N. 1990. Analysis of Pressure-Falloff Tests Following Cold-Water Injection. *SPE Form Eval.* **5**(3): 293-302. SPE-18111-PA.

Bratvold, R.B. 1989. *An Analytical Study of Reservoir Pressure Resnpose Following Cold Water Injection.* PhD Dissertation, Stanford University, CA.

Brill, J. P. and Mukherjee, H. 1999. *Multiphase Flow in Wells.* Monograph Series Vol. 17, Society of Petroleum Engineers. Richardson, Texas, USA.

Buckley, S.E. and Leverett, M.C. 1942. Mechanism of Fluid Displacement in Sands. *Trans AIME.* **146**(01): 107-116. SPE-942107-G.

Cardiff, M., Barrash, W. 2014. Analytical and Semi-analytical Tools for the Design of Oscillatory Pumping Tests. *Groundwater.* **53**(6), 896-907.

Carter, R.D. and Tracy, G.W. 1960. An Improved Method for Calculating Water Influx. *Trans AIME.* **219**(01): 415-417.

Chacin, J., Schmidt, Z., Doty, D., et al. 1994. Modeling and optimization of plunger lift assisted intermittent gas lift installations. *SPE Adv. Technol.* **2**(01):25-33.

Cronquist, C. 2001. *Estimation and Classification of Reserves of Crude Oil, Natural Gas, and Condensate.* Society of Petroleum Engineers. Richardson, TX.

de Holanda, R.W., Gildin, E., Jensen, J.L. et al. 2018. A State-of-the-Art Review on Capacitance Resistance Models for Reservoir Characterization and Performance Forecasting. *Energies.* **11**(12): 1-46.

Deng, L. and Pan, Y. 2020. Machine-Learning-Assisted Closed-Loop Reservoir Management Using Echo State Network for Mature Fields under Waterflood. *SPE Reservoir Evaluation & Engineering.* **23**(04): 1298-1313. SPE-200862-PA.

Doublet, L.E. and Blasingame, T.A. 1995. Decline Curve Analysis Using Type Curves: Water Influx/Waterflood Cases. Presented at the SPE Annual Technical Conference and Exhibition, Dallas, Texas, 22-25 Oct. SPE-30774-MS.

Eckel,A.C., Abels,H.P., Merritt,R.A. 1995.Testing and practically applying pump-off controllers in

a waterflood. Western Regional Meeting, Bakersfield. Society of Petroleum Engineers. SPE-29636-MS.

Ehlig-Economides, C.A. 1979. *Well Test Analysis for Wells Produced at a Constant Pressure.* PhD Dissertation, Stanford University, CA.

Ehlig-Economides, C.A. and Ramey, H.J. 1981. Transient Rate Decline Analysis for Wells Produced at Constant Pressure. *SPE Journal.* **21**(01):98-104. SPE-8387-PA.

Fair, W. B. Jr. 1981. Pressure Buildup Analysis with Wellbore Phase Redistribution. *SPE J.* **21**(2): 259-270. SPE-8206-PA.

Fetkovich, M.J. 1971. A Simplified Approach to Water Influx Calculations – Finite Aquifer Systems. *Journal of Petroleum Technology.* **23**(07): 814-828. SPE-2603-PA.

Fetkovich, M.J. 1980. Decline Curve Analysis Using Type Curves. *Journal of Petroleum Technology.* **32**(06): 1065-1077. SPE-4629-PA.

Fokker, P.A., Renner, J., Verga, F. 2012. Applications of harmonic pulse testing to field cases. SPE Europec/EAGE Annual Conference. SPE-154048-MS.

Fokker, P.A., Verga, F. 2011. Application of harmonic pulse testing to water-oil displacement. *J. Petrol. Sci. Eng.* **79**(3): 125-134.

Fokker, P.A., Borello, E.S., Verga, F. et al. 2017. Harmonic pulse testing for well and reservoir characterization. Presented at the SPE Europec Featured at 79th EAGE Conference and Exhibition. SPE-185815-MS.

Fokker, P.A., Borello, E.S., Verga, F. et al. 2018. Harmonic pulse testing for well performance monitoring. *J. Petrol. Sci. Eng.* **162**: 446-459.

Galas, C.M., Churcher, P.L. and Tottrup, P. 1994. Predictions of Horizontal Well Performance in a Mature Waterflood, Weyburn Unit, Southeastern Saskatchewan. *Journal of Canadian Petroleum Technology.* **33**(09): 29-35.

Gasbarri, S., Gupta, A., Wiggins,M. et al. 1997. Inflow performance of reservoirs produced by intermittent lift methods. PETSOC Annual Technical Meeting. Calgary, Petroleum Society of Canada.

Habte, A.D. and Onur, M. 2014. Laplace-Transform Finite-Difference and Quasistationary Solution Method for Water-Injection/Falloff Tests. *SPEJ.* **19**(03): 398-409. SPE-168221-PA.

Hagoort, J. 2004. Ramey's Wellbore Heat Transmission Revisited. *SPE J.* **9**(4): 465-474. SPE-87305-PA.

Hasan, A. R., Kabir, C. S., and Lin, D. 2005. Analytic Wellbore-Temperature Model for Gas-Well Testing. *SPE Res Eval & Eng.* **8**(3): 240-247. SPE-84288-PA.

Hasan, A. R., Kabir, C. S., and Wang, X. 1997. Development and Application of a Wellbore/Reservoir Simulator for Testing Oil Wells. *SPE Form Eval.* **12**(3): 182-188. SPE-29892-PA.

Hazebroek, P., Rainbow, H., and Matthews, C. S. 1958. Pressure Fall-Off in Water Injection Wells. Transactions of the Society of Petroleum Engineers, Vol. 213, Part 1, SPE-925-G.

Hollaender, F., Hammond, P., Gringarten, A., 2002. Harmonic Testing for Continuous Well and Reservoir Monitoring. Presented at the SPE Annual Technical Conference and Exhibition, San Antonio, Tex. SPE-77692-MS.

Huff, M.E. III 1988. *Pressure Transient Testing of Intermittent Gas Lift Wells.* PhD Dissertation. Texas Tech University.

Izgec, O. and Kabir, C.S. 2010. Quantifying Nonuniform Aquifer Strength at Individual Wells. *SPE Reservoir Evaluation & Engineering.* **13**(02): 296-305. SPE-120850-PA.

Jongkittinarukorn, K., Last, N., Escobar, F.H. et al. 2020. A New Decline-Curve-Analysis Method for Layered Reservoirs. *SPE Journal.* **25**(04): 1657-1669. SPE-195085-PA.

Kabir, C. S. and Hasan, A. R. 1998. Does Gauge Placement Matter in Downhole Transient-Data Acquisition? *SPE Res Eval & Eng* **1**(1): 64-68. SPE-36527-PA.

Kamal, M. 2009. *Transient Well Testing.* Society of Petroleum Engineers Monograph Series, Vol. 23. Richardson, TX.

Kazemi, H., Merrill, L.S. and Jargon, J.G. 1972. Problems in Interpretation of Pressure Fall-Off Tests in Reservoirs With And Without Fluid Banks. *Journal of Petroleum Technology.* **24**(09): 1147-

1156. SPE-3696-PA.

Kuchuk, F. J. 1986. Generalized Transient Pressure Solutions with Wellbore Storage. SPE-15671-MS.

Kuchuk, F. J., Onur, M., and Hollaender, F. 2010. *Pressure Transient Formation and Well Testing: Convolution, Deconvolution and Nonlinear Estimation.* Vol. 57, first edition. Oxford, UK: Elsevier Science.

Kuo, C.H. 1972. Determination of reservoir properties from sinusoidal and multirate flow tests in one or more wells. *Soc. Petrol. Eng. J.* **12**(06):499-507. SPE-3632-PA.

Lee, J., Rollins, J.B. and Spivey, J.P. 2003. *Pressure Transient Testing.* SPE Textbook Series Vol 9. Richardson, TX.

Levitan, M.M. 2003. Application of Water Injection/Falloff Tests for Reservoir Appraisal: New Analytical Solution Method for Two-Phase Variable Rate Problems. *SPEJ.* **8**(04):341-349. SPE-87332-PA.

Liang, X., Weber, D.B., Edgar, T.F. et al. 2007. Optimization of Oil Production Based on a Capacitance Model of Production and Injection Rates. Presented at the SPE Hydrocarbon Economics and Evaluation Symposium, Dallas, Texas, 1-3 Apr. SPE-107713-MS.

Martin, J.C. 1959. Simplified Equations of Flow in Gas Drive Reservoirs and the Theoretical Foundation of Multiphase Pressure Buildup Analyses. *Trans AIME.* **216**(01): 321-323.

Matthews, C. and Russell, D. 1967. *Pressure buildup and flow tests in wells.* SPE Monograph Series Vol. 1, Dallas, TX.

McCoy, J., Becker, D., Podio, A. 1999. Timer control of beam pump runtime reduces operating expense. Proceedings of the Annual Southwestern Petroleum Short Course. Lubbock, Texas Tech University.

Ogbe, D., Brigham, W. 1987. Pulse testing with wellbore storage and skin effects. *SPE Form. Eval.*. **2**(01): 29–42. SPE-12780-PA.

Perrine, R.L. 1956. Analysis of Pressure-Buildup Curves. *Drilling and Production Practice.* API. 482-509.

Raghavan, R. 1989. Well-Test Analysis for Multiphase Flow. *SPE Formation Evaluation.* **4**(04): 585-594. SPE-14098-PA.

Raghavan, R. 2009. A note on the theoretical foundations for multiphase pressure analysis for flow in porous media. *J Petrol Sci Eng.* **68**(1-2): 81-88.

Ramakrishnan, T. S. and Kuchuk, F. J. 1993. Pressure Transients during Injection: Constant Rate and Convolution Solutions. *Transp Porous Media.* **10**(2): 103-136.

Ramey, H. J. 1962. Wellbore Heat Transmission. *J Pet Technol.* **14**(4): 427-435. SPE-96-PA.

Rosa, A.J., 1991. *Reservoir Description by Well Test Analysis Using Cyclic Flow Rate Variation.* PhD thesis. Stanford University, CA.

Rosa, A.J., Horne, R.N., 1997. Reservoir description by well test analysis using cyclic flow rate variation. *SPE Form. Eval.* **12**(04):247-254. SPE-22698-PA.

Sayyafzadeh, M., Pourafshary, P., Haghighi, M. et al. 2011. Application of transfer functions to model water injection in hydrocarbon reservoir. *J Petrol Sci Eng.* **78**: 139-148.

Spindler, R. P. 2011. Analytical Models for Wellbore-Temperature Distribution. *SPE J.* **16**(1): 125-133. SPE-140135-PA.

Spivey, J.P., Lee, W.J., et al. 1993. Production data analysis for wells that have been subject to periodic curtailment. SPE Gas Technology Symposium. SPE-26182-MS.

Stehfest, H. 1970. Algorithm 368: Numerical inversion of Laplace transforms. *Commun. ACM.* **13**: 47-49.

Sun, H. 2015. *Advanced Production Decline Analysis and Application.* Gulf Professional Publishing.

Takacs, G. 2015. *Sucker-rod Pumping Handbook.* Gulf Professional Publishing.

Thakur, G.C. 1991. Waterflood Surveillance Techniques – A Reservoir Management Approach. *Journal of Petroleum Technology.* **43**(10): 1180-1188. SPE-23471-PA.

Theis, C.V., 1935. The relation between the lowering of the piezometric surface and the rate and duration of discharge of a well using groundwater storage, *Am. Geophys. Union Trans.* **16**: 519-524.

Thiele, M.R. and Batycky, R.P. 2006. Using Streamline-Derived Injection Efficiencies for Improved Waterflood Management. *SPE Reservoir Evaluation and Engineering.* **9**(02): 187-196. SPE-84080-PA.

Turki, L. Demski, J.A. and Grader, A.S. 1989. Decline Curve Analysis in Composite Reservoirs. Presented at the SPE Eastern Regional Meeting held in Morgantown, West Virginia, Oct 24-27. SPE-19316-MS.

Uzun, I., Kurtoglu, B. and Kazemi, H. 2016. Multiphase Rate-Transient Analysis in Unconventional Reservoirs: Theory and Application. *SPE Reservoir Evaluation & Engineering.* **19**(04): 553-566. SPE-171657-PA.

Verigin, N.N. 1952. On the Pressurized Forcing of Binder Solutions Into Rocks in Order to Increase the Strength and Imperviousness to Water of the Foundations of Hydrotechnical Installations. *Isvestia Akademii Nauk SSSR Odt. Tehn. Nauk.* **5**:674-687. (in Russian).

Willis, T.B. 2013. The Appeal of Mature Fields. *SPE The Way Ahead.* **9**(03): 2.

Yang, Z. and Urdaneta, A. 2017. A Practical Approach to History Matching Premature Water Breakthrough in Waterflood Reservoir Simulation: Method and Case Studies in South Belridge Diatomite Waterflood. *SPE Reservoir Evaluation & Engineering.* **20**(03): 726-737. SPE-174006-PA.

Yang, Z. 2009. Analysis of Production Decline in Waterflood Reservoirs. Presented at the SPE Annual Technical Conference and Exhibition, New Orleans, Louisiana, 4-7 Oct. SPE-124613-MS.

3 Overview and Surveillance of the Mature Windalia Waterflooded Field

The opening chapter provides an example field overview for a mature asset where classical reservoir surveillance methods are applied to improve reservoir management. The purpose of this chapter is to introduce readers to a typical mature asset and understand some usual challenges. The paper was presented in 2016 at the SPE Asia Pacific Oil & Gas Conference and Exhibition, held in Perth, Australia.

Statement of Authorship

Title of Paper	Increasing Water Injection Efficiency in the Mature Windalia Oil Field, NW Australia, Through Improved Reservoir Surveillance and Operations
Publication Status	☑ Published ☐ Accepted for Publication ☐ Submitted for Publication ☐ Unpublished and Unsubmitted work written in manuscript style
Publication Details	O'Reilly, D.I., Hunt, A.J., Sze, E.S., Hopcroft, B.S., Goff, B.H. and Haghighi, M. 2016. Increasing Water Injection Efficiency in the Mature Windalia Oil Field, NW Australia, Through Improved Reservoir Surveillance and Operations. Presented at the SPE Asia Pacific Oil & Gas Conference and Exhibition held in Perth, Australia, 25-27 October. SPE-182339-MS.

Principal Author

Name of Principal Author (Candidate)	Daniel O'Reilly		
Contribution to the Paper	Literature review, pressure transient case studies, preparation of graphs, writing the manuscript. Acted as corresponding author.		
Overall percentage (%)	80%		
Certification:	This paper reports on original research I conducted during the period of my Higher Degree by Research candidature and is not subject to any obligations or contractual agreements with a third party that would constrain its inclusion in this thesis. I am the primary author of this paper.		
Signature		Date	24 Nov 2020

Co-Author Contributions

By signing the Statement of Authorship, each author certifies that:

i. the candidate's stated contribution to the publication is accurate (as detailed above);

ii. permission is granted for the candidate in include the publication in the thesis; and

iii. the sum of all co-author contributions is equal to 100% less the candidate's stated contribution.

Name of Co-Author	Manouchehr Haghighi		
Contribution to the Paper	Principal supervision of the work. Manuscript review and assessment.		
Signature		Date	01/12/2020

Name of Co-Author	Ash Hunt		
Contribution to the Paper	Manuscript review and assessment. Assisted with preparation of field history chart (Figure 7).		
Signature		Date	24 - Nov - 2020

Name of Co-Author	Ewen Sze		
Contribution to the Paper	Manuscript review and assessment.		
Signature		Date	25-Nov-2020

Name of Co-Author	Brad Hopcroft		
Contribution to the Paper	Assisted with preparation of maps (Figure 5).		
Signature		Date	26-Nov-2020

Name of Co-Author	Bree Goff		
Contribution to the Paper	Chevron Team Leader responsible for work planning and oversight. Manuscript review and assessment. Bree Goff		
Signature		Date	30 Nov 2020

SPE-182339-MS

Increasing Water Injection Efficiency in the Mature Windalia Oil Field, NW Australia, Through Improved Reservoir Surveillance and Operations

DI O'Reilly, Chevron Australia Pty Ltd, The University of Adelaide; AJ Hunt, ES Sze, BS Hopcroft, and BH Goff, Chevron Australia Pty Ltd; M Haghighi, The University of Adelaide

This paper was prepared for presentation at the SPE Asia Pacific Oil & Gas Conference and Exhibition held in Perth, Australia, 25-27 October 2016.

Abstract

This paper demonstrates how good technical evaluations and focused operational application can enhance the value of a mature asset. The Windalia reservoir underlies Barrow Island (BWI), situated 56 km from the coast of Western Australia, and has produced oil since 1965. Waterflooding commenced shortly after initial production, in 1967, and remains the main drive mechanism in the field today. Throughout the life of this onshore field, water injection and oil production have varied according to asset strategy and economic conditions. In this case study, we share how recent improvements made in the areas of Reservoir Surveillance and Operations activities have increased water injection efficiency and total oil recovery.

Through the use of new methods and workflows, the BWI Sub-Surface team was able to target specific areas of the field to distribute water to in order to increase injection and maximise oil production. For example, new workflows were built with the real-time PI monitoring system to analyse Pressure Fall Off (PFO) tests from each of the 147 waterflood patterns in detail. Capacitance-Resistance-Modeling was also leveraged to guide individual well target injection-rates. Operationally, several projects were also initiated to increase water injection into the right areas of the field.

The new Reservoir Management approach has significantly increased the volume of water being injected into the areas of need, supporting improved levels of oil production. For the first time in almost 10 years, the stream-day water injection rate has exceeded 90,000 bwipd. The results from PFO transient interpretation and pattern balancing proved effective in directing water to low-pressure, high-GOR areas of the field. They also provided valuable information about formation perm-thickness and skin. The phenomenon of water-cycling was also largely avoided, owing to close monitoring of production well tests and water injector transient surveys.

The present work addresses reservoir and operational aspects of Australia's largest active waterflood. The lessons shared are highly applicable to a low oil price environment, as they show how fit-for-purpose and low-cost acquisition of reservoir data can lead to improved field performance.

Introduction

The Windalia reservoir is undergoing the largest operational waterflood in Australia. Over 400 producers and 200 water injectors have intersected this reservoir, which produced at a peak oil rate of almost 50,000 BOPD (Ellis et al. 1999). Sustained water injection was also achieved at rates of over 100,000 BWIPD after the turn of this century. The asset has undergone investment and operation for 51 years as of 2016, situated alongside the flagship Gorgon Project on BWI, Australia.

To compare, other active waterfloods in the country include the Stag (McDiarmid et al. 2001), Enfield (Hamp et al. 2008) and Stybarrow (Hill et al. 2008) fields, all of which are offshore oilfields and also located in Western Australia. These fields have been developed with a much sparser well pattern and have not undergone the same level of long-term secondary recovery as the Windalia. In addition to these fields, the Cliffhead field (Daniel and Roberts 2009) in the offshore Perth Basin and Pyrenees FPSO development (Napalowski et al. 2012) also provide pressure support through several water injection wells. Some onshore Cooper Basin fields in Australia have also undergone small-scale pilot waterflood projects (the Charo and Growler fields), but at lower injection rates than the Windalia. Most other oil developments in Australia throughout Cooper Basin, the Bass Strait, North West Shelf and Timor Sea are purely primary depletion developments due to higher aquifer pressure support and excellent reservoir quality. The low reservoir quality (4–5 mD) of the Windalia reservoir (Haynes et al. 2013) and poor aquifer support necessitated a large scale waterflood from very early on in the field's life.

The present study is the first available to comprehensively review the history and development of the Windalia waterflood, along with the latest strategy for its operation and Reservoir Management. The sections will be broken up as follows. In the Introduction, we will discuss a short history of Barrow Island hydrocarbon development, followed by a summary of current practice in Waterflood Reservoir Management. Next, we will provide a detailed description of the Windalia Background, including its geology and development history. Finally, the most recent activities in the field will be discussed in the Windalia Waterflood Reservoir Management section.

BWI Oil Field History

Barrow Island (BWI) is situated in the northern Carnarvon Basin, 56 km from the coast of Western Australia (Fig. 1). The island spans 27 km NS x 11.5 km EW. Barrow No. 1, the first well on the BWI anticline, was drilled in 1964 with deep Jurassic targets at depths of up to 9,785 ft (McTavish 1965; Casey and Konecki 1967). A Drill Stem Test (DST) measured production rates of 985 BOPD from some of the upper Jurassic sections. Earlier in 2016, this well was recompleted and returned to service after many years of downtime, and still produces oil at commercial rates.

Figure 1—Location map of Barrow Island (BWI) L1H lease, Australia

The original oil development on BWI is one of the earliest of its kind in Australia. Geological field mapping began as early as 1954 (Ellis et al. 1999), with the first well drilled at the estimated structural crest 10 years later (Parry 1967; Campbell et al. 1984). The targets were originally in the deep Jurassic intervals, but the major discovery was later in time and was the shallow Windalia of Cretaceous age.

The Windalia oil reservoir was discovered soon after in 1965 during drilling of the F36 well (Barrow No. 4), which originally targeted the Jurassic reservoirs. This well flowed without stimulation which is now considered unusual for a typical Windalia producer. The presence of irregular higher permeability carbonate anomalies assisted inflow in F36 (O'Reilly 2016b). Initial production under natural flow was 125 bopd, prompting an expanded development of the Windalia reservoir (Crank et al. 1973).

This case study only concerns itself with the Windalia reservoir on BWI. In 2016, the Windalia reservoir accounted for the majority of oil production on BWI. The remainder is produced from pools in the Gearle, M3, Mardie B, Tunney, Malouet and Jurassic intervals (Fig. 2). The Windalia was originally drilled at an 80-acre production well spacing, however over time some areas have been infill drilled to as low as 40/20-acre well spacing with producers and injectors of varying patterns. A larger review of these details will be provided later.

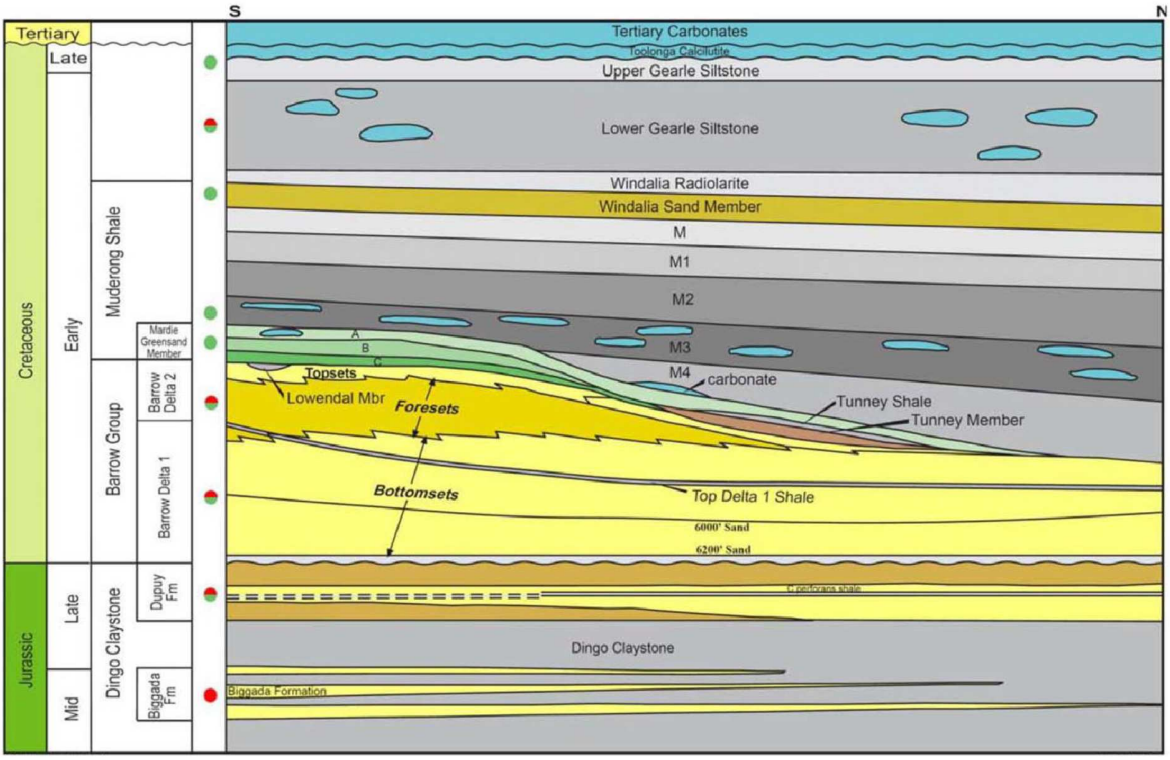

Figure 2—Barrow Island straigraphy (Ellis et al 1999). The Windalia sand averages 110ft net interval, starting at approximately 2,200ft TVDSS.

The naming of wells and grid reference relates to the early 40 acre well spacing (Campbell et al. 1984). Each block is denoted alphabetically from A – U block, though not all blocks contain wells intersecting the Windalia reservoir. The blocks are then further divided into an 8 x 8 grid of 40 acre well spacing. For example, the F36 well is on the third row and sixth column of the southern F-block part of the field. Infill wells are differentiated by adding a letter to the end of the well name, e.g. M36A and M36B infill wells.

Waterflooding is a key part of maintaining the deliverability for many onshore fields, particularly those with high API crude, low permeability and shallow reservoir intervals. This was the reason for introducing a waterflood to the Windalia reservoir after only two years' primary production. The long-term effect of the waterflood has been positive for both EUR and sustaining economic oil production for a long period.

Waterflood Reservoir Management

There is a large part of oilfield literature dedicated to waterflood reservoir management and the optimisation of field performance. Much of this theory has been used to guide the operation of the BWI reservoirs. One influential work is that of Terrado et al. (2007), who also spent time studying the Windalia. Their paper, which focuses on other global waterflood cases, emphasises analysis on different scales: Field, Block, Pattern and Well levels. A review of voidage replacement ratios, recovery factors, pore volumes injected, water cuts, property maps, Hall plots etc. can provide insights into which areas of a field might require further optimisation or development. These techniques have been leveraged for this field. The metrics will be discussed later.

Fundamentals to the theory, development and production forecasting of a waterflood field are described by Willhite (1986) and Craig (1971). The Reservoir Management of waterfloods, on the other hand, is best reviewed by Thakur and Satter (1998) and Satter and Thakur (1994), in addition to the article discussed earlier. These three references provide a description of the types of data acquisition and reservoir surveillance activities (PFOs, PBUs, metering) that are required for best practice waterflood operation, and

the appropriateness of classical methods vs. modern reservoir simulation. They are helpful background reading for the present paper.

Windalia Background

Reservoir Description

The Windalia is a greenish-grey sandstone of very fine grain size. The rock is Cretaceous in age and deposited in a middle to outer marine shelf environment. It is sealed by the overlying Windalia Radiolarite and Gearle Siltstones and trapped by a three-way anticline with structural fault closure in the south. Average permeability and porosity are 5.7 mD and 28% respectively (Crank 1973). Average gross thickness is 120 ft (36.6 m). The reservoir fluid is a light 36° API oil with solution GOR of 220 scf/bbl, with initially saturated reservoir pressure of 995 psia (Alexander et al. 1981; Emanuel et al. 1993). Further properties are shown in Table 1.

Table 1—Windalia reservoir properties (adapted from Emanuel et al. 1993)

Rock and Reservoir Data	
Initial reservoir temperature, °F	150
Initial reservoir pressure, psia	995
Datum depth, subsea ft	2050
Average pay thickness, ft	110
Average porosity, %	21
Initial water saturation %	45
Formation Water Data	
Specific gravity	1.07
Initial FVF, rb/stb	1.03
Viscosity, cP	1.00
Oil Data	
Bubblepoint pressure, psia	995
API gravity	36.0
FVF at P_b, rb/stb	1.145
Viscosity at P_b, cP	0.65
Gas Data	
Solution gas gravity	0.815
Solution GOR, scf/stb	221
B_g at P_b, rb/Mscf	2.77

The current petrophysical interpretation of the Windalia stratigraphy separates the rock into 9 distinct layers (Fig. 3). Broadly, the Windalia can be considered in two separate groups, the lower (8–9) and upper layers (1–6), separated by the middle shale (layer 7). The lower layers consist of lower quality mudstone and sandy mudstone facies. The middle shale is a laterally extensive layer of sub-mD rock that acts as a baffle between the upper and lower Windalia (Moo and Tweedy 1991). The upper Windalia is a mixture of higher reservoir quality rock: layers 4–6 are the coarsest layers, consisting of sandstone and small amounts of sandy mudstone, and layers 1–3 are a mixture of sandy mudstone and muddy sandstone. Some parts

of the field also contain carbonate concretions or fractures with carbonate-filled cement. These areas have been targeted for acid stimulation treatments in the past.

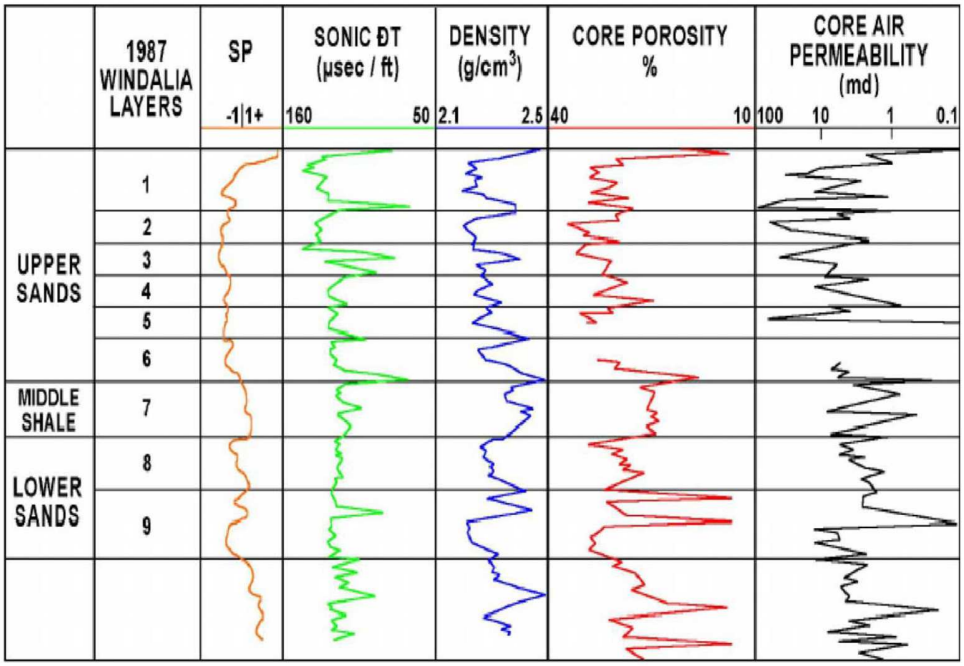

Figure 3—Representative layering and facies types for Windalia reservoir, G52 well (after Schlumberger 1967)

A core photograph of the lithologies is shown in Fig. 4.

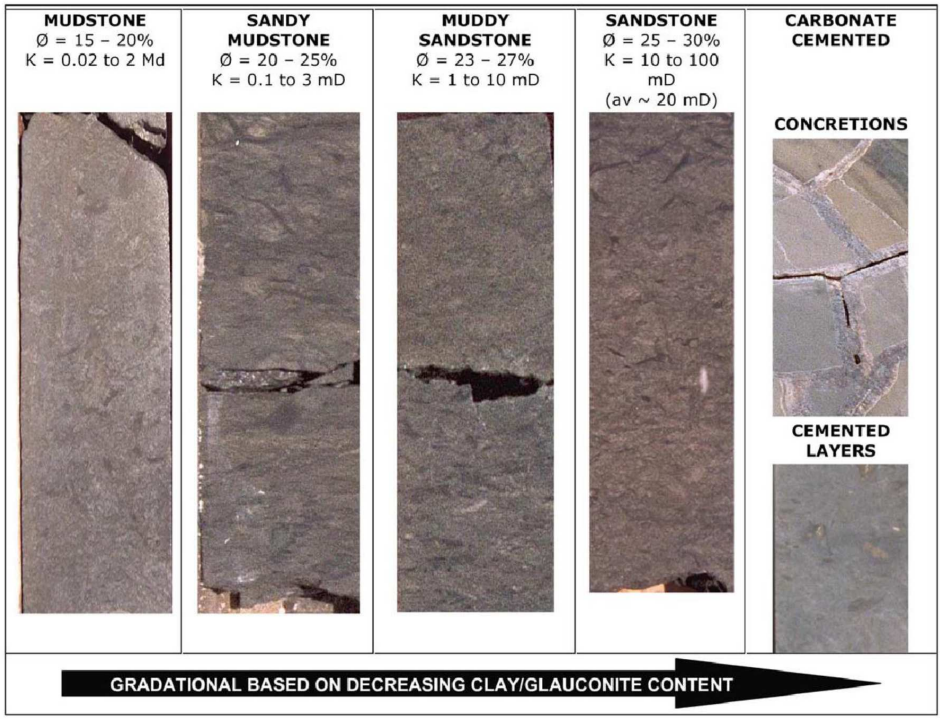

Figure 4—Representative core sections of Windalia sand member lithologies

Windalia original oil in place (OOIP) estimates are between 750 MMBBL – 1 BBBL (Emanuel et al. 1993; Fraser and Bruce 1998). The field was originally at bubble point pressure prior to development, and contained a gas cap in the northern area. The location of the gas cap was likely due to compartmentalisation since it was downdip in the structure. This high GOR area was spared from the initial development but heavily infill drilled in later years.

History of Development and Operations

1965 – 1990. Production from the Windalia reservoir began in June 1965 with the F36 production well (Barrow No. 4), which is still online under production today. Over the next three years, an 80-acre spaced primary development was drilled across the field with oil development wells. Almost all of the production wells in the field have been developed with some form of near wellbore stimulation. This was required to ensure deliverability from the low to moderate permeability sands.

During the initial field development, the gas cap area in Q-block was avoided. Wells initially drilled in this northern area had high GORs and the area was seen as less favourable, also due to a degradation of reservoir properties away from the crest of the field and lower oil saturation. It was only developed in later years.

The production network on BWI was split into several satellite separator stations, with flowlines from each producer meeting at common station manifolds. Currently, eight separator stations are in operation across the island. Combined fluid streams are pumped to a Central Processing Facility where oil is separated and sent to storage tanks. This oil is loaded onto tanker ships periodically.

After initial decline rates of up to 40% per annum in the first three years, secondary recovery was considered. The original pilot waterflood was proposed in the south west of the field (A, G, B and H blocks) under the consultation of H Dykstra. Core and fluid analyses indicated a favourable endpoint mobility ratio of 0.6. After several analytical studies (Dykstra 1968a-c) and the poor primary depletion performance, a waterflood pilot was proposed.

Pilot injection commenced in October 1967 and showed promising uplift in neighbouring production wells. As shown in Fig. 5a, the original south-western water injection wells were infill drilled in a well spacing of 40-acre using the 5 spot pattern. Commencing in 1969, the central part of the field was drilled at a 40 acre well spacing using the inverted 9 spot injection pattern. Soon after 1970, the Q-block gas cap area was drilled with producers and injectors at 40 acre well spacing with the 5 spot water injection pattern. Source water for the waterflood was obtained from dedicated wells producing under gas lift from the deeper Flacourt aquifer (Fig. 2). These water source wells were spaced evenly around the island at 8 separate stations, connected to injection wells with Carbon Steel flowlines. Injection wells were not completed specifically with stimulation but have been designed to inject water at high enough THP to achieve injectivity.

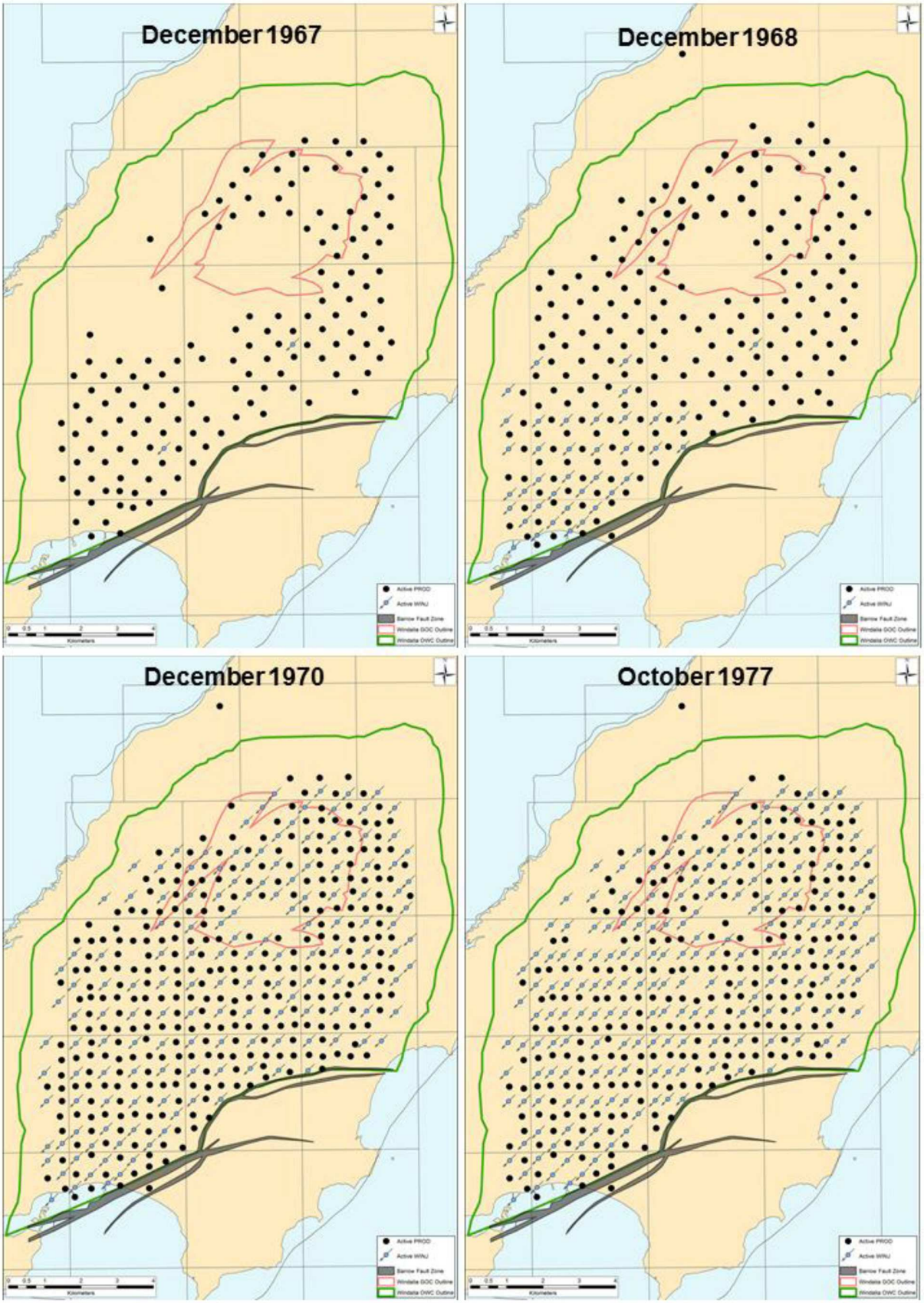

Figure 5a—Windalia Production and Injection well development over time

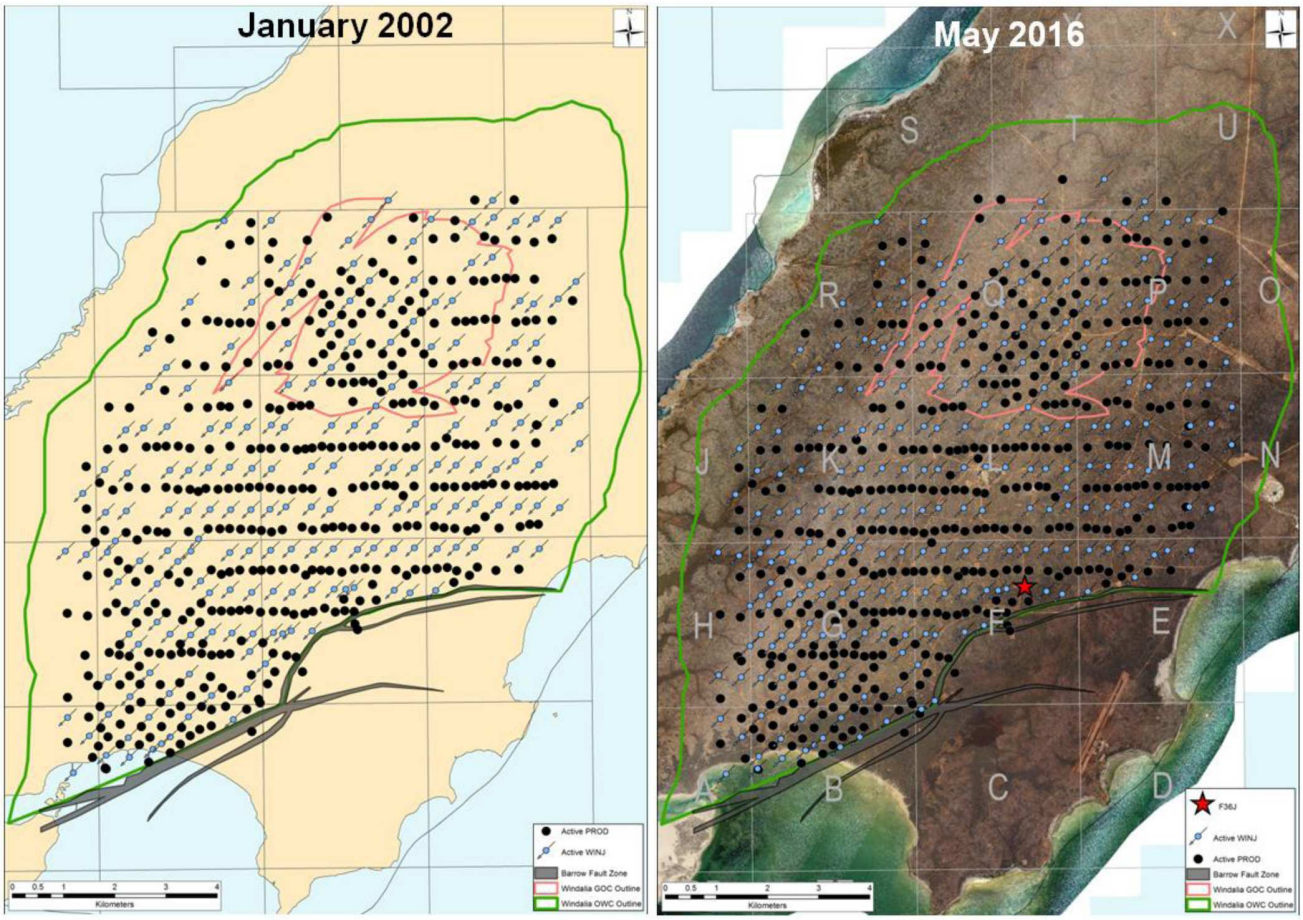

Figure 5b—Windalia Production and Injection well development – The Windalia discovery well (F36) is marked with a red star on the 2016 map.

Post-1972, rapid production well water breakthrough began at high water cuts, particularly in the K-block wells. An investigation found that the injection patterns used were not ideal for the Windalia; it was discovered that the producer-injector orientation was initially perpendicular to the minimum horizontal stress direction. Stress maps available in the work of Hillis et al. (2000) show that the direction of minimum stress surrounding BWI is consistently north-south. It is best that producer-injector alignment is in the direction of minimum horizontal stress to avoid water channeling inside the reservoir through pre-existing natural fractures. This resulted in a re-alignment to the direct line drive pattern, where producer-injectors were orientated from north to south (Williams 1977).

Pattern re-alignment of the field occurred throughout the mid to late 1970s, with mostly producer-injector conversions and some infill drilling. The excessive water cut subsided and oil rates stabilised. The Q-block and south-western block areas were not converted to line drive and still remain as various spot patterns. Today, injection rates in these parts of the fields are managed carefully to avoid problems with water cut.

Artificial lift was installed in production wells during the 1970s. During the early period, gas lift was predominant with some beam pump installations also on the island (Watson 1970). Today, gas lift has been completely decommissioned and production relies only on beam pumped wells (Fig. 6). Our experience has been that production rates and reliability with beam pumps are much higher than gas lift for this onshore, high water cut operation. Gas lift decommissioning was also a result of a mature infrastructure and the costs associated with its refurbishment. Beam pumps were originally powered by gas engines and online 24 hours per day. Dynamometer cards were taken manually by operators periodically by visiting wellsites and pumping speed was matched to inflow as much as possible.

Figure 6—Photograph of B41B and B41C beam pump units, producing from the Windalia formation

From the mid-70s to mid-80s, over 125 infill wells were drilled in the Q, G and B block areas, most of which were producers. This is seen in the producer count in Fig. 7, along with production performance for the field. The well spacing was reduced in these blocks to 20 acres. Since water injection did not change substantially in the period, the oil decline continued over the decade.

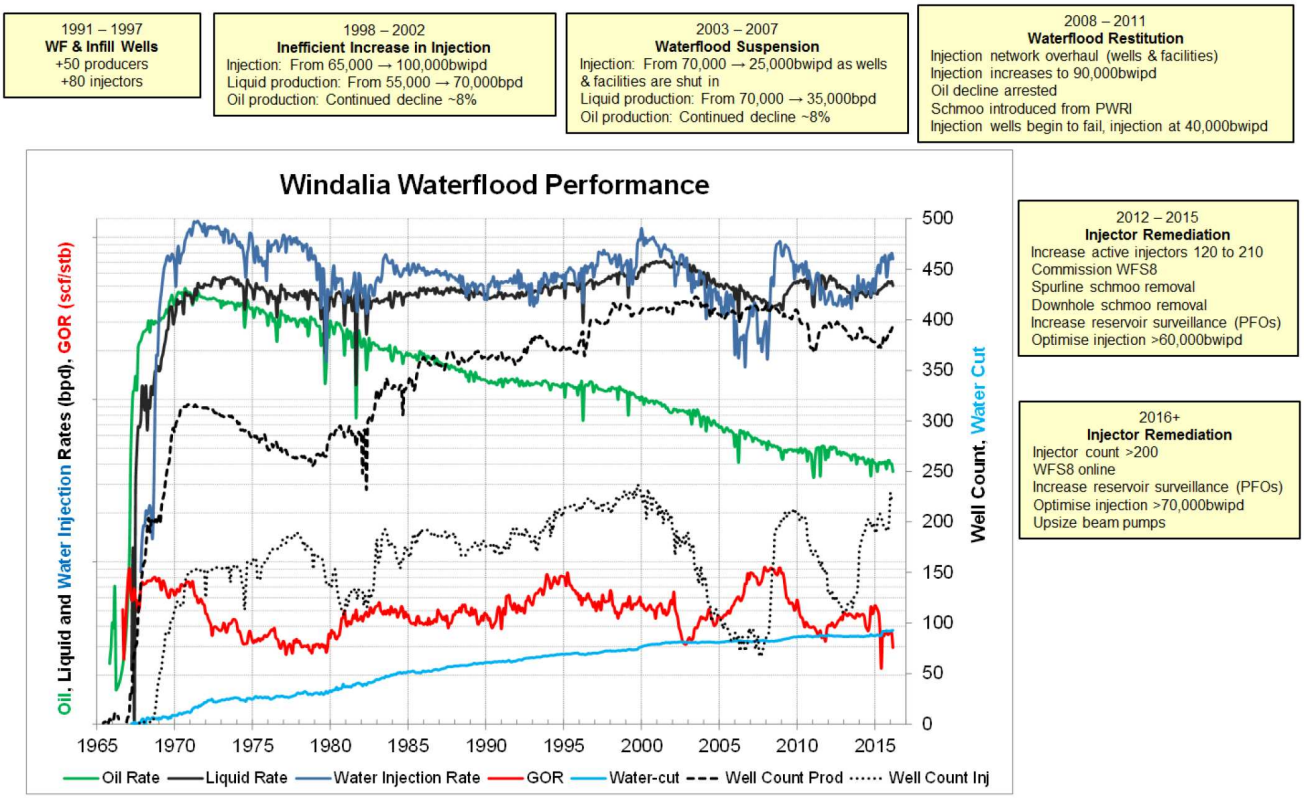

Figure 7—Chart depicting rate performance of the Windalia reservoir. Chart scales removed for confidentiality purposes.

Numerous well re-stimulation campaigns also occurred, starting in the 1980s. Several technology improvements allowed for higher quality stimulation treatments with improved well productivity for existing wells.

1990s. From 1991 – 1997, another large infill drilling campaign occurred with 50 producers and 80 injectors added to the field across most areas. The resulting patterns across the field vary now because of these infill periods (Fig. 5, 2002). This resulted in a plateau in oil rate through most of the 1990s (Fig. 7).

In the mid-1990s, Pump Off Controllers (POCs) were installed on the majority of beam pumps in the field. Electric motors were used with power supplied from the central power station, with fuel from associated gas. This reduced pump failures significantly as the pumps would stop running before fluid pounding issues occurred in the downhole pump. Some gas engine pumps remained on beam pumps in isolated parts of the field where it was impractical to run power lines. The target for the Barrow Island POCs is to operate wells for 80% of the day and run 20–30 cycles. It is best to have beam pumps sized to pump wells off with an extra 20% spare capacity to allow for additional recovery after field shutdowns (as per recommendations of Neely and Tolbert 1988). It is likely that POCs also helped the field oil rate stabilise.

2000 – 2008. Prior to 2000, oil production begun to decline at 8% per annum. In the year 2000, water injection increased to almost 100,000 bwipd in an effort to cease this. This water injection was not balanced as well as current injection is field-wide, as the surface network configuration was different to the current day. The balance of pressures was not favourable across injection wells. Furthermore, it seems that the production network was not managed in such a way that the lifting requirements of each beam pump matched the injection of neighbouring wells. Many wells reached 24 hour run time and the producer fluid levels built up over the period. This was an example of injection that was not properly managed. G block suffered the most during this period with at least 20 undersized beam pumps, which was unfortunate since this is the most prolific area of the field. The voidage replacement in this block was excessive (approaching 2.0) and production wells were not sized adequately to yield the benefits. Oil production for the reservoir continued to decline at 8% per annum.

During the mid 2000s, nine PCP pumps were also installed in the field with some success. The vast majority of production wells remained on beam pump, and a few high rate, high GOR wells were selected for a pilot on PC pump. These remain in operation today.

A period of waterflood suspension followed in the mid-2000s. During 2003–2007, water injection rates declined significantly as the Carbon Steel injection network aged and was progressively decommissioned. Water injection and water source wells suffered failures and these were not repaired until later in the decade. The number of injectors online dropped below 100. In the case of the water source wells, most were suspended indefinitely due to corrosive downhole issues in casing strings. This period of low injection resulted in a poor oil decline rate of up to 8%, shown in Fig. 7.

The last 8 infill wells in the Windalia were drilled and completed in 2007.

2008 – 2011. Following the decline of the waterflood, a new "Waterflood Restitution" project was executed in 2008 to restore the injectors and surface network to service. This project was assisted by climbing oil prices during the mid-2000s. The main achievements during the project were:

- All ANSI 600 Carbon Steel flowlines were replaced by a completely new Glass Reinforced Epoxy (GRE) flowline network. The injector surface pipe network moved from satellite stations with isolated flowlines to a network connected via a 20 km ringmain pipeline. The GRE flowlines are not prone to the same corrosion problems as steel, and are more flexible for lying across terrain.
- Produced Water Filtration (PWF) was added to assist with the new strategy of Produced Water ReInjection (PWRI). Treated produced from water from the settling tanks was now available for reinjection into the waterflood network. Previously, all produced water was disposed into dedicated Flacourt disposal wells. These changes can be seen in the water source graph in Fig. 8.

- Remote monitoring was added to all injection wells – water injection rates, tubing head pressure and annulus pressure. This assisted with integrity monitoring and was also leveraged for reservoir surveillance activities, which will be discussed later.

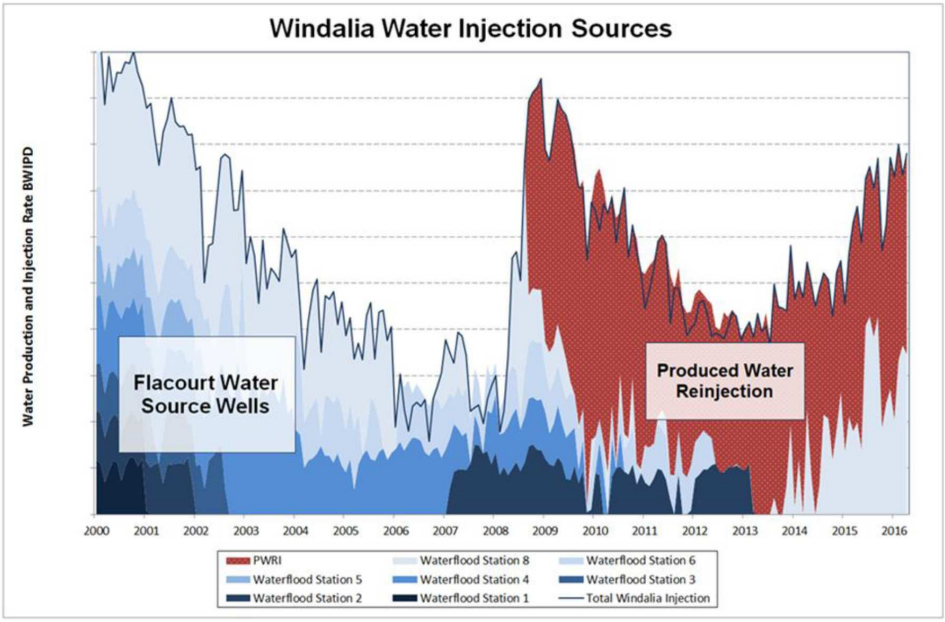

Figure 8—Waterflood injection rates and source water summary. Chart scales removed for confidentiality purposes.

The rejuvenation of the waterflood network during this period was very effective and injection rates climbed to above 90,000 bwipd (Fig. 7). Oil production decline was momentarily arrested and actually experienced a slight increase towards the end of 2011. The producing GOR reduced significantly as reservoir pressure increased.

Unfortunately the water injection began to decline, largely due to problems caused by Oil In Water (OIW) and suspended solids in the PWRI water. Some flowlines had been reduced in cross section by a thick material called "schmoo"; this term is used to describe the thick, organic and inorganic material that is a combination of oil, corrosion inhibitor, produced fines and some cases scale. Again, the injector count dropped to almost 100 as injectors also suffered downhole corrosion problems related to the schmoo. The formation of this material on tubular walls is known to reduce the effectiveness of corrosion inhibition and hence increase the risk of corrosive failures in wellbores.

For many years, EOR has been considered for the Windalia reservoir. Screening studies ruled out most forms of tertiary recovery for the reservoir due to the gravity of the oil, low permeability, shallow reservoir depth and lack of supply for injection gas (Taber et al. 1997; Haynes et al. 2013). However, there were indications that a novel chemical flood could show promise (Widjanarko et al. 2010). The proposal involved dosing a polymer at injection wells to in a similar fashion to well stimulation, extending sweep and recovering oil that was bypassed by the current flood streamlines (Fletcher and Morrison 2008). A small pilot of 3 injector wells was initiated in 2009. It is estimated that oil production increased by almost 40% in the pilot area (Leon et al. 2011; Haynes et al. 2013). In the current economic climate, expanding the EOR project poses a challenge.

2012 – 2015. Recognising the challenges that schmoo had caused, the asset underwent an intensive period of injector remediation and network cleanout from 2012 onwards. An additional workover rig was introduced onto BWI in 2013 that helped restore the injector count to above 200 wells online. Problematic GRE spurlines were manually cleaned to clear out deposits from flowlines and increase delivery pressures

to the injection wells. New chemicals have also been introduced to dissolve OIW at the central processing facility.

In 2013, two new water source wells (WSW8B and WSW8C) were drilled to assist with the future waterflood water supply on BWI from a clean, abundant source. The wells were completed with 13-Cr production casing and liner; this ensures a much longer life for these wells as compared to previous water source wells on the island. Corrosion failures were common in the past. Each well currently produces 25,000 bwipd under ESP (Electrical Submersible Pump) artificial lift. These wells have also contributed to the current rejuvenation of the waterflood.

At the end of 2015, injection returned to above 80,000bwipd, with a field instantaneous VRR of 1.3–1.4. Liquids production has increased significantly and oil production decline has been arrested. With the learnings from prior periods, the BWI asset is now better prepared to maintain water injection for a sustained period.

Current Waterflood Strategy 2016+. The current asset strategy, to be outlined further in following sections, is to maximise both injected and produced liquids within facility constraints. It is understood that increases to oil production will follow from this strategy. In the sections following we will discuss the current strategy on BWI for waterflood management. Given the reduction in oil prices since 2014, the asset has focused largely on base business activities relating to existing wells (Goff et al. 2016). This has meant that the team has been focused on optimising production and injection from existing wells.

Discussion on Stratification – Analogous Fields

The stratified nature of the Windalia has been discussed extensively in other articles. The Upper and Lower Windalia have been swept very differently; we expect current reservoir pressure and water saturation are much higher in the higher reservoir quality Upper Windalia. This is despite the majority of wells being perforated across both layers. There are several studies that provide evidence for this:

- Production logging during the 1990s showed low liquids contribution from Lower Windalia
- Injection logging during the 1990s showed low injectivity into the Lower Windalia
- Openhole logs of infill production wells drilled in the 1990s vs. Original wells in the 1960s showed reduced oil saturation in the Upper Windalia but near original saturation in the lower zone
- Wells selectively completed into the bottom zone (e.g. M36B) were depleted further than wells completed in both the Upper and Lower Windalia. The lower zone had a lower reservoir pressure and was not swept as effectively by the waterflood.

These findings led to several conformance control and targeted zonal well projects, with limited success. In the current day, the layered behavior is mostly relevant in how it provides hints for how injection and production in the field should be managed.

When searching for operational analogues recently, we were not only concerned with reservoir properties but also the type of waterflood operation. For many decades Operators have used conformance control techniques to improve the vertical displacement efficiency of stratified waterflood reservoirs, however we found on BWI from a pilot study that polymer gels were ineffective in reducing water cycling, with only small improvements seen in offset producers. It is known that conformance control is often more difficult for wells injecting above the water gradient (Thakur and Satter 1998), which is the case for the Windalia reservoir. Yet the first course of treatment for vertical stratification problems is normally conformance control or selective completion. Since it has not been practical to apply this treatment across BWI wells, stratified analogues were sought that did not have the luxury of applying this treatment. They are very helpful when guiding the current strategy.

Many onshore waterflood operations in the United States experienced trouble when displacing multiple layers (Parrish and Meadows 1965). In the East Burbank pool (Warner 1968), the operator recognised it was vital that "tremendous" volumes of water must be injected and produced in order to recover oil from all layers in the stratified reservoirs. The utility of high injection rate and high pressure-drops during the displacement was "indisputable" under their stratified condition. The problem is also described by Brown (1989). Thakur (2009) also gives a description of the problem of injection without conformance control.

The best physical explanation and technique for handling the problem without conformance control is given by Ghauri et al. (1974) for the West Texas Denver Unit Project. At high producing bottomhole pressures, some of the high oil-saturation, low reservoir pressure layers would be blocked out of production. It was essential for their operation that beam pumps were properly pumped off to minimise bottomhole pressure and allow flow of all strata (see Fig. 9). Jenkins and Eggert (2002) also describe the same strategy. Terrado et al. (2007) confirm the importance of pumping wells off, which they say reduces the chance of crossflow between different layers. These fields are very similar operationally to what we seek on BWI to maximise oil rate.

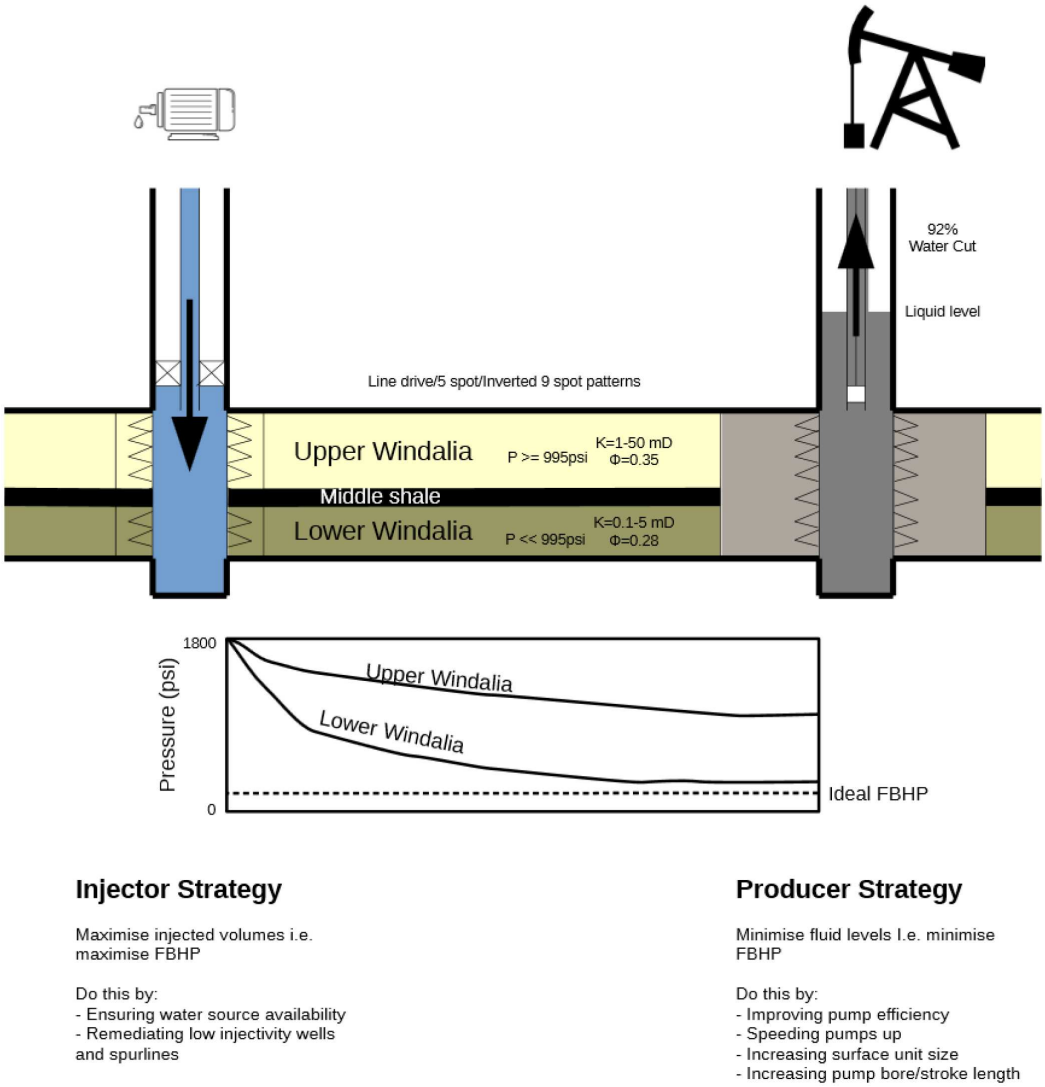

Figure 9—Water injection and liquid production strategies for the Windalia reservoir

There are also several operational implications that stratification has that will be discussed in the "Water Cycling" section.

Windalia Waterflood Reservoir Management

Reservoir Surveillance

Reservoir surveillance has been a highly important activity for the management of the Windalia waterflood. Due to various constraints, most monitoring was done on the water injection wells. It can often be difficult to justify shutting production wells for pressure buildup analysis, and since the 2014 reduction in oil price it has been increasingly difficult to justify losses in oil production. Furthermore, for reasons we will discuss in following sections (water cycling), we have seen that oil losses during shut-in periods are often not recovered as initial production when wells are returned online due to the constraints of beam pumping rates and transient water production from the reservoir. For this reason, reservoir surveillance has focused on the surveillance of water injectors. When an injector is closed for PFO survey, water is normally redistributed around the network and no net loss is incurred.

The use of wellhead gauges for pressure transient interpretation has been verified as a viable technique in the literature, especially for single-phase fluids where measurements are not distorted by phase separation (Kabir et al. 2015; Spyrou et al. 2013; Burnett et al. 1965). In fact, since water is almost incompressible, correction to reservoir datum depth was achieved using a fixed water gradient of 0.433 psi/ft. This methodology was also validated by comparing the results against a campaign of slickline retrievable downhole pressure gauges on BWI in 2014. After validation was complete, the asset relied on surface gauges only for the water injectors. The only time we have experienced gas migration to the top of a wellbore in an injection well was for a well that had been shut in for over 10 years, in a high GOR area of the field. It seems that gas percolation, even in low reservoir pressure areas, takes a substantial period of time to reach the wellbore. In some cases it was also verified that the entire wellbore fluid column was water by bleeding off a small volume of water at the top of the tubing. In all cases examined, water was the only wellbore fluid present.

The Miller-Dyes-Hutchinson (MDH) method (Miller et al. 1950) of shut-in analysis was used, where pressure is plotted versus the logarithm of shut-in time, $\log(\Delta t)$ (Lee et al. 2003), which neglects time-dependent effects of injection prior to shut-in (c.f. Horner plots with t_p inclusion). This is appropriate since the Windalia water injection wells are constantly in operation (long t_p) and have normally reached a stabilised condition. As is commonly done for watered-out reservoirs (Abacioglu 1997), single phase well testing theory has been applied to interpret the data. The method was used in 2014–2015 on over 100 injection wells to characterise reservoir pressure, permeability-thickness and wellbore skin around the field. The overall workflow is shown in Fig. 10. Some example charts of PFO analysis are shown in Fig. 11, and a map of results is shown in Fig 12. With formation properties determined, reservoir pressure was calculated for a circular reservoir of constant-pressure at radius r_e (Dake 2001). The straight-line falloff is extrapolated to $\Delta t_s = \frac{1686.6\varphi\mu c_t r_e^2}{k}$, for pressure at r_e.

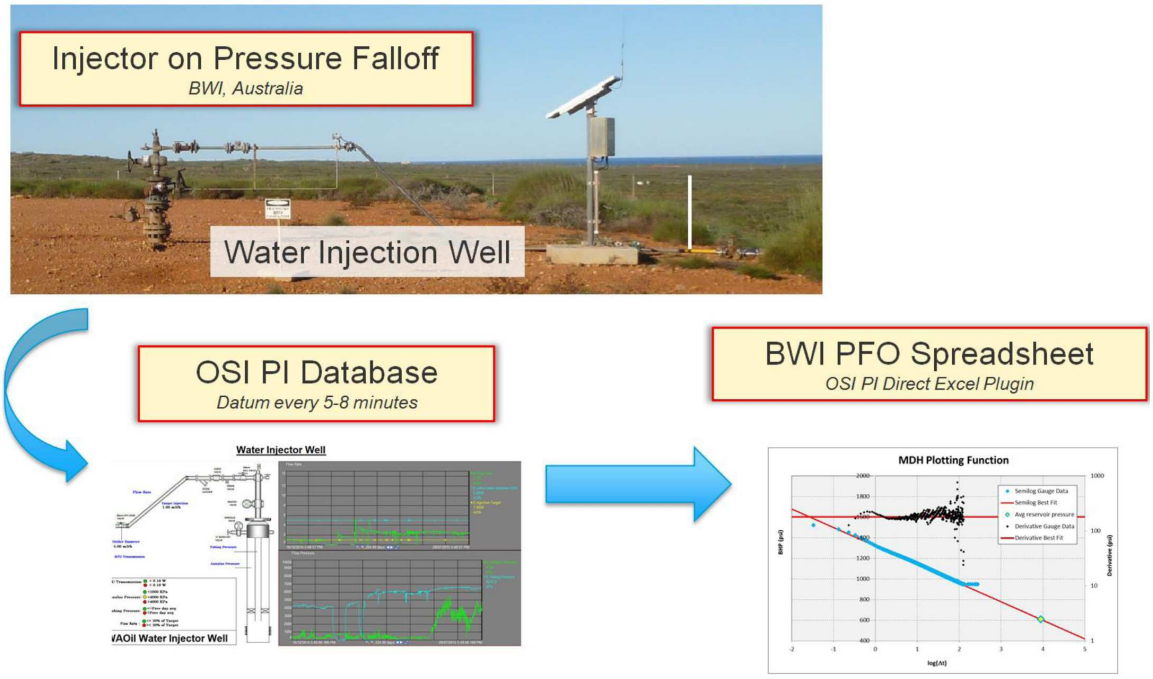

Figure 10—Waterflood injector surveillance process for the Windalia

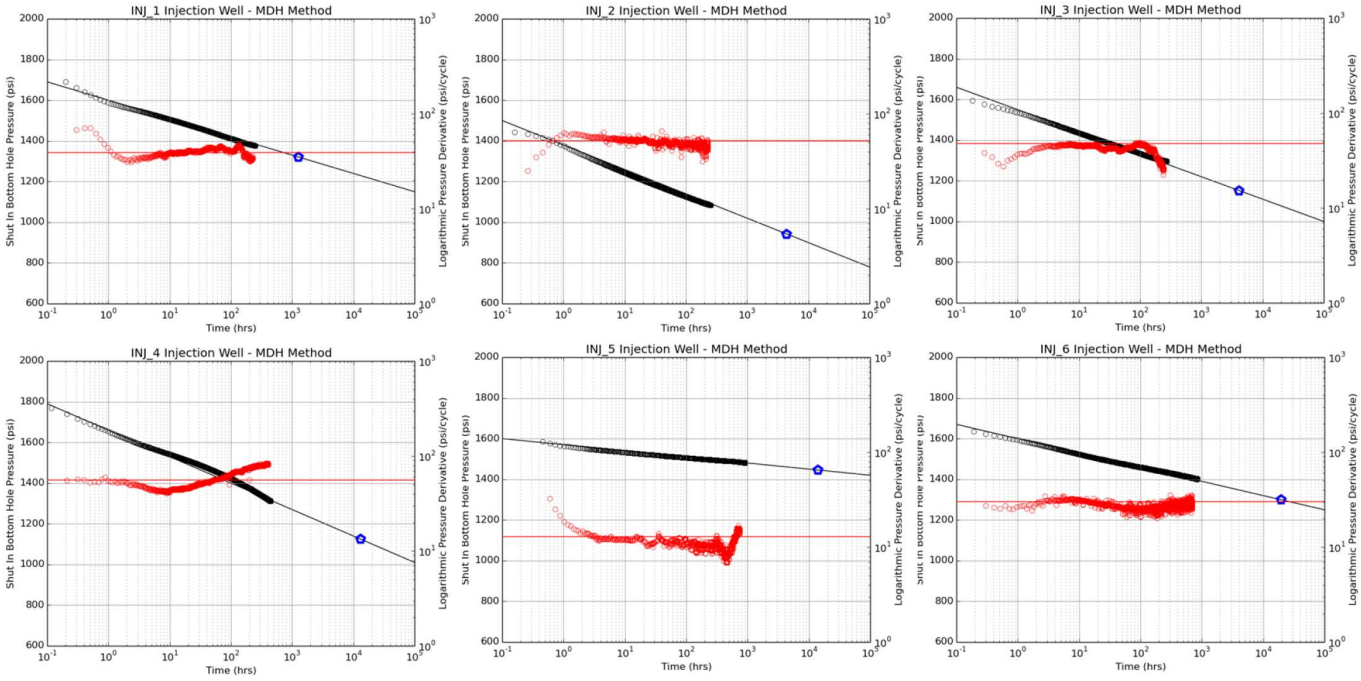

Figure 11a—Pressure fall off surveillance – Infinite Acting Radial Flow cases. The red data correspond to the pressure derivative. The blue marker in each graph corresponds to the reservoir pressure calculated from the falloff.

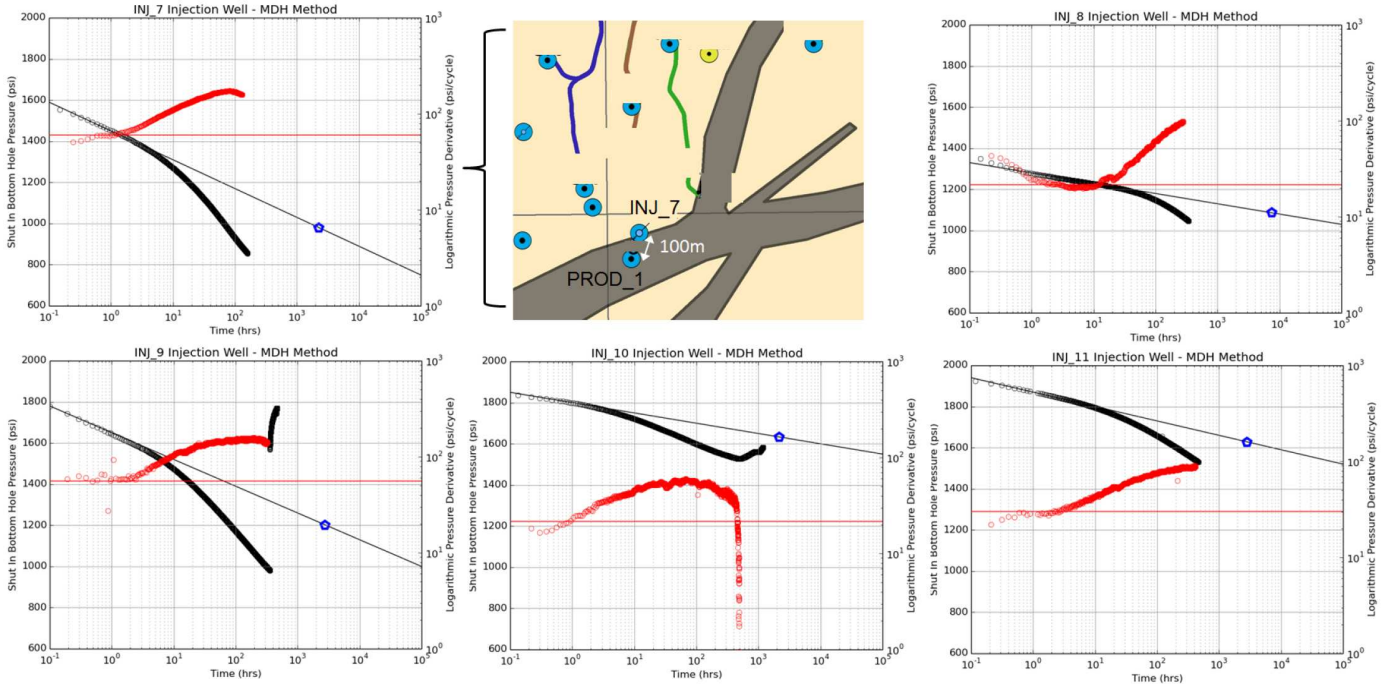

Figure 11b—Pressure fall off surveillance – Wells exhibiting interference effects. These surveys are amenable to transient interference analysis. The red data correspond to the pressure derivative. The blue marker in each graph corresponds to the reservoir pressure calculated from the falloff.

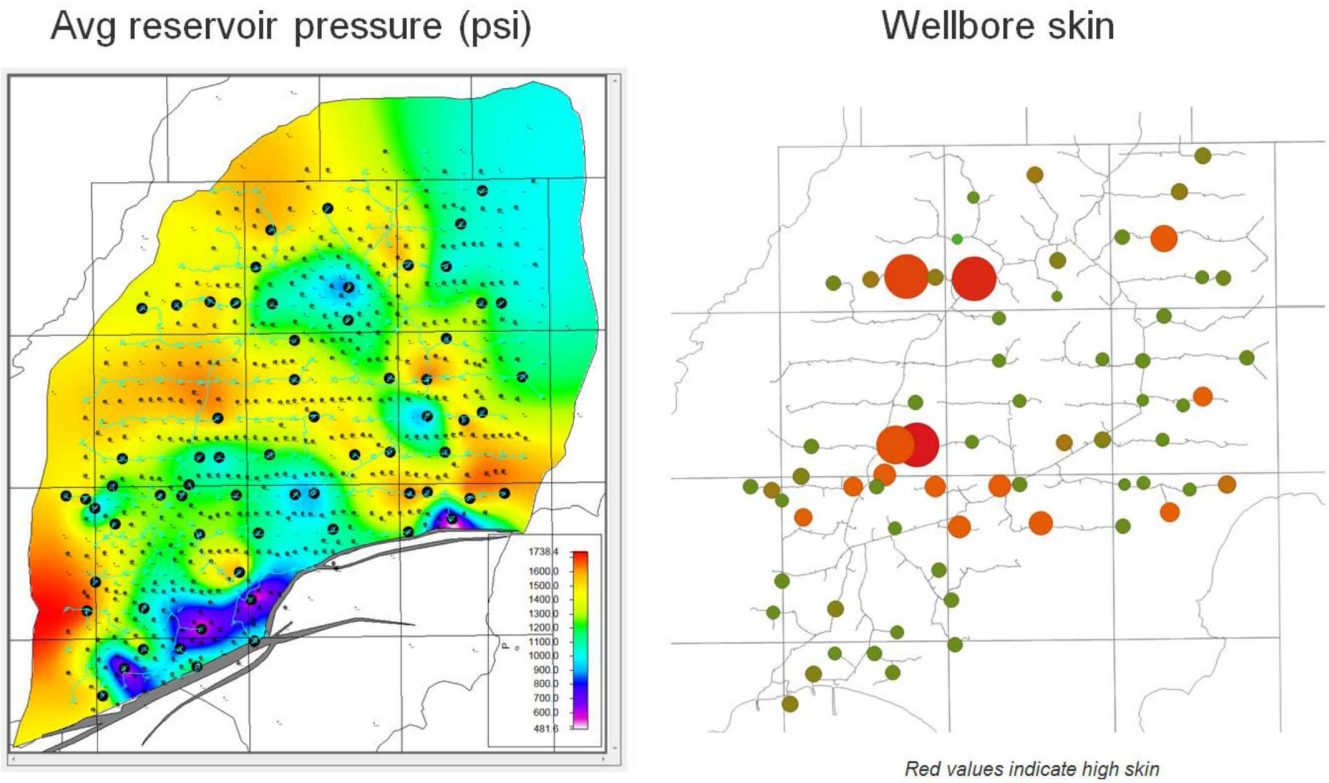

Figure 12—Maps depicting the results of PFO surveys from 2014–2015. The blue/ purple regions on the pressure map correspond to low pressure areas in the field.

Perhaps most importantly, the extrapolations for average reservoir pressure led to a large target for injected water (and hence high VRR) into low pressure areas of the field. Understanding that the reservoir

pressure was depleted allowed for large VRRs, when high values may otherwise cause concerns due to risks or water cycling at production wells. These parts of the reservoir were experiencing fillup. Another important use of PFOs was for the identification of permeability-thickness and wellbore skin damage. Some of the wells experienced injectivity problems and were assigned to slickline cleanout programs.

There is also one alternative method that is considered novel when quantifying the productivity of beam pumped wells when considering rate transients only; this is discussed by O'Reilly (2016a). We have had moderate success applying the technique to some of our cyclic beam pumped wells.

Injection Well Management

Injection Target Rate Setting. Currently the field injection target is derived from the capacity of BWI facilities (source water, produced water available for injection and total production capacity). On an individual injection well basis, this also means that injection rates must be managed to not exceed *maximum* beam pump withdrawal plus a small margin (target VRR=1.1–1.2), which may lead to building excessive fluid levels in the production wells (c.f. early 2000s in G block). The exception here is for areas of the reservoir that are still experiencing periods of fill up. It is also preferred that beam pumps are upsized as much as possible to avoid restriction of the injection targets. Currently the field is injecting at a VRR of 1.3–1.4, since parts of the reservoir are still filling up. When the maximum lifting capacity of the beam pumps is encountered, the target will be lower at 1.1–1.2.

At the current stage of increased water injection, most injectors are unchoked and not constrained by an upper target; however, a handful of wells are constrained in areas of the field where several injectors are online or beam pump units are smaller and cannot lift large rates. Care is taken (Fig. 13) to monitor the voidage replacement in each injector pattern and block, and as a result some injectors are choked for this purpose. Projects are underway to increase beam pump sizes in some of these areas.

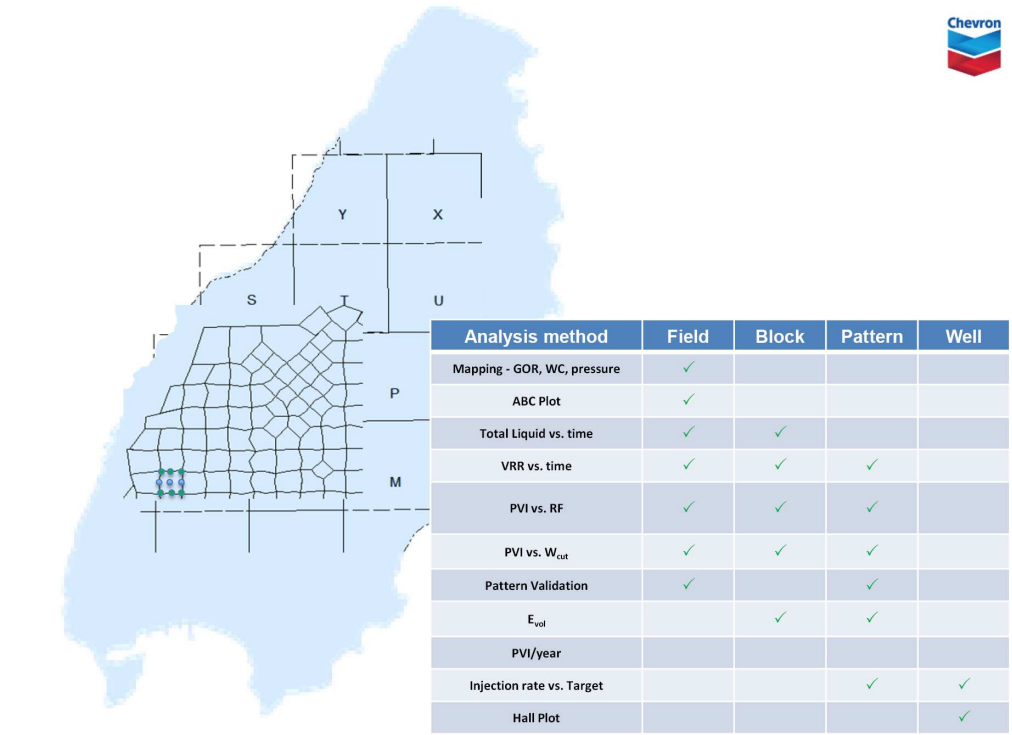

Figure 13—Windalia waterflood reservoir monitoring parameters as per Terrado et al. (2007)

Under periods of lower water supply, the CRM was used to guide individual injector targets to best optimise oil rate. This is consistent with recommendations from Terrado et al. (2007), where choking back injectors can largely be appropriate under the conditions of scarce waterflood water availability.

Liaison Between Office and Operations. A close relationship is held between the Perth subsurface team and BWI Waterflood Operations staff. During weekly correspondence, we discuss the following areas for any injectors of concern:

1. Injection rate not exceeding target or orifice plate meter upper limit
2. Annulus pressures monitored for a tubing/annulus pressure match, indicating failed packer or tubing
3. Wells are queued for PFO survey to measure reservoir pressure, kh and skin
4. Possible telemetry issues at the RTU (Remote Telemetry Unit) - e.g. gauge or battery problems

Monitoring these items allows the waterflood to be run in a seamless manner. Monthly meetings are also held between office and Field Operations to discuss broader field performance and project matters. An example waterflood performance chart is shown in Fig. 14. In addition to this, quarterly trips are made to the field where engineers inspect well leases and perform adjustments on individual injection rates for all wells.

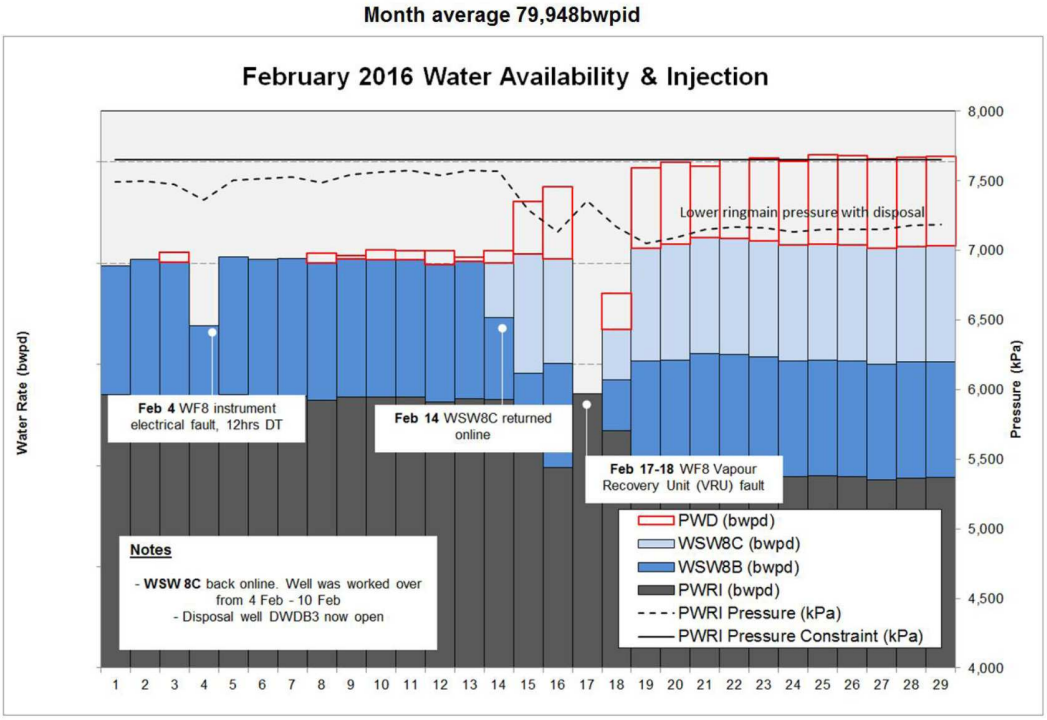

Figure 14—Monthly dashboard (February 2016) for the Windalia Waterflood

Production Well Management

Liaison Between Office and Operations. Weekly meetings are also held between Perth office staff and BWI Production Operations to review production wells at each separator station. These meetings were an initiative introduced into the asset in 2015. On BWI, each production well is tested through a dedicated 3-phase test separator on a 60 day cycle. Furthermore, annulus fluid levels are also regularly shot on wells that are 24 hours run time to ensure the proper optimisation of each well. During the weekly meeting, some of the key items discussed are:

- Review of production wells with recent deviations in well test

- Identify beam pumps requiring increased fluid capacity – e.g. 24hr RT wells with a fluid level above pump. Possible actions include:
  - Larger pump bore size
  - Larger surface unit (permitting larger stroke length)
  - Speeding up current strokes per minute (SPM)
  - Workovers for pumps operating at low production efficiency
- Adjustments to POC off-time (time spent idle during a production cycle)
- Identify possible stimulation candidates (O'Reilly et al. 2016a)

One of the most important outcomes of this meeting is the assurance that fluid levels are maintained as close to the pump intake as possible (Fig. 9). This ensures that all waterflood benefits are captured at the production system by minimising the flowing bottomhole pressure (FBHP), in accordance with the Muskat (1949) relationship between steady state injected and produced liquids in a line drive system:

$$i = \frac{0.003541kh\Delta p}{\mu\left[\ln\left(\frac{a}{r_w}\right)+1.571\frac{d}{a}-1.838\right]} \quad (1)$$

where Δp denotes the difference between injector and producer BHP (oilfield units). This relationship confirms that higher pressure drops across the reservoir will result in higher production rates (in the steady state system, injected rate [i] = produced rate [q]).

Water Cycling. The water cycling phenomenon requires a combined understanding of production and injection management and deserves specific attention. It is difficult to find an exact definition of 'water cycling' in the literature; for our purposes, we define it as an unfavourable relationship between an injector and producer that causes an uncharacteristically high water cut at the production well. Water is recycled from injection wells to production wells. Some engineers have defined the issue more broadly as production wells that are withdrawing excessive quantities of liquid, but the main concern should relate specifically to the high water cut. We have seen water cycling in waterflood patterns both in the short and long term. Internally, there were numerous theories as to why the Windalia reservoir experienced water cycling. Obviously, some areas of the field are simply swept more than others, resulting in generally higher water cuts. However, there are some other operational and time-dependent aspects that must also be considered.

One proposal within the team was that injection wells of particularly high rates led to streamlines bypassing areas of reservoir pay (a rate-dependency). The theory was certainly a possibility but it was disproven as a current cause by available pressure fall off surveys at the injection wells. The negative pseudo-skin was not changing significantly over the periods studied during 2014–2016, which indicated no substantial changes to the near-wellbore geometry and the injector streamlines. However, several parts of the field still had concerning areas of rapidly increasing water cut at producers in recent times, which seemed uncharacteristic.

Another obvious explanation for water cycling is *areally* heterogeneous reservoir properties. In parts of a field, lenses of high quality rock can channel water away from other producers and lead to early breakthrough and high water cut at some producers. This was seen in parts of the Windalia (K-block) during the field's history, and related to high permeability carbonate anomalies in the reservoir (O'Reilly et al. 2016b). Several wells in this block actually maintained natural flow capacity at high water cut up until early 2014. However, these carbonates are an irregular occurrence and do not explain all of the recent field performance we have seen.

Water cycling in the Windalia is also referenced in several other papers (Fletcher and Morrison 2008; Widjanarko et al. 2010), without specific mention of the physical mechanism. In 1991, Moo and Tweedy discussed the unswept portion of the Lower Windalia and planning target production wells in undepleted areas of the lower zone. Furthermore, during the early 1990s production and injection logging surveys also confirmed uneven injection into the two layers. It is these results that may explain water cycling.

The most feasible explanation of recent changes in water cycling relates to the stratified nature of the Windalia reservoir rock. The same problem was described by Ghauri et al. (1974) in the West Texas Denver Unit. As discussed earlier, the Windalia is separated into two producing layers: the Upper and Lower Windalia separated by the Middle Shale. Within these layers, there is also a reasonable degree of heterogeneity, resulting in high intra-layer Dykstra-Parsons coefficients (V=0.9). This results in two stratification problems at different scales. We believe that the majority of recent water cycling problems in the Windalia relate to uneven contribution from the layering, based on different reservoir pressures and properties of each layer and strata within. Water cycling becomes most problematic at high injection rates when production wells are loading with fluids in the annulus (Fig. 9); the high FBHP at the producer tends to block out the depleted Lower Windalia. This has been seen in several wells where the injector and producer are closely spaced (<100 m). Closely spaced wells necessitate careful injector and producer Reservoir Management.

The concept of water cycling has been described in other works by some related terms: thief zones, water channeling, conformance issues, early breakthrough, lenticular/layered/stratified reservoirs, heterogeneous waterfloods, and can to some extent be predicted using the classical reservoir engineering methods of Dykstra Parsons or Stiles.

There is an important operational aspect to water cycling. It is a problem that can be pervasive at high water injection rates and constrained liquid withdrawal at production wells (e.g. with beam pumps at set capacities). In a vertically homogeneous reservoir there should be no concern, but seldom does such a situation exist, and the Windalia seems to depart from ideal behavior. As a result there has been a focus on increasing the size of beam pumps on the island, particularly in the high productivity areas, to draw the liquid levels down and reduce FBHP at production wells.

Operations Philosophy. One final remark will be made about the production well operations philosophy. During recent 2015–2016 production shut-ins, transient periods of excessive water cut were noted after producers were returned to service. This was measured at the central facility and at individual test separator stations. It is suspected that this relates to the Windalia stratification and also some unloading of water from the annulus in production wells after operations resume. Ultimately, downtime must be minimised at production wells because of this, while upsets at water injection wells are more tolerable but not ideal. The phenomenon of transient water cut has become prevalent during the recent periods of high water injection on BWI. It is important to maintain a stable operating condition to reduce the amount of water produced.

Production Forecasting and Waterflood Optimisation

For reserves estimation, economic analysis and business planning, a Capicitance Resistant Model (CRM) is used to forecast oil production (Sayarpour 2009; Gan et al. 2012). There are some similarities between CRM and a decline curve approach; the relationship is shown in Fig. 15. CRM is more powerful for fast history matching and handling variable water injection rate schedules.

- Classical DCA and CRM share several similarities and a few differences
- The main advantages with CRM are:
  - Built for fast history matching and injector allocation automatically
  - Flexibility for handling changes in injection rate with forecasts

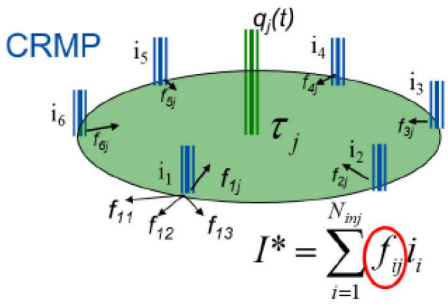

	Parameter	CRM	DCA (Waterflood)
Liquid rate	Allocation of forecasted injection water to producers	f_{ij} – matched from history	"f_{ij}" typically geometric weights
	Time delay between injected water and produced liquid	τ_j – matched from history	None
Oil rate	Oil cut method	Gentil's method (2005) **log(WOR)** vs. **log(CWI)**	A range of methods - RAC's preference for DCA is **log(WOR)** vs N_p

Figure 15—Use of CRM for production forecasting and comparison with decline curves. The graphic in this figure has been adapted from Sayarpour et al. (2009)

Regarding waterflood optimisation, CRM has been used to manage individual injection rate targets based on a constrained supply of source water available on BWI. During the 2012–2014 period of injection decline, CRM was used to allocate the scarce supply of water to the most valuable injectors. Since water availability is no longer a concern for the asset, the problem is currently less important, and individual injectors receive a supply of water up to the maximum allowable facility arrival pressure. Nonetheless, CRM remains an excellent tool for production forecasting for a large waterflood field.

Conclusion

An account has been provided for the recent history and management of Windalia secondary recovery. In summary:

- Two periods of time were compared – early 2000s and 2015 onwards. Our current strategy to Reservoir Management and operations is a large improvement over this earlier period. In spite of a slightly lower field injection rate, the oil decline has now been arrested, compared to an 8% decline during the 2000s.
- The recent use of reservoir surveillance and PFO surveys ensured that high VRR areas of injection were into areas of low reservoir pressure and being subjected to fillup rather than overinjection – Beam pumps in the area would still be sized adequately and not susceptible to water cycling
- In the short to medium term future, upsizing beam pumps to handle the high produced liquids is a focus area for the asset team.

Acknowledgements

The Barrow Island oilfield is operated by Chevron Australia Pty Ltd on behalf of the Barrow Island Joint Venture partners, which includes Chevron Australia Pty Ltd, Santos Offshore Pty Ltd and Mobil Australia Resources Company Pty Ltd. We thank Chevron Australia and the Joint Venture partners for their permission to publish this work. From BWI Operations, the authors would like to thank Ross Fenwick, Johan Henrick, Matthew Whitcombe and Richard Peverell.

Abbreviations

ABC	After Before Compare (Terrado et al. 2007)
BHP	Bottomhole Pressure
BWI	Barrow Island
BWIJV	Barrow Island Joint Venture
CRM	Capacitance Resistance Model
CWI	Cumulative Water Injected
DCA	Decline Curve Analysis
DST	Drill Stem Test
ESP	Electrical Submersible Pump
FBHP	Flowing Bottomhole Pressure
FPSO	Floating Production Storage and Offloading Unit
MDH	Miller Dyes Hutchison
OOIP	Original Oil In Place
POC	Pump Off Controller
PCP	Progressive Cavity Pump
PFO	Pressure Fall Off
PWRI	Produced Water Reinjection
RM	Reservoir Management
SIMOPS	Simultaneous Operations
SPM	Strokes Per Minute
SRP	Sucker Rod Pump
THP	Tubing Head Pressure
VRR	Voidage Replacement Ratio
WOR	Water Oil Ratio
WSW	Water Source Well

Nomenclature

a	Distance between injection wells in line drive pattern (ft)
B	Formation volume factor (rb/stb)
c_t	Total rock and fluid compressibility (1/psi)
d	Distance from producer to injector in line drive pattern (ft)
i	Injection rate (stb/d)
h	Reservoir thickness (ft)
k	Permeability (mD)
p_w	Wellbore pressure at sandface (psi)
q	Oil production rate (stb/d)
r_e	External radius of circular reservoir (ft)
s	Steady state skin factor
Δp	Pressure drop between injector FBHP and producer FBHP (psi)
Δt	Shut-in time during transient survey (hrs)
Δt_s	Shut-in time extrapolation on MDH chart for reservoir pressure evaluation (hrs)
t_p	Producing or injecting time prior to shut-in (hrs)
V	Dykstra Parsons coefficient
φ	Porosity
μ	Viscosity (cP)

References

Abacioglu, Y., Reynolds, A.C. and Oliver, D.S., 1997. Estimating heterogeneous anisotropic permeability fields from multiwell interference tests: A field example. Presented at the SPE Annual Technical Conference and Exhibition, San Antonio, Texas, 5–8 October. Society of Petroleum Engineers. SPE-38654-MS.

Alexander, R., Kagi, R.I. and Woodhouse, G.W. 1981. Geochemical correlation of Windalia oil and extracts of Winning Group (Cretaceous) potential source rocks, Barrow Subbasin, Western Australia. *AAPG Bulletin*, **65**(2): 235–250.

Allard, D.N., Hillyer, M.G. Gerbacia, W.E. and Rychener, L.M. 1999. Empirical risk assessment of infill drilling locations, Barrow Island, Australia. Presented at the SPE Annual Technical Conference and Exhibition. SPE-56816.

Behrens, R.A., Jones, R. C. and Emanuel, A.S. 1999. Implementation of a Streamline Method for Flow Simulation of Large Fields. *Journal of Canadian Petroleum Technology* **38**(13).

Brown, C.A. 1989. *Problems in Secondary-Recovery Water Flooding: Chapter 8 (Oil Field Development Techniques: Proceedings of the Daqing International Meeting)*. AAPG.

Burnett, P., Ryan, R. and Elliott, C.L. 1965. Estimating Gas-Water Contacts in Aquifer Gas Storage Fields Using Shut-In Wellhead Pressures. Presented at the SPE Gas Technology Symposium, Shreveport, LA, Nov11–12. SPE-1303.

Cameron, J.C. 1967. Australia's Oil and Gas Potential–A Review of the Main Sedimentary Basins. Presented at the 7th World Petroleum Congress.

Campbell, I. R., Tait, A. M., and Reiser, R. F. 1984. Barrow Island oilfield, revisited. *Australian Petroleum Exploration Association Journal*, **24**(1): 289–298.

Casey, J.N. and Konecki, N.C. 1967. Natural Gas–A Review of its Occurrence and Potential in Australia and Papua. Presented at the 7th World Petroleum Congress.

Clark, J., and Salsbury, B. 2003. Well Abandonment Using Highly Compressed Sodium Bentonite-An Australian Case Study. Presented at the SPE/EPA/DOE Exploration and Production Environmental Conference. SPE-80592.

Craig, F. 1971. *The Reservoir Engineering Aspects of Waterflooding*, SPE Monograph Vol **3**.

Crank, K. 1973. Geology of Barrow Island oil field. *Australian Petroleum Exploration Association Journal*, **13**(1): 49–57.

Dake, L.P. 2001. *The Practice of Reservoir Engineering (Revised)*. Elsevier.

Daniel, S. and Roberts, J. 2009. The Cliff Head Field Development—Flow Assurance and Production Chemistry in a Marginal Field Context. *SPE Projects, Facilities & Construction*, **4**(2): 19–26. SPE-115612.

Durkee, E. F. 1980. Petroleum developments in Australia in 1979. *AAPG Bulletin*, **64**(11): 1862–1879.

Dykstra, H. 1968a. *Limited Scale Water Flood, Windalia Sand*. Internal Report, WAPET, Perth, Western Australia.

Dykstra, H. 1968b. *Pilot Water Flood, Windalia Sand*. Internal Report, WAPET, Perth, Western Australia.

Dykstra, H. 1968c. *Full Scale Water Flood Predictions, Windalia Sand*. Internal Report, WAPET, Perth, Western Australia.

Ellis, G. K., Pitchford, A., and Bruce, R. H. 1999. Carnarvon Basin-Barrow Island Oil Field. *Australian Petroleum Exploration Association Journal*, **39**(1): 158–176.

Emanuel, A.S., Tang, R.W., McKay, D.M. and Ellis, M.H. 1993. A Hybrid Simulation Study of the Windalia Sand Waterflood. Presented at the SPE Annual Technical Conference and Exhibition. SPE-26477.

Fletcher, A.J. and Morrison, G.R. 2008. Developing a Chemical EOR Pilot Strategy for a Complex, Low-Permeability Water Flood. Presented at the SPE Symposium on Improved Oil Recovery. SPE-112793.

Fraser, I. and Bruce, R.H. 1998. Petroleum Developments in Western Australia. Paper presented at the Offshore Technology Conference, Houston, Texas, 4–7 May. OTC-8906.

Gan, W.Y., Hartanto, L., and Haynes, A.K. 2012. Forecasting and optimisation of the mature Windalia waterflood based on a capacitance resistance model (CRM). Paper presented at the APPEA Conference and Exhibition, Adelaide, Australia.

Ghauri, W.K., Osborne, A.F. and Magnuson, W.L. 1974. Changing Concepts in Carbonate Waterflooding-West Texas Denver Unit Project-An Illustrative Example. *Journal of Petroleum Technology*, **26**(06): 595–606.

Goff, B.H., Scott, M., Mitisek, B. 2016. Barrow Island - A Case Study into Production Optimisation and Operating Expenditure Focus to Mitigate Low Oil Price Impacts. Presented at the Asia Pacific Oil and Gas Conference and Exhibition, Perth, Australia, 25–27 October. SPE-182271.

Hamp, R., Bada, I.A., Mee, B. and Dunggan, T. 2008. Early Reservoir Management Insights from the Enfield Oil Development, Offshore Western Australia. Presented at the SPE Asia Pacific Oil and Gas Conference and Exhibition, Perth, Australia, 20–22 October. SPE-116915.

Haynes, A.K., Clough, M.D., Fletcher, A.J., and Weston, S. 2013. The Successful Implementation of a Novel Polymer EOR Pilot in the Low Permeability Windalia Field. Presented at the SPE Enhanced Oil Recovery Conference. SPE-165253.

Hill, R.A., O'Halloran, G., Napalowski, R., Wanigaratne, B., Elliott, A.A. and Jackson, M.A. 2008. Development of the Stybarrow Field, Western Australia. Presented at the SPE Asia Pacific Oil and Gas Conference and Exhibition, Perth, Australia, 20–22 October. SPE-115373.

Hillis, R.R. and Reynolds, S.D. 2000. The Australian Stress Map. *Journal of the Geological Society, London*, **157**: 915–921.

Jenkins, C.D. and Eggert, T. 2002. Increasing Reserves Through Optimized Waterflooding: The Long Beach Unit, Wilmington Field, California. Paper presented at the AAPG Annual Meeting, Houston, March.

Kabir, A., Saavedra. S.L., Utaibi, A. and Basri, M. 2015. Use of Wellhead Data for Pressure Transient Analysis for HPHT Gas Wells. Presented at the SPE Saudi Arabia Section Annual Technical Symposium and Exhibition, Al-Khobar, Saudi Arabia, 21–23 April. SPE-178004.

Kegg, B. 1998. A Small Joint Venture Operator's Approach To Intergrated EH & S Management. Presented at the SPE Asia Pacific Oil and Gas Conference and Exhibition. SPE-50135.

Lee, J., Rollins, J.B. and Spivey, J.P. 2003. *Pressure Transient Testing*. SPE Textbook Vol. **9**.

Lee, W., and Mantecon, J.C. 1994. Sucker-Rod Pumping Wells Optimisation Using a Spreadsheet Database on Barrow Island, Western Australia. Presented at the SPE Asia Pacific Oil and Gas Conference. Society of Petroleum Engineers. SPE-28766.

Leon, D. et al 2011. Barrow Island EOR Polymer Pilot Part 2—Results and Way Forward. Paper presented at the APPEA Conference and Exhibition, Perth, Australia.

Mantecon, J.C. 1993. Gas-lift optimisation on Barrow Island, Western Australia. Presented at the SPE Asia Pacific Oil and Gas Conference. SPE-25344.

McDiarmid, A., Ivor, A., Ion, A. and Thompson, J. 2001. Experience of a Reservoir Waterflood Failure and Remediation Treatment in the Stag Reservoir, Australia. Presented at the SPE Asia Pacific Improved Oil Recovery Conference, Kuala Lumpur, Malaysia, 8–9 October. SPE-72117.

McTavish, R.A. 1965. *Barrow No. 1 Well Completion Report*. Internal Report (Available from WA DMP). WAPET, Perth, Western Australia.

Miller, C.C., Dyes, A.B. and Hutchinson, C.A. 1950. The estimation of permeability and reservoir pressure from bottom hole pressure build-up characteristics. *Journal of Petroleum Technology*. **2**(04): pp. 91–104.

Moo, T.J., and Tweedy, M.W. 1991. Planning and Drilling Australia's First Medium-Radius Horizontal Wells. Presented at the SPE Asia-Pacific Conference. SPE-23013.

Muksat, M. 1949. *Physical Principles of Oil Production*. McGraw-Hill.

Napalowski, R., Loro, R., Anderson, C.J., Andresen, C.A., Dyrli, A.D. and Nyhavn, F. 2012. Successful Application of Well Inflow Tracers for Water Breakthrough Surveillance in the Pyrenees Development, Offshore Western Australia. Paper presented at the SPE Asia Pacific Oil and Gas Conference and Exhibition, Perth, Australia, 22–24 October. SPE-158423.

Neely, A.B. and Tolbert, H.O. 1988. Experience With Pumpoff Control in the Permian Basin. *Journal of Petroleum Technology*. **40**(05): 645–649.

O'Reilly, D.I., Hopcroft, B.S., Nelligan, K., Ng, G., Goff, B.H. and Haghighi, M. 2016a. A Lean Six Sigma Approach to Well Stimulation on Barrow Island, Australia. Presented at the Asia Pacific Oil and Gas Conference and Exhibition, Perth, Australia, 25–27 October. SPE-182323.

O'Reilly, D.I., Haghighi, M., Flett, M.A. and Sayyafzadeh, M. 2016b. Pressure and rate transient analysis of artificially lifted drawdown tests using cyclic Pump Off Controllers. *Journal of Petroleum Science and Engineering*. **139**: 240–253.

Parrish, F. and Meadow, P., 1965. *Oil recovery from 17 water-injection projects in Clay, Jack, Montague, and Wise Counties, Tex* (Vol. **6603**). US Dept. of the Interior, Bureau of Mines.

Parry, J.C. 1967. The Barrow Island Oilfield. *Australian Petroleum Exploration Association Journal*, **7**(2): 130–133.

Ryan, M. G. Practical Aspects of Managing HSE in a Remote Oilfield Operation. 2002. Presented at the SPE International Conference on Health, Safety and Environment in Oil and Gas Exploration and Production. SPE-73925.

Satter, A. and Thakur, G.C. 1994. *Integrated petroleum reservoir management: a team approach*. PennWell Books.

Sawiris, R., Howes, C.S., Rodriguez, J.A., and Foley, W.L. 2015. Uncertainty and Risk Management Plans are Critical for Team Alignment and Better Decision Quality. Paper presented at the SPE Annual Technical Conference and Exhibition. Society of Petroleum Engineers. SPE-174392.

Sayarpour, M., Zuluaga, E., Kabir, C.S. and Lake, L.W. 2009. The use of capacitance–resistance models for rapid estimation of waterflood performance and optimization. *Journal of Petroleum Science and Engineering*. **69**(3): 227–238.

Schlumberger. 1967. *Barrow No. G-52 - Induction Electrical Log (openfile available at DMP website)*, Schlumberger Australia Pty Ltd. 16 July.

Spyrou, C.E., Nurafza, P.R. and Gringarten, A.C. 2013. Well-head Pressure Transient Analysis. Presented at the EAGE Annual Conference & Exhibition, London, UK, 10–13 June. SPE-164871.

Stephenson, B., and Mollan, B. 1997. Unforeseen Geology Creates a Need For an Integrated Team Effort In Geosteering a Horizontal Well to Success In Northwest Australia. *Journal of Canadian Petroleum Technology*, **36**(9).

Terrado, M., Yudono, S., Thakur, G. 2007. Waterflooding Surveillance and Monitoring: Putting Principles in to Practice. *SPE Reservoir Evaluation & Engineering*, **10**(05): 552–562. SPE-102200.

Terrado, R.M., Yudono, S. and Thakur, G.C. 2007. Waterflood Surveillance and Monitoring: Putting Principles Into Practice. *SPE Reservoir Evaluation & Engineering*, **10**(05): 552–562.

Taber, J.J., Martin, F.D. and Seright, R.S. 1997. EOR Screening Criteria Revisited—Part 1: Introduction to Screening Criteria and Enhanced Recovery Projects. *SPE Reservoir Engineering*, **12**(3): 189–198. SPE-35385-PA.

Thakur, G.C. 1995. The Role of Technology and Decision Analysis in Reservoir Management. Presented at the SPE Middle East Oil Show Bahrain. SPE-29775.

Thakur, G.C. and Satter, A. 1998. *Integrated waterflood asset management*. PennWell Books.

Warner, G.E. 1968. Waterflooding a Highly Stratified Reservoir. *Journal of Petroleum Technology*, **20**(10): 1179–1186.

Watson, R.J. 1970. *Artificial Lift Review, BWI Windalia Pools*. Internal Report, WAPET. Perth, Western Australia.

Widjanarko, W., Hartanto, L., Leon, D., Scott, J., Fletcher, A., and Costelloe, P. 2010. The Design and Application of a Polymer EOR Trial on Barrow Island. Paper presented at the APPEA Conference and Exhibition, Brisbane, Australia, 16–19 May.

Willhite, P.G. 1986. *Waterflooding*. SPE Textbook Series Vol **3**.

Williams, C.T. 1977. An Analysis of the Production Performance of the Windalia Sand Reservoir of the Barrow Island Oil Field. *APEA Journal*, **17**(1): 105–113.

4 Pressure and Rate Transient Analysis of Beam Pumped Oil Wells

The forthcoming chapter outlines analytical solutions to transient reservoir flow problem where production starts and stops continually. This problem was first observed by the author in the Windalia field but is commonplace in mature fields with artificial lift wells (of which the beam pump is one example). A large amount of production performance data from beam pump controllers are left unused by engineers. This chapter provides a method of calculating reservoir properties from the start-stop performance of beam pumps and is complementary to existing methods used by engineers. It is published in the Journal of Petroleum Science and Engineering.

Statement of Authorship

Title of Paper	Pressure and Rate Transient Analysis of Artificially Lifted Drawdown Tests Using Cyclic Pump Off Controllers
Publication Status	☑ Published ☐ Accepted for Publication ☐ Submitted for Publication ☐ Unpublished and Unsubmitted w ork w ritten in manuscript style
Publication Details	O'Reilly, D.I., Haghighi, M., Flett, M.A. and Sayyafzadeh, M. 2016. Pressure and Rate Transient Analysis of Artificially Lifted Drawdown Tests Using Cyclic Pump Off Controllers. *Journal of Petroleum Science and Engineering*. **139**: 240-253.

Principal Author

Name of Principal Author (Candidate)	Daniel O'Reilly		
Contribution to the Paper	Problem formulation, derivation of mathematical model, preparation of graphs, writing the manuscript. Acted as corresponding author.		
Overall percentage (%)	80%		
Certification:	This paper reports on original research I conducted during the period of my Higher Degree by Research candidature and is not subject to any obligations or contractual agreements with a third party that would constrain its inclusion in this thesis. I am the primary author of this paper.		
Signature		Date	25 Nov 2020

Co-Author Contributions

By signing the Statement of Authorship, each author certifies that:

i. the candidate's stated contribution to the publication is accurate (as detailed above);

ii. permission is granted for the candidate in include the publication in the thesis; and

iii. the sum of all co-author contributions is equal to 100% less the candidate's stated contribution.

Name of Co-Author	Manouchehr Haghighi		
Contribution to the Paper	Principal supervision of the work. Problem formulation, manuscript review and assessment.		
Signature		Date	01/12/2020

Name of Co-Author	Matthew Flett		
Contribution to the Paper	Problem formulation, reviewed the manuscript and provided feedback		
Signature		Date	25/11/2020

Name of Co-Author	Mohammad Sayyafzadeh		
Contribution to the Paper	Problem formulation, reviewed the manuscript and provided feedback		
Signature		Date	26/11/2020

Journal of Petroleum Science and Engineering 139 (2016) 240–253

Contents lists available at ScienceDirect

Journal of Petroleum Science and Engineering

journal homepage: www.elsevier.com/locate/petrol

Pressure and rate transient analysis of artificially lifted drawdown tests using cyclic Pump Off Controllers

Daniel I. O'Reilly [a,*], Manouchehr Haghighi [b], Matthew A. Flett [a], Mohammad Sayyafzadeh [b]

[a] Chevron Australia Pty Ltd, 250 St Georges Tce, Perth 6000, Australia
[b] University of Adelaide, Adelaide 5005, Australia

ARTICLE INFO

Article history:
Received 23 September 2015
Received in revised form
14 December 2015
Accepted 18 January 2016
Available online 29 January 2016

Keywords:
Artificial lift
POC
Well testing
Pressure transient
Rate transient
Drawdown testing

ABSTRACT

In this paper it is shown that the classical well testing equations, with minor adaptations, may be extended to intermittently produced Pump Off Controller (POC) wells. We develop a framework for using the well-known well test equations on continuous POC well testing data. Two types of controller will be examined: the timer-based POC and the load-cell based POC. For the former, a modified constant rate drawdown test will be presented. For the latter, it will be shown that a modified constant flowing bottomhole pressure drawdown test can be applied, or if preferred, a more rigorous type curve.

The proposed method has the advantage of allowing approximate determination of reservoir properties at low cost, using frequently available production data. As ageing oilfields frequently have hundreds of wells producing under artificial lift, it is not economical to perform a traditional well test on all wells. Using the proposed method, it is possible to test every well in a field without the expense of a Pressure Build Up (PBU) survey. The high level interpretation is not intended to compare to a high resolution PBU and pressure derivative study, but it does serve as a very useful tool in scoping analysis. The method is useful for identifying wells with high skin or low permeability. Examples shown in this paper validate the theory against a numerical model and shed new light on POC transient decline field data.

1. Introduction

This novel approach is motivated by the need to quickly assess the productivity of multiple wells at low cost. This may include both permeability-thickness (kh) and skin (s) of an artificially lifted well, depending on the measured data available. Shutting in a well for conventional build-up analysis will cost operators money and the recovery of flushed production may often not account for lost barrels. Alternatively, when a well is brought online, it naturally enters a state of transient production, often referred to as a "drawdown test." When artificially lifted wells restart production after a period of inactivity, their behaviour is an example of this. The drawdown test itself has been extensively studied in the literature (Earlougher, 1977).

With both continuous pressure and rate data available, the methods within can be used to calculate both permeability and skin. This will provide valuable information regarding the state of impairment of a production well. However, we also provide secondary methods to assess the average permeability (but not skin) of wells where only limited production and pressure data are available. These methods are the focus of the paper and still provide helpful information about the productivity of a well, especially within the context of a field with known, anticipated permeability ranges. The choice of analysis method depends on the field data available and will be discussed later in the paper.

The first type of drawdown test studied is the case of constant rate production. When the production rate is held constant, a variation in bottomhole flowing pressure is observed. The line source solution (Lee et al., 2003) to this flow condition for an infinite reservoir is probably one of the most widely used equations in pressure and rate transient analysis. When combined with superposition or convolution analysis, the solution can be applied to a wide range of producing wells. Pressure build-up analysis techniques can also be derived from these solutions, but that will not be pursued in this paper.

The second type of drawdown test is the case of constant pressure production. In this case, the pressure at the reservoir sandface is maintained at a constant while the production rate declines as a transient. This boundary condition is less common but several solutions have been presented previously (Ehlig-Economides, 1979). Unfortunately these solutions are less mathematically convenient than the line source solution, and the inversion from Laplace space must be done numerically. Many simplifications have been proposed, and the simplest is that a

* Corresponding author.
E-mail address: dan.oreilly@chevron.com (D.I. O'Reilly).

http://dx.doi.org/10.1016/j.petrol.2016.01.030
0920-4105/

Nomenclature

Δp_s	pressure loss due to skin (psi)
Δt_{Dp}	producing time
Δt_{Ds}	shut-in time
ϵ	error term
μ	viscosity (cP)
$\overline{\overline{p}}_D$	dimensionless pressure, averaged from cycle 1 to cycle C
$\overline{p}_D$	dimensionless pressure, averaged over a single cycle C
$\overline{q}$	fluid rate, averaged over a single cycle C
ϕ	porosity (pu)
τ	integration variable
$\tilde{q}_D$	dimensionless rate in Laplace space
B	formation volume factor (rb/stb)
C	total number of cycles
c	cycle index used in summation
c_t	total compressibility (1/psi)
h	thickness (ft)
k	index for production or shut-in interval, or permeability (mD)
k'	permeability (mD) including effect of skin
n	total number of production and shut-in intervals
p	pressure (psi)
p_D	dimensionless pressure
p_i	initial reservoir pressure (psi)
p_{sD}	dimensionless pressure including skin
p_{wf}	bottomhole flowing pressure (psi)
q	fluid rate (bbl/day)
q_D	dimensionless rate
r_D	dimensionless radius
r_w	radius of wellbore (ft)
s	skin
t	time (h)
t_D	dimensionless time
W	Lambert-W function
Ei	exponential Integral
log	logarithm (base 10)

rearrangement of the logarithmic line source solution can be acceptable at higher values of dimensionless time (Earlougher, 1977).

Somewhere in between these two drawdown tests are the cases of smoothly varying pressure and rate. The use of this method has been gaining popularity (Ehlig-Economides et al., 2009; Palacio and Blasingame, 1993). In some cases, the line source solution can still be used for this analysis (Kucuk and Ayestaran, 1985; Kuchuk, 1990; Gladfelter et al., 1955), however caution must be taken. The best approach in this case, particularly if the changes in rate or pressure are not smooth, is to use convolution or deconvolution analysis to interpret such data (Lee et al., 2003).

Artificial lift wells that are operated by POCs are stopped and started intermittently based on controller logic (McCoy et al., 1999; Eckel et al., 1995). Because of this, their transient behaviour is quite complicated. There are clear trends in the behaviour of some POC wells; for example, wells using a load cell POC often experience a smooth decline in total daily runtime when they are returned to service. We propose the idea that, on an average basis, these data may be interpreted much like a classical drawdown well test. However, modifications must be made to understand how to interpret the averaged data.

Previously, there have been studies in the area of intermittent artificial lift production, however the work has not provided a general solution method applicable to all POCs. One study has focused on modelling the behaviour of intermittent gas lift and plunger lift wells using reservoir simulation (Gasbarri et al., 1997). The method was neither analytic nor general enough to perform interpretation across a range of reservoirs and wells. In another work (Huff III, 1988), a more analytical approach was developed but only specifically investigated intermittent gas lift wells. We propose a theory that is general for a range of controllers.

The use of artificial lift and associated analysis will continue to gain popularity into the future. This will occur as conventional fields decline in pressure. It will also occur in unconventional oil and gas fields (e.g. shale oil and coalbed methane), where formations must be dewatered prior to hydrocarbon production, or where artificial lift is requisite for oil recovery. Sucker Rod Pumps or Progressing Cavity Pump lift are frequently used in this process, amongst others. The analysis methods in this paper may be of assistance when such wells are produced using POC and drawdown-like production occurs.

The first section of this paper will explain the operation of POCs on artificial lift wells. We separate the types of POCs into different categories. In the second section, a mathematical model will be developed to represent some of these mechanisms. The third section will outline how some of the theory can be used with standard semi-log analysis, and the final section will present field and synthetic case studies.

2. POC operation and parameters

2.1. POC mechanism

Artificial lift is installed in wells that are no longer capable of lifting fluids to the surface using the reservoir's natural energy. The most common type of artificial lift is the Sucker Rod Pump (example photograph shown in Fig. 1). In these completions, a rod string is connected to a plunger that actuates a ball and seat valve downhole. Historically, these wells were originally allowed to run 24 h per day. Eventually operators discovered that this was contributing to the failure of pump components as the pump was often not properly primed with reservoir fluids downhole. For some portion of the day, the reservoir was so depleted that the pump plunger would pound against a low fluid level.

The POC was invented to overcome this problem and offered a way for operators to produce a well for a period of time and stop the pump from reciprocating for the remainder of the day. Nowadays POCs of varying complexity exist in the oil field. These are described in the next section.

2.2. Types of POCs

POCs are designed to start, stop or otherwise modify an artificially lifted well depending on a set of inputs defined by an operator. Since their inception, numerous models have been released, each with a slightly different mode of operation. For the purposes of analysis in this paper, POCs available in the market are separated into four categories shown in Table 1.

The first type of operation, denoted Type 0, is a well that is controlled completely manually by an operator. The operator starts and stops a pump based on their prior understanding or field experience as to how the well best performs. This need not be a POC device at all, or it could be one in which the operating parameters (such as off-time) are frequently changed. These devices do

Fig. 1. Sucker Rod Pump units and POCs in California, United States (Photo by Colin G Palmer/Creative Commons).

Table 1
Types of POCs available and their notation in this paper.

Type	Operation	Uptime	Relative equipment cost
Type 0	Manual start/stop by operator		Low
Type I	Timer	<24 h	Low
Type II	Load cell + timer	<24 h	Medium
Type III	Variable Speed Drive controller	24 h	High

not form repetitive or logical patterns in production and will not be considered heavily in this work. If a rate/cycle time/BHP history are maintained for these wells, it may be possible to use convolution analysis to interpret the data.

This paper will only focus on Type I and II controllers. These controllers follow fixed on/off patterns and are pervasive in oil fields, and simple methods of interpretation will be proposed. Firstly, the Type I controller is a POC that is based on a timer. The well will produce for a specified duration (Δt_{Dp} in dimensionless terms), and is then shut in for another period of time (Δt_{Ds}). This POC is also known as an interval timer. It is common in the United States to set the producing time for wells to 15 min (McCoy et al., 1999). Another variation of the Type I controller is known as a percentage timer, where the well operates a fixed percentage of the day.

Type II controllers include the addition of a load cell that measures the force exerted on the polished rod at the surface. This allows for real time tracking of the fluid load in the pump and controls based on the current inflow conditions. When inflow has almost ceased and the fluid level in the well is low, the sucker rod plunger may pound against a partially filled chamber. When this occurs, the Type II controller will automatically switch the well off (within some tolerance). It then shuts down for a specified amount of time (again referred to as Δt_{Ds}). The difference here is that only the time that the well is shut-in is set inside the controller; the producing time varies and is purely controlled by the well's inflow. A wellbore schematic for this type of well is shown in Fig. 2.

The early production transience experienced by Type I and II controllers is slightly different but we propose that this amounts to either a constant rate or constant pressure drawdown test respectively. Clearly, on an average basis, the timer POC produces a continuous amount of fluids over time if the operational parameters are not changed. Similarly, since the Type II controllers are produced until the bottomhole pressure reaches a constant value (before pounding occurs), they may be thought of as constant pressure drawdown tests on an average basis. The pressure and rate profiles are shown for both types of controllers in Figs. 3 and 4.

In recent times, the Type III controller has also been introduced, whereby the well is powered by a Variable Speed Drive motor that can effectively speed up or slow down as operationally required. This type of POC operates continuously over a 24 h period and does not usually shut in. If the Type III controller is used to maintain constant BHP, it is an exact drawdown study at constant BHP. This will be achieved after an initial period of wellbore storage. If the speed is adjusted manually and arbitrarily by an operator, a convolution or deconvolution method should be used for interpretation. Again, this type of POC will not be the focus of this paper. It has already been considered in the literature for Rate Transient Analysis (Clarkson et al., 2014).

2.3. Proposed drawdown testing procedures

When a well is either returned to service or brought online for the first time, it begins with a higher-rate transient period of production. Some operators refer to this as "flushed production." During this period, it is possible to complete a drawdown test. We now describe the data that should be obtained in the field in order to perform transient analysis for each type of controller (Type I or II).

Type I. Much like a conventional drawdown test, BHP data will be required for this type of analysis. There are two common methods to estimate BHP: either install a downhole gauge or periodically shoot acoustic fluid level surveys (McCoy et al., 1999). The latter method is considered less accurate due to the lower frequency of data acquisition and the inference of BHP from fluid level, yet it is much cheaper. When setting the time or percentage a well is producing, it is important to remember that the well will be in an initially flushed state. It is suggested to weight the well's production period higher than normal.

Type II. After a Type II well is brought online, the cycle time will gradually diminish as the reservoir settles into pseudo-steady or steady state production. Commonly, SCADA (Supervisory Control and Data Acquisition) systems record this information. The diminishing cycle time can then be used for drawdown interpretation. The runtime data should be correlated against separator well test rates to predict phase rates during well startup. Alternatively, if the well is continuously monitored under multiphase metering, those data should be used in preference. We will spend more time discussing the interpretation methods in following sections.

For best quality of drawdown data, it is suggested that both pressure and rate data are again acquired for the Type II controller. In this way, we propose that normalised semi-log analysis could be used to interpret the data. However, if the pressure data are not obtained, there is an interesting opportunity for analysis based on knowing the fluid pound pressure alone (knowing the pressure at each time when the POC shuts in the well). We propose two interpretation methods based on this situation when only scarcer data are available. The first method involves assuming the drawdown test is, on an average basis, a constant FBHP test. This will only lead to approximate results, as the test is not truly constant

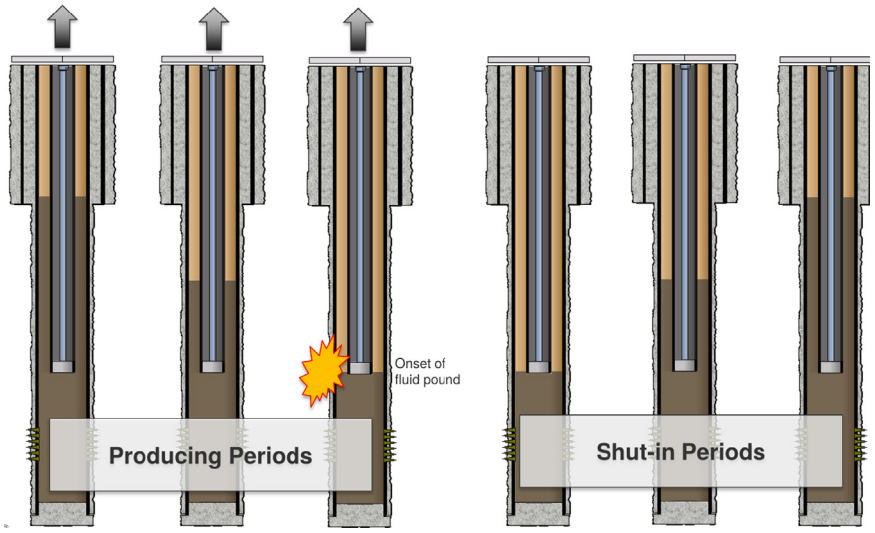

Fig. 2. Wellbore schematic of Type II POC mode of operation for tubing pump with open annulus.

FBHP. The second method is to use a precise type curve that we develop in this paper, which will be discussed further.

The drawdown testing procedures and interpretation methods shown in red in Table 2 will form the focus of this paper. These methods appear to be unstudied in the literature so far. We suggest a range of interpretations in this table that are possible depending on the data available. If continuous pressure and rate data are both available, it is possible to use the equations developed within to match directly $p(t)$ or $\overline{p}(t)$ by adjusting reservoir properties in the proposed models. In some cases it may be preferred to match $\overline{p}(t)$, which is defined as the average FBHP during a single cycle.

3. Mathematical formulation

Equations are now developed that convert the unsteady, cyclic operation of POC controllers into smoothed and averaged data that are suitable for standard drawdown semi-log analysis methods. This part is primarily divided into two sections, one for Type I and the other for a Type II controller. The general principle applied is the superposition of constant rate production and shut-in periods using the readily available infinite acting radial flow solution for constant rate production. Superposition can be used on Partial Differential Equations that are linear or have been linearised and involves combining many solutions across different time periods. POC wells are then easily modelled as a series of alternating constant rate production and shut-in periods.

3.1. Dimensionless variables and line source solution

Henceforth the following variables, expressed in terms of oilfield units, will be used to express the reservoir inflow (Lee et al., 2003):

$$p_D = \frac{kh}{141.2 q_{\text{const}} B\mu}(p_i - p), \tag{1}$$

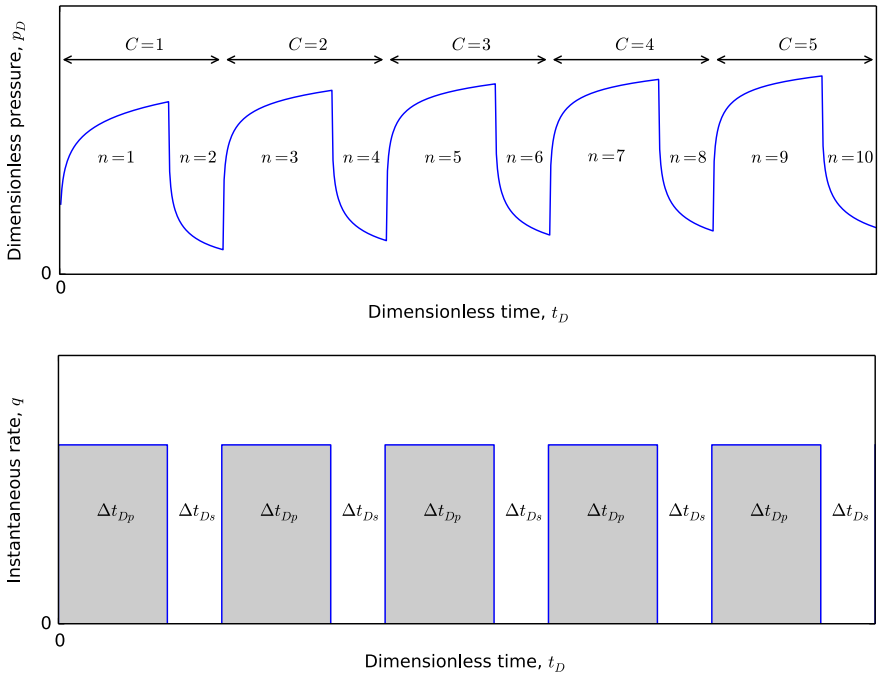

Fig. 3. Generic pressure and rate plots for Type I POC, showing nomenclature.

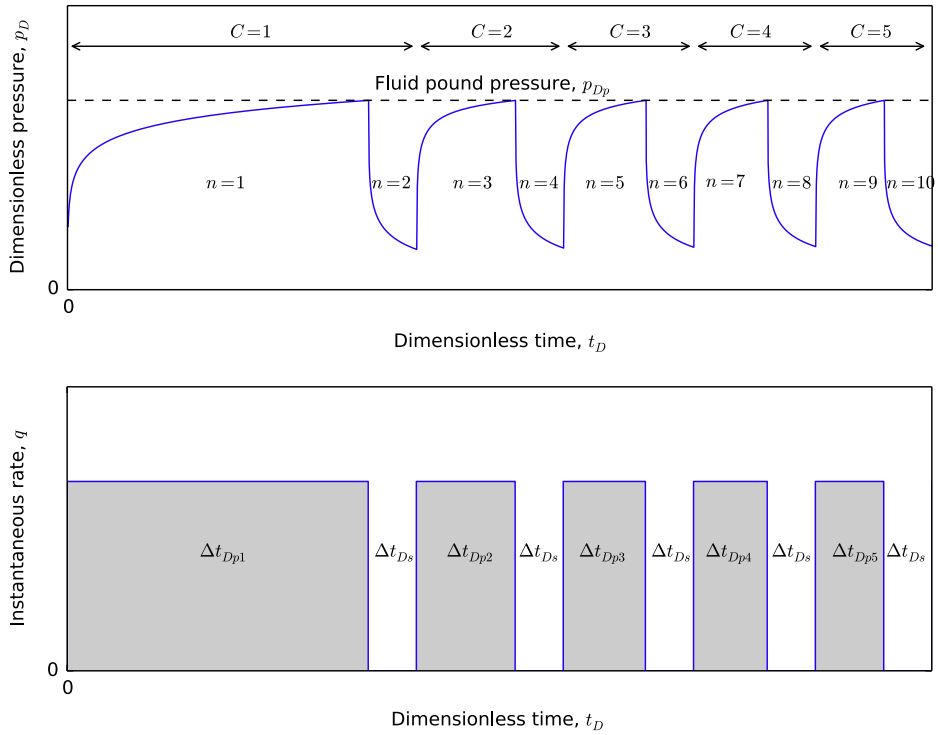

Fig. 4. Generic pressure and rate plots for Type II POC, showing nomenclature.

Table 2
Proposed drawdown testing procedures and associated interpretation techniques.

POC Type	Pressure data	Rate data	Possible interpretation methods	k	s
Type 0	✓	✓	$p(t)$ vs t – Use Eq. 9 as model	✓	✓
	✓	✓	$\overline{p}(t)/\overline{q}(t)$ vs $\log t$ – Normalised semi-log analysis	✓	✓
Type I	✓	✓	$p(t)$ vs t – Use Eq. 10 as model	✓	✓
	✓	✓	$\overline{p}(t)$ vs $\log t$ – Semi-log analysis	✓	✓
Type II	✓	✓	$p(t)$ vs t – Use Eq. 13 as model	✓	✓
	✓	✓	$\overline{p}(t)/\overline{q}(t)$ vs $\log t$ – Normalised semi-log analysis	✓	✓
	Pound only	✓	$\overline{p}/\overline{q}(t)$ vs $\log t$ – Constant FBHP drawdown	✓	
	Pound only	✓	Type curves from this work (Figure 6)	✓	

$$t_D = \frac{0.0002637kt}{\phi\mu c_t r_w^2}, \tag{2}$$

$$q_D = \frac{141.2qB\mu}{kh(p_i - p_{\text{const}})} \tag{3}$$

$$\text{and} \quad s = \frac{kh\Delta p_s}{141.2qB\mu} \tag{4}$$

These dimensionless variables are used for the radial flow, constant rate drawdown solution to the radial diffusivity equation. Dimensionless pressure is used for a constant rate drawdown solution, while dimensionless rate is used for constant BHP drawdown. The well-known line source solution at the wellbore for transient flow at the wellbore is, for $t_D \geq 10$:

$$p_D = -\frac{1}{2}\text{Ei}\left(-\frac{1}{4t_D}\right) \tag{5}$$

For $t_D \geq 25$, this solution is approximated by the logarithmic (base 10) equation shown below:

$$p_D = 1.152\log(2.246t_D) \tag{6}$$

3.2. Convolution

The theory of superposition and convolution will be relied upon to develop relations. The convolution integral expresses the changing wellbore pressure as a function of the varying sandface rate[1]:

[1] Note that the convolution equations use a slightly different definition of dimensionless rate: $q_D = q/q_{\text{ref}}$. This is the only time this definition of q_D will appear in the paper.

$$p_{wD}(t_D) = \int_0^{t_D} \frac{\mathrm{d}q_D(\tau)}{\mathrm{d}\tau}[p_{sD}(t_D - \tau)]\,\mathrm{d}\tau \tag{7}$$

where $p_{sD} = p_D(t_D) + s$ for rates at the sandface. For a discrete schedule of rates, this can be expressed as

$$p_{wD}(t_D) = \sum_{i=1}^{n} (q_i - q_{i-1})_D p_{sD}(t_i - t_{i-1})_D \tag{8}$$

which will be used as a basis to develop equations for a POC well starting and stopping.

3.3. Type 0 controllers

For completeness, a formula is given below for a general case of Type 0 controller with both varying producing and shut-in times. The other two controllers are considered as special cases of the below equation, where $p_D(t_D)$ is the line source solution:

$$p_{Dn}(t_D, n) = \sum_{k=1,\text{odd}}^{n} \left\{ p_D\left[t_D - \sum_{j=1}^{(k-1)/2} \Delta t_{(Dp)j} - \sum_{j=1}^{(k-1)/2} \Delta t_{(Ds)j} \right] + s \right\} - \sum_{k=2,\text{even}}^{n} \left\{ p_D\left[t_D - \sum_{j=1}^{k/2} \Delta t_{(Dp)j} - \sum_{j=1}^{(k-2)/2} \Delta t_{(Ds)j} \right] + s \right\} \tag{9}$$

3.4. Type I controllers

The first type of controller represents a type of distorted constant rate drawdown test after the well is brought to production. The distortion results from the periodic stopping and starting of the well, as defined by the parameters set in the controller. It will be shown that these distortions can be removed using corrections, and the classical theory can then be applied. The Type I controller will generally be more difficult to use field data from, as compared to Type II, but the formulation here serves as a useful introduction to Type II.

A general pressure and rate plot is shown in Fig. 3 for the Type I POC. The well is opened for production for a duration of Δt_{Dp} and then shut-in for a period of Δt_{Ds}. This process is repeated. The superposition or convolution equation can be expanded to form the equation below for the exact pressure during operation of a POC well:

$$p_{Dn}(t_D, n) = \sum_{k=1,\text{odd}}^{n} \left\{ p_D\left[t_D - \frac{k-1}{2}(\Delta t_{Dp} + \Delta t_{Ds}) \right] + s \right\} - \sum_{k=2,\text{even}}^{n} \left\{ p_D\left[t_D - \frac{k}{2}\Delta t_{Dp} - \frac{k-2}{2}\Delta t_{Ds} \right] + s \right\} \tag{10}$$

The even terms represent production periods, while the odd terms represent shut-in periods. The goal is to represent Eq. (10) in a simpler form. We propose

$$\bar{p}_D(t_D) = a p_D(t_D) + bs \tag{11}$$

where the equation is valid for all n and the constant a needs to be determined. It is shown in Appendix A that a simplified expression for a and b is

$$\bar{p}_D(t_D) = \frac{\Delta t_{Dp}}{\Delta t_{Dp} + \Delta t_{Ds}}\left[p_D(t_D) + s \right] \tag{12}$$

This simplification states that the average corrected pressure in the wellbore is simply the dimensionless pressure function multiplied by the time ratio that the well is online and producing. It is necessary to compare the accuracy of Eq. (12) with the full convolved Eq. (10). It is shown in Appendix A that, for the Exponential Integral solution (Eq. (5)), the approximation of Eq. (12) represents the *average* behaviour of the convolved solution for C > 20 cycles to accuracy within 1–2%.

To summarise the appendix results, the averaged equation is best applied to wells with a higher proportion of production time vs. shut-in time, if BHPs are sampled randomly. However, during flushed production on a drawdown test as a well is brought online, this is commonly the case anyway. The approximation is also less kind to wells with extreme values of skin (positive or negative). An example following will show the appropriate use of this approximation.

3.5. Type II controllers

After starting production, the Type II controller can behave like a classical constant pressure drawdown analysis, providing that corrections are applied before well test interpretation. Provided wellhead backpressure and pump setting depth are known, the BHP may be assumed constant and hence gauge or fluid level tests are not required. This is a distinct advantage of the Type II controller in terms of data analysis. Rate data are required for this style of analysis.

A graph showing the production and BHP characteristics of a Type II controller is shown in Fig. 4. In this type of well, the BHP is only allowed to decline to the fluid pound pressure, p_{Dp}, before the well is forcibly shut in by the POC controller, after time Δt_{Dp1}. This is measured by the load cell on the surface. The pump stops for duration Δt_{Ds} and this ends one cycle. For the next cycle, the well produces for a shorter duration Δt_{Dp2}, due to the nature of infinite acting radial flow, before it is again shut-in for Δt_{Ds} duration. For C number of cycles, it can be observed that $\Delta t_{Dp1} < \Delta t_{Dp2} < .. < \Delta t_{DpC}$. This is a result of the average near-wellbore pressure depleting during drawdown; the amount withdrawn each cycle decreases. The average production rate of the well during this period hence declines over time, similar to a constant BHP drawdown test.

Let us start by developing a convolved function, similar to that of Type 1 equations:

$$p_{Dn}(t_D, n) = \sum_{k=1,\text{odd}}^{n} \left\{ p_D\left[t_D - \sum_{j=1}^{(k-1)/2} \Delta t_{(Dp)j} - \frac{k-1}{2}\Delta t_{Ds} \right] + s \right\} - \sum_{k=2,\text{even}}^{n} \left\{ p_D\left[t_D - \sum_{j=1}^{k/2} \Delta t_{(Dp)j} - \frac{k-2}{2}\Delta t_{Ds} \right] + s \right\} \tag{13}$$

The key difference here is that the producing duration ($\Delta t_{(Dp)j}$) now varies for each cycle and is not a constant. Again, the odd values of k apply to producing times and the even values apply to shut-in periods. The important step of determining the values of $\Delta t_{(Dp)j}$ that correspond with each time to reach fluid pound, p_{Dp}, is discussed in Appendix B. In this section, we will present the results.

3.5.1. Constant FBHP method

As seen in Fig. 4, the BHP across cycles is not constant but varies with time. *The problem to solve is what the average pressure should be to perform standard semi-log analysis on the rates that are measured*. It would not be appropriate to select p_{Dp} since this pressure is clearly not the average. The actual pressure, however, may be relatively close to this value, depending on operating conditions. In this section, we will solve for this average pressure using superposition over time.

Similar to Type I controllers, we seek an averaged equation to the constant BHP drawdown test in the form of:

$$\bar{q}_D(t_D) = \frac{1}{1.152\,\log(2.246 t_D) + s} \tag{14}$$

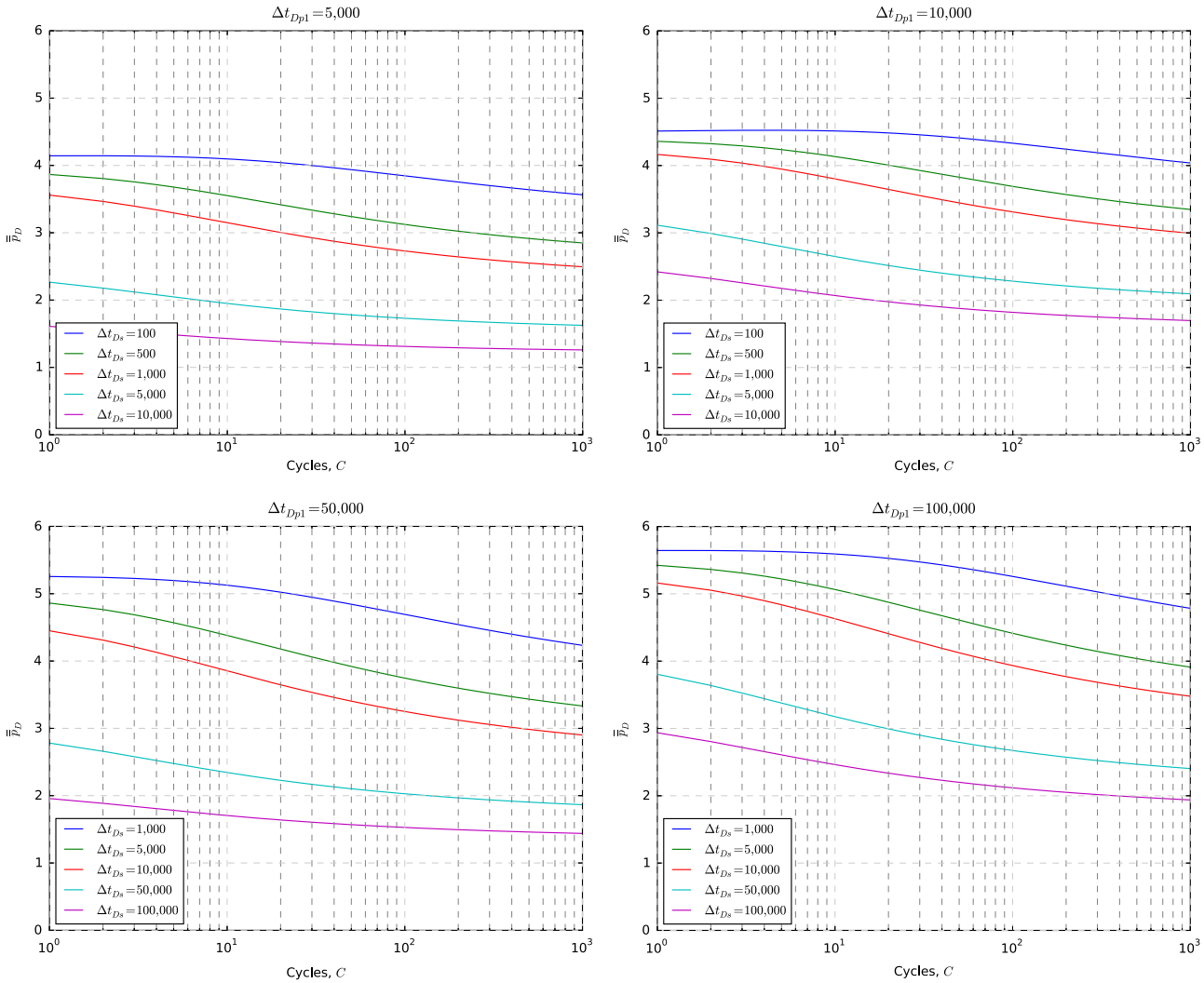

Fig. 5. Average pressure curves across all cycles for Type II controllers – skin s=0.

This equation is appropriate for standard semi-log analysis. In this averaged rate equation, it is necessary to declare a constant, average value of pressure (recall definition of dimensionless rate in Eq. (3)). To find p_{const}, Eq. (13) is integrated and averaged over the total number of cycles in the drawdown period. Note: the use of the logarithmic Eq. (14) as an approximation to the exact constant BHP drawdown solution is discussed in Appendix C. This average will be referred to as $\overline{\overline{p}}_D$, since it is across many cycles.

The determination of $p_{D\text{const}}$ and hence p_{const} follows. Using the curves in Fig. 5, three values are needed, i.e. $p_{D\text{const}} = \overline{\overline{p}}_D = f(\Delta t_{Dp1}, \Delta t_{Ds}, C)$. The last two terms have already been discussed and are the dimensionless shut in duration and total number of cycles. The first term is the duration of the first production period Δt_{Dp1}, which can be calculated from:

$$\Delta t_{Dp1} = \frac{1}{2.246} 10^{(p_{Dp}-s)/1.152} \tag{15}$$

This implies that the skin and permeability must be known *a priori*, or at least can be estimated and recursively updated if required. Of course, the fluid pound pressure at the end of each production period, p_{Dp}, must also be known. Using Fig. 5, it is then possible to determine the average dimensionless BHP required for semi-log analysis.

It will be worthwhile to review the shape of the curves in Fig. 5. Each curve represents the average dimensionless pressure drawdown encountered by a POC well with particular operating characteristics, Δt_{Dp1} and Δt_{Dps}. The average pressure is evaluated from cycle C=1 to cycle C=C, and thus it represents the appropriate average that should be used across these particular cycles if the semi-log method of interpretation is used with field data. The curves indicate that the average drawdown pressure decreases with higher cycles. This is a direct result of the well spending more time online during the first cycle than it does in subsequent cycles (which can be seen in Fig. 4).

We suggest the following steps for calculating the average pressure over a number of cycles:

1. Assume skin is zero since we can only calculate the average permeability k'.
2. Use expected permeability from reservoir to calculate dimensionless pound pressure and Δt_{Dp1} from Eq. (15).
3. Knowing the number of cycles that the POC has run, read the average dimensionless pressure from Fig. 5.
4. Perform standard semi-log analysis (Section 4.2) using constant, average FBHP (and ensuring the skin from interpretation is approximately 0).
5. Calculate the average permeability k'.
6. Compare with assumed permeability and iterate from dimensionless graphs if required.

3.5.2. *Type curve method*

A method will now be shown for interpretation of Type II data

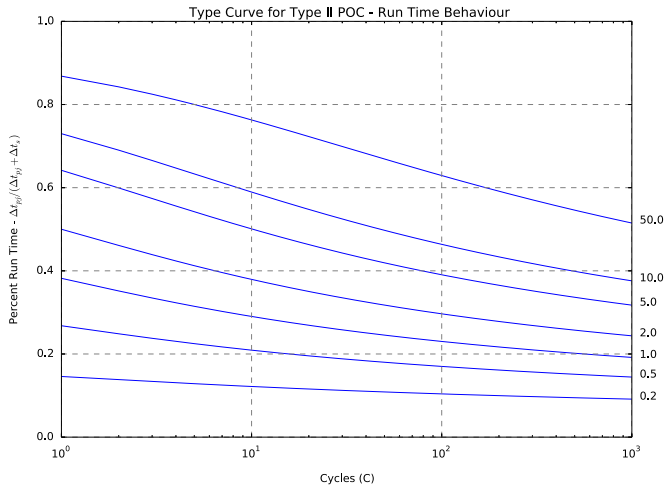

Fig. 6. Type curve method for Type II controllers – $\Delta t_{p1}/\Delta t_s$ is marked for each curve.

that is more rigorous than the constant FBHP assumption. A type curve will be used for the interpretation of results, rather than the use of a semi-log plot. The chart is shown in Fig. 6; the percentage run time for each cycle (producing time over total cycle time) is plotted against the number of cycles. This dimensionless plot has been prepared using the polynomial solution method described in Appendix B, i.e. Eq. (36).

Each type curve in the chart represents a different ratio of $\Delta t_{p1}/\Delta t_s$ – production time during first cycle divided by shut-in time each cycle. The production time during first cycle turns out to be a very important parameter and it will be used to infer permeability from these rate and fluid pound pressure data. The logarithmic line source solution (Eq. (6)), with skin, can be expressed in field units as

$$\frac{kh\Delta p_p}{141.2qB\mu} - s = 1.152\log\left(\frac{0.00059227k\Delta t_{p1}}{\phi\mu c_t r_w^2}\right) \tag{16}$$

Assuming skin is 0, the solution to permeability is then found:

$$k' = -\frac{70.64qB\mu \mathrm{W}\left(\frac{-23.9\phi c_t r_w^2 h\Delta p_p}{qB\Delta t_{p1}}\right)}{h\Delta p_p} \tag{17}$$

where $W(x)$ is the Lambert-W function. Permeability here is denoted k' instead of formation permeability k. This is to remind readers that this total permeability may include the effects of skin, since this method with only pound-pressure data available does not allow the separation of k and s (refer Table 2). The definition is similar to the average permeability, k_J, calculated from pseudo-steady state drawdown (Lee et al., 2003). The Lambert-W function (Corless et al., 1996) may either be solved numerically or with a symbolic mathematics package, e.g. Mathematica. There are also analytical approximations available (Barry et al., 2000).

Summarising the above, follow the steps below to use the suggested type curve:

1. Plot percent runtime of POC for each cycle vs. the number of cycles from the start of drawdown.
2. Find the best fit type curve from Fig. 6.
3. Read off or interpolate the associated ratio $\Delta t_{p1}/\Delta t_s$ from the graph.
4. Since Δt_s is known from the POC operation, calculate Δt_{p1}.
5. Solve for k' from Eq. (17).

An example to follow will clarify use of the above type curve.

4. Semi-log interpretation of drawdown data

This section describes application of the simplified equations using analytical well testing equations. Standard semi-log analysis is a well-established method for interpreting drawdown tests in the oil industry. Lee et al. (2003) have summarised the methods for interpreting kh and s from semi-log charts.

4.1. Type I POC – constant rate drawdown semi-log analysis

For constant rate analysis, the difference between original reservoir pressure and BHP is plotted vs. the logarithm of time ($\Delta\bar{p}(t)$ vs. $\log_{10} t$). A slope, m, is determined from these data, from which reservoir properties are inferred. The equations below are valid for the oilfield unit system:

$$k = \frac{162.6\bar{q}B\mu}{mh} \tag{18}$$

$$s = 1.151\left[\left(\frac{p_i - p_{wf,1\,\mathrm{h}}}{m}\right) - \log\left(\frac{k}{\phi\mu c_t r_w^2}\right) + 3.23\right] \tag{19}$$

In this paper we proved that it is appropriate to use $\bar{q}$ in the permeability equation, which is the average production rate over time (follows from Eq. (12)), rather than the instantaneous rate q that a well is pumping at.

4.2. Type II POC – constant BHP drawdown semi-log analysis

For constant FBHP drawdown analysis, $\frac{p_i - p_{wf,\mathrm{const}}}{\bar{q}(t)}$ is plotted vs. $\log_{10} t$. The slope m' is used for interpretation. Reservoir properties for a Type II POC can then be calculated as follows, again in oilfield units (Lee et al., 2003):

$$k = \frac{162.6B\mu}{m'h} \tag{20}$$

$$s = 1.151\left[\frac{1}{m'}\left(\frac{p_i - p_{wf,\mathrm{const}}}{\bar{q}}\right)_{1\,\mathrm{h}} - \log\left(\frac{k}{\phi\mu c_t r_w^2}\right) + 3.23\right] \tag{21}$$

The value for $p_{wf,\mathrm{const}}$ can be determined from Fig. 5. The instantaneous pumping rate, q, must be known. This should be known from operational data (stroke length, SPMs, etc.).

5. Examples

Three case studies will follow to illustrate application of the derived equations.

5.1. Synthetic example – Type I POC

This case study illustrates the appropriate use of the developed Eq. (12) for a Type I POC (constant average rate production). We examine a case with the following dimensionless properties:

- $\Delta t_{Dp} = 5000$
- $\Delta t_{Ds} = 500$
- $s = 0$.

This case is attractive for use with the proposed equation because

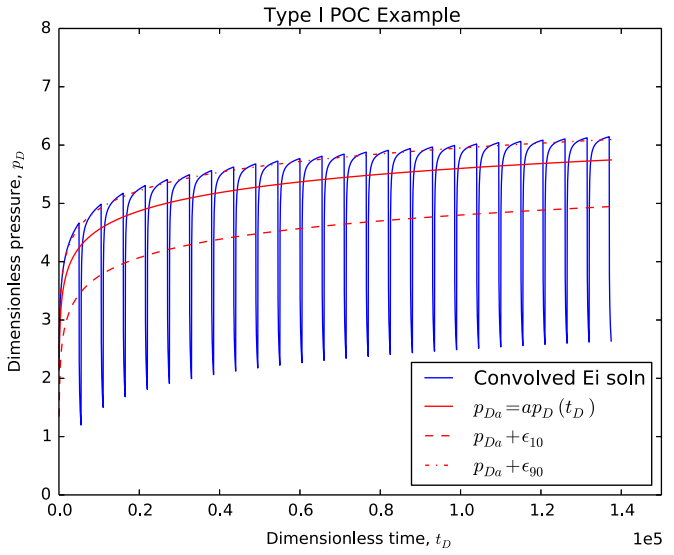

Fig. 7. Dimensionless pressure profile for Type I POC example. (For interpretation of the references to colour in this figure caption, the reader is referred to the web version of this paper.)

the ratio of producing time to shut-in time is high, i.e. the well is mostly online. This situation may be common when bringing a well online that has been offline for an extended period (drawdown test). It is also preferred to have lower values of skin, in this case 0.

The results for a forecast of dimensionless pressure are shown in Fig. 7. The convolved equation (Eq. (10)) is shown in blue, for the Exponential Integral solution. The averaged pressure equation is then shown in the solid red line. The dotted red lines show anticipated deviation between the two solutions. That is to say, there is a 10% chance that these curves (or worse) could be sampled in the case of pure random sampling of bottomhole pressure. An associated error with kh or s would result. It is obviously preferred to sample the continuous BHP using a gauge or likewise, but in this case the error is not large. The relative error also diminishes over time.

5.2. Synthetic example – Type II POC (type curve method)

The COMSOL software has been used to model the radial diffusivity equation and compare results with the proposed method. We will show the use of the type curve for Type II POCs for three separate sets of reservoir properties. The reservoir properties and results of analysis are shown in Table 3. The details of Finite Element simulation within COMSOL are given in Appendix D. The proportion of run time vs. number of cycles is shown in Fig. 8. After calculating Δt_{p1} from the chart, we used Eq. (17) to solve for permeability k'.

Results in Case A indicate a very close agreement between k' and the formation permeability k. This is expected, as the well contains no skin damage. In Cases B and C, the wells contain skin damage and skin enhancement respectively. As expected the well with skin damage ($+2$) has an impaired value of average permeability ($k'=55.2$ mD vs. $k=80$ mD). The well with reservoir stimulation (-2) has an enhanced permeability ($k'=157.8$ mD vs. $k=80$ mD).

These examples demonstrate that the total, averaged permeability k' can be used to diagnose problematic wells with only fluid pound pressure data available.

Table 3
Type curve interpretation of numerical results. Permeability (model and interpreted) and skin marked in bold for comparison purposes.

Property	Case A	Case B	Case C
p_i (psi)	400	500	500
p_p (psi)	50	375	450
r_w (ft)	0.4	0.4	0.4
B (rb/stb)	1.3	1	1
μ (cP)	2	0.7	0.7
ϕ (pu)	0.25	0.2	0.2
c_t (1/psi)	1e−5	3e−4	3e−4
h (ft)	100	20	20
k (mD)	**10**	**80**	**80**
s	**0**	**2**	**−2**
Δt_s (h)	0.5	0.15	0.15
C (cycles)	100	500	500
q_{pump} (stb/d)	200	300	300
From type curve			
$\Delta t_{p1}/\Delta t_s$	4	15	20
$\Rightarrow t_{p1}$ (h)	2	2.25	3
Interpreted k' (mD)	**10.1**	**55.2**	**157.8**

5.3. Field example – Type II POC (constant FBHP method)

A field case study is now shown using published data from the Midway Sunset field (Acton, 1981). POC run-time data were available for several wells in the field which has been undergoing cyclic steam recovery. The wells were run in cyclic steam operations; wells are periodically injected with steam and then wells flow oil back using beam pump artificial lift. The beam pumps used a POC that operated on a load cell and timer and hence fit the definition of a Type II POC. Reservoir data are available for this field in several other papers (Sims et al., 1950; Rivero et al., 1975). BHP gauge data were not available.

Fig. 9 shows a semi-log analysis of data for two wells in the field. Each plot contains data in two colours: the blue points plot assume that p_{wf} is a constant equal to the fluid pound pressure and the red points use a corrected average pressure from the convolution theory taken from Fig. 5. We assume a reasonable number of 100 cycles for $\Delta t_{Dp1}=5,000$ and $\Delta t_{Ds}=500$. Reading from the charts, this leads to $\bar{p}_D=3$, which is about 80% of the actual fluid pound dimensionless pressure. Hence the slope of the red points in the semi-log interpretation is 80% that of the blue points.

On both graphs, there is a deviation from the semi-log straight line after 1000 h. At this time the POC is running at approximately constant run time and the transient period of production has ceased. One interpretation of this is that the transient has reached a physical or pattern boundary. The slope (relating to formation kh) and intercept (relating to skin, s) during the transient period for both cases are summarised in Table 4. If the corrections proposed in this paper were not used, permeability-thickness could be overestimated by 20%. Note that since only fluid pound pressure data are available, we cannot truly separate the permeability and skin terms. Since the average FBHP from the curves in Fig. 5 assumes $s=0$, a consistent interpretation from semi-log graphs should honour this and calculate k' rather than k. We still suggest that this is a fast and approximate method for interpreting reservoir data; it is preferred over assuming constant $p_{wf}=p_p$.

The no-flow boundary condition in this example was encountered late enough to leave usable infinite-acting reservoir information for transient interpretation. In a densely drilled field with small well spacing, the transient period may be so short that

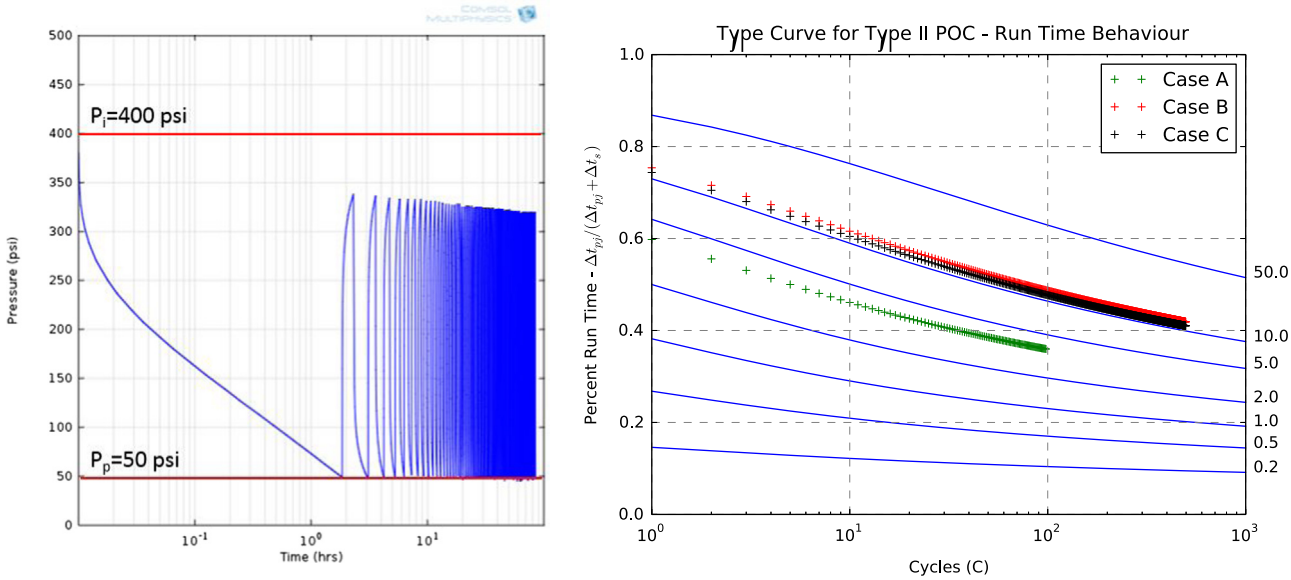

Fig. 8. COMSOL simulation of Type II POC for Case A (left), type curve results for all cases (right).

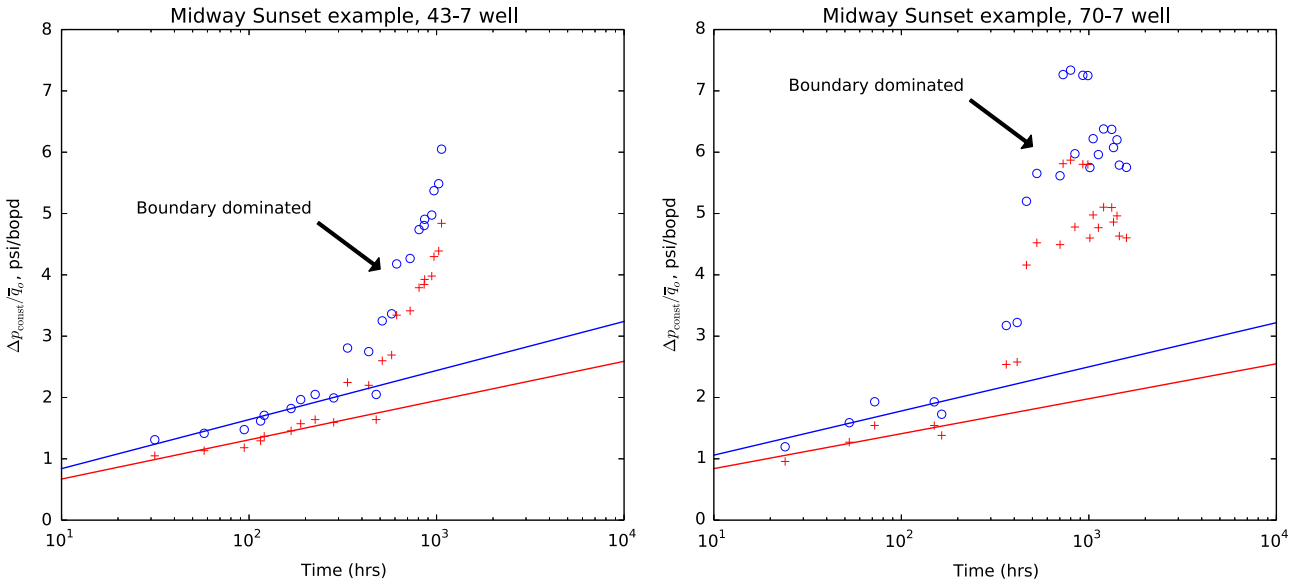

Fig. 9. Semi-log graphs for Type II POC wells from the Midway Sunset field. (For interpretation of the references to colour in this figure caption, the reader is referred to the web version of this paper.)

Table 4
Slope and intercept data for semi-log interpretation in field example.

Well	Using $p_{wf,\text{const}} = p_{\text{pound}}$		Using $p_{wf,\text{const}} = 0.8p_{\text{pound}}$	
	m' (psi/bopd/cycle)	$\left(\frac{p_i - p_{wf,\text{const}}}{\bar{q}}\right)_{1\text{ h}}$ (psi/bopd)	m' (psi/bopd/cycle)	$\left(\frac{p_i - p_{wf,\text{const}}}{\bar{q}}\right)_{1\text{ h}}$ (psi/bopd)
43-7	0.7	0.8	0.6	0.6
70-7	0.5	1.1	0.4	0.9

the analysis method discussed may be unusable. It is recommended that, similar to standard semi-log or Horner analysis, a reasonable period of transient flow is analysed.

6. Further work

The authors recommend several further developments with this theory that can be made.

- For those operators sampling the pressure of Type I POCs randomly (e.g. with sonolog), it is possible to develop a stochastic approach to the match for reservoir properties. This is an alternative to simply averaging pressure measurements to achieve a fit. It is not recommended to sample too sparsely with pressure measurements, otherwise errors become large.
- The consideration of wellbore storage is a topic that is worth discussion. It is possible to extend the solutions in this paper for the inclusion of wellbore storage. As was done in Appendix B for Type II controllers, it is possible to create an averaged solution with the integration of storage, either in the form of changing

annulus liquid level or compressible fluid storage. The solutions in this paper are still highly useful as a limiting solution for those cases where storage is negligible.

- While this paper has confined itself to Type I and Type II controllers, some POCs exist with more complicated logic that adjust the offtime, Δt_{Ds} dynamically. This is done in order to maximise the run time of a well while maintaining a preferred number of cycles per day. It is possible to derive similar equations for this type of POC, too.
- This paper has considered only infinite acting radial flow. Development of solutions and interpretation methods for other flow regimes (linear and spherical) and boundary conditions (closed and steady-state influx) would be of help for interpreting other forms of data.
- It would be valuable to compare the new type curve method for Type II controllers against field data (logs, PBUs, etc.) to validate results further.
- Downhole pump efficiency or changes in fluid phase rates are not considered. Pressure loss in annulus due to fluid friction is not considered. The effect of these on transient drawdown should be studied in future.

7. Conclusion

Solutions have been shown that the classical well test theory for drawdown analysis is extended for easy and economical use with Pump Off Controller wells.

1. Through simple corrections, the Type I and Type II POC can use averaged data to infer permeability and skin in wells undergoing a drawdown-like test. This approach is helpful for fast screening of reservoir properties.
2. A field case study has been shown that outlines the use of aforementioned theory to Type II controllers.
3. A synthetic case study has been presented for Type II controllers that shows the use of a type curve to calculate average permeability k'.
4. Early-time flow regime identification is not possible as the proposed models require several cycles (e.g. at least 20 cycles for Type I controllers) before they strictly apply.
5. The theory applies to wells with little or no wellbore storage. Examples are artificially lifted wells where the annulus is separated with a packer (or a casing pump), or wells with a small producing annulus.

Acknowledgements

The authors would like to thank Chevron Australia for their permission to publish this work and the University of Adelaide for their cooperative research. The first author appreciates thoughtful reviews from Karen DiDomenicis and Gary Reedy (Chevron). This work is the opinion of the authors and does not necessarily reflect that of Chevron Australia.

Appendix A. Derivation of average pressure method for Type I controller

A.1. Convolved function

We repeat the equation for the convolved dimensionless pressure (Eq. (10)):

$$p_{Dn}(t_D, n) = \sum_{k=1,\text{odd}}^{n} \left\{ p_D\left[t_D - \frac{k-1}{2}(\Delta t_{Dp} + \Delta t_{Ds}) \right] + s \right\} - \sum_{k=2,\text{even}}^{n} \left\{ p_D\left[t_D - \frac{k}{2}\Delta t_{Dp} - \frac{k-2}{2}\Delta t_{Ds} \right] + s \right\} \tag{22}$$

Over C cycles, the average pressure can be calculated by integrating this function:

$$\overline{\overline{p}}_D = \frac{1}{C(\Delta t_{Dp} + \Delta t_{Ds})} \sum_{c=1}^{C} \left[\int \left(p_D(t_D) + s \right) dt_D \right]_{(c-1)\Delta t_{Dp} + c\Delta t_{Ds}}^{c(\Delta t_{Dp} + \Delta t_{Ds})} \tag{23}$$

Note that $\overline{\overline{p}}_D$ is averaged from the first cycle to cycle C, whereas the pressure $\overline{p}_D$ is only averaged over a single cycle. The relationship between cycles and production interval n is shown in Fig. 3 ($C = n/2$). This equation can also be expressed as

$$\overline{\overline{p}}_D = \frac{1}{C(\Delta t_{Dp} + \Delta t_{Ds})} \left(\sum_{c=1}^{C} \left[\int p_D[c(\Delta t_{Dp} + \Delta t_{Ds})]\, dt_D - \int p_D[(c-1)\Delta t_{Dp} + c\Delta t_{Ds}]\, dt_D \right] + sC\Delta t_{Dp} \right) \tag{24}$$

A.2. Average function over convolution interval

We aim to select a single, averaged function of

$$p_D(t_D) = a p_D(t_D) + bs \tag{25}$$

to represent the convolution in an averaged way. Integrating this function over C cycles,

$$\overline{\overline{p}}_D = \frac{1}{C(\Delta t_{Dp} + \Delta t_{Ds})} \left(a \int p_D[C(\Delta t_{Dp} + \Delta t_{Ds})]\, dt_D + b\left[\int s\, dt_D \right]_0^{C(\Delta t_{Dp} + \Delta t_{Ds})} \right) \tag{26}$$

It is now necessary to determine a and b by comparing the average values for the two functions in Eqs. (24) and (26). Setting the two equations equal and simplifying:

$$a \int p_D[C(\Delta t_{Dp} + \Delta t_{Ds})]\, dt_D + bsC(\Delta t_{Dp} + \Delta t_{Ds}) = \sum_{c=1}^{C} \left\{ \int p_D[c(\Delta t_{Dp} + \Delta t_{Ds})]\, dt_D - \int p_D[(c-1)\Delta t_{Dp} + c\Delta t_{Ds}]\, dt_D \right\} + sC\Delta t_{Dp} \tag{27}$$

The skin terms will drop out of the equation if we set

$$b = \frac{\Delta t_{Dp}}{\Delta t_{Dp} + \Delta t_{Ds}} \tag{28}$$

The a coefficient will now be analysed. Through rearrangement of the last equation, a may be expressed as

$$a = \sum_{c=1}^{C} \left\{ \int p_D[c(\Delta t_{Dp} + \Delta t_{Ds})]\, dt_D - \int p_D[(c-1)\Delta t_{Dp} + c\Delta t_{Ds}]\, dt_D \right\} \Big/ \int p_D[C(\Delta t_{Dp} + \Delta t_{Ds})]\, dt_D \tag{29}$$

We propose that

$$a \approx \frac{\Delta t_{Dp}}{\Delta t_{Dp} + \Delta t_{Ds}} \tag{30}$$

and seek to find the conditions for which this is approximately

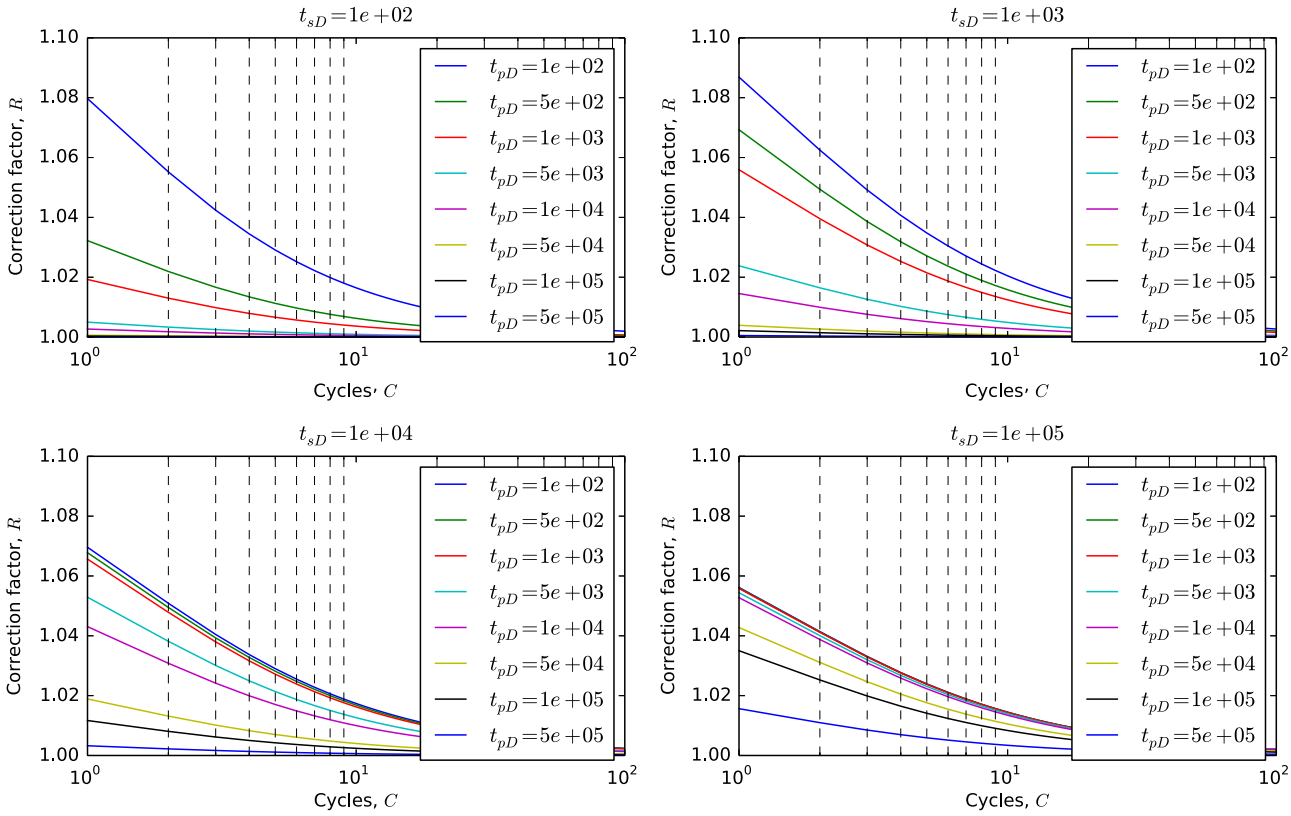

Fig. 10. Correction factor R, or ratio between Eqs. (24) and (26).

true. The quotient between Eqs. (24) and (26) will now be presented for the case of the Exponential Integral solution. The integral of the Exponential Integral is:

$$p_D = -\frac{1}{2}\,\mathrm{Ei}\left(-\frac{1}{4t_D}\right) \tag{31}$$

$$\int p_D t_D = -\frac{1}{2}\left[e^{-(1/4t_D)} + \left(\frac{1}{4}+t_D\right)\mathrm{Ei}\left(-\frac{1}{4t_D}\right)\right] + \text{const} \tag{32}$$

We will denote this quotient as R. The result is plotted across a range of dimensionless producing and shut-in times below (Fig. 10).

It is seen that for $C > 20$ cycles, in all cases, the value of R approaches unity. This is true to accuracy of greater than 2%. We have shown that this relationship is true for $\bar{p}_D$, it is also very straightforward to prove similarly for $\bar{p}_D$, if average pressure over a single cycle is plotted instead.

Appendix B. Derivation of average FBHP for Type II controller

We repeat the equation for the convolved dimensionless pressure of a Type II controller (Eq. (13)).

$$p_{Dn}(t_D, n) = \sum_{k=1,\text{odd}}^{n}\left\{p_D\left[t_D - \sum_{j=1}^{(k-1)/2}\Delta t_{(Dp)j} - \frac{k-1}{2}\Delta t_{Ds}\right] + s\right\} - \sum_{k=2,\text{even}}^{n}\left\{p_D\left[t_D - \sum_{j=1}^{k/2}\Delta t_{(Dp)j} - \frac{k-2}{2}\Delta t_{Ds}\right] + s\right\} \tag{33}$$

There is an advantage to using the logarithmic approximation to the line-source solution (Eq. (6)). We use this approximation for p_D, and rearrange the skin term so it only appears during production periods:

$$\frac{p_{Dn} - \left[(-1)^n + n \bmod 2\right]s}{1.152} = \sum_{k=1,\text{odd}}^{n}\log\left[2.246\left(t_D - \sum_{j=1}^{(k-1)/2}\Delta t_{(Dp)j} - \frac{k-1}{2}\Delta t_{Ds}\right)\right] - \sum_{k=2,\text{even}}^{n}\log\left[2.246\left(t_D - \sum_{j=1}^{k/2}\Delta t_{(Dp)j} - \frac{k-2}{2}\Delta t_{Ds}\right)\right] \tag{34}$$

We need to solve for the $\Delta t_{(Dp)j}$ terms. Now that the equation is in terms of the logarithmic solution, these terms are more easily isolated by removing the t_D variable. The following equation is obtained by examining the end of each production period. The below equation applies at the end of each production period only. The number of the production period, N, is defined as $N = (n+1)/2$.

$$\text{Solving for } \Delta t_{(Dp)N}\begin{cases} 0.4452_*10^{0.868(p_{Dp}-s)} = \Delta t_{(Dp)1}, & N = 1 \\ 0.4452_*10^{0.868(p_{Dp}-s)} = \dfrac{\prod_{i=1}^{N}\left[\sum_{j=i}^{N}\left(\Delta t_{(Dp)j}\right) + (N-i)\Delta t_{Ds}\right]}{\prod_{i=2}^{N}\left[\sum_{j=i}^{N}\left(\Delta t_{(Dp)j}\right) + (N+1-i)\Delta t_{Ds}\right]}, & N > 1 \end{cases} \tag{35}$$

An N-th order polynomial is generated $N > 1$, and may be solved using any equation solving method, such as the secant method. The most economical way to solve the equation using the secant method is in the form:

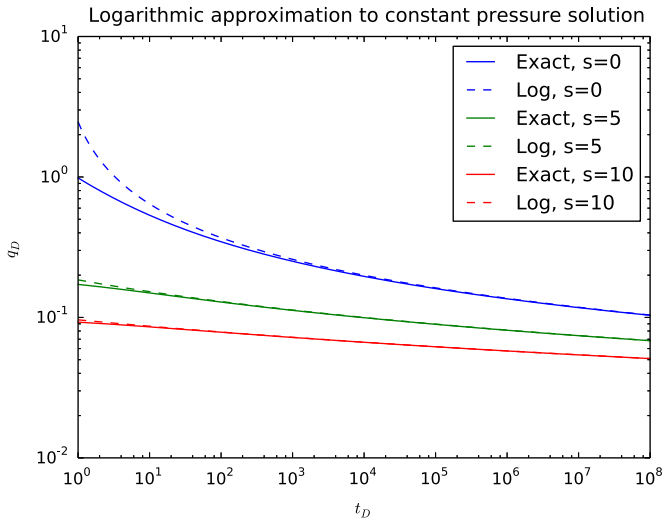

Fig. 11. Comparison between exact and logarithmic solutions for constant pressure drawdown.

$$f(\Delta t_{(Dp)N}) = \frac{\prod_{i=1}^{N}\left[\sum_{j=i}^{N}\left(\Delta t_{(Dp)j}\right) + (N-i)\Delta t_{Ds}\right]}{\prod_{i=2}^{N}\left[\sum_{j=i}^{N}\left(\Delta t_{(Dp)j}\right) + (N+1-i)\Delta t_{Ds}\right]} - 0.4452_{*}10^{0.868(p_{Dp}-s)} = 0 \tag{36}$$

which is solved successively at each N, knowing the producing time from prior cycles. The average equation for pressure from the 1st to last cycle,C is then calculated from:

$$\overline{p}_D = \frac{1.152}{\left(\sum_{c=1}^{C}\Delta t_{(Dp)c} + C\Delta t_{Ds}\right)}\sum_{c=1}^{C}\left\{\left(\sum_{j=c}^{C}\Delta t_{(Dp)j} + (C+1-c)\Delta t_{Ds}\right)\log\left(2.246\left[\sum_{j=c}^{C}\Delta t_{(Dp)j} + (C+1-c)\Delta t_{Ds}\right]\right) - \left(\sum_{j=c+1<C}^{C}\Delta t_{(Dp)j} + (C+1-c)\Delta t_{Ds}\right)\log\left(2.246\left[\sum_{j=c+1<C}^{C}\Delta t_{(Dp)j} + (C+1-c)\Delta t_{Ds}\right]\right) - \Delta t_{(Dp)c}\right\} \tag{37}$$

The results of this solution method were shown earlier in the paper in Fig. 5. It is possible to develop the exact pressures (rather than relying on the figure) using the equations in this section of the appendix.

Appendix C. Approximation of constant pressure solution

The constant pressure solution to the radial diffusivity equation with infinite outer boundary condition has been studied thoroughly. The exact solution at the wellbore is given as (Ehlig-Economides, 1979)

$$\tilde{q}_D(u) = \frac{K_1(\sqrt{u})}{\sqrt{u}\left[K_0(\sqrt{u}) + s\sqrt{u}K_1(\sqrt{u})\right]} \tag{38}$$

where K_0 and K_1 are modified Bessel functions of the second kind. The Stehfest (1970) algorithm can be used to numerically invert this solution into real space for q_D. At $t_D \geq 8\times10^4$, it has been shown that the logarithmic approximation below may be used with less than 1% error, which is simply inverse of the logarithmic solution.

$$q_D = \frac{1}{1.152\log(2.246t_D) + s} \tag{39}$$

The dimensionless groups in the equation above are consistent with those shown earlier. We plot a comparison between Eqs. (38) and 39 in Fig. 11.

Appendix D. Radial diffusivity equation in COMSOL multiphysics

The slightly compressible 1D radial diffusivity equation, in field units, is as follows:

$$\frac{1}{r}\frac{\partial}{\partial r}\left(r\frac{\partial p}{\partial r}\right) = \frac{\phi\mu c_t}{0.0002637k}\frac{\partial p}{\partial t} \tag{40}$$

The following boundary conditions are applied in a numerical model for constant rate production in a bounded reservoir. To model an infinite-acting case, r_e is modelled as a large number so that the transient does not reach the boundary over the period of interest.

$$p(r, t=0) = p_i \tag{41}$$

$$\left(\frac{\partial p}{\partial r}\right)_{r=r_e} = 0 \tag{42}$$

$$r\left(\frac{\partial p}{\partial r}\right)_{r=r_w} = \frac{141.2qB\mu}{kh} \tag{43}$$

For periods where the well is not producing, the boundary condition in Eq. (43) is changed to $q=0$. When skin factor is included,

$$p_w(t) = p(t) + s\frac{141.2qB\mu}{kh} \tag{44}$$

References

Acton, J.F., 1981. Pump-off Controller Application for Midway-Sunset Cyclic Steam Operations. SPE 9915.
Barry, D., Parlange, J.-Y., Li, L., Prommer, H., Cunningham, C., Stagnitti, F., 2000. Analytical approximations for real values of the Lambert W-function. Math. Comput. Simul. 53 (1), 95–103.
Clarkson, C.R., Qanbari, F., et al., 2014. A semi-analytical forecasting method for unconventional gas and light oil wells: a hybrid approach for addressing the limitations of existing empirical and analytical methods. In: SPE Annual Technical Conference and Exhibition, Amsterdam, Society of Petroleum Engineers.
COMSOL Multiphysics User's Guide 4.3a.
Corless, R.M., Gonnet, G.H., Hare, D.E., Jeffrey, D.J., Knuth, D.E., 1996. On the Lambert-*W* function. Adv. Comput. Math. 5 (1), 329–359.
Earlougher, R.C., 1977. Advances in Well Test Analysis. Richardson TX, Society of Petroleum Engineers of AIME.
Eckel, A.C., Abels, H.P., Merritt, R.A., 1995. Testing and practically applying pump-off controllers in a waterflood. In: Western Regional Meeting, Bakersfield. Society of Petroleum Engineers. pp. 241–248.
Ehlig-Economides, C.A., 1979. Well Test Analysis For Wells Produced At Constant Pressure (Ph.D. thesis). Stanford University.
Ehlig-Economides, C.A., Martinez, H., Okunola, D.S., et al., 2009. Unified pta and pda approach enhances well and reservoir characterization. In: Latin American and Caribbean Petroleum Engineering Conference, Cartagena. Society of Petroleum Engineers.
Gasbarri, S., Gupta, A., Wiggins, M., et al., 1997. Inflow of performance of reservoirs produced by intermittent lift methods. In: Annual Technical Meeting. Calgary, Petroleum Society of Canada.
Gladfelter, R., Tracy, G., Wilsey, L., et al., 1955. Selecting wells which will respond to production-stimulation treatment. Drilling and Production Practice.
Huff III, M.E., 1988. Pressure Transient Testing of Intermittent Gas Lift Wells (Master's thesis). Texas Tech University.
Kuchuk, F.J., 1990. Gladfelter deconvolution. SPE Form. Eval. 5 (3), 285–292.
Kucuk, F., Ayestaran, L., 1985. Analysis of simultaneously measured pressure and sandface flow rate in transient well testing. J. Pet. Technol. 37 (2), 323–334.
Lee, J., Rollins, J., Spivey, J., 2003. Pressure Transient Testing. SPE Textbook Series.

Richardson. Society of Petroleum Engineers.
McCoy, J., Becker, D., Podio, A., 1999. Timer control of beam pump run time reduces operating expense. In: Proceedings of the Annual Southwestern Petroleum Short Course. Lubbock, Texas Tech University, pp. 74–86.
Palacio, J., Blasingame, T., 1993. Decline Curve Analysis Using Type Curves: Analysis of Gas Well Production Data. Paper SPE 25909, pp. 12–14.
Rivero, R., Heintz, R., et al., 1975. Resteaming time determination case history of a steam-soak well in midway sunset. J. Pet. Technol. 27 (6), 665–671.
Sims, W., Frailing, W., et al., 1950. Lakeview pool, midway-sunset field. J. Pet. Technol. 2 (01), 7–18.
Stehfest, H., 1970. Algorithm 368: numerical inversion of Laplace transforms. Commun. ACM 13, 47–49.

5 Steady-State Productivity Analysis of Beam Pumped Oil Wells

The previous chapter solved the problem of transient reservoir flow for pump controllers undergoing start-stop operation. The method of superposition was was used to account for the variation in flow rate.

This problem of cyclic production is developed further in the next chapter. In the chapter, boundary dominated flow is considered (steady or pseudo steady state), which occurs after a long period of production. An alternative solution approach is used. Noting the cyclic nature of flow in long term production, harmonic solutions to the radial diffusivity equation are applied. This method draws from the reservoir pulse testing literature. This paper has been published in the Journal of Petroleum Science and Engineering.

Statement of Authorship

Title of Paper	Productivity Determination for Cyclic Production Using Steady State Harmonic Theory – Application to Artificial Lift Wells
Publication Status	☑ Published ☐ Accepted for Publication ☐ Submitted for Publication ☐ Unpublished and Unsubmitted w ork w ritten in manuscript style
Publication Details	O'Reilly, D.I., Haghighi, M., Flett, M.A. and Sayyafzadeh, M. 2019. Productivity Determination for Cyclic Production Using Steady State Harmonic Theory – Application to Artificial Lift Wells. *Journal of Petroleum Science and Engineering*. **172**: 787-805.

Principal Author

Name of Principal Author (Candidate)	Daniel O'Reilly
Contribution to the Paper	Problem formulation, derivation of mathematical model, preparation of graphs, writing the manuscript. Acted as corresponding author.
Overall percentage (%)	80%
Certification:	This paper reports on original research I conducted during the period of my Higher Degree by Research candidature and is not subject to any obligations or contractual agreements with a third party that would constrain its inclusion in this thesis. I am the primary author of this paper.
Signature	Date: 25 Nov 2020

Co-Author Contributions

By signing the Statement of Authorship, each author certifies that:

i. the candidate's stated contribution to the publication is accurate (as detailed above);

ii. permission is granted for the candidate in include the publication in the thesis; and

iii. the sum of all co-author contributions is equal to 100% less the candidate's stated contribution.

Name of Co-Author	Manouchehr Haghighi
Contribution to the Paper	Principal supervision of the work. Problem formulation, manuscript review and assessment.
Signature	Date: 01/12/2020

Name of Co-Author	Matthew Flett
Contribution to the Paper	Problem formulation, reviewed the manuscript and provided feedback
Signature	Date: 25/11/2020

Name of Co-Author	Mohammad Sayyafzadeh		
Contribution to the Paper	Problem formulation, reviewed the manuscript and provided feedback		
Signature		Date	26/11/2020

Journal of Petroleum Science and Engineering 172 (2019) 787–805

Contents lists available at ScienceDirect

Journal of Petroleum Science and Engineering

journal homepage: www.elsevier.com/locate/petrol

Productivity determination for cyclic production using steady state harmonic theory – Application to artificial lift wells

Daniel I. O'Reilly[a,*], Manouchehr Haghighi[b], Matthew A. Flett[c], Mohammad Sayyafzadeh[b]

[a] Chevron Australia Pty Ltd, The University of Adelaide, Adelaide, 5005, Australia
[b] The University of Adelaide, Adelaide, 5005, Australia
[c] Chevron Australia Pty Ltd, 250 St Georges Tce, Perth, 6000, Australia

ARTICLE INFO

Keywords:
Artificial lift
POC
Well testing
Pulse testing
Productivity index

ABSTRACT

In this paper we derive new solutions to the problem of harmonic flow in a bounded porous medium with inclusion of wellbore storage and skin. We present new solutions to varying radial boundary conditions and pay special attention to the cases of pseudo steady and steady state flow. These solutions have a new, special application to cyclically produced wells undergoing artificial lift under these conditions.

It is normally difficult for engineers to determine the Productivity Index (PI) or permeability of production wells undergoing cyclic operation. The relationship between bottomhole pressure, cycles, run time % and formation properties is quite non-linear, which we will illustrate here. However, the new theory allows simple determination of PI for such wells. The results will have application to artificially lifted wells or those wells intentionally pulsed in bounded reservoirs. A calculation method is shown for this type of problem along with field application.

1. Introduction

A large part of reservoir engineering literature concerns itself with constant-rate solutions to the governing diffusivity equations (Lee et al., 2003). These useful solutions are easily extended to other rate schedules via superposition or convolution. It is possible to modify the solutions to include wellbore storage and skin. There are some situations however, where other types of solutions may be practical. We turn our attention to two cases: pulse testing and wells produced in a cyclic manner for a long duration (e.g. artificially lifted wells on timer-type controls). It is common for artificial lift systems to produce intermittently (Chacin et al., 1994; Hernandez et al., 1999a; b; Kravits et al., 2011). For sucker rod pumps, the vast majority of wells are most economic when producing with the cyclic pump controllers (Eckel et al., 1995; McCoy et al., 1999).

Pulse testing is used in a reservoir with two or more wells where a transmitting well produces or injects intermittently and the pressure signal is recorded at an observation well. From this pressure signal, it is possible to interpret reservoir properties between the two wells (namely transmissibility kh/μ and storativity ϕc_t) (Kamal et al., 1975). Much of the original work in this area focused on a reservoir with homogeneous properties and pulses of only a few cycles, and used the conventional methods of constant-rate solutions (e.g. line-source well) combined with superposition of producing and shut-in periods (Brigham et al., 1970; Kamal et al., 1975). More recently, researchers have developed solutions for heterogeneous permeability profiles using a harmonic rate rather than the constant-rate solution (Ahn, 2012, Ahn and Horne, 2010, 2011).

By studying the pressure response in the reservoir from a harmonic-rate signal, it is possible to study the reservoir in a slightly different way. Rigorous solutions are readily available in the Laplace domain for a harmonic sine or cosine varying rate signal (Businov and Umrichin, 1960; Rosa, 1991; Streltsova, 1988; Kuo et al., 1972). These relationships define the pressure response as a well is open from its undisturbed state and its rate is varied harmonically. Eventually, after a few cycles (or periods), the transience dies out and the pressure signal seems to also vary harmonically. Specific solutions for this later-time behaviour has been captured in recent work (Ahn, 2012; Rosa, 1991; Rosa and Horne, 1997). It is possible to force solutions by assuming a periodic pressure solution signal, using the complex embedding approach. We also use that method here.

Reservoir studies in the harmonic domain have been gaining popularity when interpreting pressure data. Several researchers have used a Fourier transform of a cyclic pump rate to characterise groundwater reservoirs (Cardiff and Barrash, 2014, Fokker et al., 2012, 2013). Pumping tests in groundwater aquifers are considered important when

* Corresponding author.
E-mail address: dan.oreilly@chevron.com (D.I. O'Reilly).

https://doi.org/10.1016/j.petrol.2018.08.074
Received 15 January 2018; Received in revised form 10 August 2018; Accepted 27 August 2018
Available online 31 August 2018

calculating the size of the resource (Raghavan, 2004). In reservoir engineering, harmonic testing has also gained attention (Hollaender et al., 2002; Zenith et al., 2015), even in the area of water–oil displacement (Fokker and Verga, 2011). A similar harmonic approach has been used by Garcia et al. (2014), Garcia et al. (2016), Sousa et al. (2017a) and Sousa et al. (2017b), who focus on unstable flows introduced by wellbore effects, e.g. slugging. Recently, we have studied a rate transient type phenomenon seen in cyclic artificial lift wells when they are initially brought online (O'Reilly et al., 2016). The difference between our previous work and this study is that we now study the productivity of wells that have been online for a considerable duration and are in either pseudo-steady or steady state production. Our previous study only considered the case of an artificially-lifted well placed in an infinite acting reservoir. The periodic production effects for an infinite acting reservoir have also been studied elsewhere (Spivey et al., 1993).

There is also a distinct analogy between pulse testing and cyclic artificial lift wells that is understudied. The majority of work in pulse testing research focuses on the observation well and inference of reservoir properties in-between. Only recently, some researchers have also studied transient analysis of pulse testing at the oscillating well (Fokker et al., 2017, 2018). We believe that there is worth in applying the existing solutions *at the production well itself*, to infer its Productivity Index. In this way it is possible to understand productivity indices of some wells that may previously not have been considered – e.g. artificial lift wells that are opened and closed based on a timer or bottomhole pressure. It is not accurate to assume that said wells are producing at constant pressure and hence methods are needed to correct for the cyclic operation. The classic P.I. equations assume constant, stabilised BHP. At the oscillating well itself, wellbore storage and skin may be very important (Ogbe et al., 1987).

The solutions in the current paper build on the prior work in the area of pulse testing. We show new solutions for various boundary conditions where both wellbore storage and skin are considered.

2. Cyclic production & injection

There are numerous reasons that a well may need to be produced intermittently. The first reason is intentional pulse testing; this is a classical well test method used to infer reservoir properties in between a producing and observing well. Secondly, wells producing under artificial lift are frequently controller by a computer to produce for specific durations only. Otherwise, Production Operators may have practical reasons for manually switching wells on and off at defined intervals: e.g. power requirements, night/day operations (Fokker et al., 2013), or specific well feed demands.

2.1. Artificial lift

Artificial lift is key to the economic production of many oilfields. It can be used effectively in reservoirs with or without pressure support (e.g. with aquifer or waterflooding). The purpose of an artificial lift installation is to reduce the bottomhole pressure at the producing well. The pressure drop across the entire reservoir then inceases, leading to higher production rates. This is true of reservoirs producing at constant boundary pressure or the pressure depletion, although the cases are mathematically treated separately in this paper. Finally, since artificial lift operations are often run intermittently, a key part of our work is to model the time-varying nature of wells with start/stop style controllers.

2.2. Sucker rod pump off controllers

Many types of artificial lift use Pump Off Controllers (POCs) or similar to control the operation of the well:

- Sucker Rod Pumps (either timer or load-cell controllers)
- Plunger Lift (timer based or pressure-based controllers)
- Gas Lift Injection (intermittent lift controllers)

Sucker rod pumps are pervasive in the petroleum industry. With fixed-speed motors, often the inflow of the well does not perfectly match the outflow of the pump. Therefore, the controller runs the well at a constant rate until the bottomhole pressure reaches a minimum value and the well is shut in for a fixed duration. More information is provided in other references regarding their operation (Eckel et al., 1995; McCoy et al., 1999; O'Reilly et al., 2016). Some sucker rod pump POCs simply operate on a timer control.

It is worth discussing the phenomenon of "fluid pound" briefly and how it relates to the solutions in the current paper. During intermittent production, just prior to the shut-in period, the well is at maximum/peak drawdown and the bottomhole pressure reaches its minimum value. We refer to that value in this paper as the "fluid pound pressure", because for Sucker Rod Pumped wells, the POC will switch the well off just before the fluid level reaches the pump intake, and the pump plunger begins to pound against this fluid level. Using this value is certainly of interest to engineers as it is easily determined from the downhole completion type and pump setting depth. When we develop solutions and type curves in the following sections, predicting the pound pressure will allow correlation of formation properties with the pound pressure and operation characteristics (on time, off time) of a particular well. More detail on fluid pound can be found in another reference (O'Reilly et al., 2016).

3. Mathematical formulation

We will now summarise the derived solutions for harmonic rate oscillations and show how they can be applied to well producing in pulses. All these solutions are for the cases of radial flow and include wellbore storage and skin. The solution will consist of two parts:

- Oscillating-rate part of solution
- Constant-rate part of solution

For a perfect harmonic oscillation, the rate at the surface of a well can be expressed as

$$q = q_{\omega}(t) + q_{\text{const}} \tag{1}$$

For an arbitrary periodic signal, a Fourier series can be used to describe the oscillating component, i.e.

$$q = \sum q_{\omega}(t) + q_{\text{const}} \tag{2}$$

According to superposition of solutions, the pressure drop at the wellbore can be expressed as the combination of the two pressure solutions:

$$p_w = \sum p_{w,\omega}(t) + p_{w,\text{const}} \tag{3}$$

where the subscript w indicates that the pressure response is taken at the wellbore. The nomenclature for a pulsing well is shown in Fig. 1. We use this figure as the basis for forming our dimensionless units. The production well produces at surface rate q_0 for duration τ. The well then ceases production until the end of its first period (or cycle) at time T. The portion of time that a well spends online, referred to as the Run Time (RT), follows as RT $= \tau/T$.

Regarding the solution methods used here for the harmonic parts of the solution, they build on a similar method shown in another reference (Ahn, 2012). The solutions used in this paper will include the effect of both wellbore storage and skin, a necessity for modelling results at the production well.

3.1. Pulse wave Fourier Series

A pulse wave is a type of wave where the amplitude varies between

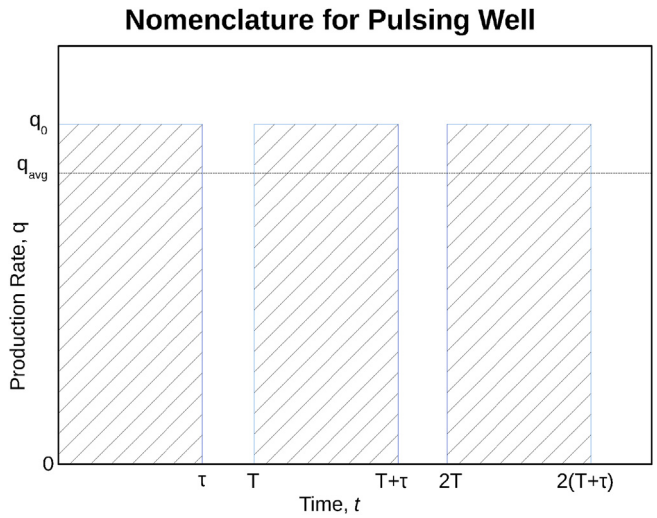

Fig. 1. Nomenclature for an intermittent production well.

either 0 and 1 at fixed times, which need not be symmetrical like the square wave. The wave is approximated through the use of a Fourier Series expansion given by the equation below. The Fourier approximation is useful as it allows us to use a sum of the harmonic solutions (in terms of cos$t$) to calculate a pressure response for a pulse wave.

$$f(t) = \frac{\tau}{T} + \sum_{n=1}^{\infty} \frac{2}{n\pi} \sin\left(\frac{\pi n \tau}{T}\right) \cos\left(\frac{2\pi n}{T} t\right) \tag{4}$$

Rather than modelling $n \to \infty$, n is limited to value $n_{\max}$ in calculations. The fixed part of this signal, τ/T, corresponds to the constant-rate portion of the pressure solution that will be applied. The harmonic term, cos$t$, will apply to the harmonic-rate solution. Fig. 2 shows $n_{\max}$ of 2, 10 and 50 for the pulse wave and how closely they approximate the shape of the wave.

The production rate will be considered as a pulse wave:

$$q(t) = q_0 f(t) = q_0 \left[\frac{\tau}{T} + \sum_{n=1}^{\infty} \frac{2}{n\pi} \sin\left(\frac{\pi n \tau}{T}\right) \cos\left(\frac{2\pi n}{T} t\right) \right] \tag{5}$$

It is proposed that the pressure relationship based on the above rate, in dimensionless units, is thus:

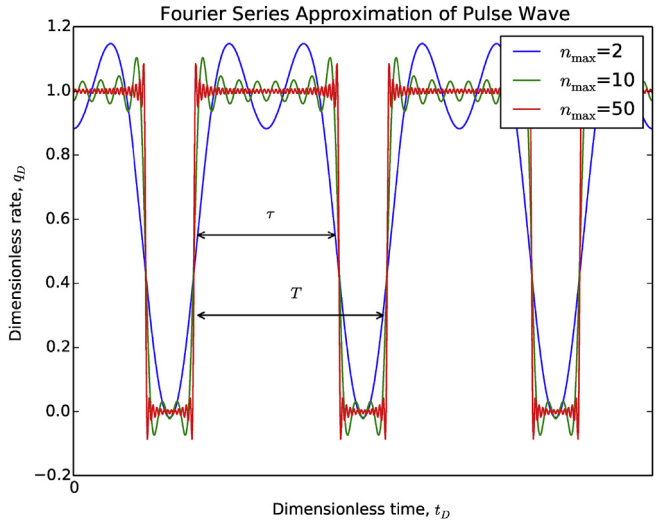

Fig. 2. Fourier Series approximation of the pulse wave used to model cyclic POC wells.

$$p_{wD}(t_D) = \frac{\tau_D}{T_D} p_{wD,\text{const}} + \sum_{n=1}^{\infty} \frac{2}{n\pi} \sin\left(\frac{\pi n \tau_D}{T_D}\right) p_{wD,\omega}(\omega_D, t_D) \tag{6}$$

with $\omega_D = \frac{2\pi n}{T_D}$.

In this text, all dimensionless groups used are defined in Appendix A.

3.2. Transient radial flow

Solutions for the case of transient response (a well placed online in a reservoir without bounds) will first be reviewed for completeness, though this work largely focuses on pseudo steady and steady state cases. The full derivations are available in the appendices. The cosine harmonic part of the solution for a boundless reservoir is:

$$p_{wD,\omega}(t_D) = \text{Re}\left\{ -\frac{s\sqrt{i\omega_D} K_1(\sqrt{i\omega_D}) + K_0(\sqrt{i\omega_D})}{C_D \omega_D K_0(\sqrt{i\omega_D}) + \frac{\omega_D K_1(\sqrt{i\omega_D})}{\sqrt{i\omega_D}}} i e^{i t_D \omega_D} \right\} \tag{7}$$

This solution for the pressure response depends on the production rate angular frequency, ω. The constant-rate part of the solution for IARF is:

$$p_{wD,\text{const}}(t_D) = -\frac{1}{2}\text{Ei}\left(-\frac{1}{4t_D}\right) + s \tag{8}$$

If including WBS and skin, the constant-rate solution is (Agarwal et al., 1970):

$$p_{wD,\text{const}}(t_D) = \int_0^{\infty} \frac{(1 - e^{-u^2 t_D}) J_0(u)}{u\left\{\left[1 - u^2 C_D s + \frac{1}{2}\pi u^2 C_D Y_0(u)\right]^2 + \left[\frac{1}{2}\pi u^2 C_D J_0(u)\right]^2\right\}} \text{d}u \tag{9}$$

Other solutions also exist in Laplace space and may be numerically inverted into the real plane if preferred.

3.3. Pseudo steady state radial flow

The PSS regime occurs during long-time production from a closed, bounded reservoir. For continually oscillating production, the constant part of production (q_{const} in Equation (1)) is treated as PSS. For the bounded reservoir case, the cosine harmonic part of the solution is:

$$p_{wD,\omega}(t_D) = \text{Re}\left\{ \frac{e^{i t_D \omega_D}[I_1(r_{eD}\sqrt{i\omega_D})(s\sqrt{i\omega_D} K_1(\sqrt{i\omega_D}) + K_0(\sqrt{i\omega_D})) + K_1(r_{eD}\sqrt{i\omega_D})(I_0(\sqrt{i\omega_D}) - s\sqrt{i\omega_D} I_1(\sqrt{i\omega_D}))]}{[iC_D\omega_D K_0(\sqrt{i\omega_D}) + \sqrt{i\omega_D} K_1(\sqrt{i\omega_D})] I_1(r_{eD}\sqrt{i\omega_D}) + [iC_D\omega_D I_0(\sqrt{i\omega_D}) - \sqrt{i\omega_D} I_1(\sqrt{i\omega_D})] K_1(r_{eD}\sqrt{i\omega_D})} \right\} \tag{10}$$

At this stage, the solution to harmonic production is in terms of the original definition of dimensionless pressure, i.e. with respect to initial reservoir pressure p_i. In this paper we will work with the drawdown with respect to the average reservoir pressure, $p_{wf} - \overline{p}$. This has the advantage of being independent of time, apart from the variation within a single cycle. To convert the solution, we define:

$$\overline{p}_{wD,\omega}(t_D) = p_{wD,\omega}(t_D) - p_{D\text{avg},\omega}(t_D) \tag{11}$$

The variable $\overline{p}_{wD,\omega}(t_D)$ is defined with respect to the absolute average reservoir pressure. The two terms on the right hand side are both dimensionless with a baseline pressure of p_i. The evaluation of the second term, the average dimensionless reservoir pressure, is covered in the Appendix.

The constant-rate part of the solution, defined as the second term on the right side of Equation (3), will now be discussed. Since it is customary in the analysis of PSS depletion to use the average reservoir pressure, $\overline{p}$. Using that in our dimensionless definition, the constant-

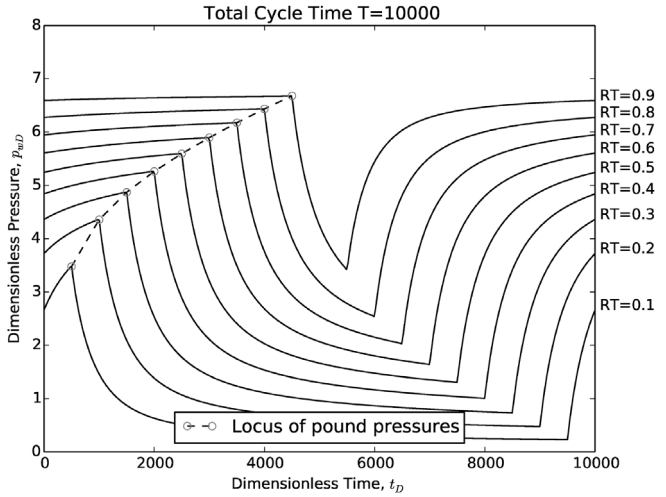

Fig. 3. Locus of fluid pound pressures across varying RT %. $r_{eD} = 10^3$, $T_D = 10^4$, $C_D = 10^2$, $s = 0$. Steady-state boundary condition at.r_{eD}.

rate part of the solution is:

$$\overline{p}_{wD,\text{const}} = \ln(r_{eD}) - \frac{3}{4} + s \tag{12}$$

3.4. Steady state radial flow

Steady state radial flow occurs when pressure at the external radius, r_e, is maintained at the initial reservoir pressure p_i over time. The cosine harmonic part of the solution is:

$$p_{wD,\omega}(t_D) = \text{Re}\left\{\frac{\begin{matrix} e^{it_D\omega_D}[K_0(r_{eD}\sqrt{i\omega_D})(s\sqrt{i\omega_D}I_1(\sqrt{i\omega_D}) - I_0(\sqrt{i\omega_D})) \\ + I_0(r_{eD}\sqrt{i\omega_D})(s\sqrt{i\omega_D}K_1(\sqrt{i\omega_D}) + K_0(\sqrt{i\omega_D}))] \end{matrix}}{\begin{matrix} \sqrt{i\omega_D}\,[(I_1(\sqrt{i\omega_D}) - C_D\sqrt{i\omega_D}I_0(\sqrt{i\omega_D}))K_0(r_{eD}\sqrt{i\omega_D}) \\ + (C_D\sqrt{i\omega_D}K_0(\sqrt{i\omega_D}) + K_1(\sqrt{i\omega_D}))I_0(r_{eD}\sqrt{i\omega_D})] \end{matrix}}\right\} \tag{13}$$

The constant-rate part of the solution is:

$$p_{wD,\text{const}} = \ln(r_{eD}) + s \tag{14}$$

Fig. 3 shows an example chart of solutions across varying run time % for a particular set of reservoir properties with the steady state boundary condition undergoing pulsing production. These curves were prepared using Equations (13) and (14), using a Fourier Series approach for p_{wD} as detailed by Equation (6). Each curve represents a well producing at a particular run time %, ranging from 10 to 90%. Marked on the curve at the peak of each cycle is the fluid pound pressure. As discussed earlier, this is the drawdown pressure experienced at the sandface just prior to the well closing in. A locus of pound pressures has been highlighted for varying run time percentages. We have calculated this locus for a variety of operating conditions later in the article, which will be useful when studying beam pump performance.

It is worth noting that numerical verification of the Steady State solution presented previously is discussed in Appendix D.

3.5. Evaluation of bessel functions

A high order precision computing environment will be required to evaluate the Bessel and hypergeometric functions in the equations. Normal floating-point precision (32 or 64 bit) will not suffice due to the large values that can result from the Bessel functions. The mpmath toolkit in Python was used for this purpose (Jones et al., 2001; Oliphant, 2007). Other mathematics packages are also suitable (e.g. Mathematica or Maple).

Table 1
Required data for permeability solution.

1	Bottomhole fluid pound pressure during each cycle, p_p
2	Reservoir pressure at the boundary or initial reservoir pressure, p_i or p_e
3	Reservoir constants: c_t, h, ϕ, μ, B, r_e, r_w, C (if applicable)
4	Flow rate during production part of cycle, q_0. See Fig. 1 for clarification – note $q_0 = q_{\text{avg}}/$ RT.
5	Duration of cycle, T, and run time %

4. Permeability solution technique for cyclic artificial lift wells

A special solution technique is developed in this section for artificially lifted wells under normal steady-state or pseudo-steady-state operation where only the fluid pound pressure is known (i.e. the pressure at which the well stops producing fluids during each cycle, which would be at maximum drawdown pressure). This solution method utilises the pressure-frequency equations previously derived to determine a well's productivity. From the known well performance data, the Productivity Index or average permeability is determined for the well. We assume the reservoir and performance data are available as per Table 1.

The dimensionless pressure at the moment of fluid pound, when the well is shut-in, is expanded as:

$$p_{wDp}(T_D, \text{RT\%}, C_D, r_{eD}) = k^*\frac{\Delta p h}{qB\mu} \tag{15}$$

The unknown to be solved for in the equation below is permeability, k^*. This permeability is linked to Productivity Index and its value, by necessity, incorporates any wellbore skin (the same definition is used in Lee et al. (2003)). It is not necessarily the true formation permeability since both factors are included. We solve the expanded equation using successive substitution, which has converged for all attempts tested using reasonable permeability initial guesses:

$$p_{wDp}\left(k^*\frac{0.0002637T}{\phi\mu c_t}, \text{RT\%}, \frac{0.894C}{\phi c_t r_w^2 h}, \frac{r_e}{r_w}\right) = k^*\left[\frac{(p_e - p_p)h}{141.2qB\mu}\right] \tag{16}$$

p_e should be replaced by $\overline{p}$ in the PSS case. This equation is of the form $f(ak^*, b, c, d)/k^* = e$, where a to e are constants. In Equation (16), the p_{wDp} expression is formed from the appropriate Fourier Series equations developed in Section 3. The solution steps below are followed:

1. Start with an initial guess of permeability, k^*. Field history and knowledge of wellbore impairment/stimulation may assist.
2. Evaluate Equation (16) using chosen reservoir model from earlier sections
3. Calculate error and iterate using a numerical method (e.g. successive substitution)

Once the permeability has been calculated, Productivity Index (PI) can be calculated from the equation below for the Steady State case:

$$J_{SS} = \frac{q}{p_e - p_{wf}} = \frac{k^*h}{141.2B\mu\ln\left(\frac{r_e}{r_w}\right)} \tag{17}$$

or for the Pseudo Steady State case:

$$J_{PSS} = \frac{q}{\overline{p} - p_{wf}} = \frac{k^*h}{141.2B\mu\left[\ln\left(\frac{r_e}{r_w}\right) - 3/4\right]} \tag{18}$$

These expressions are rearrangements of dimensionless Equations (12) and (14). Both equations have been expressed in oilfield units and are consistent with our definition of zero skin impairment (skin is included implicitly in the average permeability k^*).

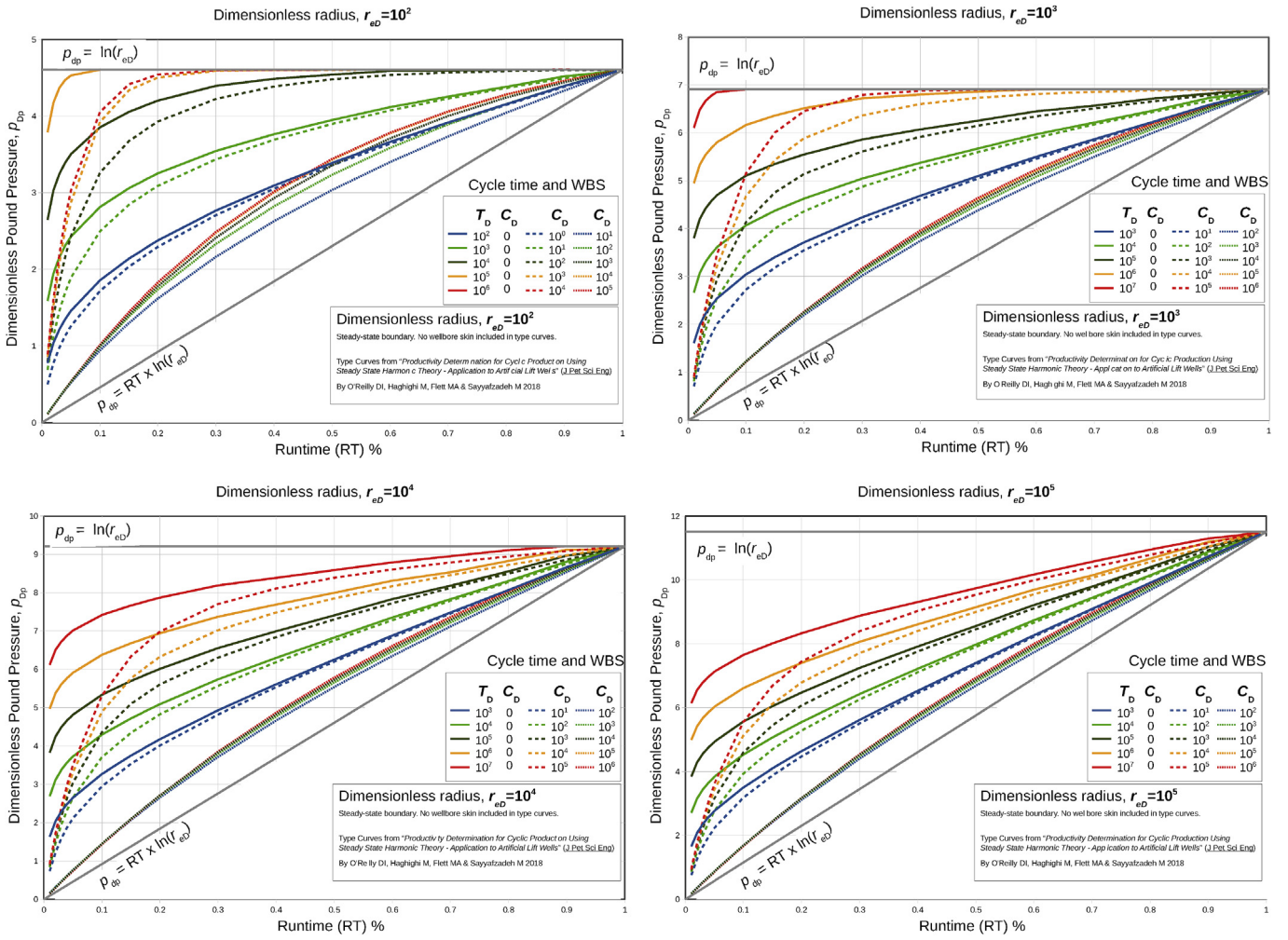

Fig. 4. Steady-state reservoir type curves for cycling well.

5. Fluid pound type curves for cyclic artificial lift wells

This section develops approximate type curves following from the solution technique described in the last section. It is an alternative to Section 4. If greater detail is needed with wellbore storage coefficients or dimensionless drainage radii, it is suggested that the full solution technique in the last section is used. Since the solution technique described in the last section does not require wellbore skin, $s = 0$ is used in all type curves.

Let us first re-examine Fig. 3, to gain an appreciation of the behaviour of dimensionless pressure vs. time for an intermittent well. All the curves in this figure have total cycle time $T_D = 10{,}000$, $r_{eD} = 10^3$ and $C_D = 10^2$. Nine curves are plotted, for varying runtime (τ/T) percentages ranging from 0.1 to 0.9. On the drawdown component of production, the maximum value of dimensionless pressure (i.e. maximum drawdown) is encountered for each curve just prior to shut-in. These points are marked with hollow circles for each case. A line is drawn through all points and is denoted the locus of fluid pound pressures. This figure illustrates how the equations from Section 3 are used to build a locus of fluid pound pressures for charting purposes.

Fig. 4 contains numerous charts for varying dimensionless external radius, total cycle time and wellbore storage for the steady state boundary condition. Fig. 6 condenses these charts into a single chart for the case of $C_D = 0$. Figs. 5 and 7 contain the same graphs for the closed outer boundary condition. Usage of the charts is similar to the iterative solution technique in Section 4, but follows a graphical method instead. The difference is that p_{wDp} is evaluated using the graph rather than using equations from Section 3.

6. Discussion

By inspecting the type curves and equations for the Steady-State boundary condition, we are able to draw conclusions for the manner in which cyclic wells operate with regards to bottomhole pressure. For the most part, the same general conclusions can be drawn from the PSS curves, with differences noted in the end of the section. In the type curves (Fig. 4), two limiting lines are drawn: $p_{Dp} = \ln r_{eD}$ and $p_{Dp} = \tau/T \ln r_{eD}$. The top curve represents the case of pure constant rate production. The lower bounding curve of slope τ/T represents a bottomhole pressure that corresponds to an "average rate" case, where the regular inflow performance relationship $\ln r_{eD}$ (for steady state) is multiplied by the fraction that the well is producing. Between those two curves, the maximum pound pressure for various operating conditions are marked as curves.

6.1. Effect of cycle time T_D and run time % (τ/T)

Let us first consider the impact of run time. All other parameters constant, the effect of increasing runtime % is a monotonic but non-linear increase in dimensionless bottomhole pound pressure (i.e. increase in drawdown at the well at the peak of the cycle). As RT tends to 100%, p_{wDp} approaches the constant-rate solution $\ln r_{eD}$, as should be expected. Now let us consider the impact of total cycle time T_D. Observing the chart for dimensionless radius $r_{eD} = 10^2$, it can be seen

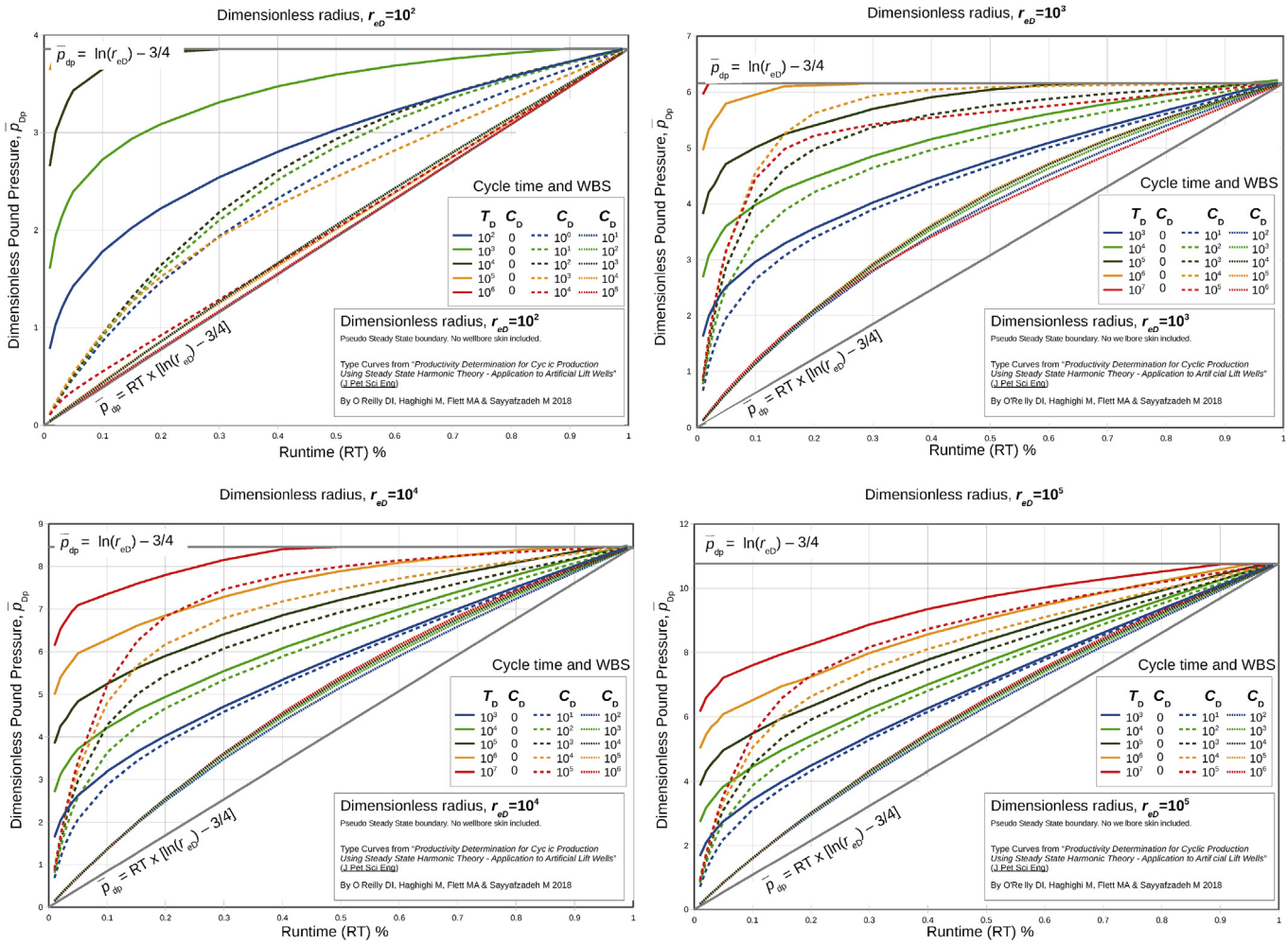

Fig. 5. Pseudo-steady-state reservoir type curves for cycling well.

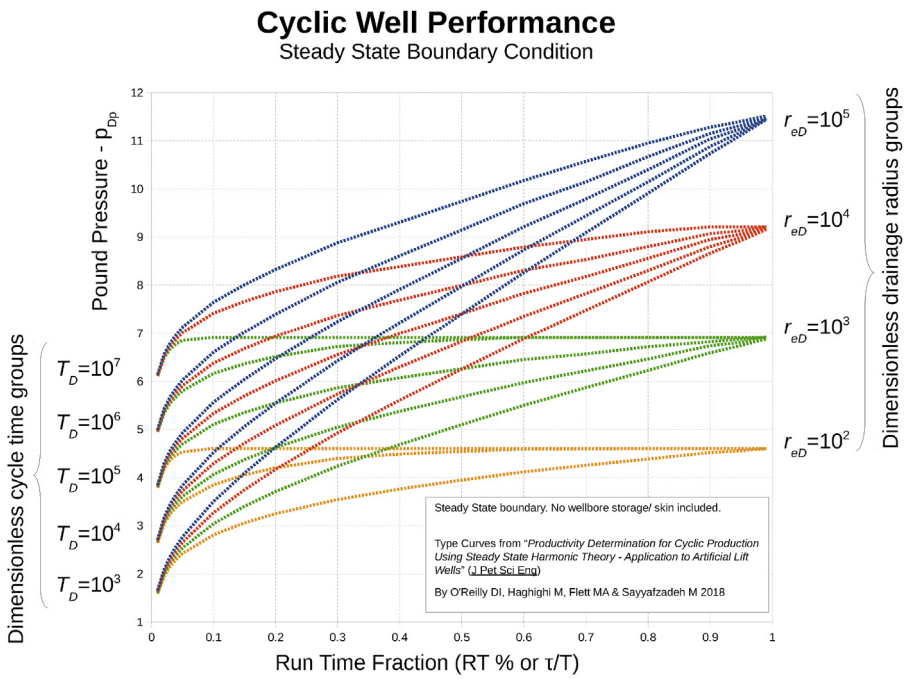

Fig. 6. Steady-state reservoir type curves for cycling well (zero wellbore storage and skin).

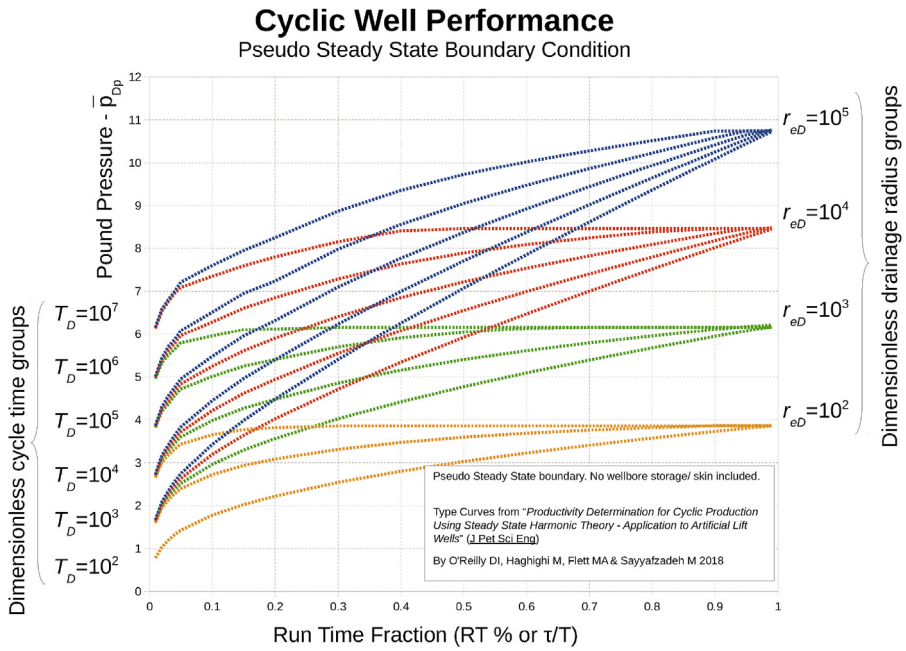

Fig. 7. Pseudo-steady-state reservoir type curves for cycling well (zero wellbore storage and skin).

that the highest value of cycle time, $T_D = 10^6$ (with $C_D = 0$), completely overlies the value for constant rate production, $p_{wDp} = \ln r_{eD}$. Conversely, lower values of cycle time tend towards the average-rate curve, $p_{wDp} = \tau/T \ln r_{eD}$. It is clear in these cases that the higher cycle time leads to an increased effect of the outer dimensionless boundary pressure, which cannot be exceeded due to physical constraints of the reservoir.

Another way to show the effect of T_D is via the use of the transfer function, H. This value is defined in Appendix E, where its limiting behaviours are discussed and proven mathematically. The transfer function denotes the amplitude of the oscilating pressure signal. In Fig. 8, some example cases are shown for H vs. frequency of production rate variation. It is seen graphically that, at lower values of production frequency (i.e. higher T_D production time), the pressure transfer function tends to a constant value, which as discussed in the previous paragraph is the constant-rate production solution. It is also seen that the infinite-acting case matches the long-time pressure responses at higher frequencies (shorter T_D). The transfer function approach is frequently used in the pulse testing literature.

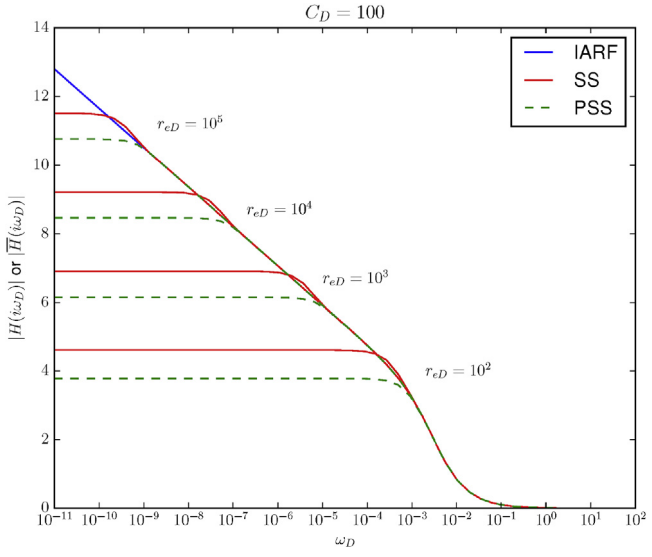

Fig. 8. Transfer function $|H|$ for IARF and SS cases and $|\overline{H}|$ for PSS case. In these curves $C_D = 100$ and $s = 0$.

6.2. Effect of drainage radius r_{eD}

Each of the four charts in Fig. 4 has been prepared for a fixed value of r_{eD}. All other parameters constant, it is observed that increasing the drainage radius increases the dimensionless fluid pound pressure, or increases the peak drawdown on the well prior to shut-in. Perhaps these results may be useful to understand when planning the density of development well spacing or understanding pump behaviour in differently drilled fields.

6.3. Effect of wellbore storage C_D

Let us now consider the impact of wellbore storage. By considering a case of constant T_D and r_{eD}, different cases of C_D can be compared in Fig. 4. In all cases it is observed that an increase in the dimensionless wellbore storage coefficient causes a decrease of the dimensionless fluid pound pressure, tending towards the limiting case of $p_{wDp} = \tau/T \ln r_{eD}$. This is because the effect of wellbore unloading and after flow effectively "smear" out the producing and shut-in periods; the rate at the sandface does not cease completely at any point but rather continues to flow in diminishing amounts during the shut-in period and vice versa during operation. This is why the curves begin to approach the average rate curve on the bottom of the graph.

6.4. Difference between PSS and SS performance

For the steady-state boundary condition, pressure is maintained at the external radius while the pressure at the inner radius may fluctuate during a cycle. Constant pressure at the outer boundary is maintained by a time-varying flux across the outer radius. In the steady-state type curves, as T_D increases, the maximum pound pressure approaches $\ln r_{eD}$, which is the normal constant-rate solution. We explain this behaviour by the damping effect that the flux across the boundary has during a cycle; all produced fluid is replaced at the boundary to maintain the constant pressure. It is therefore not possible to exceed the dimensionless inflow characteristics of the constant-rate SS solution. The same is not true of the pseudo-steady case.

For a net withdrawal of reservoir fluids, the pressure in the reservoir will deplete over time for the PSS boundary condition. Fluids are not replenished across the boundary as they are in the steady state case. In this work and in many other references, the effect is decoupled from time by introducing the average reservoir pressure $\overline{p}$ (which itself is a function of time) into the drawdown equations. The difference in stabilised constant-rate drawdown equations can be seen by comparing Equations (12) and (14) (it is a difference of constant -0.75). The concept was extended to the harmonic part of our solutions, although the formulation in Appendix C is more complicated. As such, the type curves between cases appear very similar, with a few subtle differences. The bounding lines on the charts will tend towards $\ln(r_{eD}) - 3/4$ in the PSS case rather than $\ln(r_{eD})$, as should be expected.

Almost all of the same conclusions can be drawn as for the Pseudo Steady State case, but the relationship with wellbore storage appears more complicated. For the case of $r_{eD} = 10^2$, the high C_D cases tend towards the limiting drawdown pressure boundary much more so than they did in the constant pressure outer boundary cases. Since the graph refers to the maximum fluid pound pressure at the end of the production period in the cycle, our interpretation is that the steady state boundary has enough replenishment across the boundary to allow for additional drawdown once the buildup period has ceased and production resumes. This effect is not as obvious for the higher values of dimensionless outer radius.

7. Field case study

To demonstrate field application of the new technique, field data from sucker rod lift wells will now be studied. The wells in question are pumping from a mature waterflood reservoir and use the pump controllers discussed earlier in Section 2.2. These controllers allow the well to produce at a constant rate until bottomhole pressure reaches a defined fluid pound pressure, and then well is shut for a fixed duration. During normal and prolonged operation, these wells usually produce for a fixed on-time τ. Two example wells are studied: one using Steady State analysis and the other using Pseudo Steady State. Both wells' productivity indices are benchmarked against results calculated from conventional PBU analysis.

7.1. Well data

Well data and reservoir properties from two oil production wells, OP-1 and OP-2, are shown in Table 2. The OP-1 well is in an area of the reservoir where the pressure is well maintained by surrounding water injection wells. OP-2, on the other hand, is in a structurally compartmentalised area that receives minimal waterflood support. As a result, we consider the wells to be in Steady State and Pseudo Steady State (bounded) flow regimes respectively. These cases will illustrate both solution types.

Several hundred wells currently operate within this field and generally operate with a cycle time of $T \approx 1$hrs. This is an operational preference and has been established through years of experience with sucker rod pumps. Both wells in the example fit that guide. Reservoir quality is low in the field – often less than 1mD – which is typical from the original middle marine, bioturbated depositional environment. It is normal for wells to require hydraulic fracturing prior to production. While the static reservoir properties for OP-2 are similar, the reservoir pressure and fluid withdrawal are both lower (the daily rate for OP-2 is actually 60 stb/d, since its producing rate q_0 must be multiplied by the fraction run time, RT). This is a result of the bounded depletion. Unfortunately this well does not benefit from the same pressure support that OP-1 does.

Table 2
Field data interpretation using proposed method.

	OP-1	OP-2
Reservoir data		
Inflow mechanism	Steady State	Pseudo Steady State
Reservoir pressure (psi)	p_e = 1400	$\overline{p}$ = 550
p_p (psi)	150	100
r_e (ft)	530	530
r_w (ft)	0.21	0.21
τ (hrs)	0.7	0.3
T (hrs)	1.0	1.0
C (bbl/psi)	0.01	2.5×10^{-3}
q_0 (stb/d)	163	200
B (rb/stb)	1.2	1.2
ϕc_t (cP/psi)	1×10^{-6}	1×10^{-6}
h (ft)	100	45
μ (cP)	0.6	0.6
Calculated ratios		
r_{eD}	2.5×10^3	2.5×10^3
RT %	0.7	0.3
C_D	2.0×10^3	1.0×10^3
T_D/k^* (1/mD)	1.0×10^4	1.0×10^4
p_{wDp}/k^* (1/mD)	7.57	0.99
Proposed method result		
k^* (mD)	**0.8**	**5.2**
PI (stb/d/psi)	**0.097**	**0.32**
Comparison methods		
Wireline log k (mD)	Fig. 10	–
Buildup PI (stb/d/psi)	**0.08**	**0.35**

The simplifications to multiphase transient analysis made by Perrine and Martin (Martin et al., 1959; Perrine et al., 1956) are appropriate for use in this field; that is to say, spatial saturation and pressure gradients are sufficiently small across the field. Fortunately in the case of mature waterflood reservoirs where the saturation front has long but broken through, saturation across the reservoir is reasonably uniform and the assumptions have a strong basis. The Perrine and Martin simplification allows each phase to be studied separately using the classical pressure transient analysis techniques (yielding k_o, k_w and k_g for the three phases). For convenience the fluid rates considered in these examples are combined liquid rates (oil and water).

A well completion diagram for the OP-1 well is shown in Fig. 9. During production periods, liquids are displaced inside the tubing and produced at the surface where they are combined with annular gas in a flow tee. During normal production for this well, the stagnant liquid level is located between the pump intake (marked red in the diagram) and the surface. At the end of a producing period (after τ hours), the liquid level recedes to the pump intake and production ceases. A more thorough description of this operation is discussed in other references (O'Reilly et al., 2016). This fluid pound (or onset of) pressure at perforation datum depth, shown as p_p in Table 2, has been calculated by combining the gas and liquid fluid gradients at this liquid level with the known THP. As per the sucker rod completion diagram, the wellbore storage has been calculated for a moving annular liquid level (Lee et al., 2003):

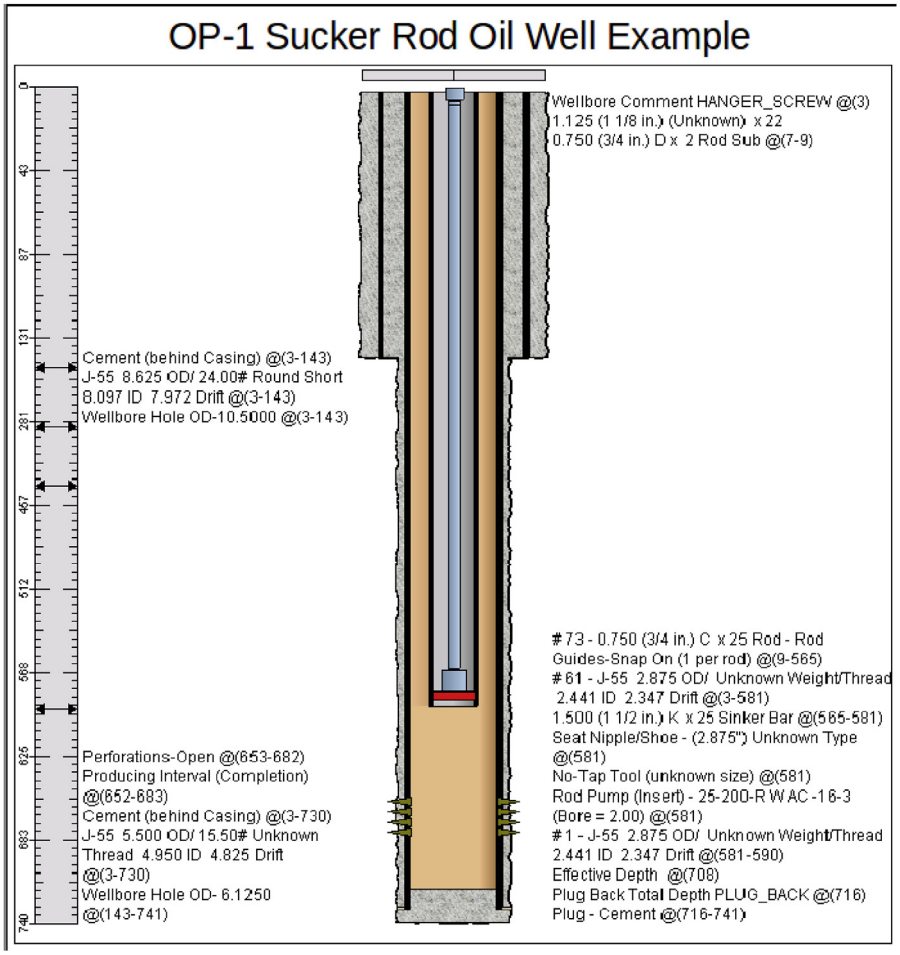

Fig. 9. Well Completion diagram for OP-1 beam pump production well.

$$C = \frac{25.65 A_{wb}}{\rho} \frac{\text{bbl}}{\text{psi}} \tag{19}$$

with A_{wb} in ft^2 and ρ in lb/ft^3.

The openhole well logs for OP-1 are shown in Fig. 10. Of particular interest in this log is the formation permeability, which is marked in the fourth track. This permeability log was calculated from a porosity-permeability crossplot relationship derived from core samples and will be useful to compare against the average permeability derived from production using our analysis technique. The porosity log is derived from the standard density log. The perforation interval is also marked. The completion diagram and well logs for OP-2 have not been shown in this paper, however they are similar.

7.2. Solution using computer iterative technique

The parameters required to calculate formation permeability k^* are shown in the "Calculated ratios" rows in Table 2. As discussed in Section 4, an initial estimate of permeability is required to begin the solution process. For both wells, 10 mD was used as the initial guess; this value may be generous for this particular reservoir but has partially been chosen to show the insensitivity of the method to initial guesses. The computed solution steps are shown in Table 3 for the OP-1 well and Table 4 for OP-2. Four iterations were completed in both cases, which seems sufficient for the permeability k^* value to converge within 1%. We certainly do not demand more accuracy from the solution, qualitatively understanding that the input field data are not within this accuracy or precision.

Final average permeability for the OP-1 well was 0.8 mD and for the OP-2 well 5.2 mD. These values are within the anticipated range of permeability in the reservoir. Using Equation (14) (or Equation (12) for PSS), we arrive at the productivity indices also shown as 0.097 stb/d/psi for OP-1 and 0.32 stb/d/psi for OP-2. It is useful to benchmark these results against the Productivity Index calculated from a full PBU survey. Comparing the permeability k^* to k derived from PBU would be erroneous, since we understand that k^* must include skin effects in its calculation whereas k is the true formation permeability. A few months prior to the timeframe studied in this work, a PBU test had been undertaken on these wells. The PBU indices, also captured in Table 2, were 0.08 stb/d/psi (c.f. 0.097 above) for OP-1 and 0.35 stb/d/psi for OP-2 (c.f. 0.32 above). These values are reasonably close to the productivity calculated using our method. The final permeability (k^*) for OP-1 is also compared against the openhole logs in Fig. 10 (this should be done cautiously since, as mentioned, k^* may include skin effects). Please note that the comparison of log-derived permeability to well-test permeability is generally only qualitative, as the log does not necessarily describe properties away from the wellbore, whereas well test-derived properties are averaged across the radius of investigation.

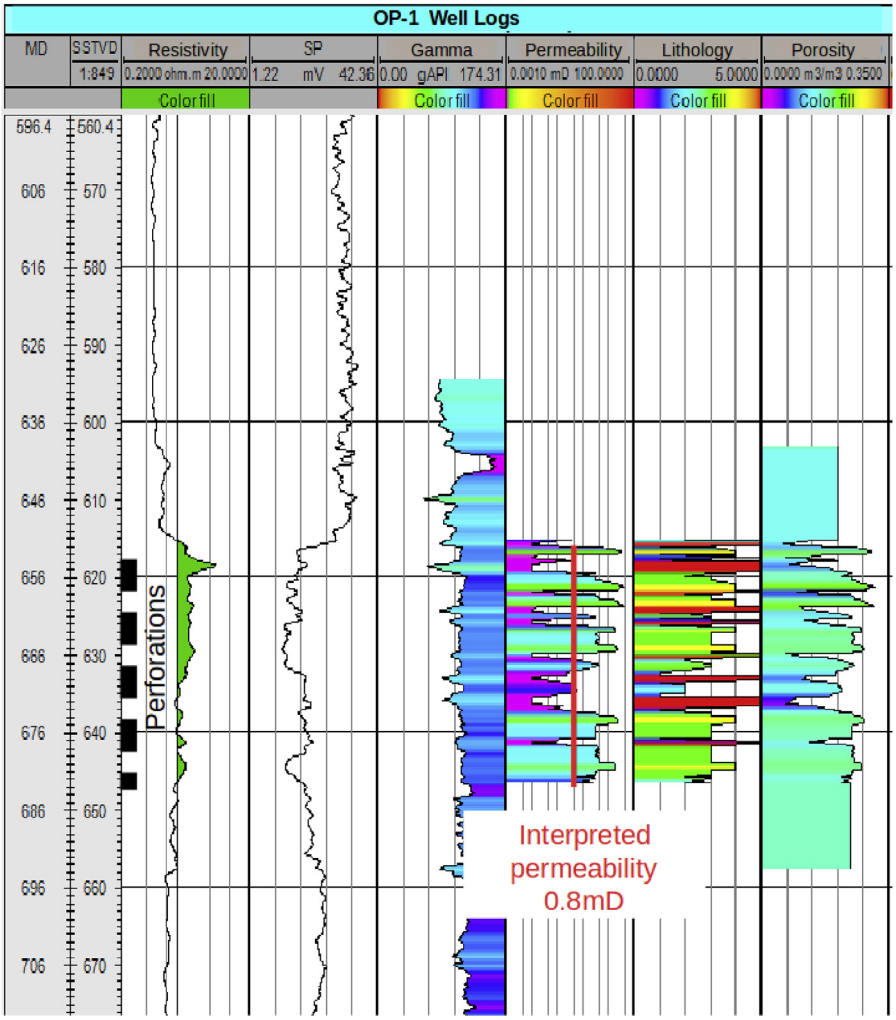

Fig. 10. Openhole logs for OP-1 beam pump production well. Interpreted permeability using proposed technique is marked on permeability log in red, resulting in PI of 0.097 stb/d/psi. PI from full PBU survey was 0.08 stb/d/psi. (For interpretation of the references to colour in this figure legend, the reader is referred to the Web version of this article.)

Table 3
Solution steps using direct technique – OP-1 well.

Property	Initial guess	Iter 1	Iter 2	Iter 3	Iter 4
k^* (mD)	10	0.936	0.780	0.772	0.771
Final PI (stb/d/psi)					0.097
T_D	1×10^5	9361	7804	7719	–
p_{wDp}	7.09	5.91	5.84	5.84	–

Table 4
Solution steps using direct technique – OP-2 well.

Property	Initial guess	Iter 1	Iter 2	Iter 3	Iter 4
k^* (mD)	10	5.715	5.275	5.195	5.18
Final PI (stb/d/psi)					0.32
T_D	1×10^5	57,150	52,745	51,951	–
p_{wDp}	5.66	5.22	5.14	5.13	–

7.3. Solution using type curves

A permeability solution using type curves is possible but not preferred. This is due to the sparseness of the dimensionless groups plotted in the curves compared to the precision available in the exact computer solution. Since the solution is still iterative, it may also require multiple lookups on a chart (Fig. 11). Results are presented in Tables 5 and 6 for OP-1 and OP-2 respectively. For the OP-1 well, an iteration on the chart was required since the recalculated dimensionless cycle time, T_D, was an order of magnitude different from the initial guess, which placed this on a different curve in the chart. The initial guess for permeability on the OP-2 well was sufficiently close to the final permeability that the recalculated T_D did not place the next solution step on a different curve, hence another iteration was not required (Fig. 12). In summary, the OP-1 well had a PI from the chart of 0.09 stb/d/psi, compared with 0.097 stb/d/psi from the direct programmed technique. Similarly, the OP-2 well had a PI from the chart of 0.33 stb/d/psi compared with 0.32 stb/d/psi from the program. These values are reasonably close but there may arise cases where using the type curves is made difficult by interpolation.

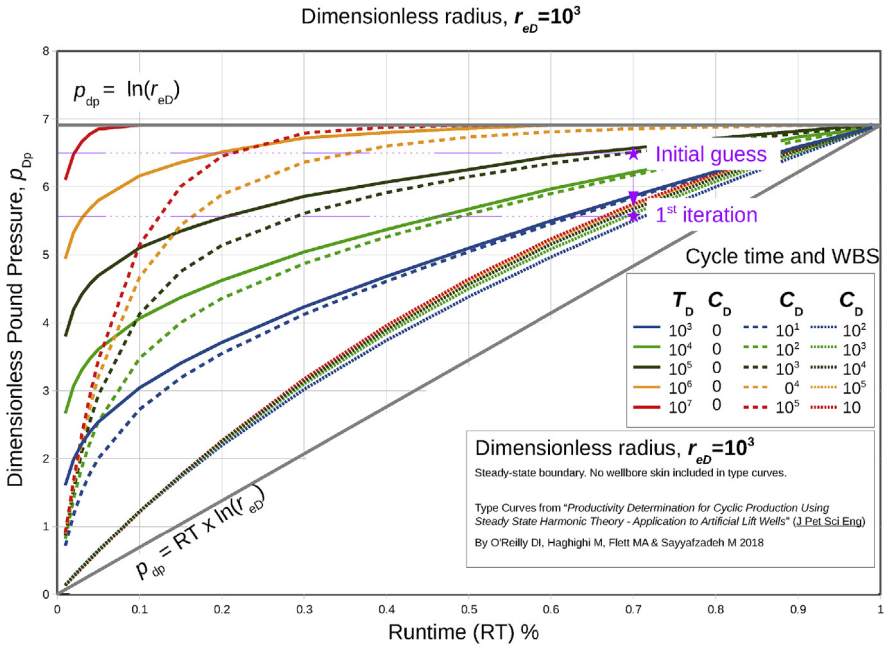

Fig. 11. Solution steps using type curve technique – OP-1 well.

Table 5
Solution steps using type curve charts – OP-1 well ($C_D \approx 1 \times 10^3$).

Property	Initial guess	Iter 1	Iter 2
k^* (mD)	10	0.86	0.73
Final PI (stb/d/psi)			0.09
T_D	1×10^5	8,600 ≈ 1×10^4	7,300 ≈ 1×10^4
p_{wDp}	6.5	5.5	5.5

Table 6
Solution steps using type curve charts – OP-2 well ($C_D = 1 \times 10^3$).

Property	Initial guess	Iter 1
k^* (mD)	10	5.3
Final PI (stb/d/psi)		0.33
T_D	1×10^5	$5.3 \times 10^4 \approx 1 \times 10^5$
p_{wDp}	5.2	5.2

8. Further work

The authors recommend several further developments with this theory that can be made.

- Development of solutions for flow geometries other than the radial case (e.g. linear or wells placed in reservoirs of polygonal shape)
- Development of solutions for unstable reservoir conditions – e.g. an uneven voidage replacement (non-steady-state)
- Application of theory to types of artificial lift wells where the pulse cycle is not applicable. Some cyclic gas-lift wells may follow a triangle-wave type rate solution.

One issue that this paper does not address is the specific type of multiphase wellbore storage that artificial lift wells may experience during shut-in periods. For most SRP completion wells, while the tubing may cease flow during shut-in, the annulus may freely flow gas with flow lines still open to separator station. This will happen until such a point that the liquid level rises in the annulus to load the BHP enough to completely cease inflow. This is an issue that needs further study. Fortunately, with the open-annulus style of Sucked Rod Pumps, phase redistribution will not occur during normal operation during off-time periods. Redistribution should only occur if the annulus is closed and gas migrates upwards against a closed flow path.

9. Conclusion

The new formulation for pulsing flow with wellbore storage and skin has been specifically developed for application to cyclic artificial lift wells. The equations have been derived for radial steady and pseudo steady flow, and for completeness, the infinite acting regime.

1. These solutions can be used to solve for the Productivity Index in long-term cyclic wells when only limited completion information is available and the pressure is known or estimated at the end of each production cycle
2. The periodic part of the solution was validated numerically and is valid within 2–3 cycles for the cases tested
3. Two field case studies showed that this method yielded similar PI values to those derived from prior pressure build up surveys
4. There are some limiting solutions when determining the expression for fluid pound pressure at the end of each producing period:
   For long cycle time T_D, $p_{wDp} \equiv$ const. rate solution (for PSS or SS).
   For short cycle time T_D or high wellbore storage C_D, $p_{wDp} \equiv$ RT % × const. rate solution (for PSS or SS).

These results were obtained through analysis of the limits of harmonic transfer functions (Appendix E) or through inspection of the produced type curves (Section 6). They may be useful limiting cases where the theory can be simplified in practice.

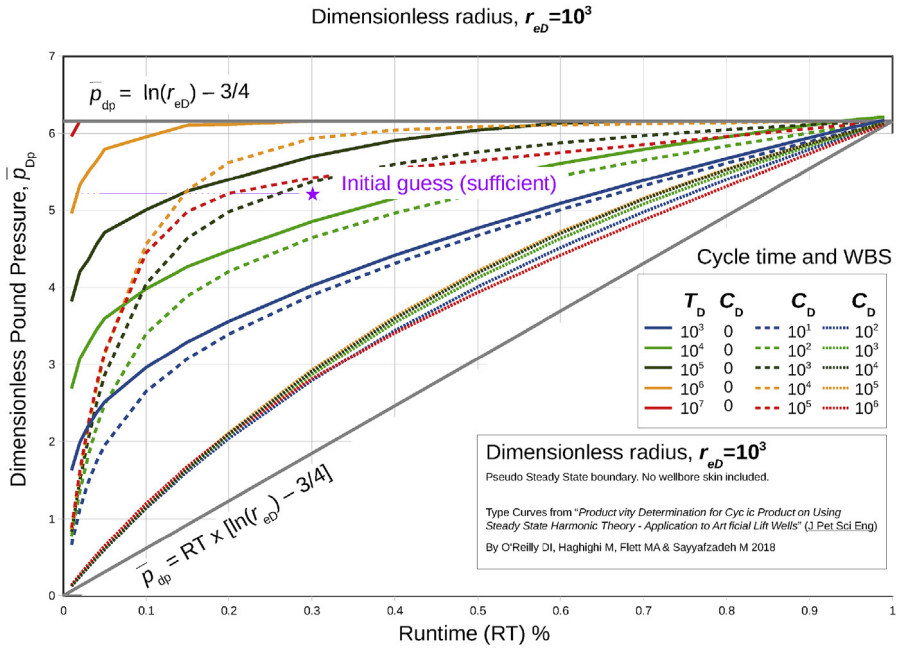

Fig. 12. Solution steps using type curve technique – OP-2 well.

Acknowledgments

The authors would like to thank Chevron Australia and JV partners for their permission to publish this work and the University of Adelaide for their cooperative research. The first author would also like to thank the anonymous peer reviewers who provided many helpful comments.

APPENDIX A. Dimensionless groups

Dimensionless groups have been used in the text to simplify expressions and generalise results. We define the groups as follows, and seek a solution $p_D(r_D, t_D)$:

$$p_D = \frac{kh}{141.2q_0B\mu}[p_i - p(r,t)], \tag{20}$$

$$\overline{p}_D = \frac{kh}{141.2q_0B\mu}[\overline{p}(t) - p(r,t)], \tag{21}$$

$$t_D = \frac{0.0002637kt}{\phi\mu c_t r_w^2}, \tag{22}$$

$$C_D = \frac{0.894C}{\phi h c_t r_w^2}, \tag{23}$$

$$r_D = \frac{r}{r_w},\ r_{eD} = \frac{r_e}{r_w}, \tag{24}$$

$$\omega_D = \frac{\phi\mu c_t r_w^2\omega}{0.0002637k},\ \text{with}\ \omega = \frac{2\pi}{T} \tag{25}$$

$$\text{and}\quad s = \frac{kh\Delta p_s}{141.2qB\mu} \tag{26}$$

APPENDIX B. Derivation of harmonic solutions

A derivation is presented here for a harmonic pulser with inclusion of both wellbore storage and skin.

B.1. General solution

The linearised radial diffusivity equation for a slightly compressible fluid is defined as

$$\frac{1}{r_D}\frac{\partial}{\partial r_D}\left(r_D\frac{\partial p_D}{\partial r_D}\right) = \frac{\partial p_D}{\partial t_D} \tag{27}$$

Now, using a separation of variables approach, specify a function, $g_D(r_D)$, to form an Ordinary Differential Equation (ODE) for a harmonic boundary condition.

$$p_D(r_D, t_D) = g_D(r_D, \omega_D)e^{i\omega_D t_D} \tag{28}$$

The PDE becomes the ODE:

$$\frac{1}{r_D}\frac{d}{dr_D}\left(r_D\frac{dg_D}{dr_D}\right) = i\omega_D g_D \tag{29}$$

or

$$r_D\frac{d^2g_D}{dr_D^2} + \frac{dg_D}{dr_D} - r_D i\omega_D g_D = 0 \tag{30}$$

This equation is the modified Bessel equation of order 0, with general solution:

$$g_D(r_D) = C_1K_0(\sqrt{i\omega_D}\,r_D) + C_2I_0(\sqrt{i\omega_D}\,r_D) \tag{31}$$

B.2. Inner boundary condition for wellbore storage and skin

In terms of pressure, the inner condition for inclusion of wellbore storage and skin is:

$$\left(r_D\frac{\partial p_D}{\partial r_D}\right)_{r_D=1} = -e^{i\omega t_D} + C_D\frac{dp_{wD}}{dt_D} \tag{32}$$

With the definition of g_D, this inner BC becomes

$$\left(\frac{dg_D}{dr_D}\right)_{r_D=1} = -1 + C_D i\omega_D g_D(1) \tag{33}$$

Finally, to compute p_{wD} with skin,

$$p_{wD} = \left[p_D - s\left(\frac{\partial p_D}{\partial r_D}\right)\right]_{r_D=1} \tag{34}$$

B.3. Solutions for different outer boundary conditions

B.3.1. Infinite system

The outer BC for an infinite system is

$$\lim_{r_D\to\infty} p_D(r_D) = \lim_{r_D\to\infty} g_D(r_D) = 0 \tag{35}$$

Combining the general solution (Equation (31)) with the inner and outer BC's (Equations (33) and (35)), the solution for $g_D(r_D)$ is:

$$g_D(r_D) = -\frac{iK_0(r_D\sqrt{i\omega_D})}{C_D\omega_D K_0(\sqrt{i\omega_D}) - i\sqrt{i\omega_D}K_1(\sqrt{i\omega_D}))} \tag{36}$$

For a cosine rate variation and the definition of g_D, dimensionless pressure is:

$$p_D(t_D, r_D) = \mathrm{Re}\left\{-\frac{iK_0(r_D\sqrt{i\omega_D})}{C_D\omega_D K_0(\sqrt{i\omega_D}) - i\sqrt{i\omega_D}K_1(\sqrt{i\omega_D}))}e^{i\omega_D t_D}\right\} \tag{37}$$

At the wellbore, we use Equation (34) to calculate p_{wD}, with the result:

$$p_{wD}(t_D) = \mathrm{Re}\left\{-\frac{s\sqrt{i\omega_D}K_1(\sqrt{i\omega_D}) + K_0(\sqrt{i\omega_D})}{C_D\omega_D K_0(\sqrt{i\omega_D}) + \frac{\omega_D K_1(\sqrt{i\omega_D})}{\sqrt{i\omega_D}}}ie^{it_D\omega_D}\right\} \tag{38}$$

B.3.2. Closed outer boundary

The outer BC for a closed outer boundary at r_{eD} is

$$\left(\frac{\partial p_D}{\partial r_D}\right)_{r_D=r_{eD}} = \left(\frac{dg_D}{dr_D}\right)_{r_D=r_{eD}} = 0 \tag{39}$$

Combining the general solution (Equation (31)) with the inner and outer BC's (Equations (33) and (39)), the solution for $g_D(r_D)$ is:

$$g_D(r_D) = -\frac{i[K_0(r_D\sqrt{i\omega_D})I_1(r_{eD}\sqrt{i\omega_D}) + I_0(r_D\sqrt{i\omega_D})K_1(r_{eD}\sqrt{i\omega_D})]}{\left(C_D\omega_D K_0(\sqrt{i\omega_D}) + \frac{\omega_D K_1(\sqrt{i\omega_D})}{\sqrt{i\omega_D}}\right)I_1(r_{eD}\sqrt{i\omega_D}) + (C_D\omega_D I_0(\sqrt{i\omega_D}) + i\sqrt{i\omega_D}I_1(\sqrt{i\omega_D}))K_1(r_{eD}\sqrt{i\omega_D})} \tag{40}$$

For a cosine rate variation and the definition of g_D, dimensionless pressure is:

$$p_D(t_D, r_D) = \mathrm{Re}\left\{ -\frac{i\left[K_0(r_D\sqrt{i\omega_D})I_1(r_{eD}\sqrt{i\omega_D}) + I_0(r_D\sqrt{i\omega_D})K_1(r_{eD}\sqrt{i\omega_D})\right]}{\left(C_D\omega_D K_0(\sqrt{i\omega_D}) + \frac{\omega_D K_1(\sqrt{i\omega_D})}{\sqrt{i\omega_D}}\right)I_1(r_{eD}\sqrt{i\omega_D}) + (C_D\omega_D I_0(\sqrt{i\omega_D}) + i\sqrt{i\omega_D}I_1(\sqrt{i\omega_D}))K_1(r_{eD}\sqrt{i\omega_D})} e^{it_D\omega_D} \right\} \tag{41}$$

At the wellbore, we use Equation (34) to calculate p_{wD}, with the result:

$$p_{wD,\omega}(t_D) = \mathrm{Re}\left\{ \frac{\begin{array}{l} e^{it_D\omega_D}[I_1(r_{eD}\sqrt{i\omega_D})(s\sqrt{i\omega_D}K_1(\sqrt{i\omega_D}) + K_0(\sqrt{i\omega_D})) \\ + K_1(r_{eD}\sqrt{i\omega_D})(I_0(\sqrt{i\omega_D}) - s\sqrt{i\omega_D}I_1(\sqrt{i\omega_D}))] \end{array}}{\begin{array}{l} [iC_D\omega_D K_0(\sqrt{i\omega_D}) + \sqrt{i\omega_D}K_1(\sqrt{i\omega_D})]I_1(r_{eD}\sqrt{i\omega_D}) \\ + [iC_D\omega_D I_0(\sqrt{i\omega_D}) - \sqrt{i\omega_D}I_1(\sqrt{i\omega_D})]K_1(r_{eD}\sqrt{i\omega_D}) \end{array}} \right\} \tag{42}$$

B.3.3. Constant pressure outer boundary

The outer BC for a constant pressure outer boundary at r_{eD} is

$$p_D(r_{eD}) = g_D(r_{eD}) = 0 \tag{43}$$

Combining the general solution (Equation (31)) with the inner and outer BC's (Equations (33) and (43)), the solution for $g_D(r_D)$ is:

$$g_D(r_D) = \frac{K_0(r_D\sqrt{i\omega_D})I_0(r_{eD}\sqrt{i\omega_D}) - I_0(r_D\sqrt{i\omega_D})K_0(r_{eD}\sqrt{i\omega_D})}{\sqrt{i\omega_D}\left((I_1(\sqrt{i\omega_D}) - C_D\sqrt{i\omega_D}I_0(\sqrt{i\omega_D}))K_0(r_{eD}\sqrt{i\omega_D}) + (C_D\sqrt{i\omega_D}K_0(\sqrt{i\omega_D}) + K_1(\sqrt{i\omega_D}))I_0(r_{eD}\sqrt{i\omega_D})\right)} \tag{44}$$

For a cosine rate variation and the definition of g_D, dimensionless pressure is:

$$p_D(t_D, r_D) = \mathrm{Re}\left\{ \frac{K_0(r_D\sqrt{i\omega_D})I_0(r_{eD}\sqrt{i\omega_D}) - I_0(r_D\sqrt{i\omega_D})K_0(r_{eD}\sqrt{i\omega_D})}{\sqrt{i\omega_D}\left((I_1(\sqrt{i\omega_D}) - C_D\sqrt{i\omega_D}I_0(\sqrt{i\omega_D}))K_0(r_{eD}\sqrt{i\omega_D}) + (C_D\sqrt{i\omega_D}K_0(\sqrt{i\omega_D}) + K_1(\sqrt{i\omega_D}))I_0(r_{eD}\sqrt{i\omega_D})\right)} e^{it_D\omega_D} \right\} \tag{45}$$

At the wellbore, we use Equation (34) to calculate p_{wD}, with the result:

$$p_{wD,\omega}(t_D) = \mathrm{Re}\left\{ \frac{\begin{array}{l} e^{it_D\omega_D}[K_0(r_{eD}\sqrt{i\omega_D})(s\sqrt{i\omega_D}I_1(\sqrt{i\omega_D}) - I_0(\sqrt{i\omega_D})) \\ + I_0(r_{eD}\sqrt{i\omega_D})(s\sqrt{i\omega_D}K_1(\sqrt{i\omega_D}) + K_0(\sqrt{i\omega_D}))] \end{array}}{\begin{array}{l} \sqrt{i\omega_D}\,[(I_1(\sqrt{i\omega_D}) - C_D\sqrt{i\omega_D}I_0(\sqrt{i\omega_D}))K_0(r_{eD}\sqrt{i\omega_D}) \\ + (C_D\sqrt{i\omega_D}K_0(\sqrt{i\omega_D}) + K_1(\sqrt{i\omega_D}))I_0(r_{eD}\sqrt{i\omega_D})] \end{array}} \right\} \tag{46}$$

It is worth nothing that the solutions derived in this appendix are analogous to Laplace-space bounded solutions available in the literature (Agarwal et al., 1970; Van Everdingen et al., 1949), with the replacement of the Laplace variable u to $u = i\omega_D$, as recognised in another reference (Hollaender et al., 2002). The method presented here is an alternative one to develop the solutions.

APPENDIX C. Average reservoir pressure in pss case

In the pseudo-steady case, it is customary to present the solution in terms of a time-dependant average reservoir pressure, $\overline{p}$. For the constant-rate part of the solution, the relationship between bottomhole flowing bottomhole pressure and average reservoir pressure is

$$\overline{p}_D = \log(r_{eD}) - 3/4 + s \tag{47}$$

Let us first examine the average pressure in the reservoir as a result of the harmonic rate variation only. We refer to this quantity as $p_{D\mathrm{avg},\omega}$. To determine this pressure, the solution from the last section (Equation (41)) is averaged volumetrically across the reservoir interval:

$$p_{D\mathrm{avg},\omega}(t_D) = \frac{\int_{r_D=1}^{r_{eD}} p_{D,\omega}(t_D, r_D)dV}{\int_{r_D=1}^{r_{eD}} dV} = \frac{2\pi\phi h}{\pi\phi h(r_{eD}^2 - 1)}\int_1^{r_{eD}} p_{D,\omega}(t_D, r_D)r_D dr_D \tag{48}$$

i.e.

$$p_{D\mathrm{avg},\omega}(t_D) = \frac{2}{r_{eD}^2 - 1}\int_1^{r_{eD}} p_{D,\omega}(t_D, r_D)r_D dr_D \tag{49}$$

Substituting Equation (42) in the prior equation and integrating using Mathematica (Wolfram Research, 0000), we found the expression is

$$p_{D\mathrm{avg},\omega}(t_D) = \mathrm{Re}\left\{ \frac{2ie^{it_D\omega_D}\left({}_0\widetilde{F}_1\left(;2;\frac{i\omega_D}{4}\right)K_1(r_{eD}\sqrt{i\omega_D}) - r_{eD}K_1(\sqrt{i\omega_D})\,{}_0\widetilde{F}_1\left(;2;\frac{1}{4}ir_{eD}^2\omega_D\right)\right)}{(r_{eD}^2 - 1)\omega_D\left(r_{eD}(C_D\sqrt{i\omega_D}K_0(\sqrt{i\omega_D}) + K_1(\sqrt{i\omega_D}))\,{}_0\widetilde{F}_1\left(;2;\frac{1}{4}ir_{eD}^2\omega_D\right) + \left(2C_D\,{}_0\widetilde{F}_1\left(;1;\frac{i\omega_D}{4}\right) - {}_0\widetilde{F}_1\left(;2;\frac{i\omega_D}{4}\right)\right)K_1(r_{eD}\sqrt{i\omega_D})\right)} \right\} \tag{50}$$

Note that $r_{eD} > 1$ and $\omega \neq 0$ for this evaluation. This is an expression for the variation in average reservoir pressure within a harmonic production cycle. We remind the reader that it is used in conjunction with Equation (11) to form the solution for pressure drop at the wellbore with respect to average reservoir pressure. Substituting, the complete expression at the wellbore is:

$$\overline{p}_{wD,\infty}(t_D) = \mathrm{Re}\left\{ \frac{\begin{array}{c} e^{it_D\omega_D} K_1(r_{eD}\sqrt{i\omega_D})\left({}_0\widetilde{F}_1\left(;2;\frac{i\omega_D}{4}\right)(r_{eD}^2(-s)\omega_D + s\omega_D - 2i) - 2i(r_{eD}^2-1)\,{}_0\widetilde{F}_1\left(;1;\frac{i\omega_D}{4}\right)\right) \\ + r_{eD}\,{}_0\widetilde{F}_1\left(;2;\frac{1}{4}ir_{eD}^2\omega_D\right)\left(K_1(\sqrt{i\omega_D})((r_{eD}^2-1)s\omega_D + 2i) + \frac{(r_{eD}^2-1)\omega_D K_0(\sqrt{i\omega_D})}{\sqrt{i\omega_D}}\right) \end{array}}{(r_{eD}^2-1)\omega_D\left(r_{eD}(C_D\sqrt{i\omega_D}K_0(\sqrt{i\omega_D}) + K_1(\sqrt{i\omega_D}))\,{}_0\widetilde{F}_1\left(;2;\frac{1}{4}ir_{eD}^2\omega_D\right) + \left(2C_D\,{}_0\widetilde{F}_1\left(;1;\frac{i\omega_D}{4}\right) - {}_0\widetilde{F}_1\left(;2;\frac{i\omega_D}{4}\right)\right)K_1(r_{eD}\sqrt{i\omega_D})\right)} \right\} \tag{51}$$

APPENDIX D. Numerical verification

A pulse wave is now compared against the numerical solution of the radial diffusivity equation using the COMSOL software. One case is compared. A similar result can been obtained if the analytical solution in Laplace space is used to compare solutions, in a similar way to Rosa (1991) who did so for the IARF flow regime. The results here are a useful addition to that work, as they confirm that the harmonic solution agrees with the full transient behaviour after only a few cycles for the special case of a square wave with a steady state boundary condition. Previously this has only been shown for the exactly sinusoidal case in the IARF regime.

The equation for radial flow in a slightly compressible fluid was solved numerically:

$$\frac{1}{r_D}\frac{\partial}{\partial r_D}\left(r_D\frac{\partial p_D}{\partial r_D}\right) = \frac{\partial p_D}{\partial t_D} \tag{52}$$

with initial condition $p_D(r_D, t_D = 0) = 0$. The inner and outer boundary conditions are

$$p(r_{eD}, t_D) = 0 \tag{53}$$

(steady state boundary) and wellbore storage condition for the inner radius,

$$\left(r_D\frac{\partial p_D}{\partial r_D}\right)_{r_D=1} = -1 + C_D\frac{dp_{wD}}{dt_D} \tag{54}$$

with p_{wD} inclusive of skin, defined as:

$$p_{wD} = \left[p_D - s\frac{\partial p_D}{\partial r_D}\right]_{rD=1} \tag{55}$$

During the production part of a cycle, Equation (54) applies. During shut-in, the right hand side of the equation is changed to $C_D\frac{dp_{wD}}{dt_D}$ alone.

Using the Fourier Series approach combined with the solution for Steady State boundary condition in Section 3.4, an analytical solution was prepared for a case with run time of 50%. The results are compared against the numerical solution in Fig. 13, with all of the dimensionless reservoir properties appearing in the caption. At early times the solutions are in disagreement. Especially during the first cycle, the analytic harmonic solution does not seem appropriate. After the third cycle, the solutions coincide and the periodic solution is in agreement for the reservoir under consideration. This results from an initial duration of transience in the reservoir before periodicity is reached and is consistent with other research (Rosa, 1991). This type of transience is distinct from the type normally discussed regarding constant-rate infinite acting radial flow, which is separated in our solution approach (Section 3.2). It is specifically the time until the periodic solution is reached.

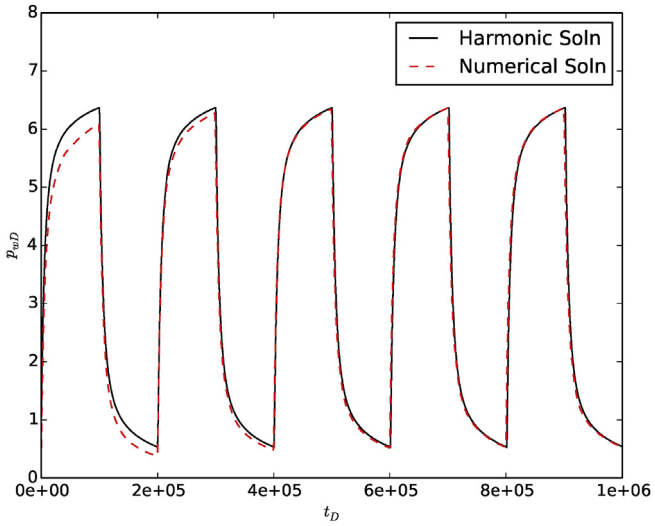

Fig. 13. Comparing numerical results (COMSOL) and harmonic solution for the steady state boundary condition, using the square pulse wave. $r_{eD} = 10^3$, $T_D = 2 \times 10^5$, $C_D = 10^3$, $s = 0$, RT= 50%.

APPENDIX E. Transfer functions and the asymptotic behaviour of pressure relationship

It is useful to express the derived equations in terms of their transfer function, $H(i\omega_D)$ (Hollaender et al., 2002; Morozov, 2013):

$$H(i\omega_D, r_{eD}, C_D, s) = \frac{p_{wD}(i\omega_D, r_{eD}. t_D, C_D, s)}{e^{i\omega_D t_D}} \tag{56}$$

This removes the periodicity of the signal and represents the magnitude of the pressure response at the peak (magnitude of the wave). We have taken the transfer function of the pressure response at the wellbore specifically (p_{wD}). In Fig. 14 we plot the modulus $|H(i\omega_D)|$ for the IARF, SS and PSS boundary conditions, for various combinations of dimensionless outer radius and wellbore storage coefficients. The cases show that at higher frequencies, the pressure response signal at the wellbore diminishes. This explains why the effect of the oscillating part of production diminishes at lower values of T_D in the type curves in this paper (e.g. Fig. 4). The reservoir behaves like a low pass filter on the pressure response from a rate signal.

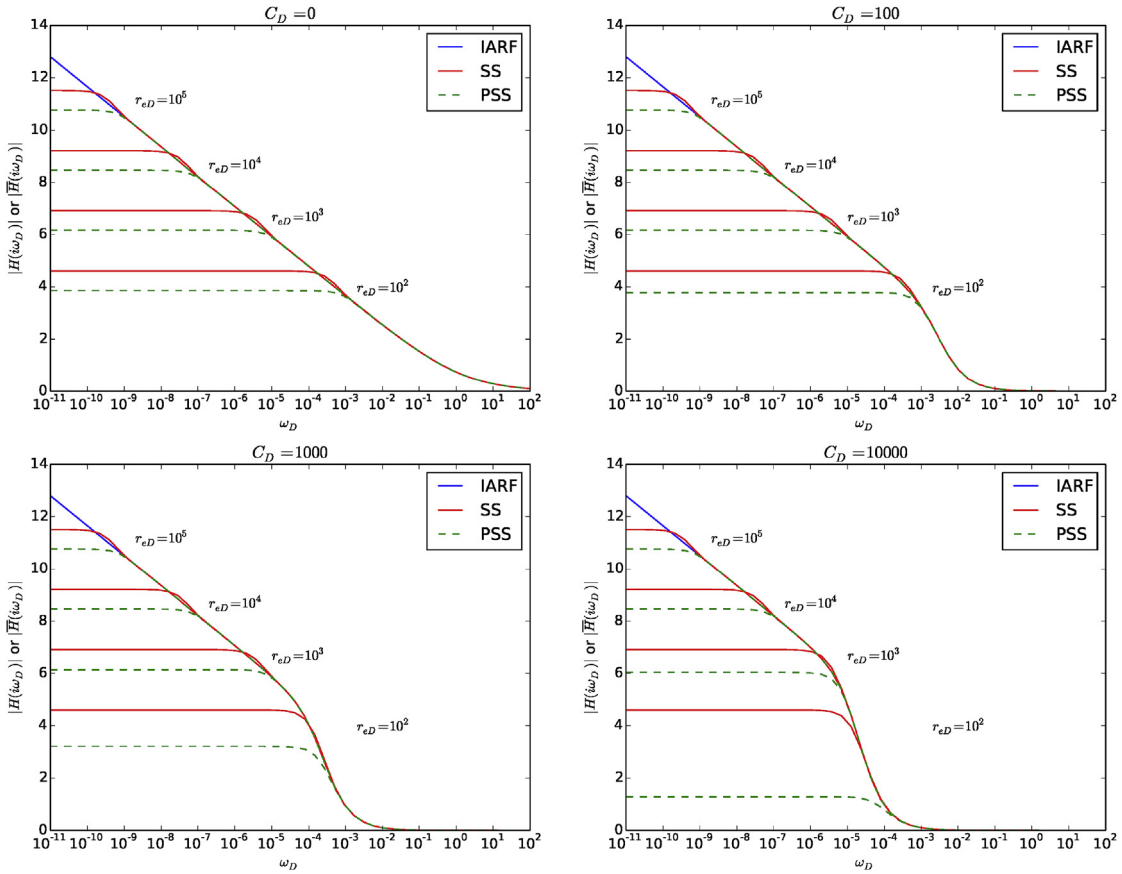

Fig. 14. Transfer function $|H|$ for IARF and SS cases and $|\overline{H}|$ for PSS case. In these curves C_D is marked and $s = 0.2$

Let us examine the behaviour for IARF, SS and PSS wellbore pressure modulus in the limits of $\omega_D \to 0$ and $\omega_D \to \infty$. For the case of $\omega_D \to \infty$, the result is simply

$$|H_{\text{IARF}}| = |H_{\text{SS}}| = |\overline{H}_{\text{PSS}}| = 0, \quad \text{as} \quad \omega_D \to \infty \tag{57}$$

for all boundary conditions, including those with the effects of wellbore storage and skin. This can be seen graphically in Fig. 14, and it can also be proven through analysis of the limit. The infinite acting case is straight forward as it contains only a few modified Bessel functions. For the cases with reservoir boundaries, we found it necessary to perform a series expansion of the modified bessel and hypergeometric functions to simplify the limit calculations.

For the case of $\omega_D \to 0$ (long wavelength),

$$|H_{\text{IARF}}| = \infty, \quad \text{as} \quad \omega_D \to 0 \tag{58}$$

which says that we will continue to deplete an unbounded porous medium. In the PSS case,

$$\left|\overline{H}_{\text{PSS}}(r_{eD}, C_D, s)\right| = \frac{r_{eD}^4\left(4s - 3 - 4\ln\left(\frac{1}{2}+\frac{i}{2}\right)\right) + 4r_{eD}^4\ln\left(\left(\frac{1}{2}+\frac{i}{2}\right)r_{eD}\right) + r_{eD}^2(4-8s) + 4s - 1}{4(r_{eD}^2-1)(2C_D + r_{eD}^2 - 1)}, \quad \text{as} \quad \omega_D \to 0 \tag{59}$$

Setting $C_D = 0$ and assuming that r_{eD} is sufficiently large so some of the terms drop out, this simplifies to

$$|\overline{H}_{\text{PSS}}(r_{eD}, C_D = 0, s)| = \ln(r_{eD}) - 3/4 + s \tag{60}$$

which is the familiar Pseudo Steady State inflow equation (c.f. Equation (12)). Finally in the SS case,

$$|H_{SS}(r_{eD}, C_D, s)| = \ln(r_{eD}) + s, \quad \text{as} \quad \omega_D \to 0 \tag{61}$$

which is identical to the Steady State inflow equation (c.f. Equation (14)). This result indicates that at sufficiently low harmonic excitation frequencies, bounded reservoirs have enough time to enter stable long-term inflow behaviour. It is a useful result that will help understand the performance of cycling wells.

There is a subtle difference between the shapes of PSS and SS curves in Fig. 14, observed just prior to reaching asymptotic values at low frequencies. It seems that the steady state line has the tendency to curve upwards from the infinite acting and pseudo steady lines before reaching the asymptotic value. It is interesting to see this behaviour in the transfer functions, but similar behaviour for these boundary conditions has been seen elsewhere, under different flow rate schedules. For build-up analysis after constant-rate production, Kumar et al. (1974), Ramey et al. (1973) noticed exactly the same type of deviation for a constant-pressure square compared with the closed square. In our particular paper we have been dealing with the circular reservoir (theirs was square shaped), so we will show a chart for the circular case to reproduce a similar phenomenon on a Horner plot, shown in Fig. 15.

The usual line source solution is used for the IARF case, without wellbore storage (Lee et al., 2003; O'Reilly et al., 2016):

$$[p_{wD}]_{\text{IARF}} = -\frac{1}{2}\text{Ei}\left(-\frac{1}{4t_D}\right) + s \tag{62}$$

For bounded reservoirs, the approximate solutions of Blasingame (1993) and Ramey (1970) are useful because they are in real space and do not require numerical inversion from Laplace space like other solutions. No wellbore storage is included in that formulation. The solutions are:

$$\begin{aligned}[p_{wD}]_{\text{SS}} &= -\tfrac{1}{2}\text{Ei}\left(-\tfrac{1}{4t_D}\right) + \tfrac{1}{2}\text{Ei}\left(-\tfrac{r_{eD}^2}{4t_D}\right) + s \\ [p_{wD}]_{\text{PSS}} &= -\tfrac{1}{2}\text{Ei}\left(-\tfrac{1}{4t_D}\right) + \tfrac{1}{2}\text{Ei}\left(-\tfrac{r_{eD}^2}{4t_D}\right) + \tfrac{2t_D}{r_{eD}^2}\exp\left(-\tfrac{r_{eD}^2}{4t_D}\right) + s\end{aligned} \tag{63}$$

These three equations were used to prepare Fig. 15 for a specific buildup case of $t_{Dp} = 10{,}000$. The dimensionless pressure shut-in function is used, $p_{wDs} = p_{wD}(t_{Dp}) - [p_{wD}(t_{Dp} + \Delta t_D) - p_{wD}(\Delta t_D)]$, which is based on superposition for the simple constant-rate buildup analysis.

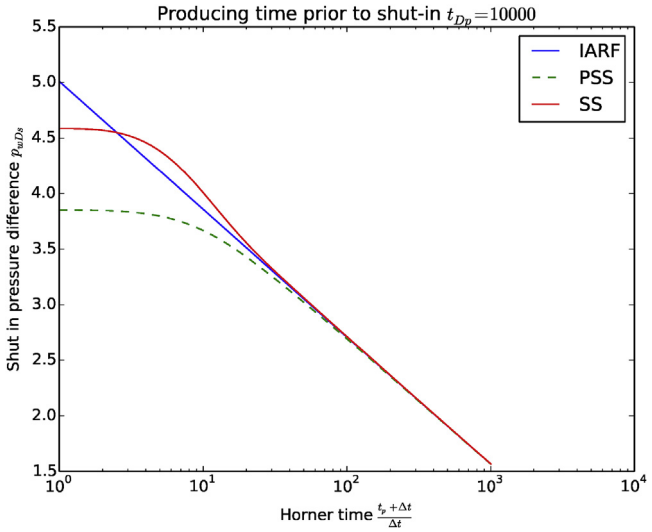

Fig. 15. Horner plot example for build-up analysis comparing different boundary conditions. In these curves $C_D = s = 0$, as per Blasingame/Ramey's formulation (Blasingame, 1993; Ramey, 1970), and $r_{eD} = 100$. The plot demonstrates an analogy of the unique difference in shapes between PSS and SS boundary condition curves that is also observed in the transfer functions in Fig. 14.3

This buildup chart illustrates that the interesting behaviour seen in the transfer functions is not unique but is also seen in buildup analysis, when Horner time is used as a plotting function. At late shut-in times (large Δt), there is a period where the bottomhole pressure in the steady state case starts to exceed that of the IARF case, before plateauing. Although not originally noted by Kumar and Ramey (Kumar et al., 1974), we expect that it is a result of the increased fluid influx into the reservoir that takes place at late time during pressure buildup. Presumably the same is true in the harmonic rate transfer functions plotted earlier, and this validates their appearance. As a final mention, this behaviour is absent from the pressure drawdown behaviour of Equation (63), and only observed during buildup.

Nomenclature

Δp_s	Pressure drop caused by wellbore skin (psi)
log	Logarithm (base 10)
μ	Viscosity (cP)
ω	Angular frequency (rad)
$\overline{p}$	Average reservoir pressure (psi)
ϕ	Porosity (pu)
ρ	Fluid density (lb/ft^3)
τ	Production duration (hrs)
$A_{wb}7$	Cross-sectional area of wellbore (ft^2)
B	Formation Volume Factor (rb/stb)
C	Wellbore storage (bbl/psi)
C_D	Dimensionless wellbore storage
c_t	Total compressibility (1/psi)
h	Thickness (ft)
i	Imaginary number $\sqrt{-1}$
I_n	Modified Bessel function of the first kind, order n
J_n	Bessel function of the first kind, order n
J_{PSS}	Productivity Index – Pseudo Steady State Flow
J_{SS}	Productivity Index – Steady State Flow
k	Permeability (mD)
k'	Permeability (mD) including effect of skin
k_g	Permeability to gas (mD)
K_n	Modified Bessel function of the second kind, order n
k_o	Permeability to oil (mD)
k_w	Permeability to water (mD)
$n_{\max}$	Number of frequencies included in discrete fourier series
p	Pressure (psi)
p_D	Dimensionless pressure
p_e	Pressure at the external radius of reservoir (psi)
p_i	Initial reservoir pressure (psi)
p_{const}	Constant-rate part of pressure solution (psi)
p_ω	Harmonic part of pressure solution (psi)
p_{wDp}	Dimensionless wellbore pressure prior to fluid pounding
p_{wf}	Bottomhole flowing pressure (psi)
q_0	Fluid rate during production part of cycle (bbl/day)
q_ω	Pure harmonic production rate (bbl/day)
q_D	Dimensionless rate
q_{avg}	Average production rate (bbl/day)
r_D	Dimensionless radius
r_e	External radius of reservoir (ft)
r_w	Radius of wellbore (ft)
s	Wellbore skin
T	Total duration of cycle (hrs)
t	Time (hrs)
t_D	Dimensionless time
u	Laplace variable
V	Reservoir Volume
Y_n	Bessel function of the second kind, order n
BHP	Bottom Hole Pressure
CHP	Casing Head Pressure
Ei	Exponential integral
IARF	Infinite Acting Radial Flow
MD	Measured Depth
POC	Pump Off Controller
PSS	Pseudo Steady State
Re	Real part of the solution
RT	Run Time %
SP	Spontaneous Potential
SS	Steady State
SSTVD	Sub Sea True Vertical Depth
WBS	Wellbore Storage

References

Agarwal, Ram G., Al-Hussainy, Rafi, HJ Ramey Jr., , et al., 1970. An investigation of wellbore storage and skin effect in unsteady liquid flow: I. analytical treatment. Soc. Petrol. Eng. J. 10 (03), 279–290.

Ahn, Sanghui, 2012. Pressure Pulse Testing in Heterogeneous Reservoirs. PhD thesis. Stanford University.

Ahn, Sanghui, Horne, Roland N., 2010. Estimating permeability distributions from pressure pulse testing. In: SPE Annual Technical Conference and Exhibition. Society of Petroleum Engineers.

Ahn, Sanghui, Horne, Roland N., 2011. The use of attenuation and phase shift to estimate permeability distributions from pulse tests. In: SPE Annual Technical Conference and Exhibition. Society of Petroleum Engineers.

Blasingame, T.A., 1993. Semi-analytical solutions for a bounded circular reservoir–no flow and constant pressure outer boundary conditions: unfractured well case. paper SPE 25479, 21–23.

Brigham, W.E., et al., 1970. Planning and analysis of pulse-tests. J. Petrol. Technol. 22 (05), 618–624.

Businov, S.N., Umrichin, I.D., 1960. Reservoir and well study under harmonic production rate. Izv. Akad. Nauk SSSr, Mekh. Mashinostr.(4).

Cardiff, Michael, Barrash, Warren, 2014. Analytical and Semi-analytical Tools for the Design of Oscillatory Pumping Tests. Groundwater.

Chacin, J., Schmidt, Z., Doty, D., et al., 1994. Modeling and optimization of plunger lift assisted intermittent gas lift installations. SPE Adv. Technol. 2 (01), 25–33.

Eckel, Andy C., Abels, Harold P., Merritt, Ross A., 1995. Testing and practically applying pump-off controllers in a waterflood. In: Western Regional Meeting. Society of Petroleum Engineers, pp. 241–248.

Fokker, Peter A., Verga, Francesca, 2011. Application of harmonic pulse testing to water–oil displacement. J. Petrol. Sci. Eng. 79 (3), 125–134.

Fokker, Peter A., Renner, Joerg, Verga, Francesca, 2012. Applications of harmonic pulse testing to field cases. In: SPE Europec/EAGE Annual Conference. Society of Petroleum Engineers.

Fokker, Peter A., Renner, Joerg, Verga, Francesca, 2013. Numerical modeling of periodic pumping tests in wells penetrating a heterogeneous aquifer. Am. J. Environ. Sci. 9 (1), 1–13.

Fokker, Peter A., Borello, Eloisa Salina, Verga, Francesca, Viberti, Dario, et al., 2017. Harmonic pulse testing for well and reservoir characterization. In: SPE Europec Featured at 79th EAGE Conference and Exhibition. Society of Petroleum Engineers.

Fokker, Peter A., Borello, Eloisa Salina, Verga, Francesca, Viberti, Dario, 2018. Harmonic pulse testing for well performance monitoring. J. Petrol. Sci. Eng.

Garcia, Artur Posenato, Silva Neto, Gilson Moura, Machado, Marcos Vitor Barbosa, de Souza Carvalho, Renato, 2014. Dynamic ipr-modeling reservoir well interactions to improve transient simulations of wells. In: SPE Latin America and Caribbean Petroleum Engineering Conference. Society of Petroleum Engineers.

Garcia, A Posenato, Cavalcanti de Sousa, P., Waltrich, P.J., et al., 2016. A transient coupled wellbore-reservoir model using a dynamic ipr function. In: SPE Annual Technical Conference and Exhibition. Society of Petroleum Engineers.

Hernandez, A., Perez, C., Navarro, U., Lobo, W., et al., 1999a. Intermittent gas lift optimization in rosa mediano field. In: Latin American and Caribbean Petroleum Engineering Conference. Society of Petroleum Engineers.

Hernandez, Ali, Gasbarri, Sandro, Machado, Miguel, Marcano, Luisana, Manzanilla, Raul, Guevara, Jose, 1999b. Field-scale research on intermittent gas lift. In: SPE mid-continent Operations Symposium, pp. 113–117.

Hollaender, F., Hammond, P., Gringarten, A., 2002. Harmonic Testing for Continuous Well and Reservoir Monitoring, Paper Spe 77692 Presented at the Spe Annual Technical Conference and Exhibition. soc. of pet. *Eng.*, San Antonio, Tex.

Jones, Eric, Oliphant, Travis, Peterson, Pearu, et al., 2001. SciPy: Open source scientific tools for Python. http://www.scipy.org/ [Online; accessed 2016-January-22].

Kamal, Medhat, Brigham, W.E., et al., 1975. Pulse-testing response for unequal pulse and shut-in periods. Soc. Petrol. Eng. J. 15 (05), 399–410.

Kravits, Matthew Stephen, Frear, Ray M., Bordwell, David, et al., 2011. Analysis of plunger lift applications in the marcellus shale. In: SPE Annual Technical Conference and Exhibition. Society of Petroleum Engineers.

Kumar, Anil, Henry, J., Ramey Jr., , et al., 1974. Well-test analysis for a well in a constant-pressure square. Soc. Petrol. Eng. J. 14 (02), 107–116.

Kuo, C.H., et al., 1972. Determination of reservoir properties from sinusoidal and multirate flow tests in one or more wells. Soc. Petrol. Eng. J. 12 (06), 499–507.

Lee, J., Rollins, J.B., Spivey, J.P., 2003. *Pressure Transient Testing*. SPE Textbook Series. Society of Petroleum Engineers ISBN 9781555630997.

Martin, John C., et al., 1959. Simplified Equations of Flow in Gas Drive Reservoirs and the Theoretical Foundation of Multiphase Pressure Buildup Analyses.

McCoy, J.N., Becker, Dieter, AL, Podio, 1999. Timer control of beam pump run time reduces operating expense. In: Proceedings of the Annual Southwestern Petroleum Short Course. Texas Tech University, pp. 74–86.

Morozov, Petr, 2013. Harmonic Testing of wells with a Vertical Fracture. In ECF19.

Ogbe, David, Brigham, William, et al., 1987. Pulse testing with wellbore storage and skin effects. SPE Form. Eval. 2 (01), 29–42.

Oliphant, Travis E., 2007. Python for scientific computing. Comput. Sci. Eng. 9 (3), 10–20.

O'Reilly, D.I., Haghighi, M., Flett, M.A., Sayyafzadeh, M., 2016. Pressure and rate transient analysis of artificially lifted drawdown tests using cyclic pump off controllers (under review). J. Petrol. Sci. Eng. 79 (3), 125–134.

Perrine, R.L., et al., 1956. Analysis of pressure-buildup curves. In: Drilling and Production Practice. American Petroleum Institute.

Raghavan, Rajagopal, 2004. A review of applications to constrain pumping test responses to improve on geological description and uncertainty. Rev. Geophys. 42 (4).

Ramey, H.J., 1970. Approximate solutions for unsteady liquidflow in composite reservoirs. J. Can. Petrol. Technol. 9 (01).

Ramey, Henry J., Kumar, Anil, Gulati, Mohinder S., 1973. Gas Well Test Analysis under Water-drive Conditions. American Gas Association.

Rosa, A.J., 1991. Reservoir Description by Well Test Analysis Using Cyclic Flow Rate Variation. PhD thesis. .

Rosa, A.J., Horne, R.N., 1997. Reservoir description by well test analysis using cyclic flow rate variation. SPE Form. Eval. 12 (04), 247–254.

Sousa, Pedro Cavalcanti de, Garcia, Artur P., Waltrich, Paulo J., et al., 2017a. Investigation of pressure profiles of reservoirs with wells under transient, unstable flow. In: SPE Annual Technical Conference and Exhibition. Society of Petroleum Engineers.

Sousa, Pedro Cavalcanti De, Artur Posenato, Garcia, Waltrich, Paulo J., et al., 2017b. Analytical development of a dynamic ipr for transient two-phase flow in reservoirs. In: SPE Annual Technical Conference and Exhibition. Society of Petroleum Engineers.

Spivey, J.P., Lee, W.J., et al., 1993. Production data analysis for wells that have been subject to periodic curtailment. In: SPE Gas Technology Symposium. Society of Petroleum Engineers.

Streltsova, T.D., 1988. Well Testing in Heterogeneous Formations. John Wiley & Sons.

Van Everdingen, A.F., Hurst, William, et al., 1949. The application of the laplace transformation to flow problems in reservoirs. J. Petrol. Technol. 1 (12), 305–324.

Zenith, Federico, Foss, Bjarne Anton, Tjønnås, Johannes, Hasan, Agus Ismail, et al., 2015. Well testing by sinusoidal stimulation. SPE Reservoir Eval. Eng.

5.1 Selected Computer Code

This Python code produces Figure 14 from the journal article.

```
# -*- coding: utf-8 -*-
"""
Created on Sun Jul 19 22:24:04 2015

@author: dan o'reilly
"""

import numpy as np
import matplotlib.pyplot as plt
import scipy.special as sp
import mpmath as mp
import matplotlib.lines as mlines
from matplotlib import rc
rc('text', usetex=True)

chart=221
for CD in [0,1e2,1e3,1e4]:
    for reD in [1e2,1e3,1e4,1e5]:
        w_a=np.logspace(-11,2,50)
        pD_iarf=list()
        pD_ss=list()
        pD_pss=list()
        for w in w_a:
            # IARF Infinite acting
            p=1j*mp.besselk(0,mp.sqrt(w*1j)) / \
                (CD*w*mp.besselk(0,mp.sqrt(w*1j))+w*mp.besselk(1,mp.sqrt(w*1j))/mp.sqrt(1j*w))
            pD_iarf.append(abs(p))
            # PSS Pseudo Steady State
            p=(mp.besselk(1,reD*mp.sqrt(w*1j))*(-2j*mp.hyp0f1(2,1j*w/4)-2j*(reD**2-1)* \
                mp.hyp0f1(1,1j*w/4)) + reD*mp.hyp0f1(2,1j*w/4*reD**2)*(mp.besselk(1, \
                mp.sqrt(w*1j))*2j+(reD**2-1)*w*mp.besselk(0,mp.sqrt(w*1j))/mp.sqrt(w \
                *1j))) / ((reD**2-1)*w*(reD*(CD*mp.sqrt(w*1j)*mp.besselk(0,mp.sqrt(w* \
                1j))+mp.besselk(1,mp.sqrt(w*1j)))*mp.hyp0f1(2,1j*w/4*reD**2)+mp.besselk \
                (1,mp.sqrt(w*1j)*reD)*(2*CD*mp.hyp0f1(1,1j*w/4)-mp.hyp0f1(2,1j*w/4)) ))
            pD_pss.append(abs(p))
            # SS Steady State
            p=( mp.besseli(0,reD*mp.sqrt(w*1j)) * mp.besselk(0,mp.sqrt(w*1j)) - mp. \
                besseli(0,mp.sqrt(w*1j)) * mp.besselk(0,reD*mp.sqrt(w*1j)) ) /( mp.besselk( \
                0,reD*mp.sqrt(w*1j))*(-1j*CD*w*mp.besseli(0,mp.sqrt(w*1j))+mp.sqrt(w*1j)*mp. \
                besseli(1,mp.sqrt(w*1j))) + mp.besseli(0,reD*mp.sqrt(w*1j))*(1j*CD*w*mp. \
                besselk(0,mp.sqrt(w*1j))+mp.sqrt(w*1j)*mp.besselk(1,mp.sqrt(w*1j))) )
            pD_ss.append(abs(p))

        plt.subplot(chart)
        plt.semilogx(w_a,pD_iarf,'b',label='IARF')
        plt.semilogx(w_a,pD_ss,'r-',label='SS')
        plt.semilogx(w_a,pD_pss,'g--',label='PSS')
        plt.xlabel('$\omega_D$')
        plt.ylabel('$|H(i\omega_D)|$ or $|\overline{H}(i\omega_D)|$')
    plt.axis([1e-11,1e2,0,14])
    plt.title('$C_D=%.0f$'%CD)
    plt.text(0.002,3.8,"$r_{eD}=10^2$")
    plt.text(1e-5,6.5,"$r_{eD}=10^3$")
```

```
plt.text(2e-7,8.5,"$r_{eD}=10^4$")
plt.text(2e-9,11,"$r_{eD}=10^5$")
plt.legend()
chart+=1
```

6 Identification of Oil Wells Requiring Reservoir Stimulation

Returning to the case of Barrow Island, Australia, examples are provided demonstrating successful production well management. In this chapter, an account is given for the identification of problematic production wells that will benefit from reservoir stimulation. The examples highlight the importance of reservoir surveillance, integrated studies and continuous improvement in mature assets. A combination of the methods can ensure prolonged oil production rates. It should be noted that Figure 13 in this chapter uses the type curves developed earlier in Chapter 2. This paper is published in the SPE Production & Operations journal.

Statement of Authorship

Title of Paper	A Lean Sigma Approach to Well Stimulation on Barrow Island, Australia
Publication Status	☑ Published ☐ Accepted for Publication ☐ Submitted for Publication ☐ Unpublished and Unsubmitted w ork w ritten in manuscript style
Publication Details	O'Reilly, D.I., Hopcroft, B.S., Nelligan, K.A., Ng, G.K., Goff, B.H. and Haghighi, M. 2018. A Lean Sigma Approach to Well Stimulation on Barrow Island, Australia. *SPE Production & Operations.* **33**(02): 393-408. SPE-182323-PA.

Principal Author

Name of Principal Author (Candidate)	Daniel O'Reilly		
Contribution to the Paper	Project manager for stimulation project, rate transient studies, preparation of graphs, writing the manuscript. Acted as corresponding author.		
Overall percentage (%)	80%		
Certification:	This paper reports on original research I conducted during the period of my Higher Degree by Research candidature and is not subject to any obligations or contractual agreements with a third party that would constrain its inclusion in this thesis. I am the primary author of this paper.		
Signature		Date	24 Nov 2020

Co-Author Contributions

By signing the Statement of Authorship, each author certifies that:

i. the candidate's stated contribution to the publication is accurate (as detailed above);

ii. permission is granted for the candidate in include the publication in the thesis; and

iii. the sum of all co-author contributions is equal to 100% less the candidate's stated contribution.

Name of Co-Author	Manouchehr Haghighi		
Contribution to the Paper	Principal supervision of the work. Manuscript review and assessment.		
Signature		Date	01/12/2020

Name of Co-Author	Brad Hopcroft		
Contribution to the Paper	Manuscript review and assessment.		
Signature		Date	26-Nov-2020

Name of Co-Author	Kate Nelligan		
Contribution to the Paper	Manuscript review and assessment. Helped with execution of workover rig activities.		
Signature		Date	25 Nov 2020

Name of Co-Author	Guan Ng		
Contribution to the Paper	Manuscript review and assessment.		
Signature		Date	25 NOV 2020

Name of Co-Author	Bree Goff		
Contribution to the Paper	Chevron Team Leader responsible for work planning and oversight. Manuscript review and assessment.		
Signature		Date	30 Nov 2020

A Lean Sigma Approach to Well Stimulation on Barrow Island, Australia

D. I. O'Reilly, Chevron Australia and University of Adelaide; **B. S. Hopcroft, K. A. Nelligan, G. K. Ng,** and **B. H. Goff,** Chevron Australia; and **M. Haghighi,** University of Adelaide

Summary

Barrow Island (BWI), 56 km from the coast of Western Australia (WA), is home to several mature reservoirs that have produced oil since 1965. The main reservoir is the Windalia Sandstone, and it has been waterflooded since 1967, whereas all the other reservoirs are under primary depletion. Because of the maturity of the asset, it is economically critical to continue to maximize oil-production rates from the 430 online, artificially lifted wells. It is not an easy task to rank well-stimulation opportunities and streamline their execution. To this end, the BWI Subsurface Team applied the Lean Sigma processes to identify opportunities, increase efficiency, and reduce waste relating to well stimulation and well-performance improvement.

The Lean Sigma methodology is a combination of Lean Production and Six Sigma, which are methods used to minimize waste and reduce variability, respectively. The methods are used globally in many industries, especially those involved in manufacturing. In this asset, we applied the processes specifically to well-performance improvement through stimulation and other means. The team broadly focused on categorizing opportunities in both production and injection wells and ranking them—specifically, descaling wells, matrix acidizing, sucker-rod optimization, reperforating, and proactive workovers. The process for performing each type of job was mapped, and bottlenecks in each process were isolated.

Upon entering the "control" phase, several opportunities had been identified and put in place. Substantial improvements were made to the procurement, logistics, and storage of hydrochloric acid (HCl) and associated additives, enabling quicker execution of stimulation work. A new program was also developed to stimulate wells that had recently failed and were already awaiting workover (AWO), which reduced costs. A database containing the stimulation opportunities available at each individual well assisted with this process. The project resulted in the stimulation of several wells in the asset, with sizable oil-rate increases in each.

This case study will extend the information available within the oil-industry literature regarding the application of Lean Sigma to producing assets. It will assist other operators when evaluating well-stimulation opportunities in their fields. Technical information will be shared regarding feasibility studies (laboratory-compatibility work and well-transient-testing results) for acid stimulation and steps that can be taken to streamline the execution of such work. Some insights will also be shared regarding the most-efficient manner to plan rig work regarding stimulation workovers.

Introduction

Economides and Nolte (2000) define reservoir stimulation as an activity to "enhance the property value by the faster delivery of petroleum fluid and/or to increase ultimate economic recovery." Well stimulation includes both hydraulic-fracture treatments (not considered on BWI) and matrix chemical treatments (acids, solvents, or other chemicals injected into the reservoir to improve reservoir properties). Generally speaking, the definition of well stimulation is restricted to activities resulting in the improvement of near-wellbore reservoir properties. In this particular work, however, we also considered options relating to workover activities and artificial-lift-design optimization.

On BWI, a recent cessation of well-stimulation treatments necessitated a closer examination of the processes in place for treatments on the island. Our interest in Lean Sigma arose from its earlier success in other projects for the BWI oil asset. After 2010, several projects had been started by team members to improve the profitability and efficiency of the BWI asset:

- Put-on-production (POP) cycle-time reduction in 2013
- Rig up/rig down improvements in 2013
- Water-injector-integrity monitoring in 2014
- Vehicle usage in 2015
- Production-performance improvements (the present work) in 2015

After these earlier projects entered the control phase, quantifiable dollar savings were recorded in each. This methodology for improving process and reducing variation has been proved within the asset and it was hoped that it would provide value for the current project.

A Lean Sigma project involves several phases: define, measure, analyze, improve, and control (DMAIC). In this paper, each section represents one or more of the interconnected phases of DMAIC and how they relate to the stimulation project. We first introduce the BWI oilfield asset and provide some description of our operations. Next, a short literature survey will be given on applications of the Lean Sigma toolbox to projects in the oil and gas industry. Finally, the DMAIC steps will be outlined in detail and related back to the success of this particular project.

BWI Background

BWI is situated in the northern Carnarvon Basin, 56 km from the coast of Western Australia **(Fig. 1).** The island spans 27 km north/south and 11.5 km east/west. Barrow No. 1, the first well on the BWI anticline, was drilled in 1964 with deep Jurassic targets at depths of up to 9,785 ft (McTavish 1965; Casey and Konecki 1967). A drillstem test measured production rates of 985 BOPD from some of the shallower Jurassic sections. Earlier in 2016, this well was recompleted and returned to service after many years of downtime, and it still produces oil at commercial rates.

This paper (SPE 182323) was accepted for presentation at the SPE Asia Pacific Oil & Gas Conference and Exhibition, Perth, Australia, 25–27 October 2016, and revised for publication. Original manuscript received for review 7 November 2016. Revised manuscript received for review 24 April 2017. Paper peer approved 2 August 2017.

Fig. 1—Location map of BWI L1H lease, Australia.

Oil is currently produced on BWI from several reservoirs: the Windalia (accounting for the majority of production), Muderong M3 (M3), Mardie B (MB), Tunney, and other Jurassic intervals. The Windalia has been waterflooded since 1967 and currently produces at a water cut of 91 to 92%, whereas the other reservoirs produce lower amounts of water because of their depletion-drive mechanism. There are currently more than 430 active producers and more than 200 active injectors on BWI. These wells are the target of the current Lean Sigma project.

Literature Survey: Lean Sigma

The use of Lean Sigma in the upstream oil and gas industry has been increasing since the early 2000s. Although borne out of the manufacturing industries in Japan, the energy industry has found many applications for Lean Sigma within its own businesses. The tools have been applied across a variety of problems, ranging from front-end-engineering design to highly operational problems.

Buell and Turnipseed (2004) have written an excellent introduction on the topic of Lean Sigma and its use in the oil industry. Several case studies are given. Of most interest to our project was the analysis of well-stimulation treatments. The authors studied a large database of historical data and found the optimal volume of acid required for an economic acid-stimulation job. Total stimulation workover time was also reduced as a result of the project. Another case study was given where the methodology for running production-logging-tool surveys was greatly improved to produce more-statistically-meaningful measurements, which resulted in a more-efficient workover program. Two more studies focused on optimizing sucker-rod-pump workovers and well-testing frequency. Overall, the projects were estimated to save at least USD 500,000 each. Buell also summarized these achievements as part of an SPE Distinguished Lecturer series (Buell 2006).

From the same operator, Popa et al. (2005) applied Lean Sigma in the Kern River Field for the purposes of production optimization. The authors recommend that the toolbox has a strong application in large fields, which is certainly the case for BWI as well. In the Kern River Field, time to POP, time to production peak, and incremental oil were all metrics that were improved as a part of their project. In addition to some artificial-intelligence techniques (Popa and Cassidy 2012b), value-stream maps (VSMs) were used to highlight inefficiencies in the process of returning a well to service after workover. Standard operating procedures, Kanbans (a scheduling system for manufacturing), and continuous-flow-production concepts were also used.

The topic of well-stimulation optimization by use of Lean Sigma has also been studied by Hejl et al. (2007) for the improvement of hydraulic-fracture-treatment design and by Juranek et al. (2010) to optimize fracture concentration, size, and other parameters through a review of the history of fracture treatments and a design of experiments, which is another Lean Sigma tool. Jati et al. (2015) have also used Lean Sigma tools in Sumatra for production enhancement and the realization of behind-pipe opportunities in their existing wellbores. The authors reported an average production improvement of 246%, with oil decline abated in their wells. There was a heavy

focus on prioritization of opportunities through data analysis of thickness, resistivity, and permeability of behind-pipe oil shows. The application of Lean Sigma for well-stimulation-process improvements is a proven technique.

Measurable improvements have also been made in oil and gas and health, environment, and safety (HES) areas with these techniques. Ghany (2010) has described the effect of the 5S (sort, set in order, shine, standardize, and sustain) method on HES performance for a major service company. Through the continual elimination of waste, training, and 5S audits, they were able to achieve more than 6 million working hours without a lost-time incident in the UAE since 2006. In Kazakhstan, a major operator was also able to demonstrate improvements made to their process-safety-information system through improved documentation and approval-process changes (Okshiev and Alteneder 2014). On the environmental side, Vargas and Scott (2015) shared reductions in energy, water, and waste as a result of following the DMAIC process.

Lean manufacturing and the continuous-improvement mantra have been used by several operators to reduce new drill costs and increase rig-work profits by reducing downtime and cutting operating expenditures (McCall et al. 2009; Charles et al. 2012; Allan et al. 2014). At the enterprise level, Eni S.p.A. has also implemented continuous improvement to structure its global portfolio and strategy (Chessa et al. 2013). Several case studies were given by the authors, ranging from oil-spill control to the reduction of planned maintenance activities.

Six Sigma alone is also a useful toolbox, particularly for the design of facilities and intricate operational problems. The focus of Six Sigma is more on reducing variability within a process, whereas lean manufacturing is focused on reducing waste. Al Adwani et al. (2011) present a case study of the use of Six Sigma on a gas-compression facility in Kuwait. Excessive glycol consumption at the plant was reduced in the dehydration unit by following the DMAIC process and using root-cause analysis. The root cause of the defect related to a reboiler-temperature setpoint and other operational values. In Central Luconia, Itua and Shamuganathan (2015) also used similar tools to assist with the front-end design of a liquefied-natural-gas (LNG) plant. Our paper focuses more on the "lean" side of Lean Sigma because of the nature of the stimulation projects.

The use of Lean Sigma in the upstream energy industry is becoming widespread and has been documented in several other cases that also demonstrate its value (Popa and Cassidy 2012b; Popa et al. 2005; 2012; Patty and Denton 2005; Basbar et al. 2016; Mustapha et al. 2015). We believe that this review of examples shows the worth of Lean Sigma to oil and gas companies, and we now proceed to the discussion of our own case study of BWI.

Problem Statement

In early 2015, the BWI subsurface team recognized that reservoir stimulation was a production opportunity that had been underutilized in recent years. In recent times, attention had been paid to drilling new wells or restoring parts of the waterflood network (O'Reilly et al. 2016a). The area of production enhancement from existing wells had been overlooked. As with any mature field, the goal was to reduce or abate production decline as much as possible.

Because of the remote location of BWI, the asset faces unique logistical and personnel challenges. It is likely that these issues had complicated reservoir-stimulation work in the past, and Lean Sigma was sought out as the tool to implement process improvements. In terms of "smart" objectives, the team wanted to see at least five stimulation jobs executed on wells in 1 year with measurable oil-rate increases.

Assembly of Lean Sigma Team and Project Timeline

During the "define" phase, it was important to assemble a Lean Sigma project team with stakeholders from all functions that would be involved in the project. In our case, it was important to involve functions spanning the planning phase (e.g., Earth science, HES) through to execution (workover engineers, operations staff). The full list of team members that were involved in the project includes:

- Project sponsor: BWI asset manager
- Project champion: BWI subsurface manager
- Project facilitator: production engineer
- Team members
  - Production engineer
  - Reservoir engineer
  - Workover engineers
  - Earth scientist/petrophysicist
  - Field-based staff
    - Production specialist
    - Wellwork supervisors
- HES specialist

In addition, external Lean Sigma black belt mentors who were experienced with the toolbox assisted throughout the duration of the project. It is advisable to include those who are familiar with the tools.

The team also agreed on a reasonable timeline for the project, in the form of a Gantt chart **(Fig. 2).** It was established that the total duration would be 5 months, after which the project would enter the "control" phase.

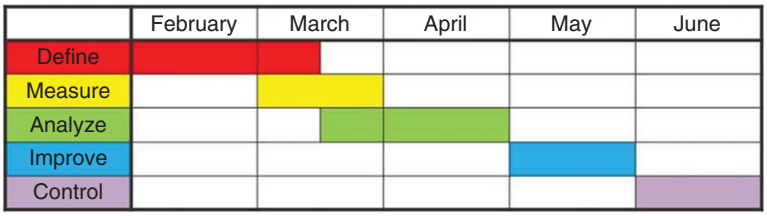

Fig. 2—Gantt chart for Lean Sigma project, 2015.

Review of Well-Stimulation Treatments Available on BWI

Throughout project "definition" and moving into the "measurement" phase, we developed a list of production-performance-enhancing activities that were available on BWI. The full collection is shown in **Fig. 3.** Some obvious well-stimulation activities are missing from

this table, such as hydraulic fracturing or hydrofluoric acid. Because of the remoteness of BWI, the lead times, handling issues, and costs associated with some options, some were simply not viable and were ruled out from the start of the project. The main production-enhancement opportunities available will now be discussed.

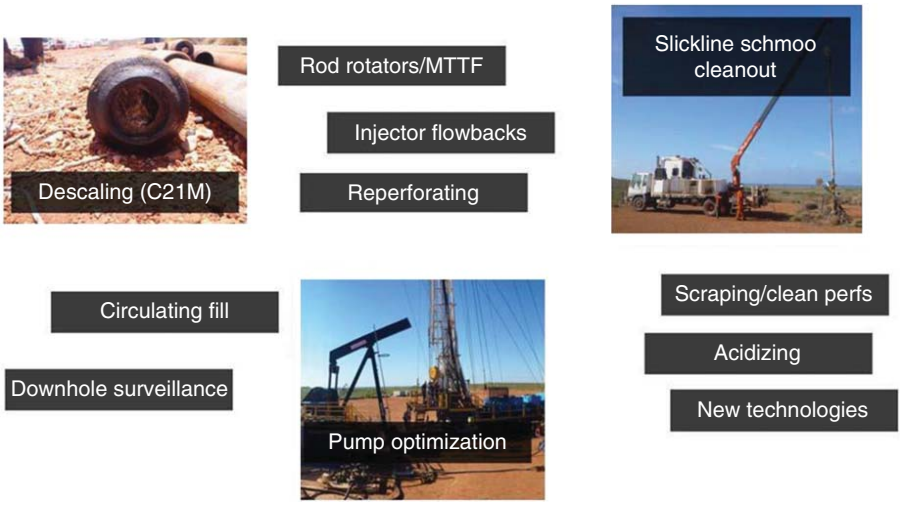

Fig. 3—Stimulation treatments available on BWI. MTTF = mean time to failure.

HCl Stimulation. HCl is a useful chemical that can be used to dissolve the reservoir matrix (production enhancement) and also precipitated scale in the tubulars or reservoir pores (removal of formation damage, which may also result from drilling-mud or completion-fluid invasion). The primary reaction taking place involves the dissolution of carbonate minerals, which can be present naturally within the rock matrix itself or in formed scale. Calcium carbonate ($CaCO_3$), or calcite/limestone, is a common example of a carbonate mineral, and when combined with HCl, the following reaction occurs:

$$CaCO_3 + 2HCl \rightarrow CO_2 + H_2O + Ca^{++} + 2Cl^{-}.$$

In the presence of an aqueous HCl solution, the carbonate ions dissolve and undergo a classical acid/base reaction. On BWI, a 15 wt% HCl solution is used and bullheaded into the reservoir.

The reservoir matrix itself can contain calcite and other carbonate minerals. Some other carbonate minerals include siderite, dolomite, and witherite. To some extent, all these minerals react when exposed to an acidic solution. When HCl is injected into a producing formation containing these minerals, they are dissolved in the rock and permeability is enhanced, leading to improved production rates.

Regarding formation damage, acid can also be used to dissolve some types of scale. The $CaCO_3$ scales are dissolved in accordance with the chemical reaction presented above. Other types of scale (e.g., barite and other sulfates) require specialized chemicals because of their low solubility in acid. Fortunately, on BWI, the majority of scale samples tested in the last 2 to 3 years have been composed of mostly $CaCO_3$. The presence of scale in the reservoir or wellbore on BWI could be caused by two factors:

- Reduction in brine pressure/temperatures (depletion in the reservoir or pressure drops through pipework), resulting in the precipitation of salts and known as self-scaling
- Mixing of different formation waters
  - Injection of nonindigenous formation water from Flacourt water-source wells into the Windalia waterflooded reservoir
  - Commingled production wells with perforations across different reservoir intervals (Windalia, M3, and MB commingled wells)

Chemical-scale inhibition is not currently installed across the BWI production network because the problem is not systemic on the island. However, on a handful of wells, we have identified scale through either steeply declining production rates or workovers when changing the downhole-pump completion. An example of a pulled pump from one workover is shown in **Fig. 4.** The plunger has been completely blocked with scale, which led to a seized pump. In another case **(Fig. 5),** thick scale (more than 1 cm) was removed when a scraper was run across the perforated interval. In both cases, we inferred that the productivity of the wells was hindered by the scale presence.

Ultimately, the removal of scale with HCl will have the effect of reducing reservoir skin or tubular blockages, and will hence increase oil production.

Sucker-Rod-Pump Optimization. All 400 + production wells on BWI are currently operated by artificial-lift completions, the majority being beam-pumped sucker-rod-pump completions. There are also a limited number of progressing-cavity-pump wells, but these are treated on an individual basis and were not considered to be within the scope of this Lean Sigma project.

The optimization of beam pumps (Takacs 2003) is an important consideration for both the Windalia waterflood and other depletion reservoirs. As an addition to the regular operating characteristics of the beam pumps (O'Reilly et al. 2016a), we studied the completion types at each well, including pump-setting depth with respect to perforations, pump-bore size, and tubing vs. insert pumps.

Finding wells with shallow pumps or small pump bores (with spare inflow capacity) represents a production-gain opportunity. As such, the goal was to catalog these opportunities in a later part of the project.

Slickline Cleanouts. Another method for the removal of solids in the wellbore on BWI is the use of slickline operations. A slickline unit is already used on the island to prepare wells for rig work, tag effective depth on injectors, or run perforation guns during recompletions. One option for production improvements is the removal of wellbore fill from producers, or fill/schmoo from injection wells. Some of the schmoo-removal work discussed by O'Reilly et al. (2016a) was achieved using slickline. Typically, a bailing tool and/or wax knife has been used to lift solids from the wellbore, with some success.

Fig. 4—Scale observed in tubing (left) and sucker-rod-pump plunger (right).

Fig. 5—Scale removed from perforations after scraper run during workover.

Reperforations. Reperforations are frequently executed on BWI, but they were considered outside the scope of this particular improvement project. They have been treated on a per-project basis because of the uniqueness of each behind-pipe opportunity and the workover/facilities requirements.

From the project-framing sessions and the discussion of alternative simulation/enhancement methodologies, the project team decided that from the previously discussed methods, the largest opportunities for improvements lay in the acidizing and pump-optimization areas, in this order of importance. These were the areas that had received the least attention recently, and it was likely that substantial process improvements could be made. A tradeoff matrix for the alternatives is shown in **Table 1.**

In this matrix, three different alternatives are compared with one another by column (acid/descaling, general pump optimization, and "new technologies"). These alternatives were assessed by the team in terms of various value drivers. By comparing the value drivers for each alternative, it was possible for the team to settle on the most-preferable alternative for production enhancement. Of highest value to the team were safety, cost, environment, production effect, lead time, and organizational capability. Certain value measures were used to quantify these drivers, such as incremental production and discounted profitability index. On the basis of the various drivers and measures, it was apparent to the team that this project would focus on improving the existing production-enhancement techniques on BWI, such as acid stimulation. The consideration of new technologies would be undertaken at a later date.

Analysis of Well-Stimulation Candidates and Database Development

We now move into the "measure" and "analyze" phases of the project, during which the existing processes were studied for the selection of stimulation candidates, ordering materials, planning workovers, and interfacing between job functions. A stimulation database containing all production and injection wells on BWI was developed. The suitability of each well to stimulation or pump-optimization improvements was stored in this catalog.

To develop the context of this project, the project team met and jointly developed process maps using several of the Lean Sigma tools. An input/process/output (IPO) diagram was created, as shown in **Fig. 6.** This diagram helps frame the important areas of this project: the end-output goals are to increase oil production after a stimulation workover, decrease the cost of stimulation jobs, and increase the number of production-improvement activities per annum. The most relevant inputs to this process are the material availability, well suitability for stimulation, and rig scheduling. The inputs serve as variable factors in the governing process, which sits in the middle of

the diagram ("Enhancement Planning and Execution"). Through measuring and analyzing this process, it is possible to identify opportunities for improvement.

Value Driver	Acid/Descaling	Pump Optimization	New Technologies
Safety	Dangerous goods	Standard workover	Unknown
Cost	Cheap materials	Low cost parts	Several new technologies are low cost
Environment	No impact without spill	Nil	Unknown
Production/Injection Impact	Proven on BWI	Good but sand risk	Potentially good
Lead Time	Issues with supply/storage	Issues with supply/storage	Longer because of new product contract
OC	Experienced WWS	Routine P/C	Requires training
Value Measures 1. Safety/environment 2. Incremental production 3. DPI	+ Proven application on BWI + Rig crews/WWS experienced with acidizing already + Wells have not been acidized in several years - Supply and storage issues	+ Routine work + Low cost - Sanding risk for lowering pumps on some wells - Supply issues	+ Large upside w/ some new technologies - Potentially complex - Rig crew/operators require training - No history of application in field

Table 1—Tradeoff matrix for alternatives.

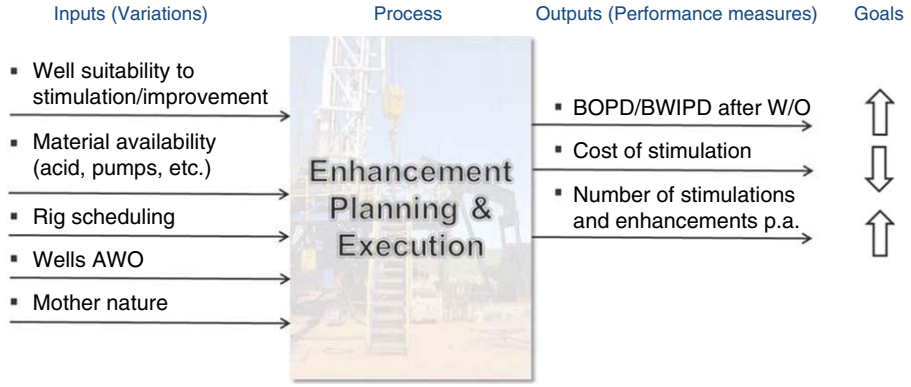

Fig. 6—IPO diagram for production-enhancement opportunities.

The project team moved to discussing how acid stimulations were executed on BWI before the beginning of the project. A VSM for this process is shown in **Fig. 7.** The VSM serves as a useful tool to measure the flow of information or material (e.g., acid chemicals) to an end user (e.g., Chevron BWI). In this diagram, the process begins at the BWI warehouse (top right) and follows counterclockwise. An order is placed for chemicals, which follows through procurement teams and to two suppliers. Supplier 1 provides the acid-additive chemicals, and Supplier 2 supplies the HCl. The lead time of Supplier 1 is much longer, and this area deserves investigation.

It was identified that there were several limiting factors that constrained the number of acid jobs being executed on the island. First, the warehouse on BWI had a limited license for the storage of corrosive fluids (HCl and additives). Second, chemical Supplier 1 had longer lead times because of interstate warehouses. These two factors combined led to difficulties in planning and executing regular acid-stimulation jobs. A cascading IPO is also shown in **Fig. 8.** Using this tool, almost the same information as in the VSM is expressed in a slightly different way. Rather than following the flow of materials, the cascading IPO looks at the processes used from start to finish of the acid job. Later in the "improve" phase, these problems would be remedied.

One important issue raised was the concern over which wells were suitable for acid-stimulation treatments. Understanding the reason for acidizing was important because we have seen that matrix-stimulation volumes need to be larger than those used for scale remediation. This resulted in the development of a database containing the candidacy of each well on BWI **(Table 2).** Of relevance to HCl stimulation, we considered the following factors:

- Scale likelihood, based on
  - Presence of scale seen from previous workover-tour reports
  - Excessive/spurious liquid-rate declines seen in production history
  - Perforation in multiple intervals (mixing of brines from each interval, resulting in scale)
- Rock-matrix response to acid
  - Windalia Sandstone: occasional occurrence of carbonate minerals in specific wells
  - M3 Sandstone: higher proportion of carbonate minerals
  - Gearle Siltstone: frequent occurrence of carbonate anomalies in wells

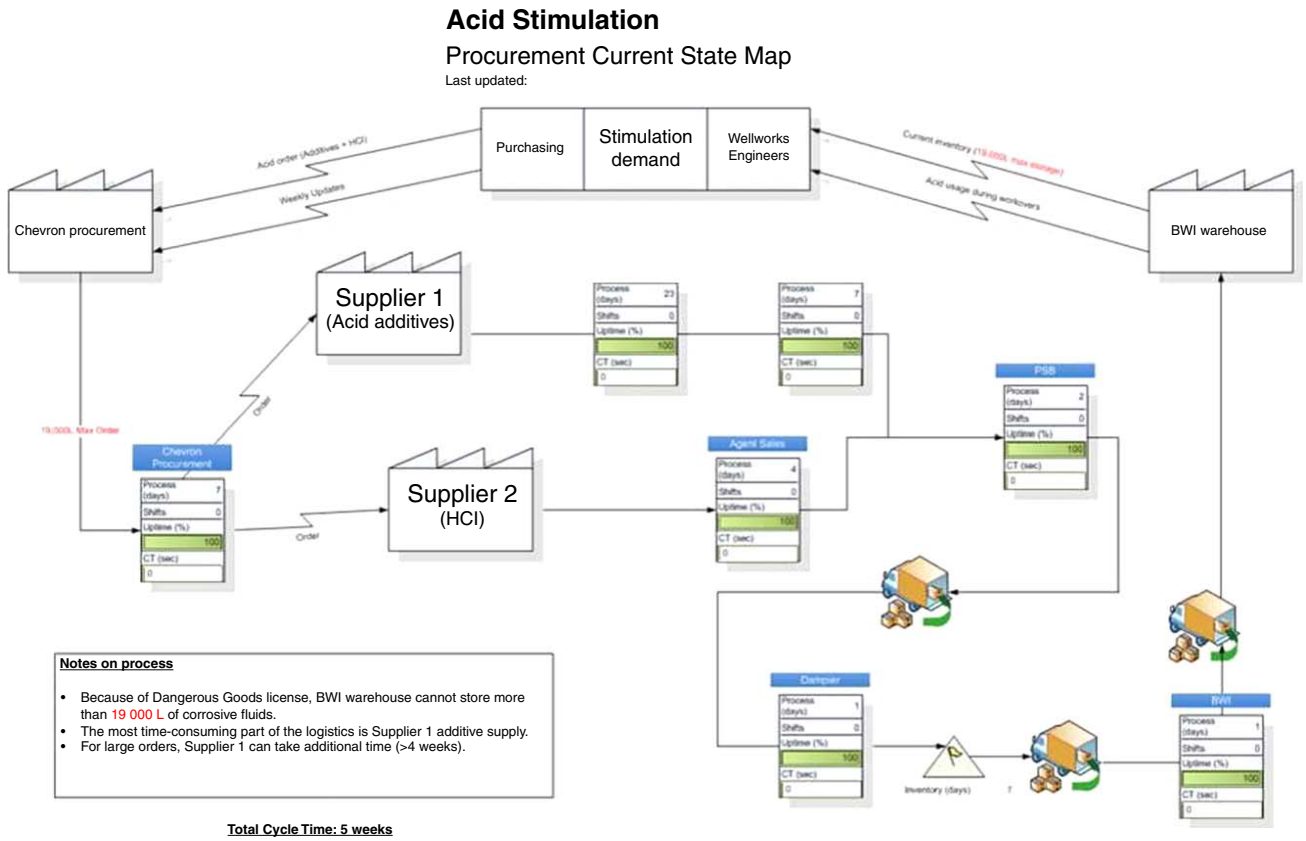

Fig. 7—Original VSM for acid stimulation.

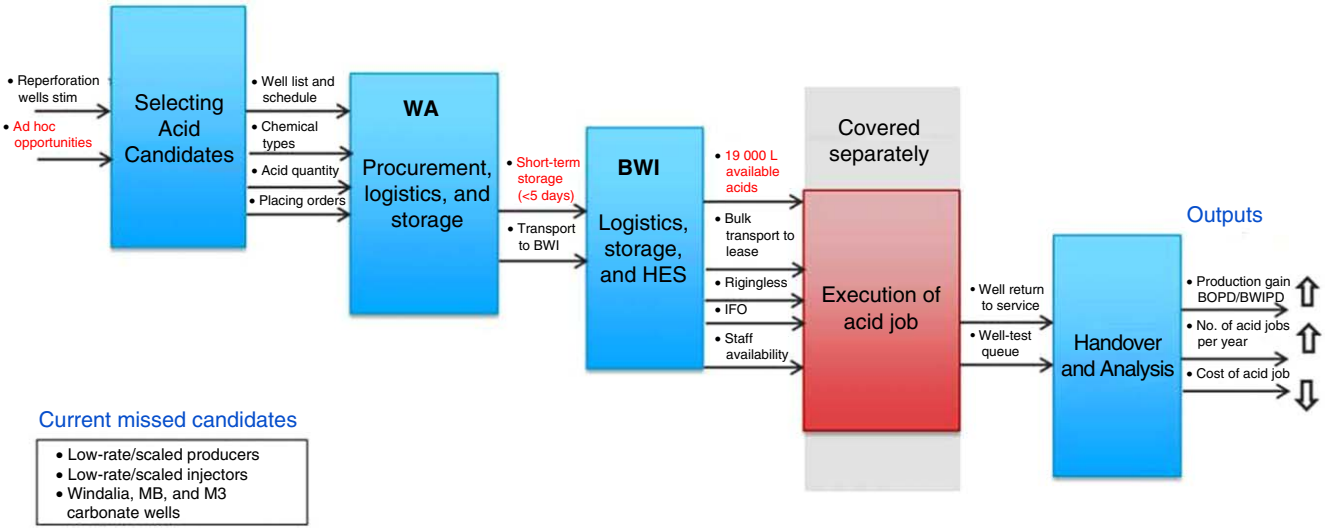

Fig. 8—Acid-job-logistics cascading IPO (current state). The primary focus was on increase of barrels of oil produced per day (BOPD) or barrels of water injected per day (BWIPD).

In the columns of Table 2, from left to right, the perforated intervals of each well are first given (Windalia, M3, MB, or Jurassic reservoirs). The next four columns indicate if the well is suitable for either a scale or matrix-acid treatment. Finally, the last two columns tabulate the sucker-rod-pump setting depth and pump-bore size, which provide an indication of whether a pump-optimization opportunity exists.

The suitability of each well and reservoir to matrix acidizing was studied carefully. In the Windalia Sandstone, for example, the majority of wells contain very little calcite (less than 3 wt%) and are unaffected by acid treatments. However, specific wells and parts of the reservoir contain very high concentrations of carbonates, and this is visible on the well logs **(Fig. 9).** For these two wells, Producer 1 is seen to contain carbonate anomalies because of unusually high resistivity and high sonic-log velocities. The anomalous carbonate composition can reach up to 50 wt% in these wells. For the same tracks in Producer 2 (right-hand side), a normal Windalia signature is seen. The wells with the largest occurrence of carbonate anomalies, or the highest deviation from a regular Windalia wireline log, are the most prospective for acid treatment. Each Windalia log in the field was categorized using a visual inspection of the logs into an integer value from 0 to 3, where 0 indicated wells with no carbonate content and 3 indicated a high presence. These were entered into the database (the ninth column of Table 2).

										1 or 0 at this stage. Wells from Prod Spec, seen scale.	General M3 wells are all prospective for acidizing		This is a relative number - the higher, the better the candidate	Pump setting depth data from LOWIS	Smaller pump bores are able to be upsized to tubing pumps
	Perfd Reservoirs					Scale/Matrix Acid Job Candidates								Sucker Rod Pump Performance
Well	Windalia	M3	MB	J		Scale Job		M3 Acid		MB Acid		Windalia Acid	Pump Above Perfs (m)	Current Bore
Well names removed	1	0	0	0	✗	0	✗	0	✗	0	●	1	0	2.25
	1	0	0	0	✗	0	✗	0	✗	0	●	2	0	0
	1	0	0	0	✓	1	✗	0	✗	0	●	1	–41	2
	1	0	0	0	✗	0	✗	0	✗	0	●	1	–46	2.5
	0	0	1	0	✗	0	✗	0	✓	1	●	0	0	0
	1	0	0	0	✗	0	✗	0	✗	0	●	1	49	2
	0	1	1	0	✗	0	✓	1	✗	0	●	0	0	0
	1	0	0	0	✗	0	✗	0	✗	0	●	1	0	2.25
	1	0	0	0	✗	0	✗	0	✗	0	●	1	–21	2
	1	0	0	0	✗	0	✗	0	✗	0	●	3	–29	2
	1	0	0	0	✗	0	✗	0	✗	0	●	2	49	2
	1	0	0	0	✗	0	✗	0	✗	0	●	2	50	2
	1	0	0	0	✗	0	✗	0	✗	0	●	3	–34	1.5
	1	0	0	0	✗	0	✗	0	✗	0	●	3	–20	1.5
	0	1	0	0	✗	0	✓	1	✗	0	●	0	0	0
	0	1	1	0	✗	0	✓	1	✗	0	●	0	–53	1.5
	1	0	0	0	✗	0	✗	0	✗	0	●	3	37	2
	1	0	0	0	✗	0	✗	0	✗	0	●	1	0	2.25

Table 2—Production-improvement opportunity-tracking database, containing information for more than 430 production wells on BWI.

One remaining issue in the design of acid treatments is the compatibility of the injected fluids with all contacted media, such as (Economides and Nolte 2000)

- Acid-mixture compatibility with formation-crude/brine mixture. Some mixtures may form an emulsion in the reservoir, and this can be investigated in a laboratory before field execution.
- Compatibility with formation-rock mineralogy. Because the Windalia is a sandstone reservoir, clays exist within the rock. There is a risk that the minerals in some formations (e.g., those containing iron) may form insoluble precipitates when combined with acid. Hydrofluoric acid is particularly known for this, although it was not used in our project.

Laboratory studies have been completed to mitigate these compatibility risks. X-ray-diffraction (XRD) tests have been performed previously on the Windalia sand, and an emulsion test was performed for the reservoir fluids and acid in 2015.

The presence of minerals containing iron was noted from the XRD **(Table 3),** which indicates that iron precipitates are possible in an unfavorable stimulation job. However, glauconite is not a known cause of formation-damage problems when acidized with a low-wt% HCl mixture. Furthermore, pyrite is present only in small quantities (less than 3 wt%). Despite this, our acid recipe **(Table 4)** includes iron-chelating agents as a conservative measure because iron precipitates may still form in reactions with tubulars and steel storage tanks. The additives ensure that iron is kept in solution.

The results of a simple and qualitative emulsion test of the acid mixture and formation fluids are shown in **Fig. 10.** This was performed on fluids from the major reservoir intervals on BWI. The results indicate that after a reasonable duration, the phases separate and do not emulsify. This is clear because there is a distinct separation between oil and brine. It is easy to perform this type of test in any laboratory.

The composition of scale is also important in the design of an acid treatment targeted at removing formation damage. We performed laboratory analysis on several scale samples removed from well workovers. Through scanning electron microscopy and energy dispersive spectroscopy, it was determined that the composition of the samples was a carbonate material **(Fig. 11),** apparent from the high calcium and oxygen elemental composition. The solubility of carbonates in HCl is excellent, so this verified the existing acid design for the treatment of these damaged wells. A completely dissolved sample of the formation scale in HCl is also shown in **Fig. 12.**

It was previously mentioned that there is value in inspecting production histories of wells to find anomalous declines indicative of formation damage (e.g., scale, fines, or fill). Particularly in waterflood reservoirs, liquid rates should match injection rates as close as possible. Visual inspection of wells in our production-allocation software highlighted wells of concern. One final method of note is a new technique we have developed for productivity-index (PI) determination purely from pump-controller rate-transient data. An exemplary case for three Windalia wells is shown in **Fig. 13.** In this dimensionless example, the PI for each well is calculated following the methods of O'Reilly et al. (2016b). This PI is then compared with expected Windalia values, from which wells with deviations can be inspected.

This type of calculation is unique because it allows for the calculation of PI in wells undergoing periodic pumping, where the well is produced and shut-in several times throughout the day (i.e., several cycles). The configuration is frequent for beam pumps on BWI (O'Reilly et al. 2016a). Conventional calculation steps for PI assume constant and stabilized production from the wellbore, whereas this new method is particularly suited to wells undergoing periodic production. In Fig. 13, the dimensionless chart plots the proportion of time that a well is running vs. the cumulative number of cycles (on and off) since it started production. We define a single cycle as the oil well being switched on and then off once. By its nature, this particular chart includes a transient drawdown-like phenomenon to calculate PI. The production of the well clearly recedes after the flush production reaches a more-stable rate. The dimensionless chart is very useful for wells that have returned to production in a relatively undisturbed reservoir. We refer the readers to O'Reilly (2016b)

for more discussion on this procedure. For oscillating wells where boundary effects have been felt already, other methods are applicable.

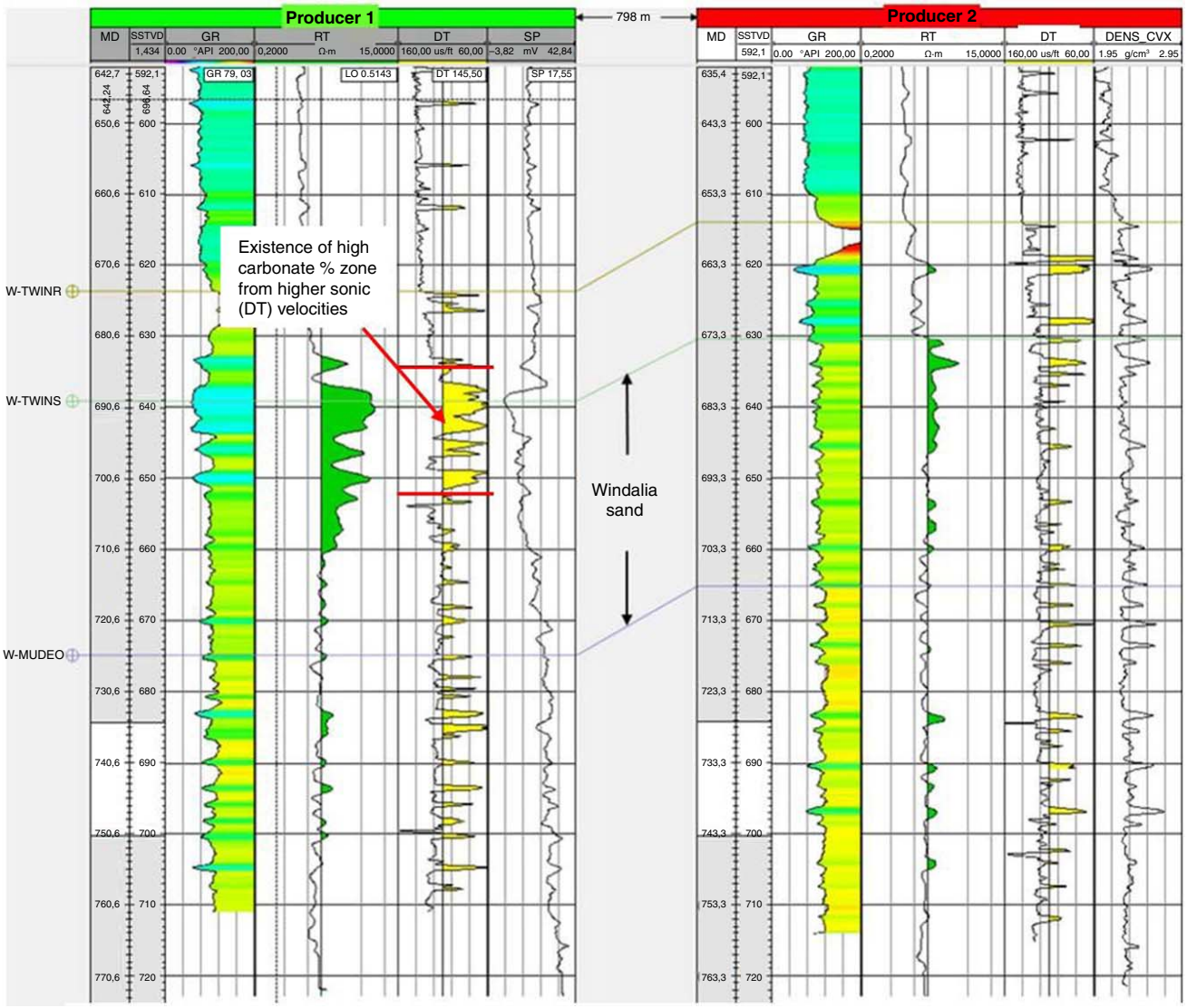

Fig. 9—Comparison of two Windalia production wells, 798 m apart on BWI. Producer 1 has evidence of anomalous carbonate layering from the resistivity track (ILD) and sonic track (DT). Producer 2 shows the regular Windalia log signatures, and is not an attractive candidate for HCl stimulation dependent on mineralogy alone.

Windalia Sandstone: Average Layer Properties (Core)

	Average *k* (md)			Mineralogy, XRD (wt%)						
Interval	Average <*p* (%)	Arithmetic	Geometric	Quartz	Feldspar	Kaolinite	Glauconite	Muscovite	Calcite	Pyrite
Gross Windalia	23.19	6.54	3.4	27.6	21.7	10.8	32.9	4.2	1.5	1.7
Layer 1	24.21	10.69	4.9	25.8	21.0	5.6	39.1	4.7	2.0	1.6
2	23.31	7.82	3.8	27.7	22.5	7.7	33.6	4.1	2.2	1.7
3	23.72	5.77	3.6	27.3	26.8	9.4	28.4	4.3	2.7	2.1
4	24.00	7.34	4.6	27.2	22.5	9.2	32.1	3.9	2.3	2.2
5	24.22	10.44	6.6	26.9	23.7	8.6	33.0	3.6	1.6	2.0
6	23.05	7.20	3.9	26.8	23.5	11.4	29.8	4.3	1.7	2.0
7	20.43	2.41	1.4	26.5	16.3	14.9	33.1	4.8	1.5	2.0
8	22.33	2.56	1.9	26.2	19.5	12.0	35.8	4.9	1.3	1.2
9	23.41	4.66	2.9	28.7	19.9	9.6	36.1	3.8	1.3	1.0

Table 3—XRD mineralogy of Windalia Sandstone core samples. This analysis represents a typical Windalia well, where calcite percentages are less than 3 wt%. Windalia wells with anomalous calcite composition (up to 50 wt%) can be targeted for HCl stimulation. Layers 1 through 6 are upper sands; Layer 7 is the middle unit; Layers 8 and 9 are lower sands. *k* = permeability.

Ingredient	Volume	Unit	No. of Packages	Package Size
Water	1,638	gal	39	bbl
Corrosion inhibitor	40	gal	8	5-gal pail
Surfactant	5	gal	1	5-gal pail
Chelating agent: Citric acid Fe-2	200	lb	4	50-lbm sack
Chelating agent/buffer: Acetic acid Fe-1	40	gal	8	5-gal pail
28% HCl	1,849	gal	7	1000-L bulk

Table 4—Example recipe for 85 bbl of 15 wt% HCl treatment.

Fig. 10—Emulsion testing of Windalia fluid sample with acid recipe (qualitative method). Sample on the left has settled for 2 minutes; sample on the right settled for 30 minutes.

Process Improvements

In the "improve" phase, the main tasks that were completed relate to the deficiencies identified in the existing stimulation processes. As noted previously, there were some gaps in the supply-chain and procurement processes that needed to be addressed.

Several options were considered to increase the quantity of available acid and decrease the lead times (**Table 5** is a selection matrix for alternative storage options). It was decided that upgrades would be made to the allowable BWI storage space for corrosive fluids. Because of the unique status of BWI and its isolation, storage space is scarcer than at other locations in the country. The operating footprint is carefully managed on BWI, and both HES and government bodies are engaged throughout the process. Acknowledging that this would take time, the chemical vendor agreed to stockpile chemicals locally in Western Australia until the BWI approvals were complete.

The improved acid-stimulation VSM is shown in **Fig. 14,** which reflects the changes as discussed. In contrast to the original-state VSM, cycle time was reduced dramatically from 5 or more weeks to 3 weeks or fewer.

Another improvement that was identified was the financial benefit associated with working over wells that were already on the rig-workover queue for pump repair. In the past, many stimulation activities were performed proactively on wells, and the rig was mobilized specifically for stimulation only. However, rod-pump or progressing-cavity-pump failures are a routine occurrence in this operation, and most wells are visited every 3 to 4 years for artificial-lift maintenance. The opportunity of reactive stimulations concurrent with pump workovers was not captured by the asset at the time. By monitoring the workover queue and using our stimulation database, it was possible to target wells that were recent failures and capture significant savings. The use of the stimulation database allowed for quick decisions on opportunities that may have been missed otherwise.

With regard to the engagement of each job function, a proposed state map with "swim lanes" was also developed **(Fig. 15).** Each swim lane (or row) indicates a different function involved in the process. Each step in the process is shown as an individual column. The functions involved are production engineers, production specialists (field-based), Perth logistics, field warehouse, and the workover team. In this work flow, candidate wells would first be selected by production engineers in Perth, under the consultation of BWI-operations production specialists. After this, logistics and workover teams would be engaged for execution of the opportunity for each well. The execution of the stimulation treatment in the field would be handled by the Well Works workover team, who would then hand the well back to production specialists on BWI. Production engineers in the Perth office would then perform analysis on the prestimulation and post-stimulation well performance. This will be discussed later in the paper.

Project Execution

After the project entered the "control" phase, the process improvements allowed for the execution of several new opportunities. The new strategy of the subsurface team was to monitor the queue of wells awaiting workover and to consult the developed stimulation database. Through a close relationship with field engineers and rig managers, it was possible to ensure that these opportunities were captured. Over the last 2 years, nine wells have been stimulated on BWI, along with many additional sucker-rod-pump-optimization workovers. Most of these wells had measurable oil gains associated with each activity.

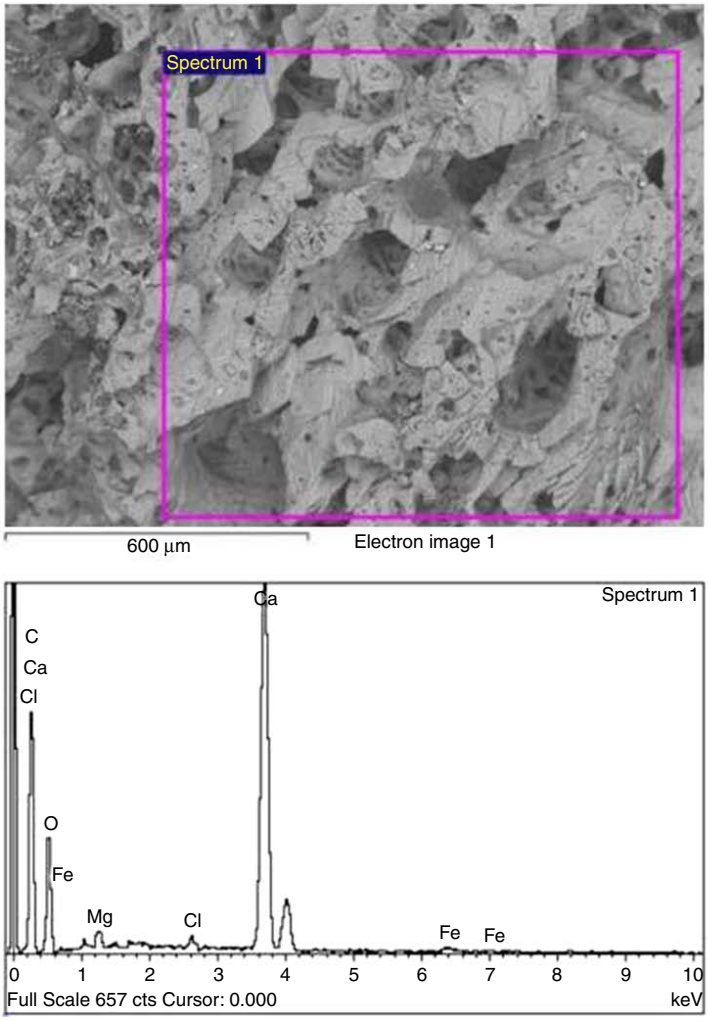

Element	(wt%)	(at%)	
O K	57.41	76.79	
Mg K	1.70	1.50	
Cl K	0.81	0.49	
Ca K	38.95	20.79	
Fe K	1.12	0.43	
Totals	100.00		

Fig. 11—2015 scanning electron microscopy and energy dispersive spectroscopy of BWI wellbore-perforations-scale sample. Composition indicates high calcite composition.

Fig. 12—HCl testing of 1-g scale sample, dissolving within 1 minute (well name removed). A small amount of scale was added to the 15% HCl solution. Gas evolved rapidly and the 1-g scale sample dissolved completely.

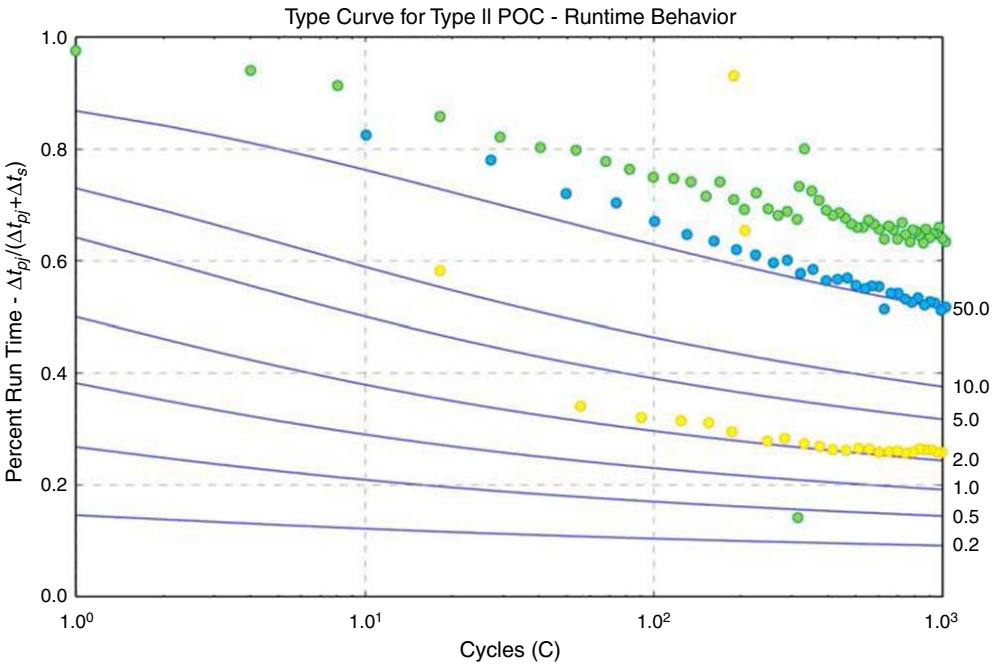

Fig. 13—Dimensionless example of rate-decline techniques used for quantification of PI of wells using pumpoff controllers (POCs). Type curves are from O'Reilly et al. (2016b). Three wells are marked in separate colors.

Lack of Acid Stimulation Jobs on BWI

Selection Matrix

Root cause: Small max storage constraint for acid on BWI

	Alternative Solutions	How well does this address root cause?	Time to implement?	Time to execute each acid job?	Cost to implement solution?	Cost to execute each acid job?	Safety and Environment Risk?	Total
	Weight	40%	20%	10%	10%	10%	10%	
1	Only extend DG license at BWI warehouse	7	2	8	9	9	7	6.5
2	Supplement with temp license storage at BWI lease	9	4	8	3	9	7	7.1
3	Supplement with storage at Perth facility c/o Chevron	8	8	6	7	7	4	7.2
4	Supplement with storage at Perth facility c/o Supplier 1	8	8	6	8	7	9	7.8

Table 5—Selection matrix for acid storage on BWI.

In **Fig. 16,** the production results of three Windalia acid-stimulation workovers are shown in a dimensionless format. The relative change in oil rate is shown for several well tests after the stimulation event. Two of these workovers were targeting carbonates, whereas the remaining one was used to treat a scale problem. Although there is some noise apparent in the charts, production gains of more than 100% were measured in the examples. Well-production tests represent the flow performance at a snapshot in time and irregularities may occur, especially after a stimulation treatment or when the well is not fully pumped off. This was the case for Well B, which only began to pump off during the last few well tests, resulting in increases in oil rate. Almost immediately, there was a gain in liquid rate after the stimulation, and it can take time to lift additional oil. It is the upward trend in oil rate for these well tests that is important.

Using the results from well tests such as these and the reduction in well-stimulation cycle time, we consider this project to be a success on BWI.

Evaluation of Post-Stimulation Well Performance

In this section, we will discuss a fit-for-purpose evaluation methodology used to compare prestimulation and post-stimulation treatment-well performance. Dimensionless well-test results have already been shown in Fig. 16. We have used a simplified but robust technique dependent on PIs to compare well performance before and after treatment. In the environment of stripper oil wells, it is not always practical to perform full pressure-transient analysis on wells both before and after stimulation treatment to assess improvements. This is because of the costs involved with executing the transient test and the deferred oil production required to perform a pressure buildup. Nevertheless, it is possible to compare the productivity of wells before and after treatment when considering their stabilized producing and operating conditions. This has been done in this project to verify the success of each treatment.

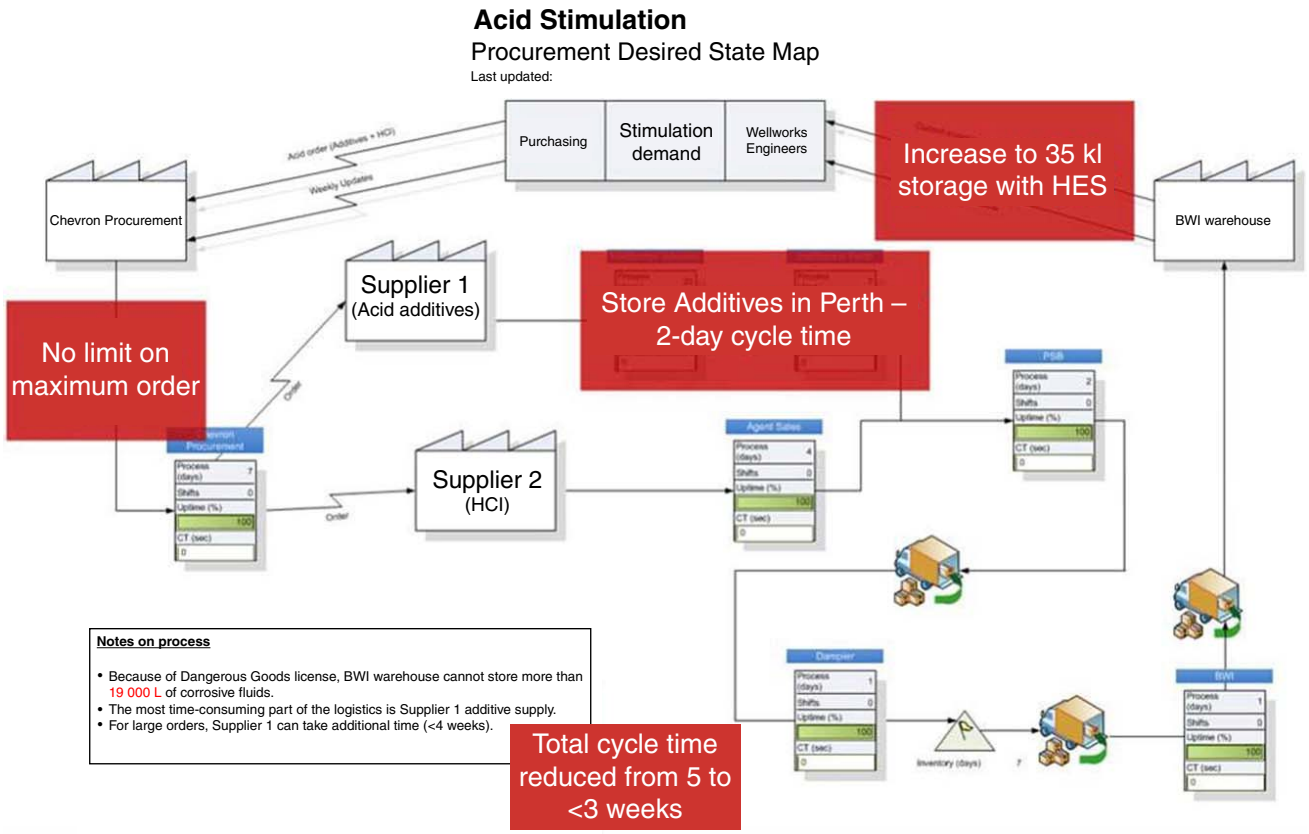

Fig. 14—Desired VSM for acid stimulation.

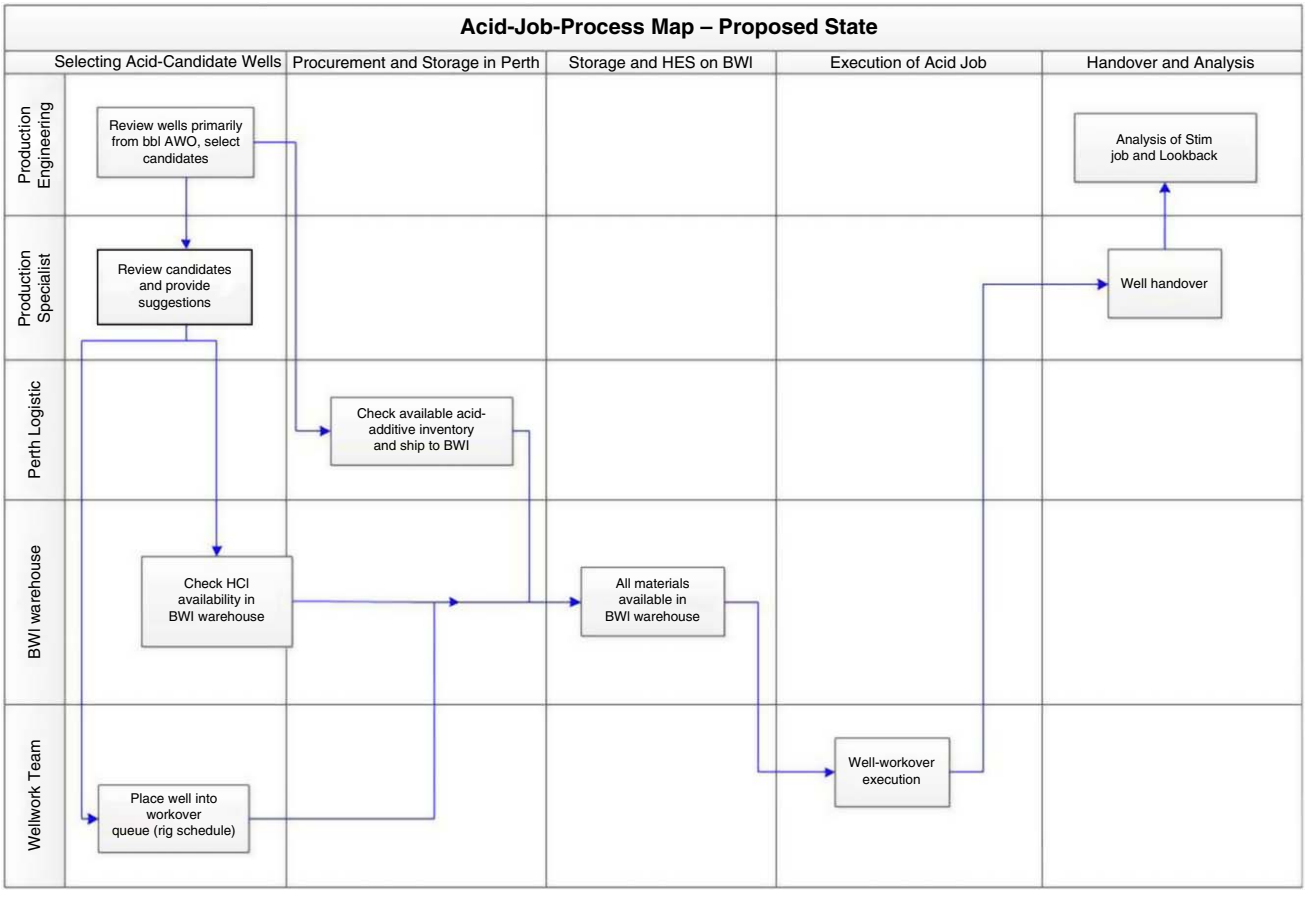

Fig. 15—Proposed state-process map for acid stimulation.

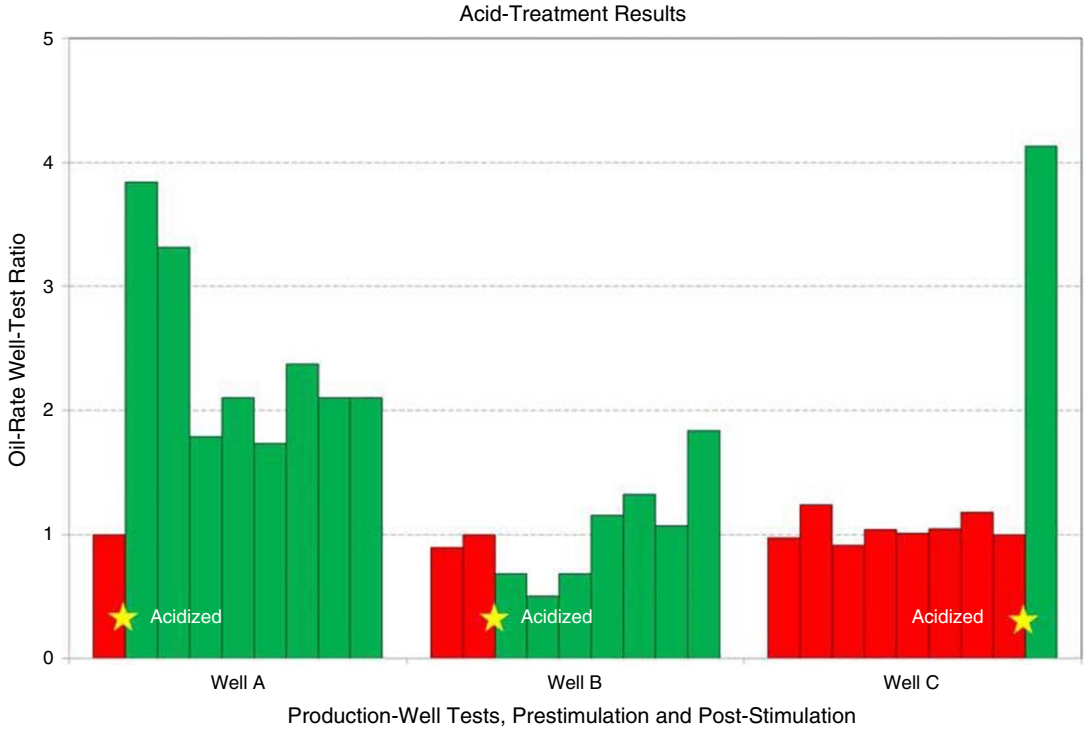

Fig. 16—Well-test results for acid treatments on production wells perforated in the Windalia sand. Each bar on the diagram indicates an individual well test. Red bars are tests before acidization, green bars are after the treatment. Well A and Well B treatments were for carbonate matrix stimulation, whereas Well C was for formation scale.

The operation of sucker-rod-pumped wells involves producing fluids through a full tubing column with a positive-displacement pump while a stagnant fluid level in the annulus exerts pressure on the sandface (Takacs 2003). In normal steady-state producing conditions, the liquid level in the annulus (hence, bottomhole pressure) is maintained at a constant, minimum level and the well produces at a constant rate. To assess the productivity of the three wells under question on BWI, only production well tests at this condition were compared with each other. If this is not the case, it is possible that the phenomenon of "flush production" can distort the comparison. Flush production occurs when a well has been shut in for a substantial period for the reservoir energy to recharge so as to produce additional fluids upon reinstatement. In the example of constant-pressure bottomhole-drawdown transient production, a large period of flush production will occur before rate stabilization. We avoided this period.

In **Table 6,** results are shown for the PI of wells before and after treatment, in dimensionless form. The methodology for calculating PI is as follows. Well tests are taken periodically (Fig. 16), and each well test is accompanied by an acoustic-fluid-level measurement. Only after both stable production and stable fluid level are obtained is the PI for this well test used. The results in Table 6 are the average of several stabilized-well tests.

The results from Table 6 indicate that in all three wells, the oil-productivity gain after stimulation was measureable.

	Expected Undamaged PI Range (Mantecon 1993)	Ratio of PI After/PI Before Stimulation Treatment
Well A	0.05–0.1 BOPD/psi	1.9
Well B	0.1–0.2 BOPD/psi	1.3
Well C	0.1–0.2 BOPD/psi	4.0

Table 6—Productivity of oil wells before and after stimulation treatment.

Conclusion

In this oil asset on BWI, Australia, we implemented Lean Sigma in a project designed to increase the frequency of well-stimulation workovers. The project was successful in that it met our primary objective, while also reducing the cost of treatments and increasing tested-oil rates after stimulation activities. The key achievements were as follows:

1. The allowable warehouse-storage space on BWI was increased for stimulation materials to improve the original supply problems.
2. A universal acid recipe was verified against rock mineralogy and fluid emulsions and used for all subsequent acid jobs on BWI.
3. An extensive database was developed to catalog all stimulation opportunities available on more than 400 producers and 200 injectors on BWI.
4. Rather than proactively working over production wells to perform stimulation, the database was compared with wells already awaiting workover after pump failure. This resulted in significant cost savings because of the reduced number of rig days required to perform a stimulation workover; 1 to 2 days' worth of rig move and performing preparations was saved.
5. The project has resulted in the successful stimulation of several wells on BWI since its inception, three of which were shared in this paper (Fig. 16). An analysis of the well performance for these cases has been discussed.

Nomenclature

C = number of cycles of beam pump operation
DENS = density log, g/cm^3
DT = sonic log, μs/ft
GR = gamma ray, °API
j = subscript used to denote current beam-pump cycle
k = permeability, mD
MD = measured depth, m
PI = productivity index, bbl/d/psi
RT = resistivity log, ohm-m
SP = spontaneous potential, mV
SSTVD = subsea true vertical depth, m
Δt_{pj} = beam-pump production time during cycle j, hours
Δt_s = beam-pump shut-in time (constant for each cycle), hours

Acknowledgments

The BWI oil field is operated by Chevron Australia on behalf of the Barrow Island Joint Venture partners, which include Chevron Australia, Santos Offshore, and Mobil Australia Resources Company. We thank Chevron Australia and the Joint Venture partners for their permission to publish this work.

References

Al Adwani, A. E., Al-Zuwayer, H., and Kapavarapu, V. M. R. 2011. Six Sigma Approach to Meet Gas Dehydration Unit Optimization. Presented at the SPE Asia Pacific Oil and Gas Conference and Exhibition, Jakarta, 20–22 September SPE-147042-MS. https://doi.org/10.2118/147042-MS.

Allan, M. E., Reese, D. W., and Gold, D. K. 2014. Application of Toyota's Principles and Lean Processes to Reservoir Management: More Tools to Overload the Toolbox or a Step Change in Our Business? *SPE Econ & Mgmt* **6** (2): 67–87. SPE-165331-PA. https://doi.org/10.2118/165331-PA.

Basbar, A. E., Al Kharusi, A., and Al Kindi, A. 2016. Reducing NPT of Rigs Operation through Competency Improvement: A Lean Manufacturing Approach. Presented at the SPE Bergen One Day Seminar, Bergen, Norway, April 20. SPE-180066-MS. https://doi.org/10.2118/180066-MS.

Buell, R. S. 2006. Operating With Integrity and Excellence in the Oilfield. Paper SPE-108815-DL presented as a Distinguished Lecture during the 2005–2006 season.

Buell, R. S. and Turnipseed, S. P. 2004. Application of Lean Six Sigma in Oilfield Operations. *SPE Prod & Fac* **19** (4): 201–208. SPE-84434-PA. https://doi.org/10.2118/84434-PA.

Casey, J. N. and Konecki, N. C. 1967. Natural Gas—A Review of its Occurrence and Potential in Australia and Papua. Presented at the 7th World Petroleum Congress.

Charles, S. R., Deutman, R., and Gold, D. K. 2012. Implementing Lean Manufacturing Principles in New Well Construction. Presented at the SPE Heavy Oil Conference Canada, Calgary, 12–14 June. SPE-157907-MS. https://doi.org/10.2118/157907-MS.

Chessa, C., Magnani, F., and De Fiorido, F. 2013. Value Creation Through an Integrated Approach to Performance Improvement. Presented at the SPE Annual Technical Conference and Exhibition, New Orleans, 30 September–2 October. SPE-166349-MS. https://doi.org/10.2118/166349-MS.

Economides, M. J. and Nolte, K. G. 2000. *Reservoir Stimulation*, third edition. New York City: Wiley.

Ghany, W. A. 2010. 5S and Its Effect on HSE Performance. Presented at the Middle East Health, Safety, Security, and Environment Conference and Exhibition, Manama, Bahrain, 4–6 October. SPE-136528-MS. https://doi.org/10.2118/136528-MS.

Hejl, K. A., Madding, A. M., Morea, M. et al. 2007. Extreme Multistage Fracturing Improves Vertical Coverage and Well Performance in the Lost Hills Field. *SPE Drill & Compl* **22** (4): 326–333. SPE-101840-PA. https://doi.org/10.2118/101840-PA.

Itua, O. J. and Shamuganathan, G. 2015. Lean Methods Application to Frontend Petroleum Engineering Project. Presented at the SPE Nigeria Annual International Conference and Exhibition, Lagos, 4–6 August SPE-178337-MS. https://doi.org/10.2118/178337-MS.

Jati, N., Rahman, F., Kurniawan, H. et al. 2015. Design of Experiment and Statistical Approach to Optimize New Zone Behind Pipe Opportunity: North Roger Block Case Study. Presented at the SPE/IATMI Asia Pacific Oil & Gas Conference and Exhibition, Bali, Indonesia, 20–22 October. SPE-176205-MS. https://doi.org/10.2118/176205-MS.

Juranek, T. A., Seeburger, D. T., Tolman, R. C. et al. 2010. Evolution of Mesaverde stimEvolution of Mesaverde Stimulations in the Piceance Basin: A Case History of the Application of Lean Six Sigma Tools. Presented at the SPE Unconventional Gas Conference, Pittsburgh, Pennsylvania, 23–25 February. SPE-131731-MS. https://doi.org/10.2118/131731-MS.

Mantecon, J. C. 1993. Gas-Lift Optimisation on Barrow Island, Western Australia. Presented at the SPE Asia Pacific Oil and Gas Conference, Singapore, 8–10 February. SPE-25344-MS. https://doi.org/10.2118/25344-MS.

McCall, J., Smart, P., and McNeil, D. 2009. Application of Continuous Improvement Methods to the Petroleum Upstream Business. Presented at the SPE Annual Technical Conference and Exhibition, New Orleans, 4–7 October. SPE-125252-MS. https://doi.org/10.2118/125252-MS.

McTavish, R. A. 1965. Barrow No. 1 Well Completion Report. Internal Report (Available from WA DMP). WAPET, Perth, Western Australia.

Mustapha, A., Umeh, N., and Adepoju, A. 2015. Deploying Continuous Improvement Methodologies to Improve Efficiency: A Way of Responding to Emerging Industry Challenges. Presented at the SPE Nigeria Annual International Conference and Exhibition, Lagos, 4–6 August. SPE-178387-MS. https://doi.org/10.2118/178387-MS.

O'Reilly, D. I., Hunt, A. J., Sze, E. S. et al. 2016a. Increasing Water Injection Efficiency in the Mature Windalia Oil Field, NW Australia, Through Improved Reservoir Surveillance and Operations. Presented at the Asia Pacific Oil & Gas Conference and Exhibition, Perth, Australia, 25–27 October. SPE-182339-MS. https://doi.org/10.2118/182339-MS.

O'Reilly, D. I., Haghighi, M., Flett, M. A. et al. 2016b. Pressure and Rate Transient Analysis of Artificially Lifted Drawdown Tests Using Cyclic Pump Off Controllers. *J. Pet. Sci. Eng.* **139** (March): 240–253. https://doi.org/10.1016/j.petrol.2016.01.030.

Okshiev, A. and Alteneder, W. 2014. Process Safety Information Management. Presented at the SPE Annual Caspian Technical Conference and Exhibition, Astana, Kazakhstan, 12–14 November. SPE-172259-MS. https://doi.org/10.2118/172259-MS.

Patty, R. and Denton, M. A. 2005. Improve Facility Project Delivery With Methods for Manufacturing Excellence. Presented at the SPE Annual Technical Conference and Exhibition, Dallas, 9–12 October. SPE-96241-MS. https://doi.org/10.2118/96241-MS.

Popa, A. and Cassidy, S. 2012a. i-field Programs Enable Operational Excellence in a Challenging Environment—Pushing the Limits of Large Data Transfer for Real-Time Monitoring and Surveillance Operations in San Joaquin Valley. *SPE Econ & Mgmt* **4** (2): 83–89. SPE-143949-PA. https://doi.org/10.2118/143949-PA.

Popa, A. S. and Cassidy, S. D. 2012b. Artificial Intelligence for Heavy Oil Assets: The Evolution of Solutions and Organization Capability. Presented at the SPE Annual Technical Conference and Exhibition, San Antonio, Texas, 8–10 October. SPE-159504-MS. https://doi.org/10.2118/159504-MS.

Popa, A., Horner, K., Cassidy, S. et al. 2012. Implementing i-field-Integrated Solutions for Reservoir Management: A San Joaquin Valley Case Study. *SPE Econ & Mgmt* **4** (1): 58–65. SPE-143950-PA. https://doi.org/10.2118/143950-PA.

Popa, A., Ramos, R., Cover, A. B. et al. 2005. Integration of Artificial Intelligence and Lean Sigma for Large Field Production Optimization: Application to Kern River Field. Presented at the SPE Annual Technical Conference and Exhibition, Dallas, 9–12 October. SPE-97247-MS. https://doi.org/10.2118/97247-MS.

Popa, A. S., Leon, H., Medel, J. et al. 2015. Data-Driven Analytics for Production Impact Assessment during Unplanned Facility System Events. Presented at the SPE Western Regional Meeting, Garden Grove, California, 27–30 April. SPE-173993-MS. https://doi.org/10.2118/173993-MS.

Takacs, G. 2003. *Sucker Rod Pumping Manual*. Tulsa: PennWell Books.

Vargas, C. M. and Scott, H. 2015. Continuous Improvement Strategy to Stimulate Sustainability and Enhance Environmental Management. Presented at the Abu Dhabi International Petroleum Exhibition and Conference, Abu Dhabi, 9–12 November. SPE-177536-MS. https://doi.org/10.2118/177536-MS.

Daniel I. O'Reilly is a production-operations adviser at Chevron Australia, currently working at the Gorgon LNG plant on BWI, Australia. Previously, he worked at Chevron on the BWI Oil Subsurface Team and the Gorgon Subsurface and Non-Operated Joint Venture Subsurface Teams. O'Reilly's main interests lie in production operations and well-test analysis. He has authored or coauthored several SPE papers and holds two patents. O'Reilly holds degrees in petroleum engineering and mechanical engineering from the University of Adelaide, Australia. He has been an SPE member since 2004, serving as the chair for the SPE Western Australian Section during 2016–2017, and he has held various other roles in that section.

Bradley S. Hopcroft is a development geologist at Chevron Australia and is currently working on the Wheatstone Project based in Perth. He has worked at Chevron Australia since 2009 across exploration, field-appraisal, development-planning, and production-operations projects, including a development geologist role on the BWI Oil Field Subsurface Team. Hopcroft holds bachelor's and master's degrees from the University of Waikato, New Zealand.

Kate A. Nelligan is a petroleum engineer at Chevron Australia and is currently working as a reservoir engineer on the Gorgon Project, which encompasses the Jansz-Io and Gorgon gas fields. She has worked at Chevron since 2012. Nelligan's previous job assignments have included being a workover-operations engineer for a waterflooded onshore oil field. She holds a combined degree in chemical and petroleum engineering from the University of Adelaide.

Guan K. Ng is the Wheatstone Project Reservoir Engineering Team Leader at Chevron Australia based in Perth. Before joining Chevron, he was a stimulation field engineer with Schlumberger, specializing in the design and wellsite execution of stimulation jobs both offshore and onshore in Canada, Russia, Qatar, UAE, and Indonesia. Ng joined Chevron Australia in 2007 and has held assignments in greenfield gas fields and brownfield oil and gas fields. His professional experience spans field appraisal and development planning, wellsite-job execution, production operations, and reservoir and production engineering. Ng holds a bachelor's degree in oil and gas engineering and a bachelor's degree in commerce from the University of Western Australia.

Bree H. Goff is the WA Oil Operations Manager, responsible for all aspects of the WA Oil operation with Chevron Australia. She joined Chevron Australia in 2004 as an Earth scientist after working for several years in the mining industry and for various service providers in the UK, Australia, and South Africa. Since joining Chevron Australia, Goff has worked in various roles within exploration and development projects, including the North-West Shelf, Wheatstone Field, and Tahiti Field. More recently, she has held several leadership roles at Chevron Australia, including acting as the BWI Gas Development Project Manager, as the Australian Business Unit's Capital Stewardship and Organizational Capability Champion, and as the WA Oil Subsurface Manager. Goff holds a first-class honors degree in geology, with a minor in pure mathematics.

Manouchehr Haghighi is an associate professor of petroleum engineering. Before joining the University of Adelaide in 2009, he was an associate professor at the University of Tehran, Iran. Previously, Haghighi was with the National Iranian Oil Company from 1995 to 1999 and Simtech, a consulting company, from 1999 to 2009. He has authored or coauthored more than 100 articles that have been published in peer-reviewed journals or presented at international conferences. Haghighi is an active member of SPE.

7 Water Injector Falloff Analysis Incorporating Wellbore Temperature Effects

The management of a mature waterflood asset is incomplete without reviewing water injection performance. One method for this is to conduct a pressure transient test; for water injectors this is referred to as the "pressure falloff test". The test can help ascertain reservoir and well properties along with average pressure in the area.

While observing pressure transient surveys on injection wells penetrating high permeability reservoirs, the author has noted that wellbore temperature effects can cause significant problems with reservoir property interpretation. The forthcoming chapter is an attempt to address this problem and interpret data from one of these field cases.

The paper is published in the SPE Production & Operations journal.

Statement of Authorship

Title of Paper	Pressure-Transient Analysis for Cold-Water Injection into a Reservoir Coupled with Wellbore-Transient-Temperature Effects
Publication Status	☑ Published ☐ Accepted for Publication ☐ Submitted for Publication ☐ Unpublished and Unsubmitted w ork w ritten in manuscript style
Publication Details	O'Reilly, D.I., Haghighi, M., Flett, M.A. and Sayyafzadeh, M. 2020. Pressure-Transient Analysis for Cold-Water Injection into a Reservoir Coupled with Wellbore-Transient-Temperature Effects. *SPE Production & Operations*. Preprint. SPE-186306-PA.

Principal Author

Name of Principal Author (Candidate)	Daniel O'Reilly
Contribution to the Paper	Problem formulation, derivation of mathematical model, preparation of graphs, writing the manuscript. Acted as corresponding author.
Overall percentage (%)	80%
Certification:	This paper reports on original research I conducted during the period of my Higher Degree by Research candidature and is not subject to any obligations or contractual agreements with a third party that would constrain its inclusion in this thesis. I am the primary author of this paper.
Signature	Date: 25 Nov 2020

Co-Author Contributions

By signing the Statement of Authorship, each author certifies that:

i. the candidate's stated contribution to the publication is accurate (as detailed above);

ii. permission is granted for the candidate in include the publication in the thesis; and

iii. the sum of all co-author contributions is equal to 100% less the candidate's stated contribution.

Name of Co-Author	Manouchehr Haghighi
Contribution to the Paper	Principal supervision of the work. Problem formulation, manuscript review and assessment.
Signature	Date: 01/12/2020

Name of Co-Author	Matthew Flett
Contribution to the Paper	Problem formulation, reviewed the manuscript and provided feedback
Signature	Date: 25/11/2020

Name of Co-Author	Mohammad Sayyafzadeh		
Contribution to the Paper	Problem formulation, reviewed the manuscript and provided feedback		
Signature		Date	26/11/2020

Pressure-Transient Analysis for Cold-Water Injection into a Reservoir Coupled with Wellbore-Transient-Temperature Effects

Daniel O'Reilly, University of Adelaide and Chevron Australia Pty. Ltd.;
Manouchehr Haghighi, University of Adelaide; **Matthew Flett,** Chevron Australia Pty. Ltd.;
and **Mohammad Sayyafzadeh,** University of Adelaide

Summary

Presented here is an analytical framework to assess the impact of transient-temperature changes in the wellbore on the pressure-transient response of cold-water injection wells. We focus attention on both drawdown and falloff periods in a well after injection. Historically, these pressure data have been used to calculate reservoir properties concerning flood-efficiency and completion properties (formation permeability/thickness, mechanical skin, and fluid-bank mobilities). One key question addressed in this paper is whether the effects of thermal heating of wellbore fluids during a falloff survey can mask the pressure signature of a two-region composite reservoir. The pressure deflections required to detect mobility changes can be relatively small compared with pressure changes induced by temperature effects in the well. The framework proposed in this paper allows for the numerical evaluation of the contribution of each.

Previously, researchers have studied multiple bank-transient-injection problems extensively for the case of reservoir flow and pressure drop, even for nonisothermal problems. The effect of temperature changes in the wellbore and overburden are seldom discussed, however. It is demonstrated in this paper that these effects can, in some cases, be substantial, and it is worthwhile to incorporate them into an interpretation model.

The results of this paper are useful for planning and designing a pressure-falloff survey to minimize the adverse effect that heating of wellbore fluid by overburden rock can have on the pressure-transient signature. The theory can also be used to analyze existing data affected by the phenomenon. A real-field case study is shown for a cold-water injector where pressure-falloff data have been affected by temperature changes. The analytical model fits the field data closely when parameters are adjusted within reservoir-property-uncertainty ranges.

Introduction

When wells are first placed online after drilling and completion, they are usually most sensitive to differences in temperature between injected water, overburden rock, and reservoir temperature. This is because the overburden surrounding the wellbore is still at its natural temperature and has not adjusted to a prolonged period of wellbore-fluid-temperature disturbance. The use of classical pressure-transient-interpretation techniques normally relies on the isothermal reservoir and wellbore condition. There are numerous wells recently placed online on the North West Shelf Venture in Australia (Flett et al. 2008; Flett and Muller 2016) that potentially fall into the category of being temperature sensitive. Results from initial pressure surveys might confound until the overburden and reservoir temperatures have equilibrated with the flowing wellbore fluids. This can apply to both production and injection wells. In this paper, attention is focused only on cold-water injection.

Aside from virgin wells, if the reservoir-pressure response is small during a transient testing (e.g., less than 10 psi) and the reservoir is in communication with the entire completion string, it is likely that transient-temperature changes will affect pressure because of fluid expansion or contraction. This can occur in cases where the injection rate is not sufficient to create a high pressure differential, or in cases where the reservoir quality is high and very little differential is required to inject. A field example shown later in the paper falls into the second category. These situations create difficulty with the interpretation of reservoir properties from pressure-transient testing—difficulty because temperature effects are also included in the results (Hasan and Kabir 2018). Another example is the injection of cold water into a hot geothermal zone. The examples necessitate a mathematical model that includes both pressure and temperature effects in the wellbore. In the past, this problem has been studied for steady-state reservoir response (Ramey 1962). Some authors have considered the case of transient temperature and pressure coupling (Izgec et al. 2007), but the work focuses on oil and gas wells. It is necessary to extend this work to cold-water injection.

The injection of cold water into reservoirs or aquifers is commonplace in the oil industry. It is usual for waterflood facilities to include several kilometers of flowlines, during which time the source water (or treated produced water) cools to ambient temperature. Slow residence times in multiple separators and treatment facilities also add to this cooling time. By the time the water has reached the injector wellhead, the temperature is much lower than the target-reservoir temperature. An example photograph of this operation is reproduced in **Fig. 1,** where a workflow is also shown for the execution and interpretation of a pressure-falloff survey. Depending on the exact conditions, it can be important to consider nonisothermal effects in the wellbore when interpreting reservoir-pressure-transient data from this type of operation. On the right-hand side of the photograph, a white valve handle is shown in the closed position, indicating that the well is shut in for a transient survey. The gray charts beneath represent real-time monitoring, which is performed by production engineers executing such tests. The spreadsheet in Fig. 1 shows a very basic pressure-transient-interpretation method. In the pressure analysis shown in Fig. 1 (O'Reilly et al. 2016a), a simplified workflow was used where isothermal density corrections were made between the wellhead gauge and the bottom of the hole. The semilog chart is used to calculate reservoir properties. This method is very basic, and although it might be applicable to some wells, others might require consideration of temperature effects for both wellbore hydraulics and afterflow into the reservoir.

This paper (SPE 186306) was accepted for presentation at the SPE/IATMI Asia Pacific Oil & Gas Conference and Exhibition, Jakarta, Indonesia, 17–19 October 2017, and revised for publication. Original manuscript received for review 9 December 2019. Revised manuscript received for review 15 May 2020. Paper peer approved 1 June 2020.

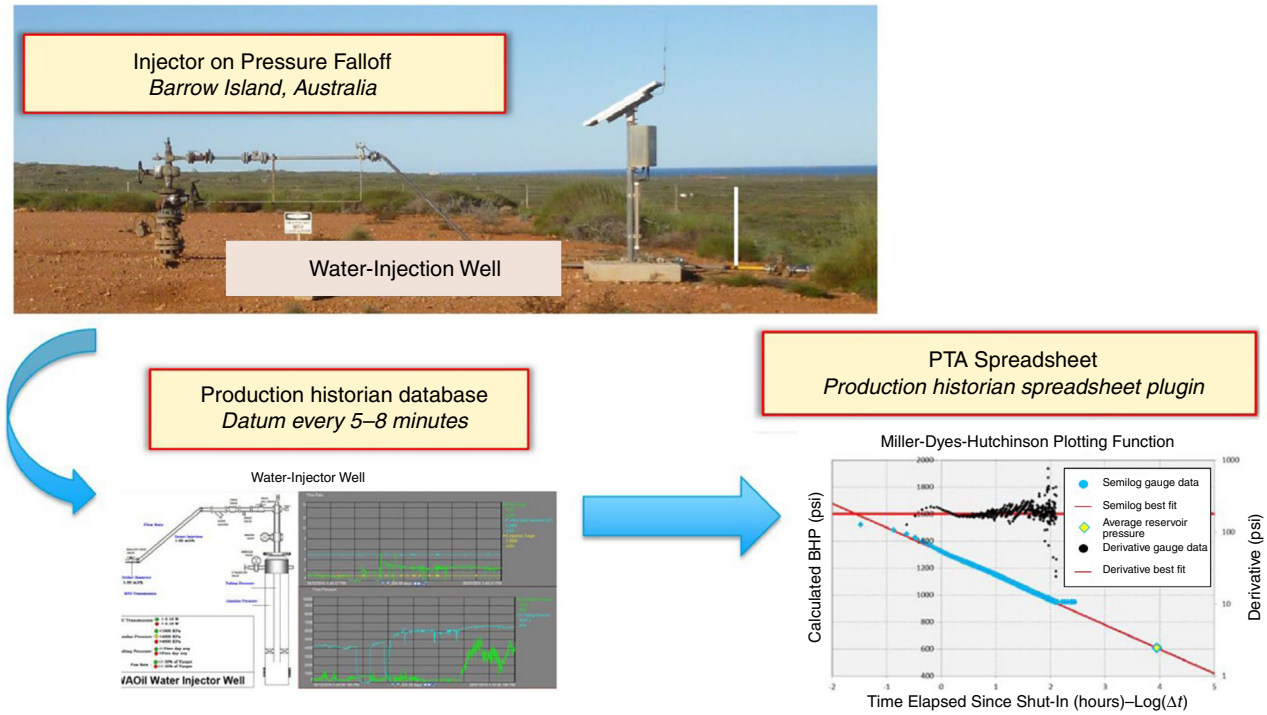

Fig. 1—Typical workflow for injector-falloff analysis (after O'Reilly et al. 2016a). BHP = bottomhole pressure; PTA = pressure-transient analysis.

Researchers have previously studied some aspects of transient-wellbore-temperature problems. Hasan et al. (2005) used analytical expressions for wellbore temperature to see the effect on the pressure-buildup response of a gas well. Their solutions share some similarities with the original work of Ramey (1962), but easily apply to an extensive range of problems. The Ramey (1962) paper has been a foundation for most studies into wellbore-temperature transience. The Hasan et al. (2005) solutions are readily computable but have previously not been applied in the context of pressure-falloff surveys in water-injection wells, which will be performed in this paper. Hakim et al. (2016) used a fully numerical coupled thermal wellbore/reservoir model to interpret results from oilwell/gas-well-pressure buildups. This numerical approach has also been used by other authors.

The petroleum literature is also rich with discussion on the pressure-transient behavior of cold-water injection in the reservoir (Hazebroek et al. 1958; Kazemi et al. 1972; Abbaszadeh and Kamal 1989), but there appears to be little in the way of transient-heating effects in the wellbore itself. The aforementioned authors went to lengths to solve the pressure response in a well with a temperature profile varying radially inside the reservoir, but an isothermal condition is assumed inside the well. Given that these effects, in their adverse case, will soil some of the subtler pressure-transient results, there is worth in discussing their impact and some mitigating factors. In our work, a simple multibank fluid model in the reservoir is combined with the transient heating of fluid in the well. An infinite-acting reservoir model is also studied.

The structure of this paper is as follows. First, the theory will be outlined and solutions combined to incorporate the effects of transient temperature on pressure response. These include a heat-transfer model for the wellbore, a temperature-transient model for the overburden rock, mechanical energy-balance equation for the wellbore fluid, and pressure-transient model for the reservoir. In the next section, example synthetic falloff signatures are given for fields undergoing cold-water injection. The examples will illustrate that poor planning of a pressure-transient test can lead to erroneous results. Field data will also be matched with the model. In the Discussion section, some recommendations and ideas are given to improve the results of transient surveys.

Methodology

It is assumed that a transient-pressure signal is measured somewhere in the well by a gauge and that these data are used to interpret reservoir properties. The appearance of temperature effects in the wellbore interfere with the recorded pressure when it is used for this purpose by altering the fluid properties. The overall methodology that is used to mathematically model this is as follows:

- Hydraulic and fluid properties inside of the well: A water-pressure/volume/temperature model is combined with the mechanical energy-balance equation to predict pressures along the well trajectory as they change with temperature.
- Transient temperature of wellbore fluid: An analytical heat-transfer model is used from the overburden rock into the tubular.
- Reservoir-pressure-response model: Analytical models are used to model the reservoir-pressure response at the bottom of the well. The following wellbore-afterflow effects are included in addition to skin:
  - Wellbore storage C_D, relating to fluid expansion/contraction with pressure changes (Agarwal et al. 1970).
  - Thermal wellbore storage α_{wD}, relating to fluid expansion/contraction with temperature changes.

By superimposing the hydraulic-well model with the reservoir model (adding the pressure responses), it is possible to predict the anticipated pressure response at any point in the well. The next section will cover this model in detail.

Development of Theory

A complete analytical model will now be developed to combine the reservoir and wellbore effects. Transient-temperature changes are considered in the wellbore but not in the reservoir itself. A sketch of this situation is depicted in **Fig. 2.** In Fig. 2, a vertical wellbore is shown for simplicity. We assume that the temperature of water injected at the surface is the same as the surface geothermal/ambient temperature. This situation is common in production operations where water is treated and stored at the surface, with a long residence time between the source of water and the injector wellhead.

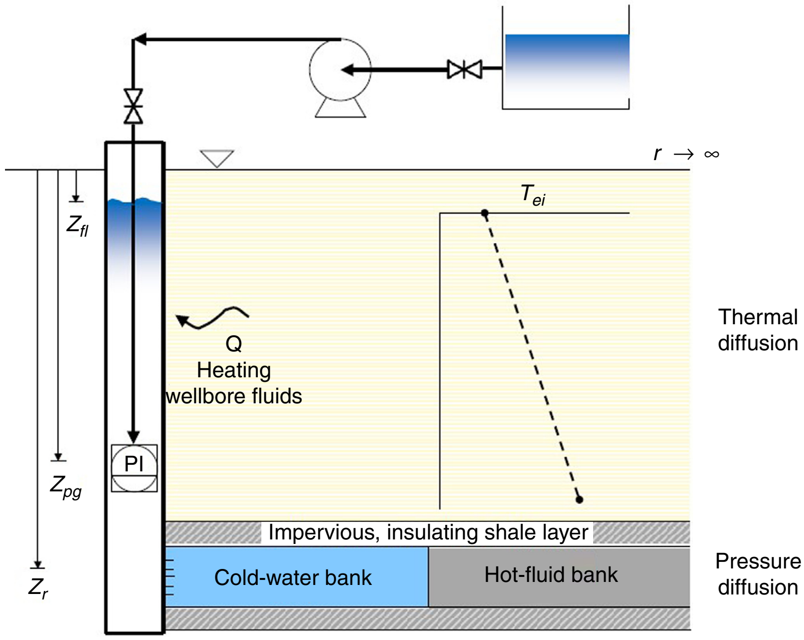

Fig. 2—Cross-sectional sketch of cold-water injection into a hot reservoir. PI = pressure indicator, denoting the pressure gauge.

Mechanical Energy-Balance Equation. The mechanical energy-balance equation is used to calculate changes in pressure within the wellbore section. For the frictionless case of single-phase water injection in a constant-diameter conduit, it is assumed that only hydrostatic forces contribute in Eq. 1 (Brill and Mukherjee 1999),

$$\frac{\mathrm{d}p}{\mathrm{d}z} = \frac{\rho g \sin\theta}{144 g_c} - \frac{f v^2 \rho}{288 g_c d} \approx \frac{\rho(T) g \sin\theta}{144 g_c}. \quad (1)$$

During flowing and shut-in for the water injector, pressure as a function of depth will be determined by gravity forces only. Note that in Eq. 1, the usual sign convention is reversed because of the direction of z shown in Fig. 2. The density term in Eq. 1 will vary with temperature along the path of the well. This effect has been studied in this paper and the solution approach is summarized in Appendix B. An equation of state (EOS) for water has been applied using a numerical technique to solve directly for pressure at each point in the wellbore. The idea is similar to the semianalytical method used by Katz (1959) for temperature-dependent wellbore-density changes for gas wells.

Thermal Wellbore Model. The thermal model is used to predict temperature changes over time in the wellbore from the external geothermal source. From the first law of thermodynamics, the energy-balance equation is derived as, for an inclined wellbore in a well producing liquid or gas (Hasan et al. 2005; Spindler 2011),

$$\frac{\partial T_f}{\partial t} = \frac{\dot{m} L_R}{m(1+C_T)}[T_{ei}(z) - T_f] + \frac{\dot{m}}{m(1+C_T)}\left[-\frac{\partial T_f}{\partial z} + \phi - \frac{g\sin\theta}{c_p g_c J}\right], \quad (2)$$

where T_f is the temperature of fluid in the wellbore and T_{ei} is the undisturbed temperature of the earth at a large distance away from the wellbore. Fluid, in this case water, flows through the well at a mass rate of $\dot{m}$ (in lbm/hr). Eq. 2 is not trivial to solve because of the presence of T_f in the $\frac{\partial T_f}{\partial t}$, $\frac{\partial T_f}{\partial z}$, and T_f terms. Nonetheless, fully analytical solutions have been presented in the literature already (Hagoort 2004; Spindler 2011). In the case of water, the terms ϕ and $\frac{g\sin\theta}{c_p g_c J} = 0$. The relaxation-distance parameter, L_R, in Eq. 2 is a term used to quantify the heat transfer into the wellbore from overburden rock,

$$L_R = \frac{2\pi}{c_p \dot{m}}\left[\frac{r_{to} U_{to} k_e}{k_e + r_{to} U_{to} T_D(t)}\right]. \quad (3)$$

Hasan et al. (2005) proposed an approximate method for solving Eq. 2, and we use their solutions in this paper. Their solution also attempts to cover both early- and late-time behavior inside the well by including the $(1 - e^{-at})$ coefficient. For the constant-rate injection-pressure-buildup period, the solution is given as

$$T_f(z,t) = T_{eiwh} + g_G z \sin\theta + \frac{1 - e^{-at}}{L_R}(e^{-zL_R} - 1)\psi, \quad (4)$$

where $a = \dot{m} L_R / [m(1 + C_T)]$ and a linear geothermal gradient has been used [i.e., $T_{ei}(z) = T_{eiwh} + g_G \sin\theta$]. Eq. 4 is adjusted in our paper to reflect water injection rather than hydrocarbon production (the focus of Hasan et al.'s paper); furthermore, Eq. 4 assumes that the temperature of injected fluid at the surface is equal to the surface geothermal temperature. The constant ψ is defined by Hasan et al. (2005), but in this single-phase liquid case, we assume $\psi \approx g_G \sin\theta$. This solution is identical to that given by Ramey (1962), with a minor difference. The appearance of the $(1 - e^{-at})$ decay term marks a difference between the two solutions and represents the authors' attempt at modeling the early-time transience in the wellbore before a full wellbore volume of fluid has been injected. At large times,

the term approaches unity and the solutions of the authors are in agreement. For long periods of injection, the difference can be small, and for the cases we studied with relatively long periods of injection, the term was not required. Removing the term and setting the gravitational constant, the equation becomes (Hasan et al. 1997)

$$T_f(z,t) = T_{eiwh} + g_G z\sin\theta + \frac{g_G \sin\theta}{L_R}(e^{-zL_R} - 1). \quad (5)$$

The relaxation-distance parameter $L_R(t)$ is time dependent in Eq. 5. If the temperature of the injected fluid at the wellhead is not equal to the surface geothermal temperature (as is assumed previously), the appropriate equation is (Ramey 1962; Hasan and Kabir 2018)

$$T_f(z,t) = T_{eiwh} + g_G z\sin\theta - \frac{g_G \sin\theta}{L_R} + \left(T_{fwh} + \frac{g_G \sin\theta}{L_R} - T_{eiwh}\right)e^{-zL_R}. \quad (6)$$

Eq. 6 also appears in a slightly different format in Ramey (1962). We maintain using a nomenclature similar to that of Hasan et al. (1997).

For the shut-in periods after injection,

$$T_f(z,t) = [T_{fo}(z) - T_{eiwh} - g_G z\sin\theta]e^{-a't} + T_{eiwh} + g_G z\sin\theta, \quad (7)$$

where $a' = L'_R/[m(1+C_T)]$. Eq. 7 represents an exponential decay. Note that a' is actually a function of time [by means of $L'_R(t)$], but it is treated as a constant in Eq. 2 when deriving the solutions discussed $\left(\text{its time rate of change is much slower than } \frac{\partial T_f}{\partial t}\right)$. Often in analysis, a single average value of L_R or L'_R is used over the analysis period.

An interesting feature of Eq. 4 is that it is not an exact solution of Eq. 2; this can be shown by resubstituting the expression into the first-order differential equation. In spite of this, this solution during injection is helpful because it is an intermediary of the transient- and steady-state wellbore-heat-flow solutions [see the Ramey (1962) solution, only steady-state wellbore-heat flow] before a full wellbore volume of fluid is injected. A lengthy discussion on this is given by Spindler (2011).

This concludes the discussion on the solutions for wellbore temperature based on energy balance.

Overburden-Temperature-Transient Model. A temperature-transient model is required for heat conduction in the hot overburden rock. Models used in other works use the infinite boundary condition, and this is considered standard. We do not change from this convention, but note that for closely spaced wells, the condition is probably inappropriate. The logarithmic approximation to the line-source solution is used here (Carslaw and Jaeger 1959), valid for $t^*_D > 25$ and at $r_D = 1$ (wellbore radius),

$$T_D(t^*_D) = \frac{1}{2}\ln\left(\frac{4}{e^\gamma}t^*_D\right). \quad (8)$$

It was previously mentioned that heat transmission into the wellbore is determined by the time-dependent term $L_R(t)$. This expression was defined previously and includes the dimensionless temperature $T_D(t^*_D)$ from the overburden-temperature model. This is the context of Eq. 8.

More intricate models have been used in other papers, but this is not considered important in the present work. It was previously shown that at long times, this constant heat-flux line-source solution is sufficient (Ramey 1962). Readers will note that Eq. 8 is identical to the pressure-drawdown solution common in petroleum and hydrology literature (by substituting p_{wD} instead of T_D) (Kuchuk et al. 2010; O'Reilly et al. 2016b). The phenomena of transient-heat conduction and pressure diffusion in porous media are mathematically equivalent.

Reservoir-Pressure-Transient Model. For simplicity's sake, we have studied both the infinite-acting radial flow (IARF) and a two-region composite model during a falloff period. Using the assumed composite model amounts to purely convective heat transfer into the reservoir rock. A composite reservoir model is used to separate the reservoir into two zones: an inner cold-water bank and, at a larger radius, a hot-fluid bank. Each zone has its own diffusivity and mobility. The IARF model implies that no fluid bank or composite reservoir has been detected yet by the pressure signal at the wellbore. Changes in rate schedule are easily accounted for through convolution or superposition. Eq. 8 is the same equation used for IARF pressure diffusion at the wellbore (replacing T_D with p_{wD} and t^*_D with t_D). Alternatively, for infinite-acting flow (van Everdingen and Hurst 1949), the solution at the wellbore in the Laplace domain is

$$\overline{p}_{uD}(u) = \frac{K_0(\sqrt{u})}{u^{3/2}K_1(\sqrt{u})}. \quad (9)$$

The solution in the Laplace domain for a two-region model is taken from (Ambastha 1989)

$$\overline{p}_{uD}(u) = C_1 I_0(\sqrt{u}) + C_2 K_0(\sqrt{u}). \quad (10)$$

The first region represents the cold-water bank and the second region represents the hot-reservoir-fluid bank. The model assumes a stationary front between regions. For an unbounded reservoir with an internal flooded region at radius R, the coefficients C_1 and C_2 are given in Appendix A. Inversion into the time domain is achieved using the Stehfest (1970) algorithm. The effects of wellbore storage and skin are combined with either solution by the convolution relation (Kuchuk 1986),

$$\overline{p}_{wD}(u) = \overline{w}_D(u)[s + u\overline{p}_{uD}(u)], \quad (11)$$

where w_D denotes the dimensionless sandface flow rate (which includes the wellbore-storage effect). Let us now consider two cases, both of which can be encountered during falloff testing. The first case, of a partially full water column in the wellbore, is comparatively simple. In the case of expansion of water caused by heating from geothermal zones outside of the wellbore, it is assumed that the water rises into an above vacuum. The second case is that of a wellbore completely filled with liquid.

Injection/Falloff with Wellhead on Vacuum. For this case, the standard relation for the wellbore-storage relation applies (Kuchuk et al. 2010),

$$\overline{w}_D(u) = \frac{1}{u} - uC_D\overline{p}_{wD}(u). \quad (12)$$

The wellbore storage here would relate to a falling liquid level, z_{fl}. In this case, temperature-dependent changes in water density are simply captured in the mechanical energy equation (Eq. 1). It is assumed that the tubing head remains on vacuum and that any change in water density from heating results in an upward expansion of the water mass without alteration of the tubinghead pressure or bottom-hole pressure. Because no additional backpressure is imposed on the sandface, there is no backflow into the reservoir or wellbore storage.

Note that for a gauge placed in the water column but above the sandface, the pressure can still be affected by temperature-related density effects as the water column becomes less dense during heating. What was discussed previously specifically relates to the exclusion of wellbore afterflow into the reservoir from thermal effects because the column might freely expand upward.

Note that it is possible for a depleted reservoir to both inject at vacuum pressure and also falloff on vacuum pressure. Injecting at vacuum (or atmospheric) pressure has been referred to in other works as a "dumpflood." We have encountered situations in field operations where waste water is disposed of simply by gravity feeding fluid from a mobile tank at surface level into the reservoir, rather than requiring a pump. This can occur because of a combination of low reservoir pressure and/or high injectivity.

Injection/Falloff with Full Column of Liquid. A wellbore filled with water results in compressive wellbore storage rather than a falling liquid level. As such, the wellbore storage itself will now also be affected by thermal changes in the well because the heating of fluids will tend to force water into the formation. In this paper, we propose the relation for constant-rate injection-pressure buildup (derived in Appendix C),

$$\overline{w}_D(u) = \frac{1}{u} - uC_D\overline{p}_{wD}(u) + u\alpha_{wD}\overline{T}_{\mathrm{Dav,inject}}(u), \quad (13)$$

and for creating shut-in pressure-falloff curves,

$$\overline{w}_D(u) = \frac{1}{u} - uC_D\overline{p}_{wD}(u) - u\alpha_{wD}\overline{T}_{\mathrm{Dav,shut\text{-}in}}(u). \quad (14)$$

Similar to the Fair (1981) approach, only one (not both) of the preceding equations should be used depending on the situation. For constant-rate injection, Eq. 13 is used for the sandface-injection rate, and for the shut-in case, Eq. 14 should be used. The equations are not intended to be used with superposition in time.

During constant-rate injection at the surface (Eq. 13), wellbore storage C_D tends to reduce injection into the sandface (sandface-injection rate w_D is defined as positive for injection) at early times as the well volume acts as a buffer to accept injected fluids. In this case, thermal expansion of the fluids during heating (α_{wD}) has the opposite effect by increasing injection into the sandstone as water heats in the well and expands into the sandface. It should be noted that in the falloff equation, wellbore storage and thermal expansion act in the same direction.

The terms in Eq. 13 have identical signs and similar forms to the wellbore-phase redistribution constant in Fair (1981). In Eq. 14 for pressure falloff, the sign of the thermal storage term is opposite to what it would be if considered as phase redistribution. In both of the works by Fair (1981, 1996), only pressure-buildup analysis (shut-in after a production period) was considered because redistribution was not considered possible in pressure-drawdown analysis. As such, an equation with the signs in Eq. 14 was not considered in these or other articles. Even so, Fair (1996) did discuss temperature-wellbore effects and how they apply to the phase-redistribution model, but they were only discussed solely for the case of pressure buildup, where wellbore storage and phase redistribution work in opposite directions. Furthermore, negative phase-redistribution parameters were not considered.

The constant α_{wD} includes such parameters as the thermal-expansion coefficient α_w, wellbore volume V_w, and injection rate w. The $T_{av}(t)$ term represents the average-column-fluid temperature as a function of time. A full derivation of this term is included in Appendix C, and discussions on its effect are presented in subsequent sections.

In the falling-liquid-level solution discussed previously, the actual falloff period is analyzed by the superposition of injecting and shut-in solutions. The calculations that follow in this paper will assume that the wells have been injecting for sufficient time so that the Miller-Dyes-Hutchinson (Miller et al. 1950) style of analysis is used (i.e., transient effects from the long injection period are ignored).

To summarize this subsection, there are two physical effects occurring when cold water is injected into a wellbore, each using different equations in this text. The two effects are the following:

- Afterflow-wellbore-storage effects relating to temperature/volume changes of water stored in the wellbore. This occurs only when the wellbore is completely filled with water. In this case, Eq. 13 for injection or Eq. 14 for shut-in are used to incorporate potential thermal-afterflow effects into the sandface flow rate. The thermal-expansion coefficient can be calculated using Eq. C-12 (Appendix C). The equation for w_D is then combined with Eq. 11 (Kuchuk 1986) with the chosen analytical reservoir model p_{uD}.
- Changes to fluid (water) properties in the wellbore over time caused by heating, which can affect the pressure measurement at the gauge if there is a reasonable standoff from the reservoir. This phenomenon can occur in wells completely filled with water, or also in partially filled wellbores where the wellhead pressure is at vacuum pressure. Both regular and thermal afterflow can occur in this situation, depending on whether the water column reaches the wellhead.

Depending on the location of the pressure gauge, if corrections to pressure need to be made according to the fluid density inside the well, Eq. 1 must then be used with the solution method discussed in Appendix B.

Temperatures inside the well are always predicted using Eq. 6 for injection and Eq. 7 for shut-in.

Thermal-Afterflow Effects: Dimensionless Type Curves

In this section, the effects of temperature on wellbore afterflow/storage will be discussed in a dimensionless context. We present the shape of curves and argue that, for many practical cases with water injection, the effect can be small. Thermal wellbore storage can have an effect during injection or the falloff period after the well has shut in. The phenomenon occurs for wells with a positive wellhead pressure (i.e., not on vacuum) on injection and falloff periods. If cold water is present in the wellbore, the water will heat and expand into the reservoir. In the case where the wellhead is on vacuum, the water will simply expand into the cavity in the tubing without entering the reservoir.

A dimensionless case is now analyzed for pressure falloff in an IARF. For this case, Eq. 14 indicates that the temperature effect on the sandface flow rate, $\alpha_{wD}\overline{T}_{Dav}(u)$, has the same sign as the pressure-related wellbore storage, $C_D\overline{p}_{wD}(u)$. During the falloff, the decrease in wellbore pressure will result in an expansion of the wellbore fluid's initial volume, and the increase in wellbore temperature will also result in expansion. The additional fluid is pushed into the sandface. The wellbore-storage and thermal-expansion terms both act against the nature of the pressure falloff: They reduce the rate at which the pressure reduces when the well is shut in, caused by forcing liquid into the reservoir.

Fig. 3 shows the results of pressure and derivatives for a range of different thermal parameters for the IARF case, with wellbore storage C_D held constant. This chart was prepared using the IARF model in Eq. 9, used with Eqs. 11 and 14. From the lines it is clear that the overall effect of heating of the fluid column is to reduce the magnitude of the pressure falloff. This can be seen by comparing the thermal cases with the isothermal case ($a'_D = \alpha_D = 0$). The case with the largest effect is $a'_D = 5\times10^{-4}$, $\alpha_D = 1{,}000$. In this case, the rate of pressure change is lower, which is also evident from the derivative.

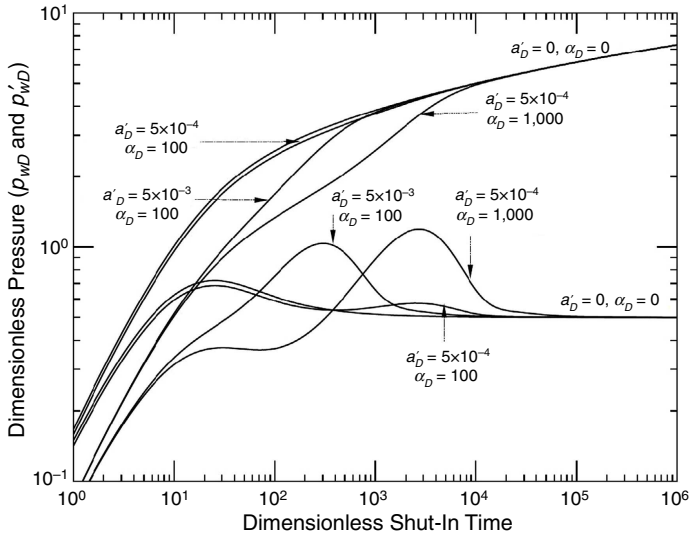

Fig. 3—Dimensionless chart for IARF reservoir model with full thermal-afterflow-model sensitivities for the pressure-falloff case; $C_D = 5$, $s = 0$.

A case will now also be shown for a pressure-falloff test in a composite reservoir. A diagram of this reservoir is shown in **Fig. 4.** The response in such a reservoir without any thermal wellbore effects is shown in **Fig. 5.** This chart was prepared using the reservoir model in Eq. 10, combined with Eqs. 11 and 12 for afterflow effects. Two fluid banks are evident in the derivative. In **Fig. 6,** the thermal model in this paper is introduced (using Eq. 14 for total afterflow) and produces similar effects as the IARF case. The wellbore storage C_D in this example already makes the identification of the inner mobility region difficult, but the thermal effects make matters worse.

It is important to discuss the dimensionless parameters a'_D and α_D (defined in Appendix C) and what values would normally be encountered during water-injection operations. From our investigation of different reservoir combinations and water properties, it seems that for regular operations, the $a'_D = 5\times10^{-4}$, $\alpha_D = 150$ case would be on the extreme end of the spectrum (and the effect of this in Figs. 3 and 6 is low compared with the other cases). Cases around this level or higher would need to occur in highly active geothermal areas. The mathematical model will have use for this application. The authors can also use the model in the future for onshore gas-disposal wells, where the thermal-expansion coefficient will be much higher.

Apart from the general physical behavior, the important result from this case is that the thermal effects for wellbore-volume expansion are small, apart from in geothermally active areas. A similar outcome was discussed by Fair (1996).

Wellbore-Temperature/Density Effects: Synthetic Cases

Three cases will now be discussed to present the ideas in this paper. These examples only incorporate changes in wellbore-fluid properties with temperature, and do not model any thermal afterflow into the sandface. The first case is a dimensional study of an injector (Injector 1, **Table 1**) supplying water to an underground aquifer undergoing IARF, where the effect of thermal changes on fluid properties in the wellbore will be studied at a pressure gauge with a small offset during the falloff period. The second case (Injector 2) will be a similar well injecting into an aquifer with two composite regions; the pressure signature will be observed incorporating thermal changes in the wellbore. In the third and final case, a water-injection well (Injector 3) will be examined in an onshore waterflood oil field, where the pressure gauge is on the surface. Each of the injectors in Table 1 is similar to actual operating wells, with results in the charts predicted from the model for illustrative purposes only.

Injector 1 Study: Aquifer, Water-Disposal Well, IARF Model. The case studies from hereon will now remove the effect of thermal wellbore storage and only study the wellbore hydraulic changes caused by fluid-property/temperature relationships. Consider Injector 1 in a fictitious reservoir, operating at vacuum-wellhead condition during injection and falloff. The injector disposes of 15,000 bbl of water injected per day (BWIPD) into a 1200-m-deep aquifer. The pressure gauge is 200 m above the top sandstone at 1000-m vertical depth. All other properties for this well are presented in Table 1. The disposed-water temperature is 30°C at the wellhead, while reservoir temperature is 60°C. Water is injected for 6 months continuously and the well is then shut in for a transient survey. The reservoir-boundary model is assumed as infinite acting.

After shut-in, **Fig. 7** shows the temperature profile in the well progressing through time. The top of sandface is shown at the base depth (1200 m), with the gauge depth (1000 m) at the shallow extent of the graph. From 0 to 25 hours, the temperature builds at the gauge from 31 to 55°C. This has a corresponding effect on the density of water inside the tubing. **Fig. 8** shows that this influences the

pressure recorded at the gauge. This chart records only the static pressure change at the gauge (relative to flowing pressure before shut-in), without the effects of the reservoir falloff itself, which will be superimposed on this. In **Fig. 9,** a log-log graph shows the combined pressure response at the gauge. Note that the pressure derivative here and elsewhere in this paper is calculated numerically using the method of Bourdet et al. (1989). An interesting feature of the thermal model is the nonmonotonic shape of the pressure response from 3 to 11 hours. At $\Delta t = 3$ hours, it is evident that the falloff has subsided and turned into a pressure buildup for several hours. This is entirely because of density changes in the water inside the tubing. The pressure profile and derivative have a similar shape to the phase-redistribution phenomena, but the equations and physics here are different.

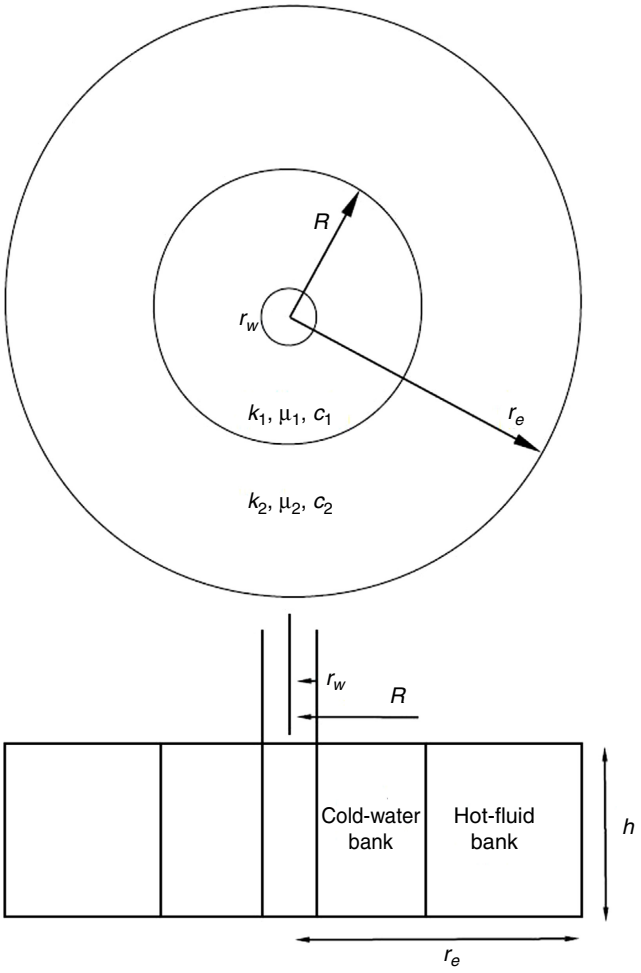

Fig. 4—Schematic of composite reservoir nomenclature used in this paper (note $R_D = R/r_w$).

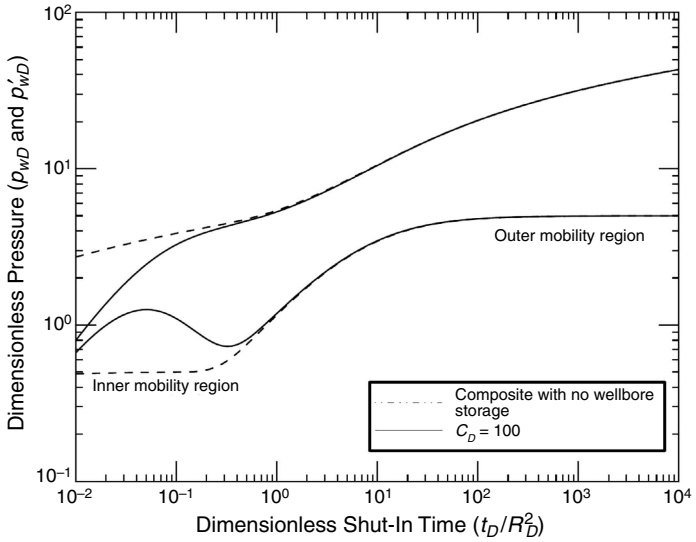

Fig. 5—Dimensionless pressure and its derivative for two-region composite model. No thermal effects included in chart. $C_D = 100$, $M = \eta = 10$, $R_D = 100$, $s = 0$.

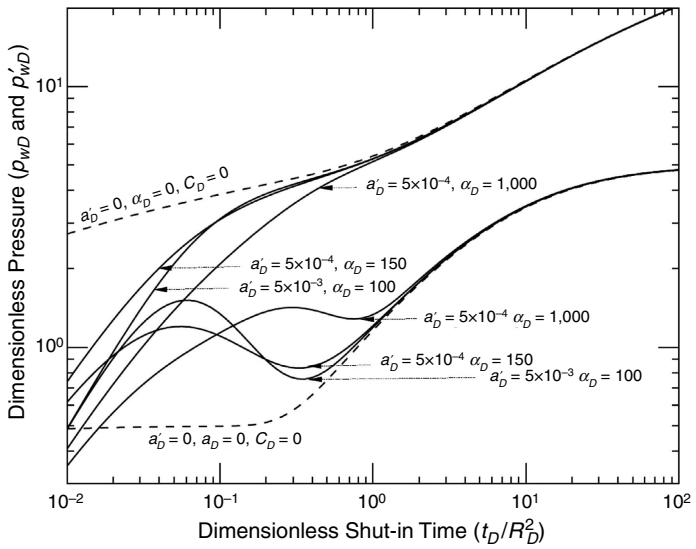

Fig. 6—Dimensionless pressure and derivative for the same case as Fig. 5; pressure-falloff case. Thermal-wellbore-storage parameters included for three cases indicated in chart.

	Injector 1	Injector 2	Injector 3
Rock and Reservoir Data			
Vertical depth to top sandstone (m)	1200	1200	620
Pay thickness (ft)	300	300	180
Average porosity (%)	0.28	0.28	0.21
Total compressibility (1/psi)	1×10^{-4}	1×10^{-4}	2×10^{-4}
Permeability (md)	2,000	2,000	10
Flowing bottomhole pressure (psig)	800	800	1,300
Injection rate (B/D)	15,000	15,000	2,000
Prior injection duration	6 months	6 months	50 years
Reservoir model	IARF	Composite $M = 2$ $\eta = 5$ $R_D = 300$	Composite $M = 2$ $\eta = 2$ $R_D = 200$
Well-Completion Data			
Total wellbore radius (ft)	1.15	1.15	0.4
Tubing inner diameter (in.)	5	5	2⅞
Wellbore storage, C_D	50	50	5
Depth of pressure gauge (m)	1000	1000	0 (surface)
Mechanical skin	0	3	0
Heat-Transfer Data			
T_{eiwh} (°C)	30	30	30
T_{fwh} (°C)	30	30	30
Geothermal gradient (°C/m)	0.025	0.025	0.025
Overall heat-transfer coefficient (Btu/°F/hr/ft^2)	8	8	8
Tubing-fluid heat capacity (Btu/lbm/°F)	1	1	1
Calculated L_R (1/ft)	1.08×10^{-5}	1.08×10^{-5}	3.96×10^{-5}
Calculated L'_R (lbm/hr-ft)	2.35	2.35	1.15
Calculated a' (1/hr)	0.13	0.13	0.19
Fluid-Property Data			
Formation volume factor, B (RB/STB)	1	1	1
Viscosity (cp)	0.6	0.6	0.8

Table 1—Reservoir and well properties for injector case studies.

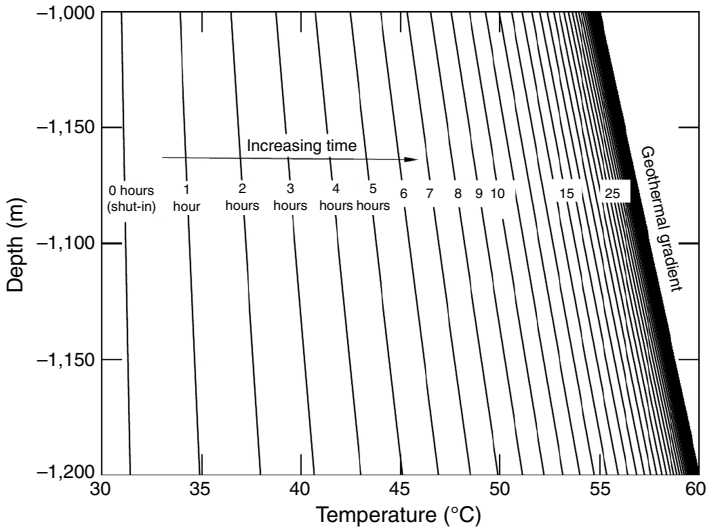

Fig. 7—Injector 1 temperature profiles inside wellbore after shut-in. Time elapsed marked on each curve. Flow rate before shut-in is 15,000 STB/D.

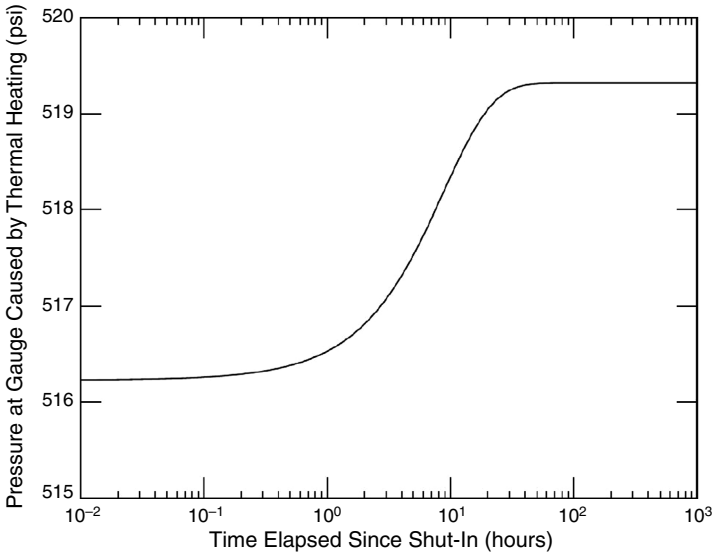

Fig. 8—Injector 1 pressure response at gauge location attributable to the thermal expansion of water alone (excludes change in pressure caused by reservoir-falloff response). Flow rate before shut-in is 15,000 STB/D.

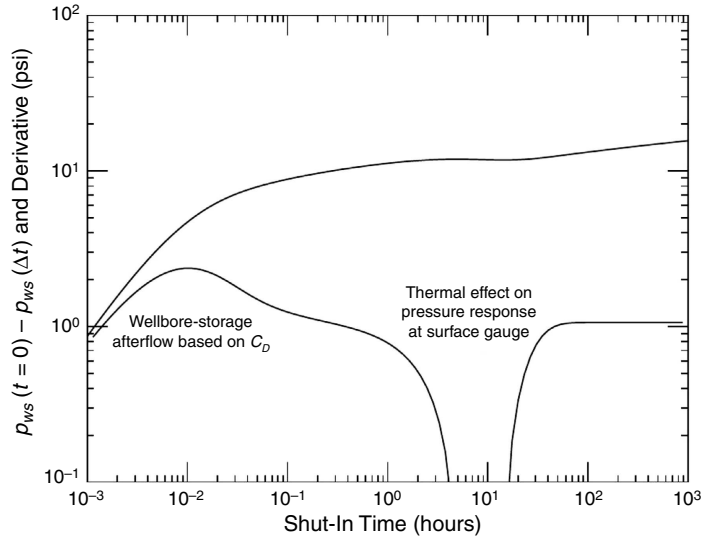

Fig. 9—Injector 1 pressure and pressure-derivative chart after shut-in. Flow rate before shut-in is 15,000 STB/D.

In this reservoir, the injectivity index is high ($kh = 600{,}000$ md-ft) and this causes very little pressure drop across the reservoir during injection operations. This causes a problem when the gauge is only slightly offset from the aquifer (200 m) because the interpretation of a transient survey for this well relies on very sensitive changes to pressure (5 to 15 psi). The changing density in the well has affected this. This exemplary case has shown one scenario in which the objectives of a pressure-transient survey might not be met because of deflections caused by temperature changes. In **Fig. 10,** different shut-in pressure responses are shown on a semilog chart for a range of prior injection flow rates. This chart shows that flowing at rates lower than 15,000 BWIPD has an adverse effect on the pressure response. The reservoir transient portion of the transient response decreases relative to the total response including thermal effects. This is useful to keep in mind when planning such surveys.

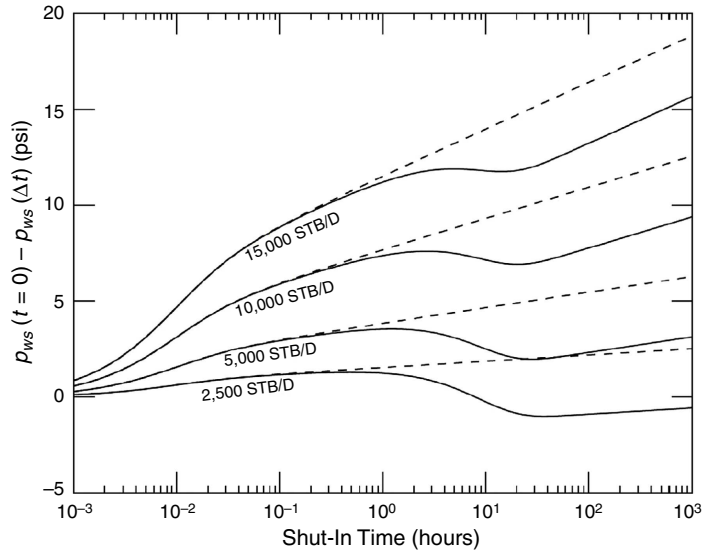

Fig. 10—Injector 1 semilog shut-in pressure curves for various flow rates leading up to shut-in. The dashed lines indicate pressure response without any thermal effects inside the well.

The pressure-turnover effect can also arise in wells with changing wellbore storage over time, but Fig. 9 indicates that it is also possible for this result to appear in wells suffering from thermal distortions in the pressure response. In this case, it is the competing effect of pressure reduction caused by the transient-reservoir response vs. pressure rise caused by the expansion of fluids in the wellbore with a gauge at a finite standoff from the sandface. The results might be surprising to engineers expecting a continuous pressure falloff.

Injector 2 Study: Aquifer, Water-Disposal Well, Composite Model. The Injector 2 well is almost identical to Injector 1, but the reservoir model used is a composite model and a positive skin of 3 units is used. In this case, we assume the mobility of the injected water is greater than that inside the aquifer. For the composite model, $\eta = 2$, $R_D = 300$, and M is varied as a sensitivity **(Fig. 11).** The flow rate is maintained at 15,000 BWIPD. Starting again at $\Delta t = 3$ hours, a pressure deflection begins in the cases. However, the cases where the outer-region mobility is further impaired ($M = 5$ and 10) suffer from less distortion and can actually be used for a reasonable pressure-transient-analysis (PTA) interpretation. This is because the impaired mobility in the outer region has caused a higher Δp in the falloff, which has masked most of the thermal effects. This case again confirms the preference for higher pressure drops.

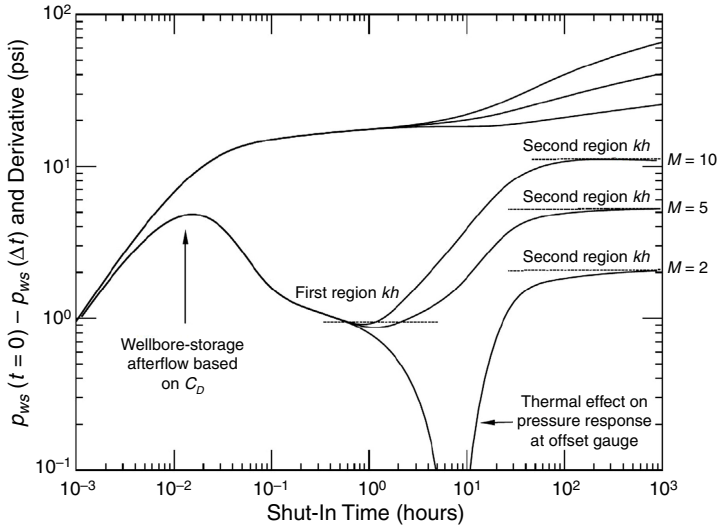

Fig. 11—Injector 2 pressure and pressure-derivative chart after shut-in. Flow rate before shut-in is 15,000 STB/D; $s = 3$, $R_D = 300$, $\eta = 5$, M is varied.

Injector 3 Study: Oil Reservoir, Waterflood Injector, Composite Model. In the last case, we examine a water injector in a mature oil field with a history of waterflooding. The injection well has been disposing on average 2,000 BWIPD water for 50 years. Injector 3 is shallower than the previous well, with top sandstone at 620 m. However, the pressure and temperature gauges are on the surface for the well. The reservoir quality in this oil field is lower ($kh = 1{,}800$ md-ft) than the aquifer studied previously, and the stabilized injection pressure at the bottom of the hole is 1,300 psi. Cold water is injected at the surface at 30°C into a reservoir of 46°C temperature. The mobility ratio for the injected water/displaced fluid is 2.

A log-log graph of the pressure and its derivative response is shown in **Fig. 12.** What is first noticeable regarding this graph is that it seems absent of any distorting wellbore effects. We remind readers that this gauge is on the surface of this onshore field, 620 m above the reservoir. This encouraging result is attributable to low reservoir quality and its impact on the high Δp encountered in the falloff. This has masked the effect of any temperature-related changes to pressure at the gauge. These data would be suitable for PTA interpretation and reservoir-property inference. We reinforce the point regarding reservoir quality in **Fig. 13,** where the permeability is increased in several cases and the pressure data are shown. In each case the thermal impact on pressure response becomes more evident. The associated pressure-derivative data are shown in **Fig. 14.** At 500 md and greater, the data are less usable.

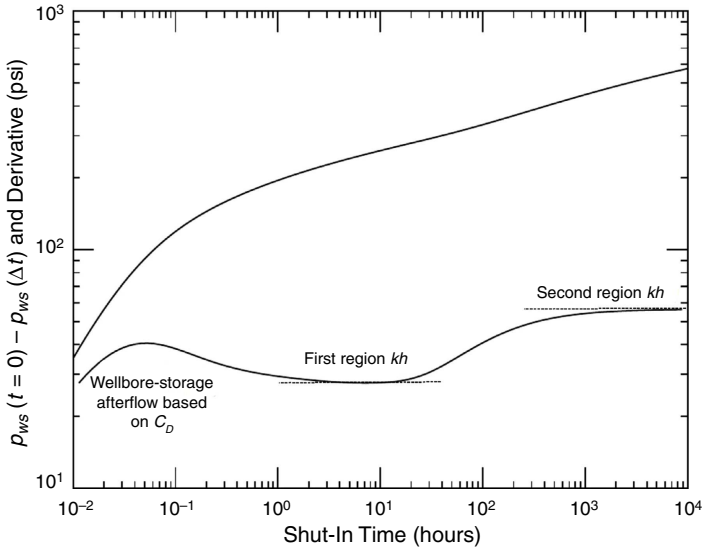

Fig. 12—Injector 3 pressure and pressure derivative after shut-in.

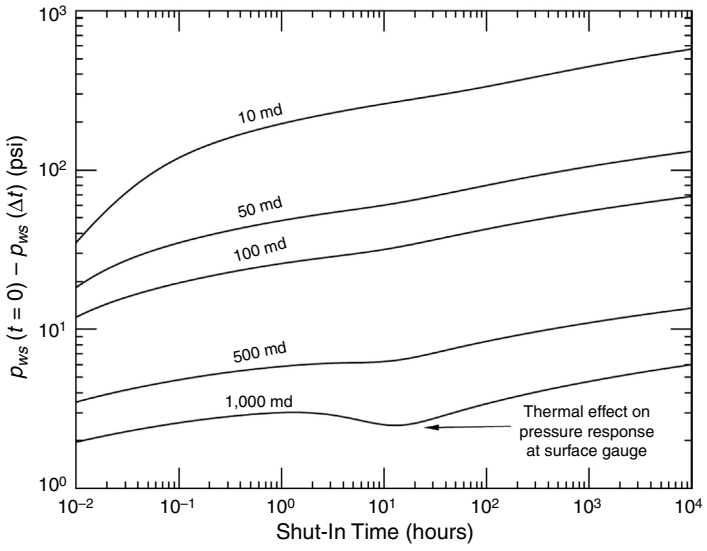

Fig. 13—Injector 3 log-log pressure vs. shut-in time with varying formation permeability.

This injector study has shown that the problem of gauge placement in a well and its usability for transient analysis is very much dependent on factors such as reservoir quality and flow rate.

Field Case Study: Onshore-Water-Injector Pressure-Falloff Test

After the synthetic cases used to illustrate model-parameter sensitivity, a real-field case study from Australia will be shown and its results compared with the analytical model. In the example, water is injected at surface temperature into perforations across multiple aquifers of up to 1600-m depth. The vertical well is cased and perforated, completed with 5½-in. tubing and a packer to isolate the casing string. The geothermal gradient for this well is within the normal ranges seen in other fields (Ramey 1962; Hasan and Kabir

2018). Because water is injected at surface temperature and the formation is not in a highly geothermally active area, thermal-wellbore-afterflow effects will be neglected. The model used to match field data therefore only considers hydrostatic wellbore-temperature/density effects, similar to the previous section.

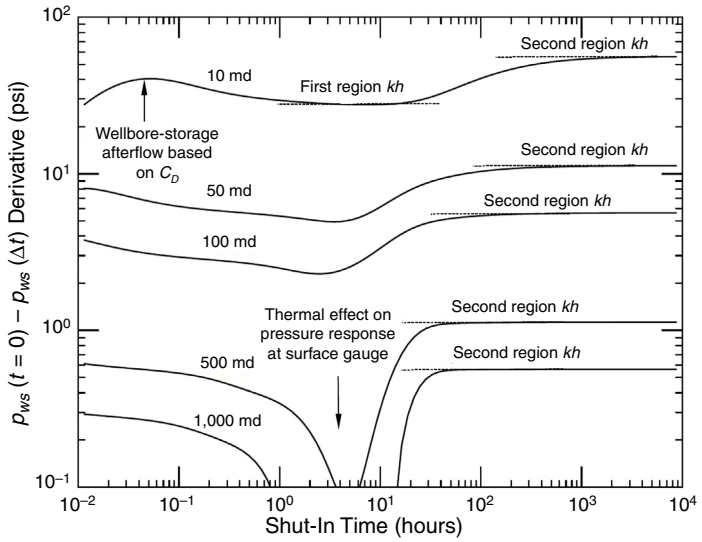

Fig. 14—Injector 3 log-log pressure vs. shut-in time with varying formation permeability. This chart is the pressure-derivative data associated with each curve in Fig. 13.

Pressure-falloff data for the water injector are shown in **Fig. 15.** A transient survey was planned specifically to ascertain aquifer properties and executed using a slickline unit with memory gauges placed more than 100 m away from the intervals. For the test, multiple stepped rates greater than 20,000 BWIPD were injected over a 4-hour duration. Pressure and temperature data were available, but the temperature variation over time was only used as a guide when furnishing the model. This was because the temperature gauge was inside the tool (shrouded by insulation), with the primary purpose of temperature compensation of the pressure measurement. The starting and endpoint temperatures were used in the model.

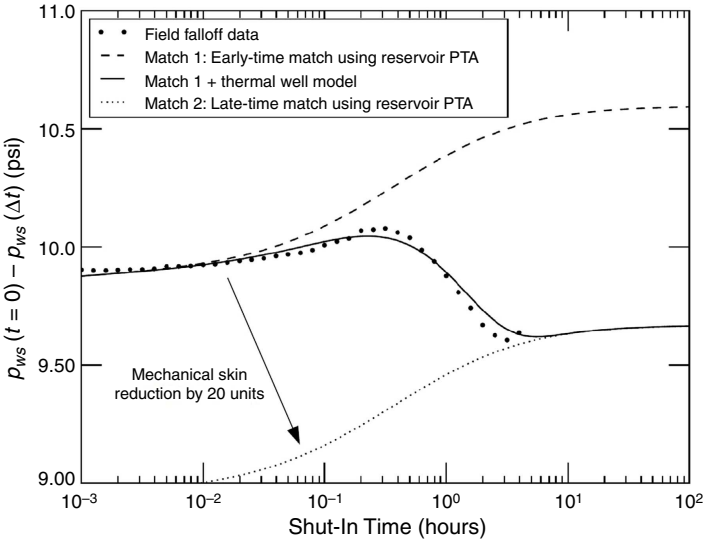

Fig. 15—Field pressure-falloff test compared with model matches (semilog chart). The solid line (full PTA/thermal model) is considered the correct match. The PTA-only match using late-time data (Match 2) results in erroneously low mechanical skin (*s* reduced 20 units from the correct interpretation).

Matching with the transient-pressure data was achieved by manual adjustment of aquifer-rock properties and wellbore/overburden-heat-transfer properties within acceptable ranges. When modeling, fluid properties for fresh water were used inside the well and aquifer (i.e., Appendix B), and the IARF aquifer model was used (Eq. 9 with superposition to account for the step-injection profile).

Fig. 15 shows two separate dashed lines depicting aquifer "PTA-only" matches (both assuming no fluid-density changes in the well). The first match is performed using early-time points ($t < 0.01$ hours) and the second match using late-time points ($t > 4$ hours). The full PTA/thermal-model match is shown as a solid continuous line and contains exactly the same match properties as the early-time match. For the full analytical model, the shapes of the pressure-transient data are traced at all times, which cannot be said for reservoir PTA alone. This is because of the hydrostatic pressure changes at the gauge away from the aquifer. It is worth noting that the difference between the early-time and late-time PTA match was the reduction of mechanical skin by 20 units (all other properties held constant). This underestimation effect is reaffirmed in the Discussion section for a synthetic semilog example.

In this field example, it is clear that matching the data without considering temperature could cause error, even as early as within the time range of 0.01 to 0.1 hours. Furthermore, the benefit to matching over the full time period is that rock properties deeper into the aquifer are calculated, provided that temperature changes are well-understood. It should be apparent in the example that the aquifer-rock properties are very favorable (small pressure increments in the falloff) and a wellbore skin is present (high pressure drop at shut-in, $S > 10$). The high permeability/thickness (kh of approximately 10^6 md-ft) of this well meant that it was susceptible to the temperature effects occurring in the time period of 0.01 to 4 hours. Using the analytical model allowed matching across the full falloff duration.

Discussion

Three synthetic cases and one field case have been shown to demonstrate the effect that geothermal heating of water in the wellbore can have on the gauge pressure for a well. The first two synthetic cases showed a well injecting and falling off into a high-quality aquifer. The third case was for a full column of water inside a shallower oilfield injection well. In that case, it is also possible for thermal expansion to force additional fluid into the reservoir during injection or falloff, but we showed earlier that these effects are generally small for water. The dominant thermal effect studied was the heating of the wellbore fluid and the corresponding effect that density change has on pressure-gauge response. The cases show that for a gauge placed at a reasonable standoff from the reservoir zone, significant deviations in pressure can occur during early time of the injection buildup or falloff. As discussed in the Introduction, these cases confirm that temperature-sensitive PTA can be required when there is a small pressure differential induced by the injection (Fig. 15), when reservoir quality is high (Figs. 13 and 14) or when the injection rate is low (Fig. 10). Other cases can include the injection of cold water into particularly geothermally active areas.

To mitigate against the distortion of pressure data in these cases, it is helpful to consider the following factors when designing an appropriate well-testing program:

- Place the pressure gauge as close to the reservoir interval as possible so that heating of water in the well does not significantly change the bottomhole pressure at the sandface (assuming rathole of small volume). With knowledge of anticipated reservoir properties, it might be possible to design the setting depth so that thermal changes do not interfere with the expected pressure response. This matter is also discussed by Kabir and Hasan (1998).
- Consider use of temperature sensors, sonolog surveys, and downhole flowmeters to use with the proposed models to quantify the effect of thermal heating. Fiber-optic temperature sensors are becoming more commonplace and can help populate a thermal wellbore model with the required data.
- A downhole shut-in tool is advisable to ensure zero flow at the sandface.
- Injection of water at temperature closer to the geothermal gradient (note: not necessarily at reservoir temperature). It is recognized that this is not always feasible in actual field operations.
- Allow sufficient time for overburden rock temperature to stabilize before shut-in in falloff surveys. The effect of temperature on an offset pressure gauge with hydrostatic pressure adjustment can be studied theoretically to see the relative impact of the expanding water on bottomhole pressure. This will help guide the required temperature stabilization. For the Injector 3 case study, the 50-year duration of injection helped minimize the heating effect.
- If possible, increase injection rates to increase the magnitude of pressure-signal change during falloff. Fig. 10 shows that the thermal effect is reduced by injecting at higher rates.

With regard to reservoir-property interpretation from PTA, it is also possible that incorrect values can be derived from the data including thermal effects. In Fig. 10 (Injector 1), it is apparent that the interpreted kh might be reasonably accurate at late time because the semilog slopes of the curves are similar, but this is only part of the picture. We examine the effects of temperature/density changes in the well on skin interpretation for the same injector in **Fig. 16.** The straight-line semilog method is used. In the interpretation, if middle-time data are used (0.1 to 0.4 hours) after conventional wellbore-storage effects cease, the skin is correctly interpreted ($s = 0$). However, if data are used after the temperature effects are felt inside the well (30 to 200 hours), the skin is underestimated ($s = -1.5$). This is the same effect as the previous field case study. All other reservoir properties are correctly interpreted from using semilog matching in both cases. Of course, during the period of wellbore-fluid heating (approximately 0.4 to 11 hours), the identification of any reservoir properties would be completely impossible. Depending on the duration of the survey, if the temperature alteration to pressure data has not diminished, the identification of a fluid bank in composite reservoirs might also be impossible (e.g., if the duration of the well test in Fig. 14 was less than 15 hours).

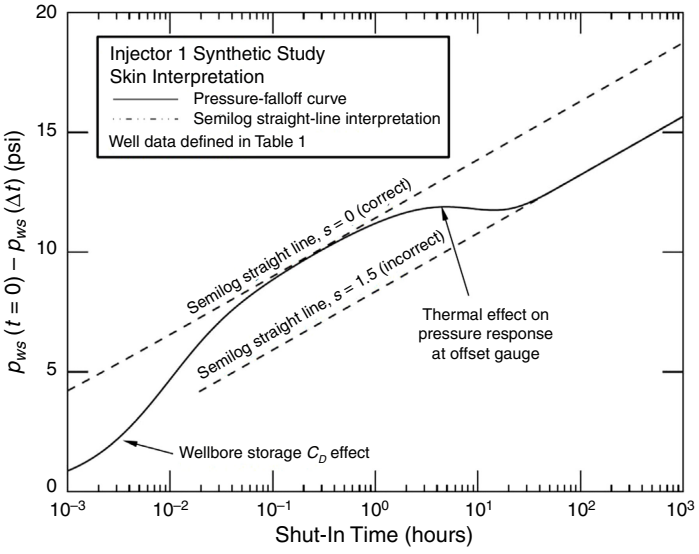

Fig. 16—Effect of temperature-density changes in the wellbore on skin interpretation (Injector 1 well, data given in Table 1).

In the case of a full water column up to the wellhead, a new solution has also been proposed in this paper that includes the expansion of tubing fluid into the reservoir. The solution accounts for the flow of water into the sandface that can occur during heating of water in the wellbore by overburden rock. This solution highlights an interesting phenomenon for reservoirs when the overburden is a significantly higher temperature than the injected-fluid temperature. This problem will be explored further in the future. One new result we have shown is that the compressible wellbore-storage and thermal-expansion terms counteract each other for the transient-injection case but work in the same direction for the transient-falloff case.

The accuracy of the analytical models is also worth discussing. First, use of the analytic transient-heat-conduction models (Eqs. 6 and 7) includes several assumptions in the derivation, namely, linear geothermal gradient, slowly varying relaxation parameter L_R (it is assumed constant in derivations of T_f), incompressible liquid, and radial-heat transfer (Ramey 1962; Hasan and Kabir 2018). In cases where these assumptions are not valid, it is best to use a full numerical model. There are also some limitations in the pressure-diffusion models selected for this study: the IARF and two-region composite models. Improved models are available that describe the physics of a moving flood front and saturation gradient (if applicable) inside the reservoir (Bratvold and Horne 1990; Ramakrishnan and Kuchuk 1993). It is likely that most aspects of our model can be combined with these solutions if it is required. When considering hydraulics inside the wellbore, Eq. 1 was simplified to remove friction and acceleration components, which is satisfactory for the shut-in case, especially for the case of water. When presenting figures on the thermal wellbore afterflow (Figs. 3, 5, and 6), it was also assumed that an average value of α_{wD} could be calculated (α_{av}) for the entire well. This constraint might need to be removed by means of full numerical modeling in cases with nonlinear temperature profiles and thermal-expansion-coefficient behavior. Note that exactly the same averaging is normally performed when calculating the wellbore-storage term C_D.

Finally, it is interesting that most commercial pressure-transient software packages currently available include very little in the way of transient-temperature effects in the wellbore. Some specialized packages exist for thermal wellbore effects, but these are often expensive and do not cater specifically to pressure transience. As we demonstrate in this paper, making those adjustments to the existing code is not necessarily difficult. However, several new parameters are introduced into the equations and these might not always be straightforward to quantify in practice.

Conclusions

A sequence of equations has been developed to incorporate the effect of thermal changes in a wellbore fluid when cold water is injected into a hot reservoir or aquifer. As injection or falloff proceeds in this case, the temperature of the water inside the well slowly rises. The following conclusions can be drawn from this work:

1. The increase in fluid temperature after cold-water injection results in an expansion of the wellbore fluid and corresponding decrease in density. In one calculated case (Fig. 8), this resulted in an increase of approximately 3 psi at the gauge.
2. For a full wellbore column of water, backflow into the reservoir caused by heating is small compared with the previous effect. This is because of the pressure/volume/temperature properties of water and normal geothermal conditions not providing significant fluid expansion.
3. It is possible that skin damage could be underestimated in PTA if the thermal effect is not accounted for.
4. The identification of fluid banks can be difficult without mitigating temperature effects in the well.
5. High-kh wells without skin damage are more susceptible to lower-quality PTA data in cold-water injection because the total pressure disturbance is lower in the reservoir, increasing the relative contribution of the thermal wellbore effects.
6. The field case study (Fig. 15) showed that using this analytical model allowed matching of pressure-transient data across the full duration of a temperature-affected falloff.

Nomenclature

a = $L_R/[\dot{m}(1+C_T)]$,1/t, 1/hr
a' = $L'_R/[m(1+C_T)]$, 1/t, 1/hr
a_1 to a_4 = parameters used in Runge-Kutta numerical method (Eqs. B4 through B8), m/L^2, lbm/ft^2
B = reservoir-fluid formation volume factor, L^3/L^3, RB/STB
c_p = tubing-fluid heat capacity, L^2/Tt^2, Btu/lbm-°F
c_t = reservoir total compressibility, Lt^2/m, 1/psi
c_1, c_2 = reservoir total compressibility of inner and outer regions, Lt^2/m, 1/psi
C = wellbore-storage coefficient, L^{4}t^2/m, bbl/psi
C_D = dimensionless wellbore-storage factor, $C_D = 0.894C/\phi hc_t r_w^2$
C_J = Joule-Thompson coefficient of fluid, LTt^2/m, ft-°F-sec^2/lbm
C_T = thermal storage parameter, dimensionless
C_1, C_2 = coefficients used in composite two-region reservoir model
d = tubing diameter, L, ft
f = friction factor, dimensionless
g = gravitational constant, L/t^2, ft/sec^2
g_c = conversion factor, dimensionless, 32.17 lbm-ft/lbf/s^2
g_G = geothermal gradient, T/L,°F/ft
h = reservoir thickness, L, ft
I_0, I_1 = modified Bessel functions of the first kind
J = conversion factor, 778 ft-lbf/Btu
k = reservoir permeability, L^2, md
k_1, k_2 = reservoir permeability of inner and outer regions, L^2, md
k_e = earth conductivity, cm^3/Tt^3, Btu/hr-ft-°F
kh = permeability/thickness product, L^3, md-ft
K_0, K_1 = modified Bessel functions of the second kind
L_R = relaxation distance, 1/L, 1/ft, $L_R = 2\pi r_{to}U_{to}k_e/cp\dot{m}/(ke + r_{to}U_{to}T_D)$
L'_R = relaxation distance used for shut-in, m/Lt, lbm/hr-ft, $L'_R = 2\pi r_{to}U_{to}k_e/c_p/(ke + r_{to}U_{to}T_D)$
L_{R0} = relaxation distance before shut in of well (constant), 1/L, 1/ft
m = mass of fluid per unit depth, m/L, lbm/ft
$\dot{m}$ = tubing-fluid mass rate, m/t, lbm/hr
M = mobility ratio of regions (in composite reservoir model), $M = (k/\mu)_1/(k/\mu)_2$

p = pressure, m/Lt^2, psi [bar when using Tait-Tumlirz EOS (Fisher and Dial 1975)]
p_D = dimensionless pressure in reservoir for injection solutions, $p_D = kh(p_{wf}–p_i)/(141.2wB\mu)$ or dimensionless pressure for fall-off solutions, $p_D = kh(p_i–p_{wf})/(141.2wB\mu)$
p_i = initial reservoir pressure, m/Lt^2, psi
p_{uD} = dimensionless pressure solution for unit step flow rate
p_{wD} = dimensionless pressure in reservoir at $r_D = 1$ (wellbore radius), includes wellbore-storage effects
p_{wf} = sandface flowing wellbore pressure, m/Lt^2, psi
p_{ws} = shut-in wellbore pressure, m/Lt^2, psi
P_0 = correlation function in Tait-Tumlirz EOS, m/Lt^2, bar
q = production rate at wellhead (positive number), L^3/t, STB/D
q_D = dimensionless sandface-production rate
q_{sf} = production rate at sandface (positive number), L^3/t, STB/D
Q = heat transfer per unit length of wellbore, Lm/t^3, Btu/hr-ft
r_{to} = tubing outer radius, L, ft
r_w = wellbore radius, L, ft
R_D = dimensionless radius of inner-reservoir region in composite model
s = mechanical skin factor
t = time, t, hours
t_D = dimensionless time relating to reservoir pressure solutions, $t_D = 0.0002637kt/(\phi\mu c_t r_w^2)$
t_D^* = dimensionless time relating to overburden-temperature solutions, $t_D^* = \alpha t/r_w^2$
T = temperature, T,°F (°C for Tait-Tumlirz EOS)
T_D = dimensionless temperature, $T_D = (2\pi k_e)(T_{wb}– T_{ei})/Q$
$\overline{T}_{\text{Dav,inject}}$ = dimensionless temperature in wellbore averaged with depth, during constant rate injection, dimensionless
$\overline{T}_{\text{Dav,shut-in}}$ = dimensionless temperature in wellbore averaged with depth, during shut-in, dimensionless
T_{ei} = undisturbed geothermal temperature of overburden rock, T,°F
T_{eiwh} = surface geothermal temperature, T,°F
T_f = temperature of wellbore fluid, T,°F
$T_{f,av}$ = average temperature of entire wellbore fluid column, T,°F
T_{fo} = initial temperature of well fluid before shut-in, T,°F
T_{fwh} = temperature of wellbore fluid at wellhead, T,°F
u = Laplace variable
U_{to} = overall heat-transfer coefficient for annular fluid, m/Tt^3, Btu/°F-hr-ft^2
v = tubing-fluid velocity, L/t, ft/sec
V_{wb} = volume of well fluid, L^3, bbl
w = injection rate at wellhead (positive number), L^3/t, STB/D
w_D = dimensionless sandface-injection rate
w_{sf} = injection rate at sandface (positive number), L^3/t, STB/D
z = depth along wellbore subsurface (positive number, measured depth), L, ft
z_{fl} = depth of fluid level in well (positive number, measured depth), L, ft
z_r = depth of reservoir (positive number, measured depth), L, ft
α = thermal diffusivity of Earth, L^2/t, ft^2/h
α_{nn} = coefficients used in composite two-region reservoir model, applies to α_{11} through α_{33}
α_w = wellbore-fluid volumetric thermal-expansion coefficient, 1/T, 1/°C
α_{wD} = thermal-wellbore-storage constant, dimensionless
γ = Euler gamma constant
Δp = pressure difference, m/Lt^2, psi
Δt = time elapsed since shut-in, t, hours
η = diffusivity ratio in composite model, $\eta = [k/(\phi\mu c_t)]_1/[k/(\phi\mu c_t)]_2$
θ = well-inclination angle from horizontal
λ = correlation function in Tait-Tumlirz EOS, L^2/t^2, bar-cm^3/g
μ = fluid viscosity, m/Lt, cp
ν = specific volume for Tait-Tumlirz EOS, L^3/m, cm^3/g
ν_∞ = specific volume-correlation function in Tait-Tumlirz EOS (Eq. B-3), L^3/m, cm^3/g
ρ = fluid density, m/L^3, lbm/ft^3
ϕ = parameter $\phi = –C_J dp/dz + v dv/dz/c_p$, T/L,°F/ft (note that for the reservoir model, ϕ denotes porosity)
ψ = lumped parameter $\psi = g_G \sin\theta + \phi + g\sin\theta/(c_p J g_c)$, T/L,°F/ft (note that for water, assume $\psi \approx g_G \sin\theta$)
$-$ = bar indicates Laplace transform
$\sim$ = same order of magnitude

Subscript
D = dimensionless

Acknowledgments

The first author would like to thank Boniface Yee (Chevron Australia Pty. Ltd.) and Joshua Beinke (Vermilion Energy) for useful discussions. The authors would also like to acknowledge helpful suggestions made by four peer reviewers. This work is solely that of the authors and does not represent the opinion of their employers.

References

Abbaszadeh, M. and Kamal, M. 1989. Pressure-Transient Testing of Water-Injection Wells. *SPE Res Eng* **4** (1): 115–124. SPE-16744-PA. https://doi.org/10.2118/16744-PA.

Agarwal, R. G., Al-Hussainy, R., and Ramey, H. J. Jr. 1970. An Investigation of Wellbore Storage and Skin Effect in Unsteady Liquid Flow: I. Analytical Treatment. *SPE J*. **10** (3): 279–290. SPE-2466-PA. https://doi.org/10.2118/2466-PA.

Ambastha, K. A. 1989. Pressure Transient Analysis for Composite Systems. Technical Report DOE/BC/14126-11, Stanford University, Stanford, California, USA (October 1989).

Bourdet, D., Ayoub, J. A., and Pirard, Y. M. 1989. Use of Pressure Derivative in Well Test Interpretation. *SPE Form Eval* **4** (2): 293–302. SPE-12777-PA. https://doi.org/10.2118/12777-PA.

Bratvold, R. B. and Horne, R. N. 1990. Analysis of Pressure-Falloff Tests Following Cold-Water Injection. *SPE Form Eval* **5** (3): 293–302. SPE-18111-PA. https://doi.org/10.2118/18111-PA.

Brill, J. P. and Mukherjee, H. 1999. *Multiphase Flow in Wells*, Vol. 17. Richardson, Texas, USA: Monograph Series, Society of Petroleum Engineers.

Carslaw, H. S. and Jaeger, J. C. 1959. *Conduction of Heat in Solids*, second edition. Oxford, UK: Clarendon Press.

Fair, W. B. Jr. 1981. Pressure Buildup Analysis with Wellbore Phase Redistribution. *SPE J*. **21** (2): 259–270. SPE-8206-PA. https://doi.org/10.2118/8206-PA.

Fair, W. B. Jr. 1996. Generalization of Wellbore Effects in Pressure-Transient Analysis. *SPE Form Eval* **11** (2): 114–119. SPE-24715-PA. https://doi.org/10.2118/24715-PA.

Fisher, F. H. and Dial, O. E. Jr. 1975. Equation of State of Pure Water and Sea Water. Report, Marine Physical Laboratory of the Scripps Institution of Oceanography, San Diego, California, USA (November 1975).

Flett, M. A. and Muller, M. 2016. Early Field Life Interference Pulse Test Design To Refine Reservoir Uncertainties: A Reservoir Surveillance Opportunity for the Wheatstone Gas Field, Australia. Paper presented at the SPE Asia Pacific Oil and Gas Conference and Exhibition, Perth, Australia, 25–27 October. SPE-182325-MS. https://doi.org/10.2118/182325-MS.

Flett, M. A., Beacher, G. J., Brantjes, J. et al. 2008. Gorgon Project: Subsurface Evaluation of Carbon Dioxide Disposal under Barrow Island. Paper presented at the SPE Asia Pacific Oil and Gas Conference and Exhibition, Perth, Australia, 20–22 October. SPE-116372-MS. https://doi.org/10.2118/116372-MS.

Hagoort, J. 2004. Ramey's Wellbore Heat Transmission Revisited. *SPE J*. **9** (4): 465–474. SPE-87305-PA. https://doi.org/10.2118/87305-PA.

Hakim, B., Fair, C., and Montague, E. 2016. The Effect of Wellbore Temperature Changes and Frictional Losses on Well Test Interpretation Results. Paper presented at the SPE Asia Pacific Oil and Gas Conference and Exhibition, Perth, Australia, 25–27 October. SPE-182329-MS. https://doi.org/10.2118/182329-MS.

Hasan, A. R. and Kabir, C. S. 2018. *Fluid Flow and Heat Transfer in Wellbores*, second edition. Richardson, Texas, USA: Society of Petroleum Engineers.

Hasan, A. R., Kabir, C. S., and Lin, D. 2005. Analytic Wellbore-Temperature Model for Gas-Well Testing. *SPE Res Eval & Eng* **8** (3): 240–247. SPE-84288-PA. https://doi.org/10.2118/84288-PA.

Hasan, A. R., Kabir, C. S., and Wang, X. 1997. Development and Application of a Wellbore/Reservoir Simulator for Testing Oil Wells. *SPE Form Eval* **12** (3): 182–188. SPE-29892-PA. https://doi.org/10.2118/29892-PA.

Hazebroek, P., Rainbow, H., and Matthews, C. S. 1958. Pressure Fall-Off in Water Injection Wells. In *Transactions of the Society of Petroleum Engineers*, Vol. 213, Part 1, SPE-925-G, 250–260. https://doi.org/10.2118/925-G.

Izgec, B., Kabir, C. S., Zhu, D. et al. 2007. Transient Fluid and Heat Flow Modeling in Coupled Wellbore/Reservoir Systems. *SPE Res Eval & Eng* **10** (3): 294–301. SPE-102070-PA. https://doi.org/10.2118/102070-PA.

Kabir, C. S. and Hasan, A. R. 1998. Does Gauge Placement Matter in Downhole Transient-Data Acquisition? *SPE Res Eval & Eng* **1** (1): 64–68. SPE-36527-PA. https://doi.org/10.2118/36527-PA.

Katz, D. L. V. 1959. *Handbook of Natural Gas Engineering*. New York, New York, USA: McGraw-Hill.

Kazemi, H., Merrill, L. S., and Jargon, J. R. 1972. Problems in Interpretation of Pressure Fall-Off Tests in Reservoirs with and without Fluid Banks. *J Pet Technol* **24** (9): 1147–1156. SPE-3696-PA. https://doi.org/10.2118/3696-PA.

Kreyszig, E. 2010. *Advanced Engineering Mathematics*, 10th edition. Hoboken, New Jersey, USA: Wiley.

Kuchuk, F. J. 1986. Generalized Transient Pressure Solutions with Wellbore Storage. SPE-15671-MS.

Kuchuk, F. J., Onur, M., and Hollaender, F. 2010. *Pressure Transient Formation and Well Testing: Convolution, Deconvolution and Nonlinear Estimation*, Vol. **57**, first edition. Oxford, UK: Elsevier Science.

Loucks, T. L. and Guerrero, E. T. 1961. Pressure Drop in a Composite Reservoir. *SPE J*. **1** (3): 170–176. SPE-19-PA. https://doi.org/10.2118/19-PA.

Miller, C. C., Dyes, A. B., and Hutchinson, C. A. Jr. 1950. The Estimation of Permeability and Reservoir Pressure from Bottom Hole Pressure Build-Up Characteristics. *J Pet Technol* **2** (4): 91–104. SPE-950091-G. https://doi.org/10.2118/950091-G.

O'Reilly, D. I., Hunt, A. J., Sze, E. S. et al. 2016a. Increasing Water Injection Efficiency in the Mature Windalia Oil Field, NW Australia, Through Improved Reservoir Surveillance and Operations. Paper presented at the SPE Asia Pacific Oil & Gas Conference and Exhibition, Perth, Australia, 25–27 October. SPE-182339-MS. https://doi.org/10.2118/182339-MS.

O'Reilly, D. I., Haghighi, M., Flett, M. A. et al. 2016b. Pressure and Rate Transient Analysis of Artificially Lifted Drawdown Tests Using Cyclic Pump Off Controllers. *J Pet Sci Eng* **139** (March): 240–253. https://doi.org/10.1016/j.petrol.2016.01.030.

Ramakrishnan, T. S. and Kuchuk, F. J. 1993. Pressure Transients during Injection: Constant Rate and Convolution Solutions. *Transp Porous Media* **10** (2): 103–136. https://doi.org/10.1007/BF00617004.

Ramey, H. J. 1962. Wellbore Heat Transmission. *J Pet Technol* **14** (4): 427–435. SPE-96-PA. https://doi.org/10.2118/96-PA.

Spindler, R. P. 2011. Analytical Models for Wellbore-Temperature Distribution. *SPE J*. **16** (1): 125–133. SPE-140135-PA. https://doi.org/10.2118/140135-PA.

Stehfest, H. 1970. Algorithm 368: Numerical Inversion of Laplace Transforms. *Commun ACM* **13:** 47–49. https://doi.org/10.1145/361953.361969.

van Everdingen, A. F. and Hurst, W. 1949. The Application of the Laplace Transformation to Flow Problems in Reservoirs. *J Pet Technol* **1** (12): 305–324. SPE-949305-G. https://doi.org/10.2118/949305-G.

Appendix A—Composite Two-Region Reservoir Model

In this appendix we repeat the equations outlined by Loucks and Guerrero (1961) and Ambastha (1989). The general solution at the wellbore is

$$\overline{p}_{uD}(u) = C_1 I_0(\sqrt{u}) + C_2 K_0(\sqrt{u}). \quad \text{(A-1)}$$

The system of equations for generalized boundary conditions is

$$\begin{bmatrix} \alpha_{11} & \alpha_{12} & 0 \\ \alpha_{21} & \alpha_{22} & \alpha_{23} \\ \alpha_{31} & \alpha_{32} & \alpha_{33} \end{bmatrix} \begin{bmatrix} C_1 \\ C_2 \\ C_3 \end{bmatrix} = \begin{bmatrix} 1/u \\ 0 \\ 0 \end{bmatrix}. \quad \text{(A-2)}$$

For a case without wellbore effects and zero skin at the interface between regions, the coefficients are defined as follows for the IARF outer-boundary case. Other boundary conditions are documented in the aforementioned articles.

$$\alpha_{11} = -\sqrt{u}I_1(\sqrt{u}), \quad \alpha_{12} = \sqrt{u}K_1(\sqrt{u}), \quad \text{(A-3)}$$

$$\alpha_{21} = I_0(R_D\sqrt{u}), \quad \alpha_{22} = K_0(R_D\sqrt{u}), \quad \alpha_{23} = -K_0(R_D\sqrt{u\eta}), \quad \text{(A-4)}$$

$$\alpha_{31} = M\sqrt{u}I_1(R_D\sqrt{u}), \quad \alpha_{32} = -M\sqrt{u}K_1(R_D\sqrt{u}), \quad \alpha_{33} = \sqrt{u\eta}K_1(R_D\sqrt{u\eta}). \quad \text{(A-5)}$$

Eq. 11 is inverted numerically using the Stehfest (1970) algorithm.

Appendix B—Temperature/Density Relations for Water

Solution of Eq. 1 for pressure yields the following expression as a function of depth and time:

$$p(z,t) = p_{wf}(t) - \frac{g\sin\theta}{144g_c}\int_z^{z_r}\rho(z,t)\mathrm{d}z. \quad \text{(B-1)}$$

Eq. B-1 assumes that the bottom of the wellbore is at the perforations and that negligible rathole volume exists. An EOS is needed to determine $\rho(p,T)$. It must capture variations of density with both temperature and pressure caused by the small deflections in signal studied here. The boundary condition (B.C.) is

$$\frac{\mathrm{d}p}{\mathrm{d}z} = \rho[p(z,t),T(z,t)]\frac{g\sin\theta}{144g_c}; \quad \text{B.C.}: p(z_r,t) = p_{wf}(t). \quad \text{(B-2)}$$

Eq. B-2 is a nonlinear ordinary-differential equation of the first order. Density is both a function of pressure and elevation in the wellbore, attributable to the vertical variation in temperature. It is possible that any EOS is used to furnish the density values. The Tait-Tumlirz EOS has been used. Recalling that $\rho = 1/\nu$, the density relation in this case is defined as (Fisher and Dial 1975)

$$\nu(p,T) = \nu_\infty(T) + \frac{\lambda(T)}{p_0(T)+p}, \quad \text{(B-3)}$$

where ν_∞, p_0, and λ are polynomial functions of temperature and defined by Fisher and Dial (1975). The input temperature (in °C) and other symbols are further discussed in the Nomenclature section. The correlating terms used in their implementation do not account for salinity; the correlation is for pure water. This EOS is indeed very accurate for liquid water, but it does not afford an easy analytical solution of Eq. B-2 for pressure along the wellbore depth. Because of this, the explicit Runge-Kutta numerical method (Kreyszig 2010) has been used to solve for pressure along the well depth.

$$a_1 = \Delta z \cdot \rho[T(z^N), p^N], \quad \text{(B-4)}$$

$$a_2 = \Delta z \cdot \rho\left[T\left(z^N + \frac{\Delta z}{2}\right), p^N + \frac{a_1}{2}\right], \quad \text{(B-5)}$$

$$a_3 = \Delta z \cdot \rho\left[T\left(z^N + \frac{\Delta z}{2}\right), p^N + \frac{a_2}{2}\right], \quad \text{(B-6)}$$

$$a_4 = \Delta z \cdot \rho[T(z^N + \Delta z), p^N + a_3], \quad \text{(B-7)}$$

$$p^{N+1} = p^N + \frac{g\sin\theta}{144g_c}\left(\frac{a_1}{6} + \frac{a_2}{3} + \frac{a_3}{3} + \frac{a_4}{6}\right). \quad \text{(B-8)}$$

For this model, p^0 and z^0 start at the sandface (depth z_r), with Δz being a negative number (the solution marches up the wellbore).

Appendix C—Analytical Wellbore Storage Including Thermal Expansion (Dimensionless Forms)

Constant-Rate-Injection Problem. To develop equations for wellbore storage including thermal effects, we start with an expression for total injection at the wellhead (w) during constant rate injection into the reservoir (resulting in a transient pressure buildup over time),

$$w = w_{sf} + \frac{C}{B}\frac{\mathrm{d}p_{wf}}{\mathrm{d}t} - \frac{\alpha_w V_{wb}}{B}\frac{\mathrm{d}T_{f,av}}{\mathrm{d}t}. \quad \text{(C-1)}$$

The use of thermal expansion in Eq. C-1 is based on the thermodynamic volume relation $d\upsilon = (\partial\upsilon/\partial p)_T\mathrm{d}p + (\partial\upsilon/\partial T)_p\mathrm{d}T$ (Moran and Shapiro 2004). Therefore, the C and α_w properties must be taken at constant temperature and pressure, respectively. Rearranging for sandface injection rate w_{sf} and dividing through by w,

$$\frac{w_{sf}}{w} = 1 - \frac{C}{wB}\frac{\mathrm{d}p_{wf}}{\mathrm{d}t} + \frac{\alpha_w V_{wb}}{wB}\frac{\mathrm{d}T_{f,av}}{\mathrm{d}t}. \quad \text{(C-2)}$$

Preparing terms for their dimensionless forms with field constants, the equation becomes

$$\frac{w_{sf}}{w} = 1 - \left[\frac{0.8936C}{\phi c_t h r_w^2}\cdot\frac{\mathrm{d}(p_{wf}(t)-p_i)kh}{141.2wB\mu}\cdot\frac{\phi\mu c_t r_w^2}{0.0002637k\ \mathrm{d}t}\right] + \left[\alpha_w\frac{0.0002637V_{wb}k}{wB\phi\mu c_t r_w^2}\cdot\frac{\mathrm{d}(T_{f,av}(t)-T_{fo})}{(T_{ei}-T_{fo})}\cdot\frac{\phi\mu c_t r_w^2}{0.0002637k\mathrm{d}t}\right]; \quad \text{(C-3)}$$

that is,

$$w_D(t_D) = 1 - C_D \frac{\mathrm{d}p_{wD}(t_D)}{\mathrm{d}t_D} + \alpha_{wD} \frac{\mathrm{d}T_{Df,av}(t_D)}{\mathrm{d}t_D}. \qquad \text{(C-4)}$$

Finally, taking the Laplace transform,

$$\overline{w}_D(u) = \frac{1}{u} - C_D u \overline{p}_{wD}(u) + \alpha_{wD} u \overline{T}_{Df,av}(u), \qquad \text{(C-5)}$$

with dimensionless groups $p_D = \frac{[p_{wf}(t) - p_i]kh}{141.2wB\mu}$, $w_D = \frac{w_{sf}}{w}$, $t_D = \frac{0.0002637kt}{\phi\mu c_t r_w^2}$, $T_D = \frac{T_f(z,t) - T_{fo}}{T_{ei} - T_{fo}}$, $\alpha_{wD} = \frac{0.0002637V_{wb}k\alpha_w}{wB\phi\mu c_t r_w^2}$, and $C_D = \frac{0.8936C}{\phi c_t h r_w^2}$.

Pressure Falloff for Shut-In Problem. The pressure-falloff relationship will now be discussed. To produce a pressure-falloff situation, the mathematics are analogous to the constant-rate-production problem (referred to as pressure drawdown for production wells). We start this problem by using the production analog,

$$q = q_{sf} - \frac{C}{B}\frac{\mathrm{d}p_{wf}}{\mathrm{d}t} + \frac{\alpha_w V_{wb}}{B}\frac{\mathrm{d}T_{f,av}}{\mathrm{d}t}. \qquad \text{(C-6)}$$

Rearranging for sandface-production rate q_{sf} and dividing through by q,

$$\frac{q_{sf}}{q} = 1 + \frac{C}{qB}\frac{\mathrm{d}p_{wf}}{\mathrm{d}t} - \frac{\alpha_w V_{wb}}{qB}\frac{\mathrm{d}T_{f,av}}{\mathrm{d}t}. \qquad \text{(C-7)}$$

Preparing terms for their dimensionless forms with field constants, the equation becomes

$$\frac{q_{sf}}{q} = 1 - \left\{\frac{0.8936C}{\phi c_t h r_w^2}\cdot\frac{\mathrm{d}[p_i - p_{wf}(t)]kh}{141.2qB\mu}\cdot\frac{\phi\mu c_t r_w^2}{0.0002637k\ \mathrm{d}t}\right\} - \left\{\alpha_w \frac{0.0002637V_{wb}k}{qB\phi\mu c_t r_w^2}\cdot\frac{\mathrm{d}[T_{f,av}(t) - T_{fo}]}{(T_{ei} - T_{fo})}\cdot\frac{\phi\mu c_t r_w^2}{0.0002637k\mathrm{d}t}\right\}; \qquad \text{(C-8)}$$

that is,

$$q_D(t_D) = 1 - C_D \frac{\mathrm{d}p_{wD}(t_D)}{\mathrm{d}t_D} - \alpha_{wD}\frac{\mathrm{d}T_{Df,av}(t_D)}{\mathrm{d}t_D}. \qquad \text{(C-9)}$$

Taking the Laplace transform,

$$\overline{q}_D(u) = \frac{1}{u} - C_D u \overline{p}_{wD}(u) - \alpha_{wD} u \overline{T}_{Df,av}(u). \qquad \text{(C-10)}$$

As mentioned previously, the problem of pressure falloff is analogous to this constant-rate-production case. As such, the q_D term will be replaced by w_D, where $w_D = w_{sf}/w_{\text{prior-injection}}$. The equation then becomes

$$\overline{w}_D(u) = \frac{1}{u} - C_D u \overline{p}_{wD}(u) - \alpha_{wD} u \overline{T}_{Df,av}(u), \qquad \text{(C-11)}$$

with dimensionless groups $p_D = \frac{[p_i - p_{wf}(t)]kh}{141.2wB\mu}$, $w_D = \frac{w_{sf}}{w_{\text{prior-injection}}}$, $t_D = \frac{0.0002637kt}{\phi\mu c_t r_w^2}$, $T_D = \frac{T_f(z,t) - T_{fo}}{T_{ei} - T_{fo}}$, $\alpha_{wD} = \frac{0.0002637V_{wb}k\alpha_{av}}{wB\phi\mu c_t r_w^2}$, and $C_D = \frac{0.8936C}{\phi c_t h r_w^2}$. Please note the difference in dimensionless pressure and sandface-rate definitions between the injection and falloff cases. The remaining groups are identical between cases. Note that an average is required for the thermal-expansion coefficient along the well depth,

$$\alpha_{av} = \frac{\int_0^{z_R} \alpha(z)[T_{ei}(z) - T_{fo}(z)]\mathrm{d}z}{\int_0^{z_R}[T_{ei}(z) - T_{fo}(z)]\mathrm{d}z}. \qquad \text{(C-12)}$$

Similarly, an average temperature would be used at each time,

$$T_{f,av}(t) = \frac{1}{z_R}\int_0^{z_R} T_f(z,t)\mathrm{d}z. \qquad \text{(C-13)}$$

The difference in behavior caused by thermal effects in the constant-rate injection and pressure falloff is shown in **Fig. C-1.** In Fig. C-1, the IARF solution without thermal effects is also shown. When excluding well-temperature effects, the IARF dimensionless pressure response is identical for constant-rate injection and falloff cases (recalling the different definitions of the dimensionless groups given in this appendix). When including thermal effects, the constant-rate-injection problem shows increased values of dimensionless pressure during the buildup over time compared with the isothermal case, as the heating liquids expand, resulting in additional injection into the sandface. For the pressure-falloff case, the same heating effect occurs, forcing liquid into the sandface, now resulting in a "diminished falloff." These two cases lie on either side of the isothermal IARF case. Note that this case with thermal afterflow is unique because storage changes the shape depending on whether it is buildup or falloff. Normally, in the case of the IARF curve, the shape of the curve does not change depending on shut-in or flowing conditions.

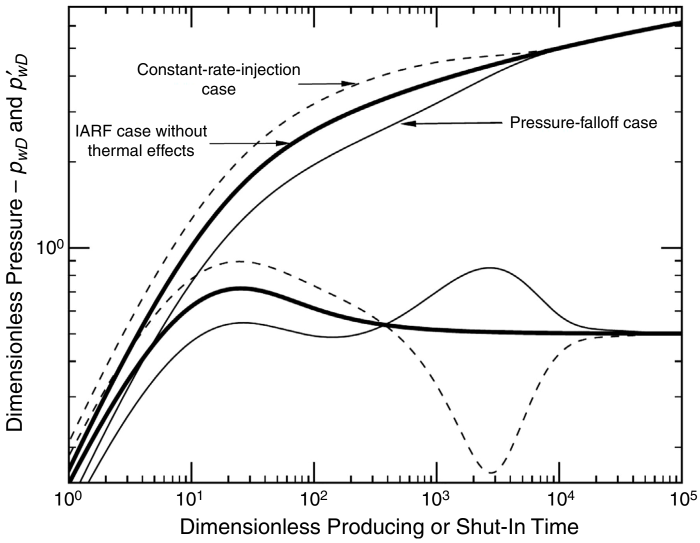

Fig. C-1—Pressure behavior for three separate cases (marked on the chart). (1) IARF case without any thermal effects. (2) Constant-rate-injection case with thermal-wellbore-afterflow effects. (3) Pressure-falloff case with thermal-wellbore-afterflow effects. Wellbore storage $C_D = 5$, thermal constants $a'_D = 5 \times 10^{-4}$, $\alpha_{wD} = 500$.

Laplace Transforms $\overline{T}_{Df}(u)$**.** Expressions are now required for the $\overline{T}_{Df,av}(u)$ function in each case. For the constant-rate-water-injection case, the fluid temperature inside the well is given by

$$T_f(t,z) = T_{ei}(z) + \frac{g_G \sin\theta}{L_R}(e^{-zL_R} - 1). \quad \text{(C-14)}$$

To calculate the average value inside the entire well ($T_{f,av}$), Eq. C-14 is integrated along depth using Eq. C-13. Recall that the time dependency will be captured in the L_R term. The dimensionless version of fluid temperature will be defined as

$$T_{Df}(t) = \frac{T_f(t,z) - T_{fo}(z)}{T_{ei}(z) - T_{fo}(z)} = \frac{T_{ei}(z) - T_{fo}(z) + \dfrac{g_G \sin\theta}{L_R}(e^{-zL_R} - 1)}{T_{ei}(z) - T_{fo}(z)} = 1 + \frac{\dfrac{g_G \sin\theta}{L_R}(e^{-zL_R} - 1)}{T_{ei}(z) - T_{fo}(z)}, \quad \text{(C-15)}$$

where T_{fo} is the temperature at the moment that injection begins. We can assume that $T_{fo}(z) = T_{ei}(z) + \dfrac{g_G \sin\theta}{L_R}(e^{-zL_{R0}} - 1)$. Therefore,

$$T_{Df}(t) = 1 - \frac{1 - e^{-zL_R}}{1 - e^{-zL_{R0}}}. \quad \text{(C-16)}$$

If the temperature does not change significantly inside the well during injection, then $L_R(t) = L_{R0}$ and consequently $T_{Df} = 0$. This is consistent with our definition of dimensionless temperature given previously. Taking the Laplace transform of this equation, assuming that $L_R(t)$ varies slowly and is approximately constant,

$$\overline{T}_{Df,\text{inject}}(u) = \frac{1}{u}\left(1 - \frac{1 - e^{-zL_R}}{1 - e^{-zL_{R0}}}\right). \quad \text{(C-17)}$$

For the falloff case, the fluid temperature inside the well is given by

$$T_f(z,t) = [T_{fo}(z) - T_{ei}(z)]e^{-a't} + T_{ei}(z). \quad \text{(C-18)}$$

In dimensionless form,

$$T_{Df}(t_D) = \frac{T_f(t_D) - T_{fo}}{T_{ei} - T_{fo}} = \frac{1}{T_{ei}(z) - T_{fo}(z)}\left\{[T_{fo}(z) - T_{ei}(z)]\exp\left(-a't_D \cdot \frac{\phi\mu c_t r_w^2}{0.0002637k}\right) + T_{ei}(z) - T_{fo}(z)\right\}$$
$$= 1 - \exp\left(-a't_D \cdot \frac{\phi\mu c_t r_w^2}{0.0002637k}\right) = 1 - \exp(-a'_D t_D), \quad \text{(C-19)}$$

where T_{fo} is the fluid temperature at the instant of shut-in. The dimensionless temperature term varies between zero and unity, when the fluid temperature has equilibrated with that of the earth. Taking the Laplace transform of this equation,

$$\overline{T}_{Df,\text{shut-in}}(u) = \mathcal{L}[T_{Df}(t_D)] = \frac{1}{u} - \frac{1}{a'_D + u}. \quad \text{(C-20)}$$

In Eq. 20, the time dynamics of heat transfer (by means of a') and reservoir flow $\left(\text{by means of } \dfrac{\phi\mu c_t r_w^2}{k}\right)$ are joined to a common dimensionless timescale. The behavior of this equation is as expected; for small values of the heat-transfer-time coefficient (a'_D), $\overline{T}_{Df} = 0$.

7.1 Selected Computer Code

This Python code produces one of the curve sets from Figure 3 in the journal article.

```
import scipy.special as sp
import math
import numpy as np
import matplotlib.pyplot as plt
import matplotlib as mpl

#------- CHART PREP  --------------------
## Set up the charting settings
mpl.rcParams['xtick.major.size']=15
mpl.rcParams['xtick.major.width']=1
mpl.rcParams['ytick.major.size']=15
mpl.rcParams['ytick.major.width']=1
mpl.rcParams['xtick.minor.size']=5
mpl.rcParams['xtick.minor.width']=1
mpl.rcParams['ytick.minor.size']=5
mpl.rcParams['ytick.minor.width']=1
plt.rc('text', usetex=True)
plt.rc('font', family='serif')
fig=plt.figure(facecolor='white')
plt.xlim([1e0,1e6])
plt.ylim([1e-1,1e1])

#------- MODEL INPUTS--------------------
#-----Thermal wellbore constants--------
# For use with the thermal storage model
a_D=5e-4
alpha_D=-1000
#------Reservoir properties-------------
# Reservoir - dimensionless
S=0
CD=5

# Stehfest inversion model
# N must be even
N=12
# Generate coefficients
c=[]
for n in range(1,N+1):
    temp=0
    for k in range(int((n+1)/2),min(n,N/2)+1):
        temp+=k**(N/2.0)*math.factorial(2.0*k)*1.0/(1.0*math.factorial(N/2.0-k)* \
        math.factorial(k)*math.factorial(k-1)*math.factorial(n-k)*math.factorial(2.0*k-n))
    c.append((-1.0)**(n+N/2.0)*temp)

# Inversion algorithm for function
def f(t,F):
    temp=0
    for n in range(1,N+1):
        temp+=c[n-1]*F(1.0*n*np.log(2.0)/t)
    return np.log(2.0)/t*temp

# Define function to be inverted (IARF)
def puD(u):
```

```
    sqt_u=np.sqrt(u)
    return sp.k0(sqt_u)/u/sqt_u/sp.k1(sqt_u)
# Wellbore function
def pwD(s):
    numerator=(a_D + s + a_D*alpha_D*s)*(S + puD(s)*s)
    denominator=s*(a_D + s)*(1 + CD*S*s + CD*puD(s)*s**2)
    return numerator/denominator
# Wellbore deriative function
def pwD_(s):
    numerator=(a_D + s + a_D*alpha_D*s)*(S + puD(s)*s)
    denominator=s*(a_D + s)*(1 + CD*S*s + CD*puD(s)*s**2)
    return s*numerator/denominator


## Chart the two curves (pressure and its derivative)
t=np.logspace(-1,6,1000)
plt.loglog(t,t*f(t,pwD_),'k')
plt.loglog(t,f(t,pwD),'k')
plt.ylabel("Dimensionless pressure")
plt.xlabel("Dimensionless shut-in time")
```

8 Rate Transient Analysis of Production Wells with Water Injector Support

The final chapter in this thesis views the reservoir as a connected system spanning from injector to producer. RTA, which is usually only applied to waterflooded wells using semi-empirical methods, is approached in a fully analytical way for waterflood fields. When deriving RTA equations for the production response in a waterflood reservoir, no assumptions are made regarding stabilised flow, which allows all transient periods to be accounted for. This work is motivated by some of the inadequacies of the classical decline curve techniques when handling production data from waterflooded fields.

The paper is published in the SPE Reservoir Evaluation & Engineering journal.

Statement of Authorship

Title of Paper	Analytical Rate-Transient Analysis and Production Performance of Waterflooded Fields With Delayed Injection Support
Publication Status	☐ Published ☐ Accepted for Publication ☑ Submitted for Publication ☐ Unpublished and Unsubmitted w ork w ritten in manuscript style
Publication Details	O'Reilly, D.I., Haghighi, M., Sayyafzadeh, M. and Flett, M.A. 2020. Analytical Rate-Transient Analysis and Production Performance of Waterflooded Fields With Delayed Injection Support. Submitted to *SPE Reservoir Evaluation & Engineering*.

Principal Author

Name of Principal Author (Candidate)	Daniel O'Reilly		
Contribution to the Paper	Problem formulation, derivation of mathematical model, preparation of graphs, writing the manuscript. Acted as corresponding author.		
Overall percentage (%)	80%		
Certification:	This paper reports on original research I conducted during the period of my Higher Degree by Research candidature and is not subject to any obligations or contractual agreements with a third party that would constrain its inclusion in this thesis. I am the primary author of this paper.		
Signature		Date	25 Nov 2020

Co-Author Contributions

By signing the Statement of Authorship, each author certifies that:

i. the candidate's stated contribution to the publication is accurate (as detailed above);

ii. permission is granted for the candidate in include the publication in the thesis; and

iii. the sum of all co-author contributions is equal to 100% less the candidate's stated contribution.

Name of Co-Author	Manouchehr Haghighi		
Contribution to the Paper	Principal supervision of the work. Problem formulation, manuscript review and assessment.		
Signature		Date	01/12/2020

Name of Co-Author	Matthew Flett		
Contribution to the Paper	Problem formulation, reviewed the manuscript and provided feedback		
Signature		Date	25/11/2020

Name of Co-Author	Mohammad Sayyafzadeh		
Contribution to the Paper	Problem formulation, reviewed the manuscript and provided feedback		
Signature		Date	26/11/2020

Analytical Rate-Transient Analysis and Production Performance of Waterflooded Fields with Delayed Injection Support

Daniel O'Reilly, University of Adelaide and Chevron Australia Pty Ltd.; **Manouchehr Haghighi** and **Mohammad Sayyafzadeh,** University of Adelaide; and **Matthew Flett,** Chevron Australia Pty Ltd.

Summary

An approach to the analysis of production data from waterflooded oil fields is proposed in this paper. The method builds on the established techniques of rate-transient analysis (RTA) and extends the analysis period to include the transient- and steady-state effects caused by a water-injection well. This includes the initial rate transient during primary production, the depletion period of boundary-dominated flow (BDF), a transient period after injection starts and diffuses across the reservoir, and the steady-state production that follows. RTA will be applied to immiscible displacement using a graph that can be used to ascertain reservoir properties and evaluate performance aspects of the waterflood. The developed solutions can also be used for accurate and rapid forecasting of all production transience and boundary-dominated behavior at all stages of field life.

Rigorous solutions are derived for the transient unit mobility displacement of a reservoir fluid, and for both constant-rate-injection and constant-pressure-injection after a period of reservoir depletion. A simple treatment of two-phase flow is given to extend this to the water/oil-displacement problem.

The solutions are analytical and are validated using reservoir simulation and applied to field cases. Individual wells or total fields can be studied with this technique; several examples of both will be given. Practical cases are given for use of the new theory. The equations can be applied to production-data interpretation, production forecasting, injection-water allocation, and for the diagnosis of waterflood-performance problems.

Introduction

Waterflooding accounts for a significant proportion of reserves recovered in many conventional oil fields. One established method to analyze and forecast the performance of producing oil fields is RTA (Ehlig-Economides and Ramey 1981; Clarkson and Pedersen 2010; Sun 2015; Poston et al. 2019). RTA seeks to resolve reservoir properties (e.g., permeability, skin, and drainage area) from available production history and operational information. The method continues to be popular for both conventional and unconventional reservoirs (Ali and Sheng 2015; O'Reilly et al. 2016b).

In its usual format, RTA is difficult to apply directly to some production data from wells or fields undergoing waterflood-pressure support. This point is clear in waterflooded-field examples given in Fetkovich (1980). Often depletion alone is assumed; alternatively, empirical decline parameters are matched (Fetkovich 1980; Ambastha and Wong 1998), or possibly a form of continuous aquifer support is applied. Frequently on production histories for waterflood fields, rapid changes in liquid rates (or discontinuities) are observed for the production wells after injection begins. These events are not satisfactorily modeled using the present RTA methods.

There are many methods available apart from RTA to analyze waterflood performance. Reservoir simulation is a powerful tool, but requires time to develop a dynamic model and run the computations. Alternatively, numerous analytical methods exist to analyze the steady-state fractional-flow performance of waterflood fields (Baker et al. 2003; Yang 2009; Li et al. 2011). These models do not pay attention to transient flow periods but focus on forecasting phase fractions for the remainder of field life. The "waterflood event" is also discussed in the context of oil-production-performance analysis by Poston et al. (2019), where it is approached in a steady-state fashion.

During the past 15 years, capacitance resistance modeling (CRM) has also emerged as a successful intermediate between reservoir simulation and the steady-state methods. Many authors have shown CRM to be an excellent history-matching, forecasting, and optimization tool to model fluid flow in waterflood fields (Gentil 2005; Liang et al. 2007; Sayarpour et al. 2009; de Holanda et al. 2018). Complicated multilayer field scenarios can also be modeled using CRM (Moreno 2013). Several other methods have emerged that are similar to CRM, where the main objective is to infer injector/producer-well connectivities and water cuts in fields with many wells (Sayyafzadeh 2011). However, most of the methods assume a 0D reservoir (assessed at an average reservoir pressure) and thus do not account for the transient effects required for RTA. The method proposed in this paper also provides an improved description of the transition period between depletion production and full steady-state waterflood support. BDF behavior is not assumed in the present work.

There are also similarities between modeling waterflooding and aquifer pressure support in reservoirs. Many mathematical solutions are available to model aquifer support (van Everdingen and Hurst 1949; Carter and Tracy 1960; Fetkovich 1971; Yildiz and Khosravi 2007; Izgec and Kabir 2010). One option available in RTA is the composite (two-zone) model of the subsurface to account for the reservoir and a large attached aquifer in the outer zone [e.g., the Ambastha (1989) model applied to RTA]. This method allows external influx into the reservoir from the aquifer. Unfortunately, these aquifer models do not perfectly describe the situation occurring during a waterflood. Because oil wells are often developed years before waterflood operations begin, there is a period of extensive decline before the start of any form of pressure support. Aquifer models in RTA analysis (including the composite model) are usually connected to the reservoir since the beginning of depletion, and this can pose problems interpreting data from waterflooded fields where pressure support did not start until later. Our model resolves this by allowing injection to start later in field life.

Doublet and Blasingame (1995) investigated the application of a waterflood RTA model. Their study served as an excellent starting point for the work in this paper, but the approach we have taken is mathematically quite different. Doublet and Blasingame (1995) solved the problem for delayed constant-rate-injection by taking the Laplace transform of a delayed unit rate-step function at the outer boundary. This function was inverted back into the time domain using an inversion algorithm; however, this inversion algorithm does

Original SPE manuscript received for review 13 December 2020. Revised manuscript received for review 27 January 2021. Paper (SPE 205371) peer approved 31 January 2021.

not perform well with discontinuities such as the delayed unit-step function. In our work, the problem is overcome by applying superposition in the time domain on basic solutions. Furthermore, we have also introduced a solution for the constant-pressure-injection problem that again involves a different solution method. Finally, some additional attention is given in our text to the treatment of multiphase flow.

The interpretation method provided in our work is very similar to the original method of Fetkovich (1980). Modifications to that type curve still occur frequently in the literature and maintain popularity (Eleiott et al. 2019). The present work will be beneficial to those interpreting production data from oil fields undergoing waterflood. With modern computing available, it is not necessarily intended that the type curves generated in this paper are used exactly in their graphical format, although that is certainly possible. Automated or assisted matching is also possible using the new model.

The structure of this paper is as follows. In the first section, the overall theory is given for the development of production-rate curves. Next, the analytical solutions will be provided for use in the model. The third part of the paper will show a set of type curves developed using the theory, intended for matching with field production data. After this, the type curves are validated against reservoir-simulation cases, and finally, several field applications are shown. A separate section is given on forecasting production using the frontal advance theory, and a case is shown for a hypothetical stratified waterflood. A discussion will highlight the limitations of this model and compare it with other mathematical techniques available.

Theory and Development of Model

The underlying analytical model in this work is dependent on solutions to the linearized radial diffusivity equation for the flow of a slightly compressible fluid in a porous medium. Gravity effects are ignored and the flow is considered as isothermal, laminar Darcy flow. Constant reservoir thickness and reservoir properties (k, ϕ, c_t) are assumed, along with a fully penetrating vertical production well. This model assumes that a production well, producing from inner radius r_w, depletes a reservoir of prescribed outer radius r_e for a period of time starting at $t = 0$, after which injection begins at this external boundary. The time that injection begins is denoted t_{inj}. Flux from injection is assumed to be evenly spread across the outer radius. This approximation is particularly useful for reservoirs with a pattern-flood configuration. Capillarity effects are ignored. A diagram of the radial geometry and boundary conditions is shown in **Fig. 1.**

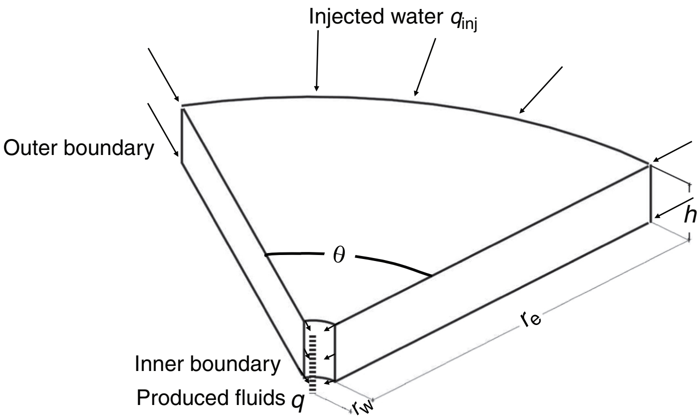

Fig. 1—Schematic of a reservoir undergoing waterflood injection at the outer boundary. Liquid production starts at constant p_{wf} at $t = 0$, while injected liquid (rate q_{inj}) can start at any time in the field life. In the model, θ = 360°.

Importantly, it is also assumed that the fluid properties of the injected fluid are the same as those of the displaced fluid. This assumption is made to develop the straightforward analytical solution, but it is shown through reservoir-simulation results that the solutions can be representative of cases where there are some differences between displacing- and displaced-fluid properties. A more thorough description on multiphase aspects is given later in the paper.

The mathematical description of total production rate from a production well in a reservoir is split into the following two time periods:

- The first period of transient production decline and BDF ($t < t_{\text{inj}}$).
- Production-rate increase immediately after the start of water injection ($t \geq t_{\text{inj}}$).

Injection at the outer reservoir boundary is considered as either constant rate or constant pressure. For the case of constant-rate injection, the two time periods are covered separately by means of superposition of a depletion solution and a separate injection solution. This is shown in Eq. 1,

$$q(t) = \begin{cases} q^{\text{depl}}(t)\,; & 0 < t < t_{\text{inj}} \\ q^{\text{depl}}(t) + q^{\text{inj-q}}(\Delta t)\,; & t \geq t_{\text{inj}}, \end{cases} \quad (1)$$

where q represents the total liquid flow at the production well, and $\Delta t = t - t_{\text{inj}}$. The depletion solution incorporates both transient and boundary-dominated effects.

For the case of constant-pressure injection, an alternative solution has been developed. This solution should be applied as

$$q(t) = \begin{cases} q^{\text{depl}}(t)\,; & 0 < t < t_{\text{inj}} \\ q^{\text{inj-p}}(\Delta t)\,; & t \geq t_{\text{inj}}. \end{cases} \quad (2)$$

It is noted that there is no superposition of solutions required during the injection period for the constant-pressure injection problem. The difference between the constant-rate and constant-pressure injection approaches is the initial starting pressure used for the solved equations $q^{\text{inj-q}}(\Delta t)$ and $q^{\text{inj-p}}(\Delta t)$.

In the constant-rate injection solution, a uniform initial pressure profile is defined and the well is assumed to be held at this fixed initial pressure. This solution is then added by means of superposition to the original depletion-production-rate solution, $q^{\text{depl}}(\Delta t)$. In this case, the incremental production caused by injection is clearly described by the $q^{\text{inj-q}}(\Delta t)$ equation. After $t \geq t_{\text{inj}}$, the sum of the two equations describes the total production at the well (Eq. 1).

For the constant-pressure injection solution, a different approach is used to solve for production at the wellbore. This is necessary because the original depletion solution uses the Neumann no-flux boundary condition at the outer radius r_e. Because the constant-pressure-injection solution is of the Dirichlet fixed-value type at r_e, superposition should not be used for the two solutions because the boundary conditions are inconsistent. Instead, a solution can be found to the problem by loading the pressure distribution after depletion, $p(r)$, as the initial condition to the problem of a step constant-pressure injection at the outer reservoir radius. As a result, the solved $q^{\text{inj-p}}(t)$ equation includes both the effects of initial production and the incremental production caused by injection. This explains the different form of Eqs. 1 and 2.

Analytical Solutions

Expressions are derived fully in Appendix A for the depletion solution, constant-rate injection part of the solution, and the constant-pressure-injection solution. The solutions will be repeated here and are expressed in terms of the dimensionless variables also defined in Appendix A.

The depletion solution, for production from a well held at a constant flowing bottomhole pressure (FBHP), is given as

$$\overline{q}_D^{\text{depl}}(u) = \frac{1}{\sqrt{u}} \cdot \frac{I_1(r_{eD}\sqrt{u})K_1(\sqrt{u}) - I_1(\sqrt{u})K_1(r_{eD}\sqrt{u})}{I_1(r_{eD}\sqrt{u})K_0(\sqrt{u}) + I_0(\sqrt{u})K_1(r_{eD}\sqrt{u})}. \quad (3)$$

This solution provides the full trace of the curves normally present on the Fetkovich (1980) decline curves for pure-depletion flow, excluding the empirical Arps (1945) curves. The depletion equation is also available in Ehlig-Economides (1979).

For the case of constant-rate injection into a reservoir with a uniform initial reservoir pressure and production well held at a fixed, initial pressure, the solution is given as

$$\overline{q}_D^{\text{inj-q}}(u) = \frac{q_{D,\text{inj}}}{r_{eD}u} \cdot \frac{I_1(\sqrt{u})K_0(\sqrt{u}) + I_0(\sqrt{u})K_1(\sqrt{u})}{I_1(r_{eD}\sqrt{u})K_0(\sqrt{u}) + I_0(\sqrt{u})K_1(r_{eD}\sqrt{u})}. \quad (4)$$

Finally, for constant-pressure injection into a reservoir with a nonuniform initial pressure and production well held at a fixed pressure, the solution is given as

$$\overline{q}_D^{\text{inj-p}}(u) = \frac{-\dfrac{p_{D,\text{inj}}}{u} + K_0\left(r_{eD}\sqrt{u}\right)\displaystyle\int_1^{r_{eD}} \xi I_0\left(\xi\sqrt{u}\right)p_{D0}(\xi)d\xi - I_0\left(r_{eD}\sqrt{u}\right)\displaystyle\int_1^{r_{eD}} \xi K_0\left(\xi\sqrt{u}\right)p_{D0}(\xi)d\xi}{I_0(r_{eD}\sqrt{u})K_0(\sqrt{u}) - K_0(r_{eD}\sqrt{u})I_0(\sqrt{u})}. \quad (5)$$

These solutions are used in Eqs. 1 or 2 to create a full production profile over time. An example case is shown in **Fig. 2.** In this log-log graph, the declining solid black line is for pure-depletion production only. There are two solid lines coming off this stem at $t_{D,\text{inj}} = 4{,}000$ and $t_{D,\text{inj}} = 10{,}000$, corresponding to two different cases of constant-rate injection starting at the outer boundary. The two injection stems also use different strengths of water injection. After a period of time, it can be observed that production at the inner well increases until it reaches a fixed, steady-state value corresponding exactly to the injection rate at the outer boundary. At the same time, a dotted line shows the production response from constant-pressure injection that terminates at an equivalent steady-state-production rate to the constant-rate-injection cases.

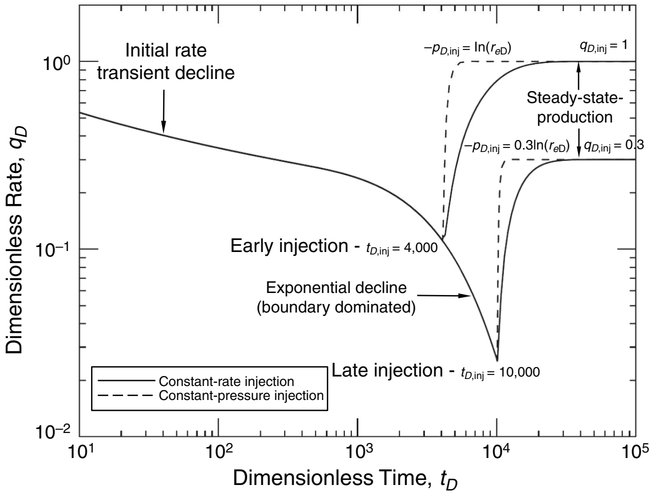

Fig. 2—Comparison of production-well response for constant-rate and constant-pressure injection at the outer reservoir radius (in this example, $r_{eD} = 50$).

At large times, Eqs. 1 and 2, utilizing the solutions in this section, reach the steady-state condition. Using our nomenclature, this can be written as

$$\lim_{t_D \to \infty} q_D(t_D) = q_{D,\text{inj}} = \frac{-p_{D,\text{inj}}}{\ln r_{eD}}. \quad (6)$$

The equivalence between constant-pressure and constant-rate injection is also marked in Fig. 2.

Fig. 2 shows that the production response at the inner well is much more rapid in the case of constant-pressure injection than for that of a constant rate. It should be recognized that while the constant-pressure case eventually ends at the same production rate at the inner well, at early times the injected volumes at the outer boundary are much higher than this terminal value. This occurs during reservoir "fill-up." In some situations, the application of the constant-pressure injection solution might be unrealistic. For a highly depleted reservoir with a low pressure, imposing a constant pressure at the outer boundary can require rates so excessive that they are not achievable in practice. For this reason, the constant-pressure injection solution should be applied carefully. In field operations where finite volumes of source water are available, it is more likely that the constant-rate injection solution is the most practical.

Waterflood Type Curves

The use of type curves is an established method for determining reservoir and well properties (Poston et al. 2019). In this section, general dimensionless curves are developed that can be overlaid with actual field or well production history. These type curves have been prepared for total liquid production and are dependent on solutions given in the prior section.

The Fetkovich (1980) decline variables are useful to scale decline curves for different reservoir sizes (r_e) onto a single graph. This allows charting of any production data on a single log-log graph for later ascertainment of reservoir size and properties. The dimensionless production-rate decline and decline time are defined as

$$q_{Dd} = q_D\left(\ln r_{eD} - \frac{1}{2}\right), \quad (7)$$

and

$$t_{Dd} = \frac{t_D}{\frac{1}{2}\left(r_{eD}^2 - 1\right)\left(\ln r_{eD} - \frac{1}{2}\right)}. \quad (8)$$

It has been noted by other authors (Ehlig-Economides 1979; Doublet et al. 1994) that these dimensionless decline groups contain a minor error in their definition, but because there is minimal impact on engineering calculations, we continue to use them for consistency.

The type curves for the constant-rate injection case are given in **Figs. 3 and 4,** using the Fetkovich decline variables (Fetkovich 1980). Fig. 3 contains injection stems for injection time $t_{Dd,\text{inj}}$ beginning very early into reservoir depletion. Later times are shown in Fig. 4. The majority of cases should be analyzed using Fig. 3 because these are probably more practical cases that incorporate some pressure depletion before the start of injection. The figures have been separated by the resolution of the different scales.

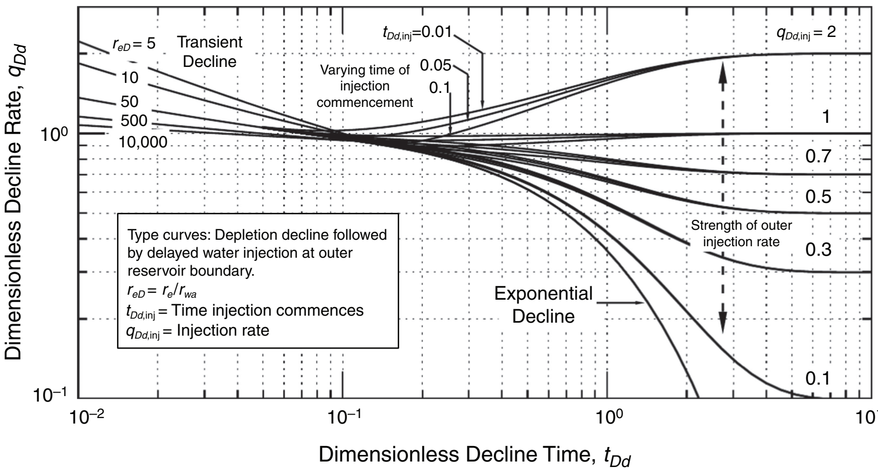

Fig. 3—Constant-rate injection type curves (stems shown for injection starting $t_{Dd,\text{inj}} \leqslant 0.1$).

The constant-pressure-injection case is shown in **Fig. 5.** Readers can compare the marked difference in production-rate response of the constant-pressure and constant-rate-injection (Fig. 4) cases. The response in the constant-pressure case is much more rapid. Here, the dimensionless pressure injection constant is defined as in Appendix A,

$$p_{D,\text{inj}} = \frac{p_{wf} - p_{e,\text{inj}}}{p_i - p_{wf}}. \quad (9)$$

For pressure gradients across the reservoir that result in production inside the well, the $p_{D,\text{inj}}$ constant defined here will be negative.

In Appendix B, type curves are also available using alternative plotting variables derived from the decline-rate integral. There is a benefit to using these charts when flow-rate/time field data contain measurement fluctuations. These terms are defined as (McCray 1990)

$$q_{Ddi} = \frac{N_{pDd}}{t_{Dd}}; \quad N_{pDd} = \int_0^{t_{Dd}} q_{Dd}(t')dt'. \quad (10)$$

When using discrete production data, integration is achieved in Eq. 9 using the scheme from Blasingame et al. (1989). The strength of this "smoothing" type curve will be demonstrated later with field examples.

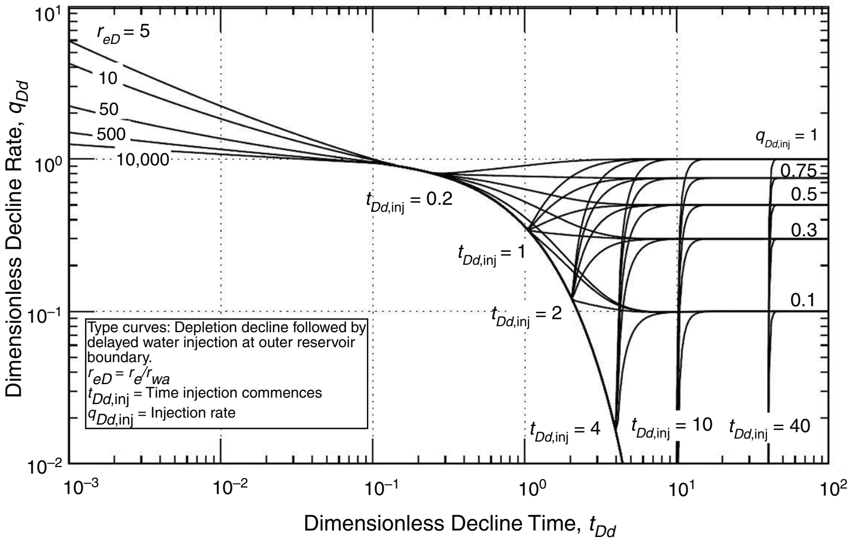

Fig. 4—Constant-rate-injection type curves (stems shown for injection starting $t_{Dd,inj} \geqslant 0.2$).

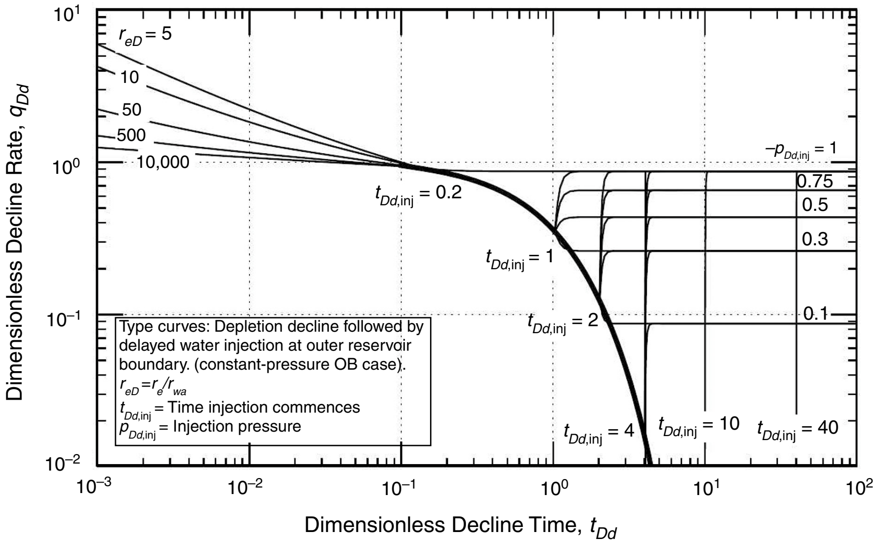

Fig. 5—Constant-pressure injection type curves. OB = outer boundary.

Type-Curve-Matching Process. Use of any of the graphs with field data will now be described. The objective of analyzing production data using type curves is to calculate unknown reservoir properties from decline behavior. First, production-rate/time data (or integral/cumulative if this chart is used) should be charted on square log-log axes, using the same-sized log cycles as the computed type curves in this paper. The field data are then overlaid on the required dimensionless type-curve graph. This can be performed using a computer. The production data chart is physically shifted until a best match is achieved with the type-curve stems. After this, a value of r_{eD} is read from the type-curve chart ($t_{Dd,\text{inj}}$ and $q_{Dd,\text{inj}}$ or $p_{D,\text{inj}}$ can also be recorded). A match ratio between the scales of actual field data and dimensionless type curves is then recorded, denoted $(q)/(q_{Dd})_{\text{MP}}$ and $(t)/(t_{Dd})_{\text{MP}}$. In accordance with the dimensionless groups defined in Eqs. 7, 8, and A-2, the unknown reservoir properties can then be determined.

When following this approach using the constant-rate-injection type curves, the usual parameter outputs from analysis are as follows (provided the other required reservoir properties are known):

- Step 1: $(q)/(q_{Dd})_{\text{MP}} \rightarrow$ permeability, k (Eqs. 7 and A-2)
- Step 2: $(t)/(t_{Dd})_{\text{MP}} \rightarrow$ apparent wellbore radius, r_{wa}, and hence skin, s (Eqs. 8 and A-2)
- Step 3: r_{eD} matched stem $\rightarrow$ reservoir outer-boundary radius, r_e (Eq. A-2)
- Step 4: $q_{Dd,\text{inj}}$ and $t_{Dd,\text{inj}}$ matches $\rightarrow$ effective water-injection rate, q_{inj}, and time of injection start, t_{inj} [Eqs. 7 and 8, and utilizing $(q)/(q_{Dd})_{\text{MP}}$]

The calculated properties in Steps 1 through 3 are identical to the Fetkovich (1980) approach for decline-curve analysis (DCA). Step 4 incorporates the new model from this work and provides insight into the influence of water injection at the production well.

Examples will follow later in this paper to serve as further demonstration.

Multiphase-Flow Considerations

The primary objective of this paper is to develop a set of curves for single-phase-liquid analysis of a transient displacement process present in waterflooded fields. Secondary to this, the fact that the displacement process is actually two or more phases needs to be discussed. Often, solutions for the single-phase slightly compressible fluid case can later be extended to multiple phases, with minor adjustments to the dimensionless variables used.

For cases where both oil and water are producing from the well, the following correction can be made when plotting field data, assuming that the reservoir is above bubblepoint pressure:

$$q_t = q_o B_o + q_w B_w, \quad (11)$$

where the q_t volumetric rate is measured at reservoir conditions (RB/D). If RB/D are used in the type-curve charts, the formation volume factor (FVF) term should be removed from the dimensionless groups when calculating the reservoir properties (Appendix A, Eq. A-2).

Consequently, the total mobility of the system is defined as

$$\lambda_t = \frac{k_o}{\mu_o} + \frac{k_w}{\mu_w} = \lambda_o + \lambda_w. \quad (12)$$

Using this approach, the type curves can be used on a total-liquid and total-mobility basis for multiphase fluids. This tactic is identical to that used by Perrine (1956) and later proved mathematically by Martin (1959), who showed that the single-phase diffusivity equation (Appendix A, Eq. A-1) could be applied to multiphase fluids by using the total mobility (λ_t), total compressibility (c_t), and total flow rate (q_t). The important assumption when using this approach is that saturation gradients in the reservoir are small (Martin 1959). The change in saturation with time does not need to be small for the Martin (1959) theory to apply to Eq. A-1, and λ_t can vary with time. However, because our type curves were derived as a solution to Eq. A-1 for the case of constant mobility λ_t, it is not strictly rigorous to allow the mobility to change dramatically over time when charting and interpreting results. Small changes in mobility for production data might be acceptable, but they must be recognized as a deviation from our underlying theory.

It is known that fluid saturations will change during the course of a waterflood, and this can affect total mobility over time. A simple way of handling this is to assume that the majority of changes occur at late times, similar to other steady-state methods (Baker et al. 2003; Yang 2009; Li et al. 2011).

In the case of constant-rate-injection during the steady-state BDF period, we can estimate the total pressure gradient at any point in the reservoir with reservoir flow equal to the external injection rate,

$$\left[\frac{\partial p(r,t)}{\partial r}\right]_{\text{BDF}} = -\frac{B_t q_t(r,t)}{2\pi r h \lambda_t(r,t)} \approx -\frac{B_w q_{\text{inj}}}{2\pi r h \lambda_t(r,t)}. \quad (13)$$

Combining with the continuity equation and integrating over the reservoir, recalling that p_{wf} is held constant,

$$\left[p_e(t) - p_{wf}\right]_{\text{BDF}} = \frac{B_w q_{\text{inj}}}{2\pi h} \int_{r_w}^{r_e} \frac{dr'}{r' \lambda_t(r',t)}. \quad (14)$$

These simplifications suggest that during the steady-state portion of the type-curve stems only, it is acceptable to include phase-flow rates that vary slowly over time. Hence, during this period, the total liquid rate can be written during boundary-dominated injection as

$$[q_t]_{\text{BDF}} = q_o(t) B_o(t) + q_w(t) B_w(t) \approx q_{\text{inj}} B_w. \quad (15)$$

As noted, this approach is identical to other steady-state methods available in the literature. The simulation case studies that follow show that using Eq. 15 for multiphase flow can result in acceptable agreement with the type-curve charts for the specific mobility ratio considered in the examples. However, the results are not necessarily general, and there will be cases where the immiscible displacement behavior exceeds the range of applicability of the type curves. This has not been tested across all ranges and is considered as further work.

It is finally worth mentioning that this treatment of two-phase flow is also equivalent to what is performed in CRM. In CRM (Sayarpour et al. 2009), when voidage replacement is set to unity, the total liquid production stays fixed at long times, while water cut changes as a function of cumulative production [e.g., the Gentil (2005) model]. Our approximation is equivalent.

Reservoir-Simulation Validation

Some case studies will now be shown from numerical reservoir simulation and compared with the analytical type curves from this work. Two-phase waterflood simulations have been run with constant-compressibility oil and water fluids using an open-source software reservoir simulator (Rasmussen et al. 2021).

A map of the cases is shown in **Table 1,** with fixed reservoir and completion properties in **Table 2.** The simulation uses a $100 \times 100 \times 1$-cell grid that is a symmetrical quarter-portion of a 20-acre drainage area. The production and injection rates have been adjusted after the simulation (multiplied by four) to account for the symmetrical sector. The grid is shown in **Fig. 6** along with diagrams of the relative permeability inputs and associated total mobility curve, $\lambda_t(S_w)$. In the diagram of the simulation model, a production well (OP) and injection well (INJE) are marked. The case is fictitious but bears some resemblance to the waterflooded reservoir discussed by O'Reilly et al. (2016a).

In all of the simulation cases, a period of production depletion is followed by delayed injection; this follows the same course as the analytical model and type curves. The five cases were run using varying S_{wi}, q_{inj}, and t_{inj}, as shown in Table 1. Cases 1 through 3 all use the five-spot pattern of injection, whereas Cases 4 and 5 use the normal nine-spot pattern. The first four cases use constant-rate injection, while the last case tests the effect of constant-pressure injection. It is also worth noting that Cases 3 through 5 had breakthrough of water before the end of their forecasted period.

	Case 1	Case 2	Case 3	Case 4	Case 5
Drainage area	$A = 20$ acres (i.e., equivalent $r_e = 526.6$ ft), $100 \times 100 \times 1$-cell grid				
Wellbore radius apparent	r_{wa}=0.8 ft				
Calculated r_{eD}	$r_{eD} = 658$				
Injection pattern	5-spot	5-spot	5-spot	Normal 9-spot	Normal 9-spot
Initial saturation condition	$S_{wi} = 1.0$ Water displacing water	$S_{wi} = 0.3$ Water displacing oil at S_{oi}	$S_{wi} = 0.6$ Water displacing oil with mobile water present	$S_{wi} = 0.3$ Water displacing oil at S_{oi}	$S_{wi} = 0.3$ Water displacing oil at S_{oi}
Total injection rate into pattern	200 BWIPD	400 BWIPD	400 BWIPD	Fixed q_{inj}; 360 BWIPD	Fixed injector FBHP = 1,300 psi
Time injection starts	$t_{inj} = 180$ days	$t_{inj} = 90$ days	$t_{inj} = 90$ days	$t_{inj} = 90$ days	$t_{inj} = 90$ days
Calculated t_{Ddinj} (from reservoir/fluid properties)	$t_{Ddinj} = 3.1$	$t_{Ddinj} = 1.1$	$t_{Ddinj} = 0.9$	$t_{Ddinj} = 1.1$	$t_{Ddinj} = 1.1$

Table 1—Case map for reservoir-simulation study. BWIPD = barrels of water injected per day.

Input Parameter	Value
Permeability, $k_x = k_y = k_z$ (md)	3
Porosity, ϕ (p.u.)	0.26
Depth to top sand (ft)	3,000
Layer thickness, h (ft)	100
Water compressibility, c_w (1/psi)	3.0×10^{-6}
Oil compressibility, c_o (1/psi)	1.0×10^{-5}
Formation compressibility, c_f (1/psi)	3.0×10^{-6}
Water viscosity, μ_w (cp)	0.6
Oil viscosity, u_o (cp)	0.65
Water FVF, B_o at p_i (RB/STB)	1
Oil FVF, B_w at p_i (RB/STB)	1.2
Wellbore radius apparent, r_{wa} (ft)	0.8
Initial pressure, p_i (psi)	1,000
Producer FBHP, p_{wf} (psi)	400

Table 2—Simulation inputs.

The results of reservoir simulation (q_t in RB/D) are shown matched to the type curves in **Figs. 7a and 7b.** In all cases, the interpreted r_{eD} transient stem compares closely with the actual value of r_{eD}=658. The interpreted time that injection starts ($t_{Dd,inj}$) can also be compared with the actual time for each case in Table 1, with similar results. Furthermore, it is clear that the general shape of the transition between the depletion curve and the steady-state-production curve is the same between reservoir simulation and type curves. It is apparent in Fig. 7b that the constant-pressure injection Case 5 has a much steeper response at the production well than its equivalent constant-rate injection Case 4.

The effect of using the radial type-curve model with production data from spot-pattern floods also appears to be small. This helps to validate the analytical model and also shows that when small mobility gradients are present in the reservoir, the type curves are representative of total liquid multiphase production behavior.

Field Case Studies

The primary application of this theory is the interpretation of production data (both transient and steady state) from waterflooded fields. For this purpose, production history from six waterflooded assets have been gathered from the literature and are analyzed here using the type curves. Each set of production data includes both transient, boundary-dominated depletion flow, and later steady-state flow from waterflood support. This allowed comparison with each portion of the type curve.

The results from all field case study type-curve matches are shown in **Table 3.** All cases are interpreted using the constant-rate-injection type curve. Most of the results are shown in a dimensionless format, with the match point also given so that the match can be

converted into reservoir properties using Eqs. 6, 7, and A-2. Each of the data sets will now be discussed. To provide a graphical example within the text, **Fig. 8** is shown for Windalia Well 1. The remainder of the examples will be discussed here, with figures appearing in Appendix C (Figs. C-1 through C-5).

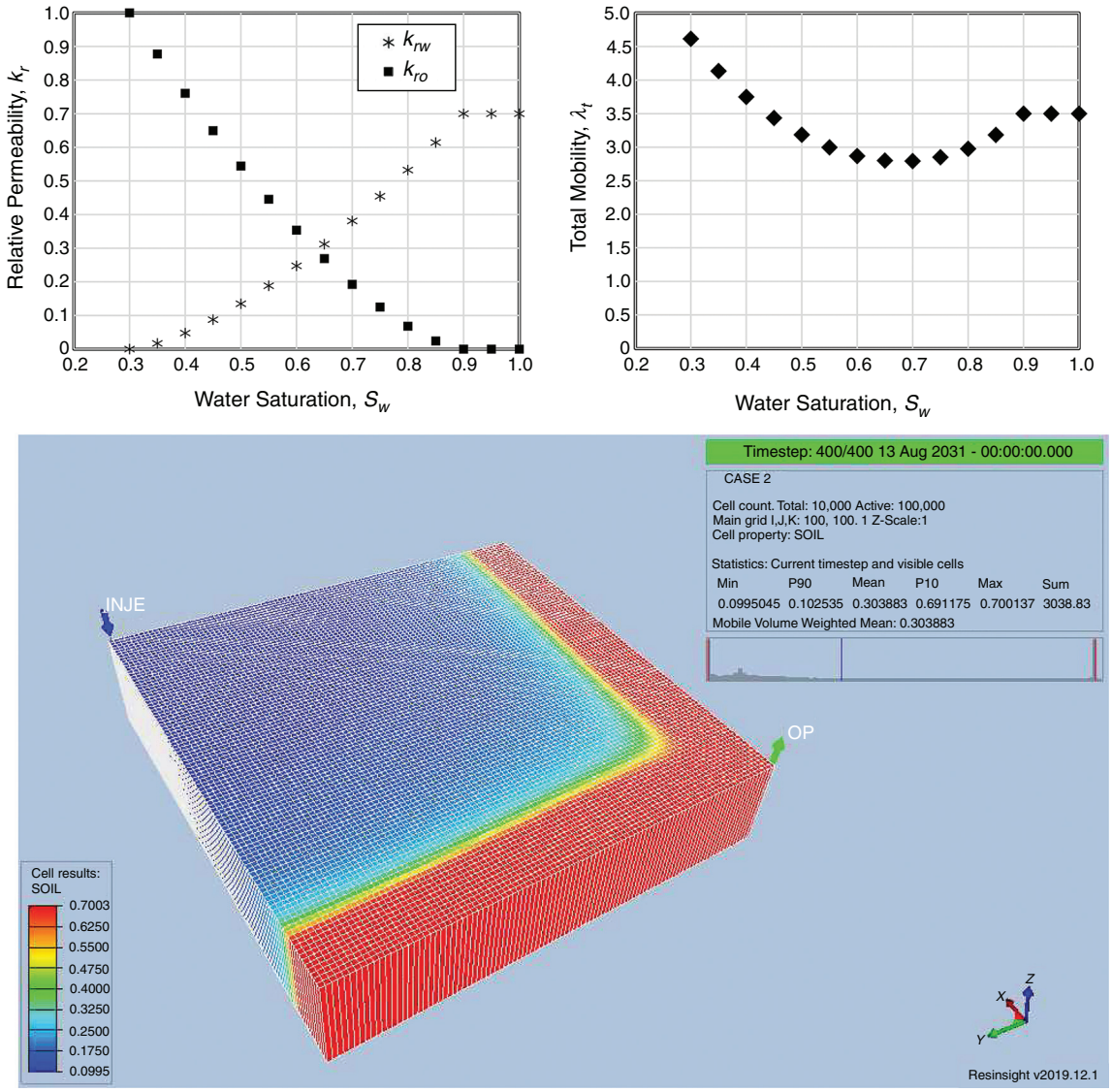

Fig. 6—Simulation-model relative permeabilities, total mobility, and graphical view of grid with oil saturation (SOIL) colored (Case 2 shown at the end of forecast).

Windalia Well 1 is discussed in Haynes et al. (2013). The production well is completed in the low-permeability Windalia reservoir, which has been waterflooded since the 1960s. The reservoir is located on Barrow Island, Australia. A description of this field is given along with reservoir properties by O'Reilly et al. (2016a). Average permeability and porosity are 5.7 md and 28%, respectively. The production data shown in Fig. 8 demonstrate a change in the field operating conditions. In the early part of production (10 to 1,000 days), total liquid rate declines because of the depletion caused by unequal voidage replacement. After this time, injection increased and a conformance enhanced-oil-recovery pilot began at the injection wells. This is shown as a rapid uplift in production rates in the q_{Dd} vs. t_{Dd} chart in Fig. 8 (top left), where the final liquid rate lies on the $q_{Dd,\mathrm{inj}} = 1$ curve. Because wells in this field are on patterns of either 20 or 40 acres, the large r_{eD}-value interpreted here is appropriate.

Alternative type-curve charts are also shown for the Windalia well in Fig. 8 and for all other examples. The bottom two diagrams in Fig. 8 use the production-decline integral q_{Ddi} (Eq. 9). Using this method, the data have been smoothed and the results are much easier to visualize on the decline charts. The response of a waterflood also takes longer to fully conclude on the decline integral charts.

For the second example, oil production from the Clyde Cowden lease [with further data available in Fetkovich et al. (1987)] is shown in Appendix C, Fig. C-1. This lease is part of the Goldsmith Field in Ector County, Texas, USA. In the Fetkovich et al. (1987) case study paper, it is noted that production from this field was first driven by primary depletion, and approximately 10 years later the reservoir was supplemented with water injection. It is clear from the analysis that the production wells were not receiving effective injection support equal to their original flow capacity; the matched stem of $q_{Dd,\mathrm{inj}} = 0.2$ shows this. This field would have benefited from additional water injection if it were possible. Because oil production was charted for this example rather than total liquid rate (which was not available), the steep decline in production toward the end can be attributed to the rising water cut.

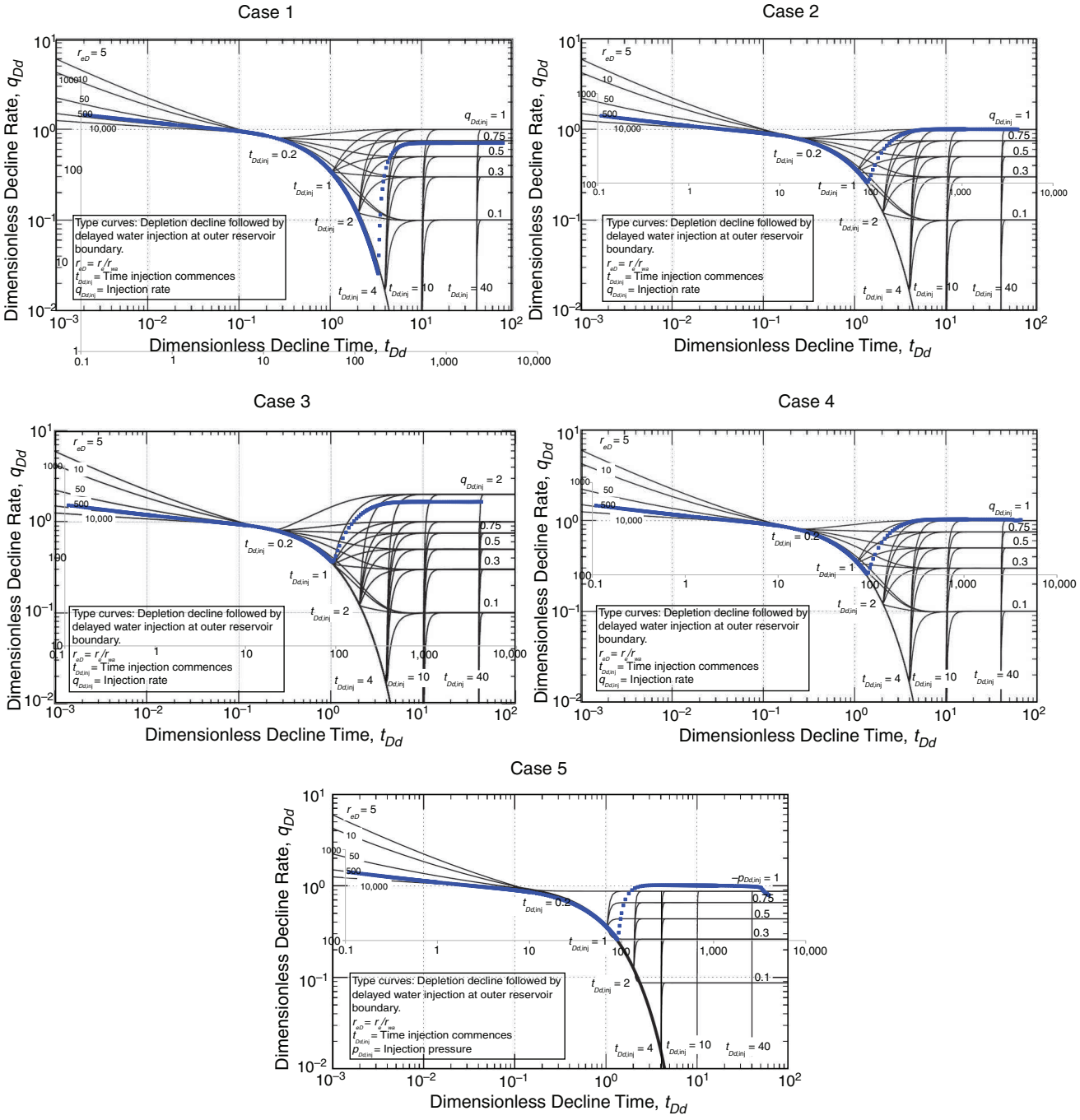

Fig. 7—(a) Simulation results (blue points) overlaid on constant-rate injection type curves (q_{Dd} vs. t_{Dd}). Cases 1 through 4 plotted. (b) Simulation results (blue points) overlaid on constant-pressure-injection type curve (q_{Dd} vs. t_{Dd}). Case 5 plotted.

Production history from the next two wells, TF 1 and PL 3, were taken from Delamaide (2018). The oil-rate match for these wells are shown in Appendix C, Figs. C-2 and C-3. These Canadian wells were drilled horizontally into heavy-oil reservoirs, and supported by a waterflood delayed from the initial depletion period. Although our type curves have been generated for the vertical well case, the match with the curve is still reasonable. Both wells show an excellent response to the waterflood event. In PL 3, it appears that the $q_{Dd,\mathrm{inj}}$ value is greater than unity, indicating excess pressure support.

The next example is the total field decline from the Sunset Triassic A Oil Field (Ambastha and Wong 1998) located in western Canada. The oil-rate data are shown with type curves in Fig. C-4. Although it seems that injection support started very quickly in Fig. C-4, the production data are a segment taken from later in the field's history. Similar to the previous well, this case shows excellent pressure support during this period, with the final $q_{Dd,\mathrm{inj}}$ between 1 and 2. Part of the declining effect at the end of these data might be caused by an increasing water/oil ratio. In an ideal case, total liquid rate should be used for these charts, but because this was unavailable, the oil-rate chart still provides insight.

The final example is Emmons Well 101 (Doublet and Blasingame 1995), shown in Fig. C-5. This well is drilled in the South Cowden Oil Field in Ector County, Texas, USA. Doublet and Blasingame (1995) also analyzed this well in their paper and noted that its erratic production performance is resolved by using the decline-rate integral function. This is also obvious on our type curves shown in Fig. C-5. It is noted that some of the irregular production rates were caused by formation damage and operational events (e.g., well plugging and cleanouts). Despite this, there is a clear pressure-support effect on the well, and a $q_{Dd,\mathrm{inj}}$ value of 0.3 was selected according to the integral charts.

	Windalia Well 1	Clyde Cowden	TF 1	PL 3	Sunset Triassic A	Emmons Well 101
Type	Well	Field	Well	Well	Field	Well
r_{eD}	5,000	1,000	50	≈500	50	10
$t_{Dd,\text{inj}}$	0.5	1.5	2	1.5	0.2	2
$q_{Dd,\text{inj}}$	1	0.2	0.5	2	2	0.3
$(q)_{MP}/(q_{Dd})_{MP}$	300 BLPD	3,300 BOPD	50 BOPD	55 BOPD	5,000 BOPD	100 BOPD
$(t)_{MP}/(t_{Dd})_{MP}$ (days)	2,500	2,000	450	500	3,300	2,500
Figure	Fig. 8	Fig. C-1	Fig. C-2	Fig. C-3	Fig. C-4	Fig. C-5
Reference	Haynes et al. (2013)	Fetkovich et al. (1987)	Delamaide (2018)	Delamaide (2018)	Ambastha and Wong (1998)	Doublet and Blasingame (1995)

Table 3—Results from type-curve matching of waterflood field case studies. BLPD = barrels of liquid per day; BOPD = barrels of oil per day.

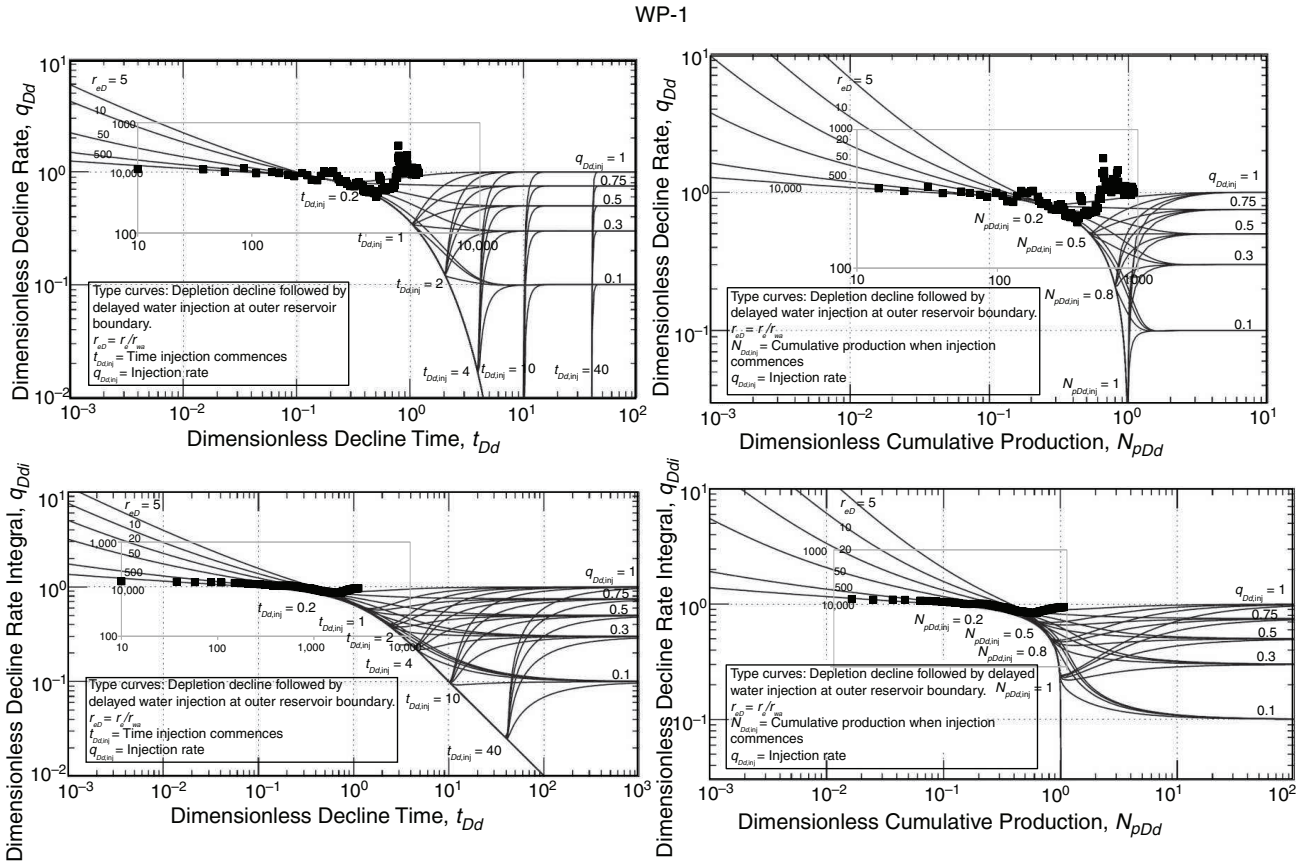

Fig. 8—Type-curve matches for Windalia Well 1 (Haynes et al. 2013). Total liquid rate (in BLPD) is plotted in black points.

The preceding cases have all been provided with quantitative dimensionless match parameters in Table 3 that can be used to ascertain further reservoir properties according to the production history. In many of the examples, a reasonable fit between field data and the type curves is observed, and this can also be considered as validation of the underlying theory.

Production-Forecasting Examples

A secondary application of the theory in this paper is production forecasting for fields when either primary, secondary, or even no production history is available. Two cases of production forecasting using the analytical model will be shown in the following subsections, where the model is used in a predictive way. The first example is for water injection into a single-layer reservoir and the second example is a two-layer reservoir.

Single-Layer Reservoir Example (S Carrabba Well 225). In this example, a well-penetrating single-layer reservoir is studied (S Carrabba Well 225). The reservoir properties for this well are given in **Table 4.** This information and the production history are taken from Doublet et al. (1994). The full history of the well is shown with red markers in **Fig. 9.** These data have been matched with a resulting $r_{eD} = 798$ outer radius. The production history of this well ends at approximately 400 days.

After the production history ends, with $t_{\text{inj}} = 500$ days, a forecast has been generated for 750 RB/D of water injection at the outer radius. The analytical model is shown as the solid lines in the graph; the black line is total liquid rate. After approximately 1,000 days, the model predicts that steady-state liquid production is obtained. After the water injection began, the Buckley and Leverett (1942)

model for water cut is used to separate the oil-rate (red) and water-rate (blue) curves. In the frontal advance theory, the travel velocity of each saturation in a radial system is expressed as

$$r\frac{dr}{dt}\bigg|_{S_w} = \alpha\frac{q_{\text{inj}}}{2\pi\phi h}\frac{df_w}{dS_w}\bigg|_{S_w} . \qquad (16)$$

Property	S Carrabba Well 225 (Fig. 9)	Multilayer Well (Fig. 10)
Permeability, k (md)	0.54	Layer 1: 2.5; Layer 2: 10
Porosity, ϕ (p.u.)	0.05	Layer 1: 0.20; Layer 2: 0.25
Layer thickness, h (ft)	300	Layer 1: 200; Layer 2: 100
Total compressibility, c_t (1/psi)	2.1×10^{-5}	2.0×10^{-5}
Wellbore radius apparent, r_{wa} (ft)	0.68	0.75
Outer reservoir radius, r_{eD}	798	700
Oil viscosity, μ_o (cp)	0.45	0.7
Oil FVF, B_o (RB/STB)	1.35	1.1
Initial pressure, p_i (psi)	3,326	1,000
Producer FBHP, p_{wf} (psi)	650	100

Table 4—Reservoir properties for production-forecasting examples.

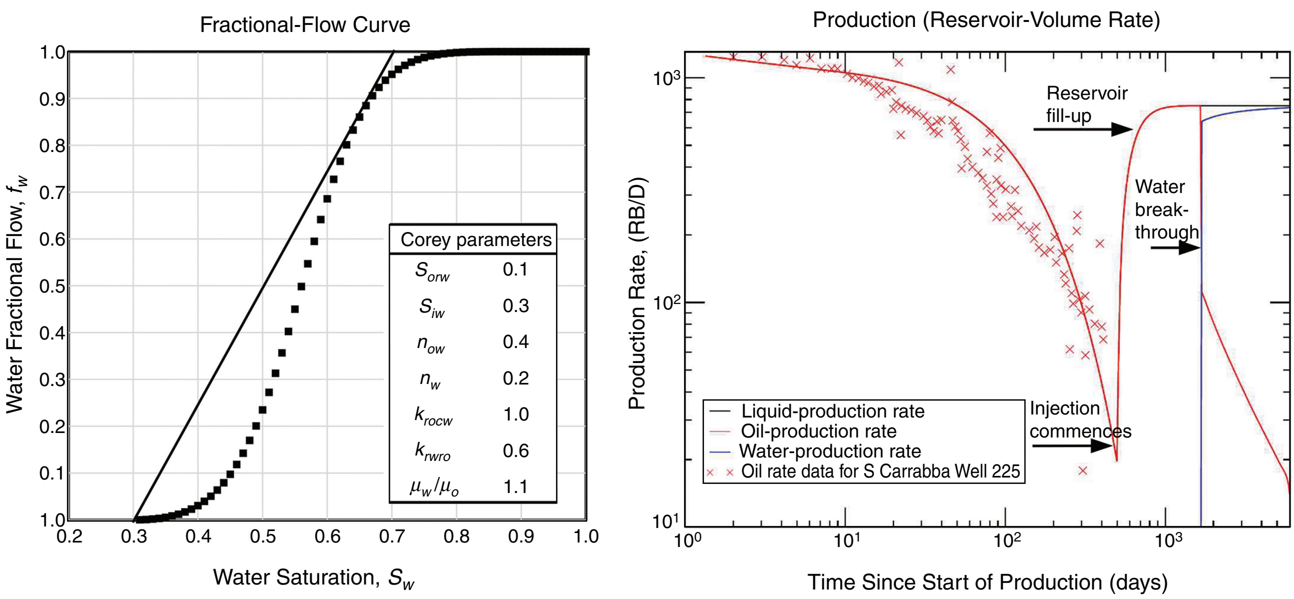

Fig. 9—Forecasting example for S Carrabba Well 225 [field data from Doublet et al. (1994)]. (Left) Fractional-flow curve for water/oil (inset shows Corey model parameters). (Right) Production forecast generated by the current model with fractional flow included.

By integrating, it is possible to determine the relationship between saturation and time at a particular radius,

$$t(S_w) = \frac{\pi\phi h}{\alpha q_{\text{inj}} f'_w(S_w)}\left(r_e^2 - r^2\right). \qquad (17)$$

$r = r_w$ is substituted in Eq. 17 to calculate fractional flow at the wellbore. Water fractional flow is here defined as

$$f_w = \frac{1}{1 + \dfrac{k_{ro}}{k_{rw}}\dfrac{\mu_w}{\mu_o}}. \qquad (18)$$

The fractional-flow curve used is shown in Fig. 9. A modified Brooks-Corey model has been used (Lake 1989; Goda and Behrenbruch 2004). Data from an analogous formation have been used as a guide when constructing the curve (Shenawi and Wu 1994).

Using the Buckley-Leverett displacement model, water breakthrough is predicted at $t = 1{,}670$ days. Because this model includes no vertical or areal heterogeneity, the breakthrough is sudden. Other effects such as gravity, viscous fingering, and capillary pressure are also not included.

In summary, Fig. 9 shows how the full rate-transient model can be applied to obtain a liquid-rate forecast for an oil well with known properties. An oil-cut model has been subsequently applied to the result. In the case that the waterflood has already started and fractional-flow production history is available, other oil-cut models can be used (Baker et al. 2003; Gentil 2005).

Multilayered Reservoir Example. DCA has previously been studied for multilayer or stratified reservoirs for reservoirs with little or no pressure support (Fetkovich 1980; Fetkovich et al. 1990; Cheng et al. 2008; Luo et al. 2011; Jongkittinarukorn et al. 2020). No reservoir crossflow between layers is assumed. From these and other references, it is not clear how the problem of water injection or aquifer support would be approached using the empirical Arps (1945) method. However, the technique in this paper should be amenable for use with multilayer reservoirs without interlayer crossflow.

A production well penetrating more than one zone imposes a common datum bottomhole pressure across all the connected zones. The same condition obviously applies to injection wells, which in our case is modeled as a flux spread evenly across r_e.

For this physical situation to apply to the current model, the constant-pressure injection solution can be used for all layers. Once a common inner- and outer-boundary pressure (p_{wf} and p_e) are applied across all the layers, the production rates from all layers are simply summed to calculate total well production. For a two-layer model, this results in

$$q(t) = q_{\text{Layer 1}}(t) + q_{\text{Layer 2}}(t). \quad (19)$$

Eq. 19 applies during all flow periods (transient, boundary-depletion dominated, and during the injection response), provided that the boundary conditions are applied consistently across the layers.

A synthetic two-layer example of this has been constructed with reservoir properties shown in Table 4. In this example, Layer 1 has a lower reservoir quality of $k = 2.5$ md and $\phi = 0.20$. For Layer 2, $k = 10$ md and $\phi = 0.25$. A common FBHP of 100 psi is set at the well and water injection starts after 60 days of depletion. The injector FBHP is set at $p_e = 1{,}000$ psi for both layers, which is the original reservoir pressure.

The model forecast for this example is shown in **Fig. 10.** It is interesting to see that the higher-quality layer (Layer 2) initially contributes the larger portion or production, but by 60 days has declined to a rate lower than the poorer-quality layer. When injection starts, the Layer 2 production rate rapidly increases to previous levels, while Layer 1 production restores more slowly.

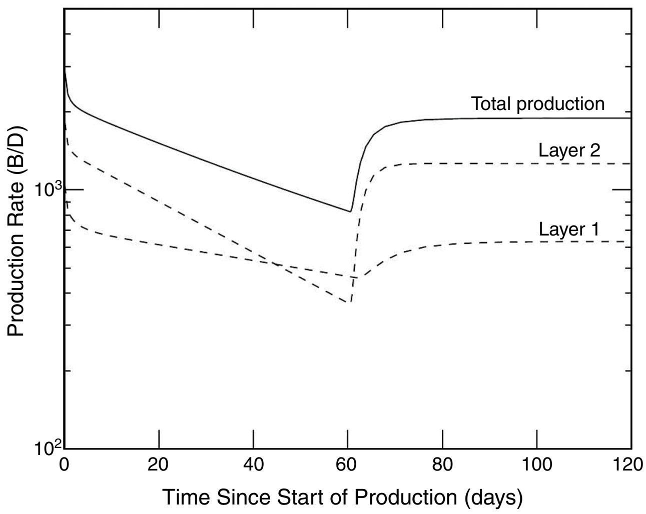

Fig. 10—Forecasting exampled for multilayer/stratified reservoir (total liquid rate shown). Layer properties given in Table 4.

Discussion

In this paper, we have proposed an extension of the RTA theory to account for the effect of water injection at the outer boundary of the reservoir. The model has been applied to numerical simulation and field cases with some success. Certain simplifications were made in this model and the associated implications will be highlighted.

Overall, the mathematical model comprises a cylindrical reservoir where slightly compressible liquid is withdrawn evenly from the inner radius and the same fluid is replenished evenly across the outer radius (Fig. 1). Constant p_{wf} production is assumed at $t = 0$, and the constant-rate or constant-pressure outer-boundary conditions are used for injection starting at $t = t_{\text{inj}}$. The application of the type curves is theoretically constrained to these production, injection, and geometrical assumptions, and in practice wells might not always be operated in this fashion. Nevertheless, the real field data show a similar form to the type curves. Single-phase liquid flow is a further limitation of the mathematical model that has only been addressed to some extent. Situations with large saturation gradients within the reservoir or mass transfer between phases will not be adequately covered by the model. A more detailed description of some of these limitations will now be given.

Multirate Injection Effects and Multiple Wells. Strictly speaking, the theory in this paper only applies to depleted fields where water injection starts instantaneously and is continuously held at a constant rate or pressure. There are many cases operationally where this does not happen, and injection rates can start and then vary drastically over time. It would be possible to use superposition with the boundary-injection solution in Appendix A, $q^{\text{inj-q}}$, to account for this over time. However, the primary intent of this paper was to provide fast, usable type curves that can be used for simple diagnostics and interpretation of waterfloods. For the analysis of long-term highly variable data, CRM might be more appropriate. Different methods of analysis should be used where they are considered appropriate.

For fields with multiple production and injection wells, the present theory does not currently easily allow for allocation of liquids to particular injectors, because only a single flux is assumed at the outer boundary of the production well. However, it is still possible to ascertain the total injection support for a producer using the model. The theory has also been developed assuming a vertical production well, but showed reasonable agreement with examples of horizontal wells (Appendix C, Figs. C-2 and C-3).

Multiphase Flow. The derivations for the liquid-flow theory assumed a unit-mobility ratio between fluids. Two-phase flow was accounted for by applying the Martin-Perrine theory (Perrine 1956; Martin 1959) during the initial transient depletion-decline period and by assuming that a steady condition is obtained quickly after the onset of injection. This raises the question of the time before steady-state attainment and the possibility of a slow-moving fluid bank during the longer-term flow period, which is not modeled in the homogeneous reservoir model in this paper.

Extensive work is currently being undertaken by other authors in the area of multiphase RTA. In spite of this attention, most of the issues relate to the depletion of unconventional fields rather than immiscible displacement. Pseudopressure and pseudotime are commonly used to linearize the multiphase diffusivity equation, converting it to a similar format to Appendix A, Eq. A-1. Raghavan (1989) discussed the use of the pseudopressure for multiphase-pressure-buildup surveys and also some implications of multiphase flow on DCA. More recently, Uzun et al. (2016) have used ideas very similar to the Martine-Perrine theory to model all phases in unconventional RTA. More complicated multiphase RTA models use both pseudopressure/time (Zhang and Emami-Meybodi 2020), or alternative solutions to the diffusivity equation using the Boltzmann transform (Hamdi et al. 2020).

Straightforward pseudogroups for time-dependent permeability, sharing some similarity with the problem at hand, were proposed by Lee (2003). Extending these ideas to incorporate the time dependencies of immiscible displacement would provide additional depth to our theory.

Finally, Simulation Cases 2 through 4 studied earlier in this text used a mobility ratio of 0.76. Despite this difference from the unit-mobility-ratio assumption in derivations, the form of the total-liquid-production decline matched the type curves reasonably well. Nevertheless, future work should consider the effect of a broader range of fluid and rock properties, including heterogeneity and other factors, on the match obtained from type-curve analysis. This extends beyond multiphase effects and should also incorporate other nonlinear effects included in complex reservoir-simulation models.

Comparison with the CRM Method. As discussed previously, CRM is a modern tool for rapid history matching of production data in waterflooded fields and is also used for oil-production-optimization problems. It is worth highlighting the differences between our method and CRM. Several different formulations exist; our discussion refers to the model in Liang et al. (2007). Two main parameters are matched in CRM when calculating total liquid production from multiple wells: the lumped time constant, $\tau_j = c_t V_p / J_j$, for the area around a production well j, and the fraction of injector i's water injected that enters the area around production well j, denoted Λ_{ij}.

Clearly our method does not allow for the matching of multiple producer- and injector-well rates, as already mentioned. The CRM terms form part of the governing differential equation, which is based on a 0D control volume surrounding each producer. For a production well held at steady FBHP, and injectors each held at a constant injection rate, I_i,

$$q_j(t) = \sum_{i=1}^{m} \Lambda_{ij} I_i - \tau_j \frac{dq_j}{dt}. \quad (20)$$

It is possible to rearrange the solution to Eq. 20 and express it in terms of dimensionless groups used in our paper (see Nomenclature), to place it in an equivalent form for comparison. The solution to the CRM Eq. 20 for a single injector well is, in terms of our variable system,

$$q_D(t_D) = \frac{\exp\left(-\frac{2t_D}{r_{eD}^2}\frac{1}{\ln r_{eD} - 3/4}\right)}{\ln r_{eD} - \frac{3}{4}} + q_{D,\mathrm{inj}}\left[1 - \exp\left(-\frac{2\Delta t_D}{r_{eD}^2}\frac{1}{\ln r_{eD} - 3/4}\right)\right]. \quad (21)$$

This format allows for a direct comparison with our method because a single injector is also assumed here. There are two terms in the solution. The first represents boundary-dominated depletion and does not include transient effects. This term is identical to the exponential decline in Fetkovich (1980) and Raghavan (1989). The second term represents the influence of the injector on total production rate, and also follows an exponential form.

Put simply, fitting production data to the CRM solution (Eq. 21) would only match the reservoir size, r_{eD}, and injection into the area, $q_{D,\mathrm{inj}}$. This is because the transient period is neglected in the 0D model. Using the RTA method proposed in this paper would also recover one additional unknown term during the transient period: mechanical skin, s. **Fig. 11** compares the depletion and injection solutions from the CRM solution (Eq. 21) with RTA solutions from this work. The difference between curves is caused by transient effects. Both methods clearly have strengths and weaknesses.

Comparison with the Doublet and Blasingame (1995) Type Curves. It is useful to compare the present method with the original work of Doublet and Blasingame (1995), which was also developed for waterflooded or aquifer-supported fields. Their unique study is one of the first we are aware of to tackle this problem. Despite having similar goals, our method is different in nature and possesses some improvements. The most fundamental difference between type curves lies in the treatment of injection at the outer boundary. In our work, injection is held at either constant rate or constant pressure, which is probably most appropriate for the waterflood problem. In Doublet and Blasingame (1995), injection is treated as a voidage-replacement-ratio (VRR) value that continually tracks the rate at the production well according to the target ratio. This marks the first difference in the approaches. In their paper, a pressure solution is first given to the problem of constant-rate production,

$$\overline{p}_{wD}(u) = \frac{1}{u\sqrt{u}}\left[\frac{K_0(\sqrt{u})I_1(r_{eD}\sqrt{u}) + K_1(r_{eD}\sqrt{u})I_0(\sqrt{u})}{K_1(\sqrt{u})I_1(r_{eD}\sqrt{u}) - I_1(\sqrt{u})K_1(r_{eD}\sqrt{u})} - q_{D\mathrm{inj}}^{\mathrm{VRR}}\frac{e^{-t_{D\mathrm{inj}}u}}{r_{eD}}\frac{K_0(\sqrt{u})I_1(\sqrt{u}) + K_1(\sqrt{u})I_0(\sqrt{u})}{K_1(\sqrt{u})I_1(r_{eD}\sqrt{u}) - I_1(\sqrt{u})K_1(r_{eD}\sqrt{u})}\right]. \quad (22)$$

The solution is then converted to the constant-pressure-production problem required for rate-decline type curves by use of

$$\overline{q}_D(u) = \frac{1}{u^2\overline{p}_{wD}(u)}. \quad (23)$$

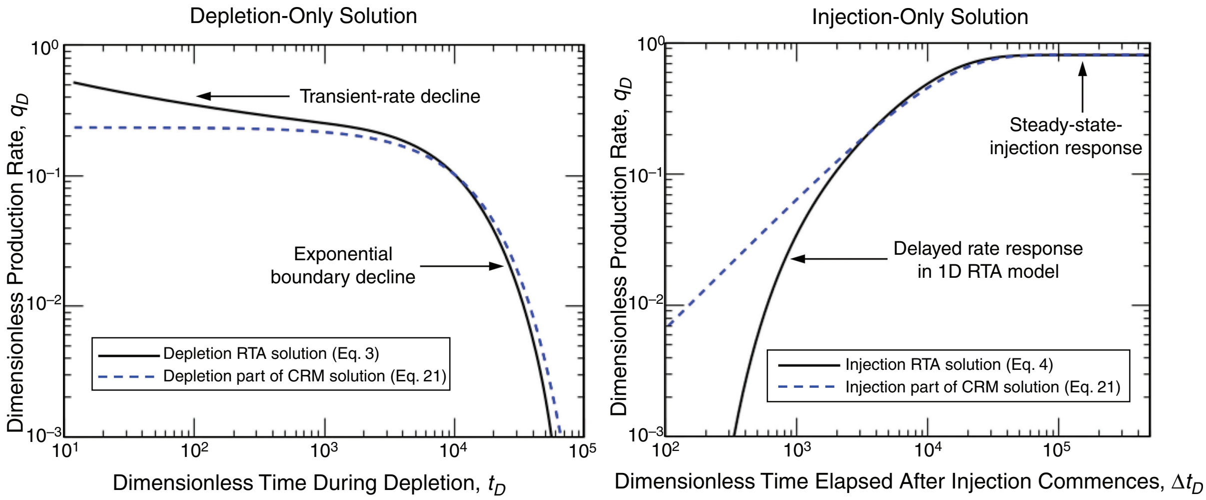

Fig. 11—Production rates from CRM solution vs. the RTA solutions. Note that the individual equations for depletion and injection have been charted separately (i.e., no prior production effects occur in the right-hand-side chart).

Eqs. 22 and 23 form the Doublet and Blasingame (1995) method for constant voidage ratio $q_{D\mathrm{inj}}^{\mathrm{VRR}}$ starting at time $t_{D\mathrm{inj}}$. A comparison of our method with the type curves developed in their paper is shown in **Fig. 12.**

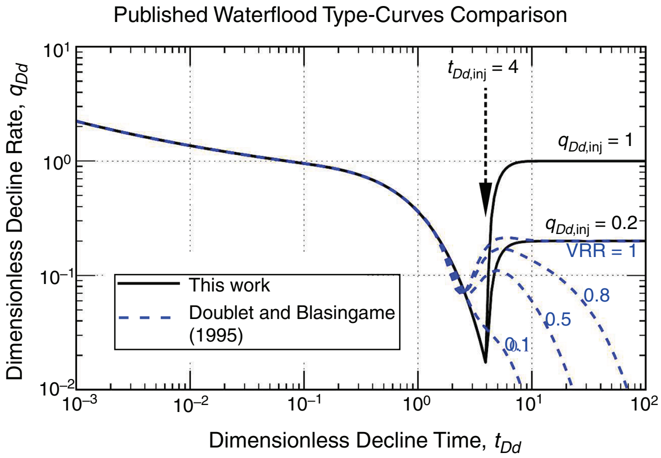

Fig. 12—Comparison of current method with Doublet and Blasingame (1995) curves (a partial set of type curves is shown for injection starting at $t_{Dd,\mathrm{inj}} = 4$).

In Fig. 12, injection starts in all type curves at $t_{Dd,\mathrm{inj}} = 4$. The difference between the steady-state injection of the present method and the VRR approach is clear. Unfortunately, because of problems that the Stehfest (1970) algorithm faces when numerically inverting functions with discontinuities, their type curves contained an artifact just before the initial injection time. The difficulty of inversion into the real domain lies in the exponential term in Eq. 22. Despite this issue, the Doublet and Blasingame (1995) type curves still remain very usable for actual production analysis. The new equations in this paper do not face this issue.

It is possible to show in the Doublet and Blasingame (1995) method that for the steady-state case (i.e., $q_{D\mathrm{inj}}^{\mathrm{VRR}} = 1.0$), production stabilizes at the rate

$$\lim_{t_D \to \infty} q_D(t_D) = \frac{2(r_{eD}^2 - 1)}{1 - r_{eD}^2 + 4t_{D\mathrm{inj}} + 2r_{eD}^2 \ln(r_{eD})}. \qquad (24)$$

This relation was not originally given in their paper and provides some insight into the shape of their type curves and the terminal steady-state rate for a given injection-start time. Eq. 24 shows that at late times of injection start, it is not possible in their model to obtain large stabilized production rates at the inner well, and the maximum limiting value is given by this equation. In Fig. 12, it is seen that the maximum rate obtained when setting VRR = 1.0 is $q_{Dd,\mathrm{inj}} = 0.2$ in their model. This is because reservoir pressure has already declined before the equal voidage replacement starts. In our model, it is possible to achieve any target production rate at the well because any injection rate can be prescribed at the outer boundary. Several of the field studies showed that this is certainly possible in practice, and highlights a limitation of the previous type curves.

Finally, in our paper we have also solved the problem of constant-pressure injection at the outer boundary (Eq. 5), which was listed as further work in the original Doublet and Blasingame (1995) text.

Rate/Pressure Normalization and Material-Balance Time in RTA. One topic not yet discussed is the application of pressure-normalized rate or rate-normalized pressure to the developed RTA theory. This practice is common in RTA analysis to account for

variable FBHP and rate in production data (Winestock and Colpitts 1965; Doublet et al. 1994; Clarkson and Pedersen 2010). These plotting groups have not been tested as part of this project. However, the depletion portion of the waterflood type curve (see Fig. 4) is definitely suited to pressure-normalized-rate adjusted production data because these curves are the same as the Fetkovich (1980) decline curves for the exponential case, for which the practice is already accepted. After steady-state injection is obtained for the production data, the pressure-normalized-rate method will also work. During the transition period between depletion decline and steady-state injection support, we have not tested the production-data-adjustment methods, but expect it would also be allowable for most of this time region.

Material-balance time is another plotting method used in RTA, the basis of which is derived from the boundary-dominated depletion period (Blasingame et al. 1991; Palacio and Blasingame 1993). Although this time-adjustment method is effective for bounded reservoirs without pressure support, it should not be used with the waterflood type curves without adjustment for injection. The introduction of external pressure support invalidates the assumption of a closed boundary. Options are available for use in this area, but they have not been explored as part of this paper.

Conclusions

The details of an RTA model tailored toward waterflooded fields have been provided in this paper, along with applications to field cases and production forecasting. The following conclusions are given as a result of this work:

1. The developed RTA model was solved analytically for unit-mobility-ratio displacement and extended to two phases through the use of the Martin-Perrine well-testing theory. Five reservoir-simulation examples assisted with validating the analytical model.
2. Multiple type-curve formats are available for reservoir-property interpretation. It is anticipated that Fig. 4 (log-log q_{Dd} vs. t_{Dd} chart) for the constant-rate injection case will be the most useful chart for engineers. Other integral formats are available for data sets containing a large amount of noise.
3. The type curves can be used to characterize the strength (q_{inj}) and type of water injection (constant-rate or constant-pressure injection, depending on the steepness of the response at the production well), in addition to the usual reservoir parameters from RTA.
4. Several waterflood field case studies have been presented. After taking into account data scatter, many of the cases follow the form of the type curves and allow interpretation of reservoir properties.
5. Injection into stratified reservoirs should be modeled using constant-pressure injection at the boundary rather than constant-rate injection. An example has been provided (Fig. 10). This type of forecast cannot be generated using existing RTA/DCA techniques.
6. To gain a complete appreciation of rate performance, total liquid rate should be used with the type curves. If only oil-rate data are available, the curves still have some diagnostic utility.

Nomenclature

A = area of reservoir, L^2, acres
B = fluid FVF factor, L^3/L^3, RB/STB
c_1, c_2 = unknowns solved during derivations
c_t = reservoir total compressibility, Lt^2/m, 1/psi
f_w = fractional flow of water
f'_w = derivate of water fractional flow with saturation
h = reservoir thickness, L, ft
I_0, I_1 = modified Bessel functions of the first kind
I_i = CRM model term, injector i flow rate, L^3/t, STB/D
J_j = CRM model term, productivity index of production well j, L^4t/m, (STB/D)/psi
k = permeability, L^2, md
k_r = relative permeability
k_{rocw} = endpoint oil relative permeability
k_{rwro} = endpoint water relative permeability
K_0, K_1 = modified Bessel functions of the second kind
n_{ow} = oil Corey exponent
n_w = water Corey exponent
N_{pDd} = cumulative production (using dimensionless decline group)
p = pressure, m/Lt^2, psi
p_D = dimensionless pressure, $p_D = (p_i - p)/(p_i - p_{wf})$ for depletion and constant-rate-injection solutions, or $= p_D = (p_{wf} - p)/(p_i - p_{wf})$ for the constant-pressure injection solution
p_{D0} = initial pressure distribution used for nonhomogeneous solution
$p_{D,\text{inj}}$ = dimensionless pressure applied to external reservoir boundary by injection well
$p_{e,\text{inj}}$ = pressure at the external reservoir boundary, m/Lt^2, psi
$p_{e,\text{inj}}$ = pressure applied to external reservoir boundary by injection well, m/Lt^2, psi
p_i = initial reservoir pressure, m/Lt^2, psi
p_{wf} = sandface flowing wellbore pressure, m/Lt^2, psi
q = production rate from inner well (positive number), L^3/t, STB/D
q_D = dimensionless production rate, $q_D = 141.2qB\mu/kh/(p_i - p_{wf})$
q_{Dd} = dimensionless decline production rate at inner well
q_{Ddi} = dimensionless decline integral production rate at inner well
$q_{D,\text{inj}}$ = dimensionless injection rate at external reservoir boundary
q_{inj} = injection rate at outer-boundary radius (positive number), L^3/t, STB/D
$q_{D\text{inj}}^{\text{VRR}}$ = dimensionless injection VRR at external boundary, Doublet and Blasingame (1995) method
q^{depl} = production at wellbore caused by primary depletion, L^3/t, STB/D
$q^{\text{inj-p}}$ = production at wellbore corresponding to constant-pressure injection at outer boundary (solution uses nonuniform initial reservoir pressure), L^3/t, STB/D
$q^{\text{inj-q}}$ = production at wellbore corresponding to constant-rate injection at outer boundary (solution uses uniform initial reservoir pressure), L^3/t, STB/D

r = radius, L, ft
r_D = dimensionless radius, $r_D = r/r_w$
r_e = external reservoir radius, L, ft
r_{eD} = dimensionless external reservoir radius
r_w = wellbore radius, L, ft
r_{wa} = wellbore radius apparent, $r_{wa} = r_{we} - s$ (includes effect of mechanical skin), L, ft
s = mechanical skin factor
S = saturation of phase
S_o = oil saturation
S_{oi} = initial saturation of oil
S_{orw} = residual oil saturation
S_w = water saturation
S_{wi} = initial saturation of water
t = time, t, hours
t' = integration variable
t_D = dimensionless time, $t_D = 0.0002637$ kt/($\phi\mu c_t r_w^2$)
$t_{D,\text{inj}}$ = dimensionless time at commencement of injection
t_{inj} = time at start of injection at outer boundary, t, hours
u = Laplace variable
v_1, v_2 = unknowns solved during derivations
V_p = CRM model term, pore volume, L^3, STB
W = Wronskian matrix
α = unit-conversion factor used in frontal advance equation, $\alpha = 4.275$ STB/D/(ft^3/hr)
Δt = $\Delta t = t - t_{\text{inj}}$, t, hours
λ = fluid mobility, $\lambda = k/\mu$, L^3t/m, md/cp
Λ_{ij} = CRM model term, fraction of injector i's rate allocated to production well j
μ = fluid viscosity, m/Lt, cp
ξ = integration variable
τ_j = CRM model term, time constant for production well j
ϕ = porosity, L^3/L^3
$\mathcal{L}$ = Laplace transform
$\bar{}$ = bar indicates Laplace transform

Subscripts

D = dimensionless
i = initial
MP = match point
o = oil
w = water
t = total liquid

Acknowledgments

The authors would like to thank management at Chevron Australia Pty Ltd. for permission to publish this paper and the anonymous peer reviewers for their useful suggestions. Author D. O'Reilly would like to thank Tom Blasingame for helpful discussions.

References

Ali, T. A. and Sheng, J. J. 2015. Production Decline Models: A Comparison Study. Paper presented at the SPE Eastern Regional Meeting, Morgantown, West Virginia, USA, 13–15 October. SPE-177300-MS. https://doi.org/10.2118/177300-MS.

Ambastha, A. K. 1989. *Pressure Transient Analysis for Composite Systems*. Technical report, Stanford Petroleum Institute, Stanford University, Stanford, California, USA (October 1988).

Ambastha, A. K. and Wong, K. H. 1998. Decline Curve Analysis for Canadian Oil Reservoirs under Waterflood Conditions. *J Can Pet Technol* **37** (1): 20–26. PETSOC-98-01-04. https://doi.org/10.2118/98-01-04.

Arps, J. J. 1945. Analysis of Decline Curves. In *Transactions of the Society of Petroleum Engineers*, Vol. 160, Part 1, 228–247, SPE-945228-G. Richardson, Texas, USA: SPE.

Baker, R. O., Anderson, T., and Sandhu, K. 2003. Using Decline Curves To Forecast Waterflooded Reservoirs: Fundamentals and Field Cases. Paper presented at the Canadian International Petroleum Conference, Calgary, Alberta, Canada, 10–12 June. PETSOC-2003-181. https://doi.org/10.2118/2003-181.

Blasingame, T. A., Johnston, J. L., and Lee, W. J. 1989. Type-Curve Analysis Using the Pressure Integral Method. Paper presented at the SPE California Regional Meeting, Bakersfield, California, USA, 5–7 April. SPE-18799-MS. https://doi.org/10.2118/18799-MS.

Blasingame, T. A., McCray, T. C., and Lee, W. J. 1991. Decline Curve Analysis for Variable Pressure Drop/Variable Flowrate Systems. Paper presented at the SPE Gas Technology Symposium, Houston, Texas, USA, 23–24 January. SPE-21513-MS. https://doi.org/10.2118/21513-MS.

Bratvold, R. B. and Horne, R. N. 1990. Analysis of Pressure-Falloff Tests Following Cold-Water Injection. *SPE Form Eval* **5** (3): 293–302. SPE-18111-PA. https://doi.org/10.2118/18111-PA.

Buckley, S. E. and Leverett, M. C. 1942. Mechanism of Fluid Displacement in Sands. In *Transactions of the Society of Petroleum Engineers*, Vol. 146, Part 1, 107–116, SPE-942107-G. Richardson, Texas, USA: SPE.

Carter, R. D. and Tracy, G. W. 1960. An Improved Method for Calculating Water Influx. In *Transactions of the Society of Petroleum Engineers*, Vol. 219, Part 1, 415–417, SPE-1626-G. Richardson, Texas, USA: SPE.

Cheng, Y., Lee, W. J., and McVay, D. A. 2008. Improving Reserves Estimates from Decline-Curve Analysis of Tight and Multilayer Gas Wells. *SPE Res Eval & Eng* **11** (5): 912–920. SPE-108176-PA. https://doi.org/10.2118/108176-PA.

Clarkson, C. R. and Pedersen, P. K. 2010. Tight Oil Production Analysis: Adaptation of Existing Rate-Transient Analysis Techniques. Paper presented at the Canadian Unconventional Resources and International Petroleum Conference, Calgary, Alberta, Canada, 19–21 October. SPE-137352-MS. https://doi.org/10.2118/137352-MS.

de Holanda, R. W., Gildin, E., Jensen, J. L. et al. 2018. A State-of-the-Art Review on Capacitance Resistance Models for Reservoir Characterization and Performance Forecasting. *Energies* **11** (12): 3368. https://doi.org/10.3390/en11123368.

Delamaide, E. 2018. Application of Conventional Forecasting Methods to Waterfloods with Horizontal Wells in Heavy Oil Reservoir. Paper presented at the SPE Annual Technical Conference and Exhibition, Dallas, Texas, USA, 24–26 September. SPE-191692-MS. https://doi.org/10.2118/191692-MS.

Doublet, L. E. and Blasingame, T. A. 1995. Decline Curve Analysis Using Type Curves: Water Influx/Waterflood Cases. Paper prepared for presentation at the SPE Annual Technical Conference and Exhibition, Dallas, Texas, USA, 22–25 October. SPE-30774-MS.

Doublet, L. E., Pande, P. K., McCollum, T. J. et al. 1994. Decline Curve Analysis Using Type Curves–Analysis of Oil Well Production Data Using Material Balance Time: Application to Field Cases. Paper presented at the Petroleum Conference and Exhibition, Veracruz, Mexico, 10–13 October. SPE-28688-MS. https://doi.org/10.2118/28688-MS.

Ehlig-Economides, C. A. 1979. *Well Test Analysis for Wells Produced at a Constant Pressure*. PhD dissertation, Stanford University, Stanford, California, USA.

Ehlig-Economides, C. A. and Ramey, H. J. 1981. Transient Rate Decline Analysis for Wells Produced at Constant Pressure. *SPE J*. **21** (1): 98–104. SPE-8387-PA. https://doi.org/10.2118/8387-PA.

Eleiott, A. C., Lee, W. J., and Moridis, N. 2019. Modified Fetkovich Type Curve Enhances Type Well Construction for Horizontal Wells with Multiple Fractures. Paper presented at the SPE/AAPG/SEG Unconventional Resources Technology Conference, Denver, Colorado, USA, 22–24 July. URTEC-2019-471-MS. https://doi.org/10.15530/urtec-2019-471.

Fetkovich, M. J. 1971. A Simplified Approach to Water Influx Calculations—Finite Aquifer Systems. *J Pet Technol* **23** (7): 814–828. SPE-2603-PA. https://doi.org/10.2118/2603-PA.

Fetkovich, M. J. 1980. Decline Curve Analysis Using Type Curves. *J Pet Technol* **32** (6): 1065–1077. SPE-4629-PA. https://doi.org/10.2118/4629-PA.

Fetkovich, M. J., Bradley, M. D., Works, M. D. et al. 1990. Depletion Performance of Layered Reservoirs without Crossflow. *SPE Form Eval* **5** (3): 310–318. SPE-18266-PA. https://doi.org/10.2118/18266-PA.

Fetkovich, M. J., Vienot, M. E., Bradley, M. D. et al. 1987. Decline Curve Analysis Using Type Curves—Case Histories. *SPE Form Eval* **2** (4): 637–656. SPE-13169-PA. https://doi.org/10.2118/13169-PA.

Gentil, P. B. 2005. *The Use of Multilinear Regression Models in Patterned Waterfloods: Physical Meaning of the Regression Coefficients*. MS thesis, University of Texas at Austin, Austin, Texas, USA.

Goda, H. M. and Behrenbruch, P. 2004. Using a Modified Brooks-Corey Model To Study Oil-Water Relative Permeability for Diverse Pore Structures. Paper presented at the SPE Asia Pacific Oil and Gas Conference and Exhibition, Perth, Australia, 18–20 October. SPE-88538-MS. https://doi.org/10.2118/88538-MS.

Hamdi, H., Behmanesh, H., and Clarkson, C. 2020. A Semianalytical Approach for Analysis of Wells Exhibiting Multiphase Transient Linear Flow: Application to Field Data. *SPE J*. **25** (6): 3265–3279. SPE-196164-PA. https://doi.org/10.2118/196164-PA.

Haynes, A. K., Clough, M. D., Fletcher, A. J. et al. 2013. The Successful Implementation of a Novel Polymer EOR Pilot in the Low Permeability Windalia Field. Paper presented at the SPE Enhanced Oil Recovery Conference, Kuala Lumpur, Malaysia, 2–4 July. SPE-165253-MS. https://doi.org/10.2118/165253-MS.

Izgec, O. and Kabir, C. S. 2010. Quantifying Nonuniform Aquifer Strength at Individual Wells. *SPE Res Eval & Eng* **13** (2): 296–305. SPE-120850-PA. https://doi.org/10.2118/120850-PA.

Jongkittinarukorn, K., Last, N., Escobar, F. H. et al. 2020. A New Decline-Curve-Analysis Method for Layered Reservoirs. *SPE J*. **25** (4): 1657–1669. SPE-195085-PA. https://doi.org/10.2118/195085-PA.

Kuchuk, F. J. and Wilkinson, D. J. 1991. Transient Pressure Behavior of Commingled Reservoirs. *SPE Form Eval* **6** (1): 111–120. SPE-18125-PA. https://doi.org/10.2118/18125-PA.

Lake, L. 1989. *Enhanced Oil Recovery*. Englewood Cliffs, New Jersey, USA: Prentice Hall.

Lee, H. J. 2003. Estimating Time-Dependent Reservoir Properties by Analyzing Long-Term Pressure Data. MS thesis, Stanford University, Stanford, California, USA.

Lee, J., Rollins, J. B., and Spivey, J. P. 2003. *Pressure Transient Testing*, Vol. 9. Richardson, Texas, USA: Textbook Series, Society of Petroleum Engineers.

Li, K., Ren, X., Li, L. et al. 2011. A New Model for Predicting Water Cut in Oil Reservoirs. Paper presented at the SPE EUROPEC/EAGE Annual Conference and Exhibition, Vienna, Austria, 23–26 May. SPE-143481-MS. https://doi.org/10.2118/143481-MS.

Liang, X., Weber, D. B., Edgar, T. F. et al. 2007. Optimization of Oil Production Based on a Capacitance Model of Production and Injection Rates. Paper presented at the SPE Hydrocarbon Economics and Evaluation Symposium, Dallas, Texas, USA, 1–3 April. SPE-107713-MS. https://doi.org/10.2118/107713-MS.

Luo, H., Mahiya, S., and Pannett, S. 2011. The Use of Rate Transient Analysis Modeling To Quantify Uncertainties in Commingled Tight Gas Production Forecasting and Decline Analysis Parameters in the Alberta Deep Basin. Paper presented at the Canadian Unconventional Resources Conference, Calgary, Alberta, Canada, 15–17 November. SPE-147529-MS. https://doi.org/10.2118/147529-MS.

Martin, J. C. 1959. Simplified Equations of Flow in Gas Drive Reservoirs and the Theoretical Foundation of Multiphase Pressure Buildup Analyses. In *Transactions of the Society of Petroleum Engineers*, Vol. 216, Part 1, 321–323, SPE-1235-G. Richardson, Texas, USA: SPE.

McCray, T. L. 1990. *Reservoir Analysis Using Production Decline Data and Adjusted Time*. MS thesis, Texas A&M University, College Station, Texas, USA.

Moreno, G. A. 2013. Multilayer Capacitance-Resistance Model with Dynamic Connectivities. *J Pet Sci Eng* **109** (September): 298–307. https://doi.org/10.1016/j.petrol.2013.08.009.

Oliver, D. S. 1990. The Averaging Process in Permeability Estimation from Well-Test Data. *SPE Form Eval* **5** (3): 319–324. SPE-19845-PA. https://doi.org/10.2118/19845-PA.

O'Reilly, D. I., Haghighi, M., Flett, M. A. et al. 2016b. Pressure and Rate Transient Analysis of Artificially Lifted Drawdown Tests Using Cyclic Pump Off Controllers. *J Pet Sci Eng* **139** (March): 240–253. https://doi.org/10.1016/j.petrol.2016.01.030.

O'Reilly, D., Hunt, A., Sze, E. et al. 2016a. Increasing Water Injection Efficiency in the Mature Windalia Oil Field, NW Australia, through Improved Reservoir Surveillance and Operations. Paper presented at the SPE Asia Pacific Oil and Gas Conference and Exhibition, Perth, Australia, 25–27 October. SPE-182339-MS. https://doi.org/10.2118/182339-MS.

Palacio, J. C. and Blasingame, T. A. 1993. Decline Curve Analysis Using Type Curves: Analysis of Gas Well Production Data. Paper presented at the Low Permeability Reservoirs Symposium, Denver, Colorado, USA, 12–14 April. SPE-25909-MS. https://doi.org/10.2118/25909-MS.

Perrine, R. L. 1956. Analysis of Pressure-Buildup Curves. *Drilling and Production Practice*, **1** January, New York, New York, USA, API-56-482.

Poston, S. W., Laprea-Bigott, M., and Poe, B. D. 2019. *Analysis of Oil and Gas Production Performance*. Richardson, Texas, USA: Society of Petroleum Engineers.
Raghavan, R. 1989. Well-Test Analysis for Multiphase Flow. *SPE Form Eval* **4** (4): 585–594. SPE-14098-PA. https://doi.org/10.2118/14098-PA.
Rasmussen, A. F., Sandve, T. H., Bao, K. et al. 2021. The Open Porous Media Flow Reservoir Simulator. *Comput Math Appl* **81** (1 January): 159–185. https://doi.org/10.1016/j.camwa.2020.05.014.
Sayarpour, M., Zuluaga, E., Kabir, C. S. et al. 2009. The Use of Capacitance-Resistive Models for Rapid Estimation of Waterflood Performance and Optimization. *J Pet Sci Eng* **69** (3–4): 227–238. https://doi.org/10.1016/j.petrol.2009.09.006.
Sayyafzadeh, M., Pourafshary, P., Haghighi, M. et al. 2011. Application of Transfer Functions To Model Water Injection in Hydrocarbon Reservoir. *J Pet Sci Eng* **78** (1): 139–148. https://doi.org/10.1016/j.petrol.2011.05.009.
Shenawi, S. H. and Wu, C. H. 1994. Compositional Simulation of Carbonated Waterfloods in Naturally Fractured Reservoirs. Paper presented at the SPE/DOE Improved Oil Recovery Symposium, Tulsa, Oklahoma, USA, 17–20 April. SPE-27741-MS. https://doi.org/10.2118/27741-MS.
Stehfest, H. 1970. Algorithm 368: Numerical Inversion of Laplace Transforms. *Commun ACM* **13** (1): 47–49. https://doi.org/10.1145/361953.361969.
Sun, H. 2015. *Advanced Production Decline Analysis and Application*, first edition. Waltham, Massachusetts, USA: Gulf Professional Publishing.
Uzun, I., Kurtoglu, B., and Kazemi, H. 2016. Multiphase Rate-Transient Analysis in Unconventional Reservoirs: Theory and Application. *SPE Res Eval & Eng* **19** (4): 553–566. SPE-171657-PA. https://doi.org/10.2118/171657-PA.
van Everdingen, A. F. and Hurst, W. 1949. The Application of the Laplace Transformation to Flow Problems in Reservoirs. *J Pet Technol* **1** (12): 305–324. SPE-949305-G. https://doi.org/10.2118/949305-G.
Winestock, A. G. and Colpitts, G. P. 1965. Advances in Estimating Gas Well Deliverability. *J Can Pet Technol* **4** (3): 111–119. PETSOC-65-03-01. https://doi.org/10.2118/65-03-01.
Yang, Z. 2009. Analysis of Production Decline in Waterflood Reservoirs. Paper presented at the SPE Annual Technical Conference and Exhibition, New Orleans, Louisiana, USA, 4–7 October. SPE-124613-MS. https://doi.org/10.2118/124613-MS.
Yildiz, T. and Khosravi, A. 2007. An Analytical Bottomwaterdrive Aquifer Model for Material-Balance Analysis. *SPE Res Eval & Eng* **10** (6): 618–628. SPE-103283-PA. https://doi.org/10.2118/103283-PA.
Zhang, F. and Emami-Meybodi, H. 2020. A Semianalytical Method for Two-Phase Flowback Rate-Transient Analysis in Shale Gas Reservoirs. *SPE J.* **25** (4): 1599–1622. SPE-201225-PA. https://doi.org/10.2118/201225-PA.

Appendix A—Derivations

General Equations. The starting point for analysis is the linearized-version partial-differential equation for the radial inflow of a slightly compressible fluid in a porous medium (Lee et al. 2003),

$$\frac{\partial^2 p_D}{\partial r_D^2}+\frac{1}{r_D}\frac{\partial p_D}{\partial r_D}=\frac{\partial p_D}{\partial t_D}. \quad \text{(A-1)}$$

At this point we will leave the equation general and prescribe no initial or boundary conditions. The following dimensionless groups are used in the governing equation and its solutions:

$$p_D=\frac{p_i-p(r)}{p_i-p_{wf}};\quad r_D=\frac{r}{r_w};\quad t_D=\frac{0.0002637kt}{\phi\mu c_t r_w^2};\quad q_D=\frac{141.2qB\mu}{kh(p_i-p_{wf})}. \quad \text{(A-2)}$$

Taking the Laplace transform of Eq. A-1, recalling that $\mathcal{L}\left(\frac{\partial p_D}{\partial t_D}\right)=u\overline{p}_D-p_D(t_D=0)$,

$$\frac{d^2\overline{p}_D}{dr_D^2}+\frac{1}{r_D}\frac{d\overline{p}_D}{dr_D}-u\overline{p}_D=-p_D(r_D,t_D=0)=-p_{D0}(r_D). \quad \text{(A-3)}$$

Eq. A-2 is a nonhomogeneous ordinary-differential equation. The independent solutions to the corresponding homogeneous problem are

$$u_1=K_0\left(r_D\sqrt{u}\right),\ u_2=I_0\left(r_D\sqrt{u}\right). \quad \text{(A-4)}$$

Once a solution is found is found in terms of pressure, the flow rate at any point in the reservoir is determined from

$$\overline{q}_D=-r_D\frac{d\overline{p}_D(r_D,u)}{dr_D}. \quad \text{(A-5)}$$

At the wellbore, $r_D=1$, and

$$\overline{q}_D|_{r_D=1}=-\frac{d\overline{p}_D(1,u)}{dr_D}. \quad \text{(A-6)}$$

In the following subsections, specific solutions will be developed for different initial and boundary conditions.

Depletion Solution. ***Solution 1: Uniform Initial Pressure, Pressure Step at r_w, Closed Boundary at r_e.*** The initial condition for the first solution is that of an undisturbed reservoir,

$$p_{D0}(r_D)=0. \quad \text{(A-7)}$$

This translates to the boundary conditions

$$r_D=1\colon\ p_D(1,t_D)=1\ \rightarrow\ \overline{p}_D(1,u)=\frac{1}{u}, \quad \text{(A-8)}$$

$$r_D = r_{eD}:\ r_{eD}\frac{\partial p_D(r_{eD},t_D)}{\partial r_D} = 0 \rightarrow r_{eD}\frac{\partial \overline{p}_D(r_{eD},u)}{\partial r_D} = 0. \quad \text{(A-9)}$$

Eqs. A-3, A-8, and A-9 form a system of equations. It is possible to show that, after algebraic manipulation,

$$\overline{p}_D^{\text{depl}}(r_D,u) = \frac{1}{u}\cdot\frac{I_1(r_{eD}\sqrt{u})K_0(r_D\sqrt{u}) + I_0(r_D\sqrt{u})K_1(r_{eD}\sqrt{u})}{I_1(r_{eD}\sqrt{u})K_0(\sqrt{u}) + I_0(\sqrt{u})K_1(r_{eD}\sqrt{u})}. \quad \text{(A-10)}$$

For flow rate at the production well,

$$\overline{q}_D^{\text{depl}}(u) = \frac{1}{\sqrt{u}}\cdot\frac{I_1(r_{eD}\sqrt{u})K_1(\sqrt{u}) - I_1(\sqrt{u})K_1(r_{eD}\sqrt{u})}{I_1(r_{eD}\sqrt{u})K_0(\sqrt{u}) + I_0(\sqrt{u})K_1(r_{eD}\sqrt{u})}. \quad \text{(A-11)}$$

This is identical to solutions available in van Everdingen and Hurst (1949) and Ehlig-Economides (1979).

Constant-Rate Injection Solution. ***Solution 2: Uniform Initial Pressure, Constant Pressure at r_w, Rate Step at r_e.*** This solution for production rate at the wellbore is intended to be added to the depletion solution by means of the principle of superposition (Eq. 1). As with Solution 1, the initial condition for the solution is that of an undisturbed reservoir,

$$p_{D0}(r_D) = 0. \quad \text{(A-12)}$$

The constant-rate injection problem at the outer reservoir boundary translates to the following boundary conditions

$$r_D = 1:\ p_D(1,t_D) = 0 \rightarrow \overline{p}_D(1,u) = 0, \quad \text{(A-13)}$$

$$r_D = r_{eD}:\ r_{eD}\frac{\partial p_D(r_{eD},t_D)}{\partial r_D} = -q_{D,\text{inj}} \rightarrow r_{eD}\frac{\partial \overline{p}_D(r_{eD},u)}{\partial r_D} = -\frac{q_{D,\text{inj}}}{u}. \quad \text{(A-14)}$$

After some manipulation, the pressure solution becomes

$$\overline{p}_D^{\text{inj-q}}(r_D,u) = \frac{q_{D,\text{inj}}}{r_{eD}u\sqrt{u}}\cdot\frac{-I_0(r_D\sqrt{u})K_0(\sqrt{u}) + I_0(\sqrt{u})K_0(r_D\sqrt{u})}{I_1(r_{eD}\sqrt{u})K_0(\sqrt{u}) + I_0(\sqrt{u})K_1(r_{eD}\sqrt{u})}. \quad \text{(A-15)}$$

For flow rate at the production well,

$$\overline{q}_D^{\text{inj-q}}(u) = \frac{q_{D,\text{inj}}}{r_{eD}u}\cdot\frac{I_1(\sqrt{u})K_0(\sqrt{u}) + I_0(\sqrt{u})K_1(\sqrt{u})}{I_1(r_{eD}\sqrt{u})K_0(\sqrt{u}) + I_0(\sqrt{u})K_1(r_{eD}\sqrt{u})}. \quad \text{(A-16)}$$

Constant-Pressure Injection Solution. ***Solution 3: Nonuniform Initial Pressure, Constant Pressure at r_w, Pressure Step at r_e.*** We now consider a general case where an initial pressure distribution is given as a general function of radius. The solution in this subsection is intended to be used in a standalone format. Once the initial pressure distribution is loaded from the depletion solution, this constant-pressure-injection solution should be used on its own. The original pressure distribution is defined as

$$p_{D0}(r_D) = f(r_D). \quad \text{(A-17)}$$

For this case, the following boundary conditions are applied:

$$r_D = 1:\ p_D(1,t_D) = 0 \rightarrow \overline{p}_D(1,u) = 0, \quad \text{(A-18)}$$

$$r_D = r_{eD}:\ p_D(r_{eD},t_D) = p_{D,\text{inj}} \rightarrow \overline{p}_D(r_{eD},u) = \frac{p_{D,\text{inj}}}{u}. \quad \text{(A-19)}$$

In this instance, because the dimensionless pressure is set to zero at the wellbore, the following definition of dimensionless pressure will be used for the equations in this subsection,

$$p_D = \frac{p_{wf} - p(r,t)}{p_i - p_{wf}}. \quad \text{(A-20)}$$

Using the definition of dimensionless pressure from the depletion solution for this case, the initial condition is furnished as

$$p_{D0}(r_D) = p_D^{\text{depl}}\left(r_D, t_{D\text{inj}}\right) - 1, \quad \text{(A-21)}$$

where the p_D^{Depl} solution was given in Eq. A-10. Here, $t_{D\text{inj}}$ is a constant representing the specific time that injection starts.

The solution to Eq. A-3 with these initial/boundary conditions can be obtained using the variation of parameters. This solution method has been used elsewhere in the area of pressure-transient analysis (Bratvold and Horne 1990; Oliver 1990; Kuchuk and Wilkinson 1991).

A general solution to Eq. A-3 is sought of the form

$$p_D = v_1(r_D)u_1 + v_2(r_D)u_2 + c_1u_1 + c_2u_2, \quad \text{(A-22)}$$

where u_1 and u_2 denote the independent solutions defined previously (Eq. A-4).

The functions $v_1(r_D)$ and $v_2(r_D)$, and the constants c_1 and c_2, are determined from the initial and boundary conditions, respectively. Using the Wronskian matrix, v_1 and v_2 are determined as

$$\frac{dv_i}{dr_D} = -p_{D0}(r_D)\boldsymbol{W}^{-1}\begin{bmatrix}0\\1\end{bmatrix} = -p_{D0}(r_D)r_D\begin{bmatrix}\sqrt{u}I_1(r_D\sqrt{u}) & -I_0(r_D\sqrt{u})\\ \sqrt{u}K_1(r_D\sqrt{u}) & K_0(r_D\sqrt{u})\end{bmatrix}\begin{bmatrix}0\\1\end{bmatrix}; \quad \text{(A-23)}$$

that is,

$$\frac{dv_1}{dr_D} = I_0\left(r_D\sqrt{u}\right)p_{D0}(r_D)r_D; \quad \frac{dv_2}{dr_D} = -K_0\left(r_D\sqrt{u}\right)p_{D0}(r_D)r_D. \quad \text{(A-24)}$$

After incorporating the boundary conditions, c_1 and c_2 are obtained. The solution for the production rate at the wellbore is then

$$\overline{q}_D^{\text{inj-p}}(u) = \frac{-\dfrac{p_{D,\text{inj}}}{u} + K_0\left(r_{eD}\sqrt{u}\right)\displaystyle\int_1^{r_{eD}}\xi I_0\left(\xi\sqrt{u}\right)p_{D0}(\xi)d\xi - I_0\left(r_{eD}\sqrt{u}\right)\int_1^{r_{eD}}\xi K_0\left(\xi\sqrt{u}\right)p_{D0}(\xi)d\xi}{I_0(r_{eD}\sqrt{u})K_0(\sqrt{u}) - K_0(r_{eD}\sqrt{u})I_0(\sqrt{u})}. \quad \text{(A-25)}$$

The definite integrals in Eq. A-25 are calculated using numerical integration.

Numerical Inversion of the Laplace-Transform Solutions into Real Domain. The equations developed for flow rate at the production well (Eqs. A-11, A-16, and A-25) are expressed in terms of the Laplace transform. For practical purposes, inversion of these equations into the real domain is required. Note that analytical inversions are not easily available, so we must resort to numerical methods. Because the equations contain no discontinuities in the real domain, they are suitable for numerical inversion using the well-known Stehfest (1970) algorithm.

Appendix B—Waterflood Type Curves Against Other Plotting Variables (Constant-Rate Injection Case)

Please see **Figs. B-1 through B-3.**

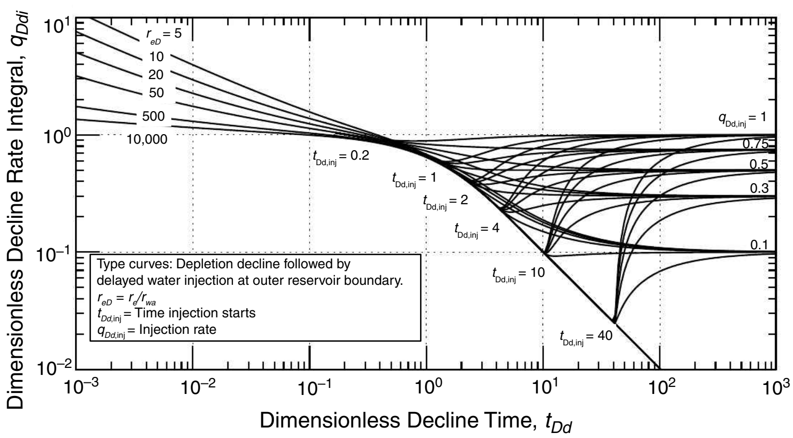

Fig. B-1—Dimensionless rate decline integral (q_{Ddi}) vs. dimensionless decline time (t_{Dd}). Constant-rate injection case.

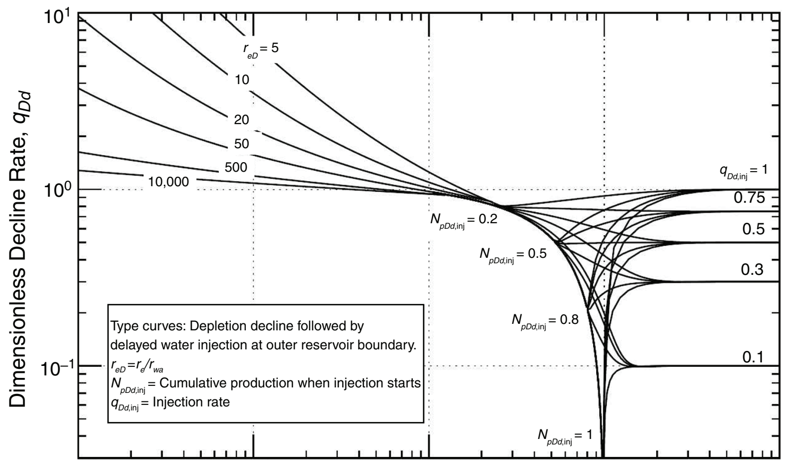

Fig. B-2—Dimensionless rate decline (q_{Dd}) vs. dimensionless cumulative production (N_{pDd}). Constant-rate-injection case.

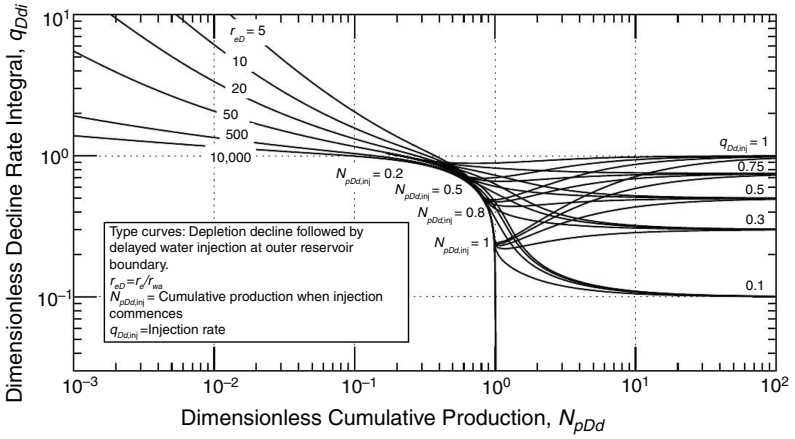

Fig. B-3—Dimensionless rate decline integral (q_{Ddi}) vs. dimensionless cumulative production (N_{pDd}). Constant-rate-injection case.

Appendix C—Additional Field-Case-Study Matches

Please see **Figs. C-1 through C-5.**

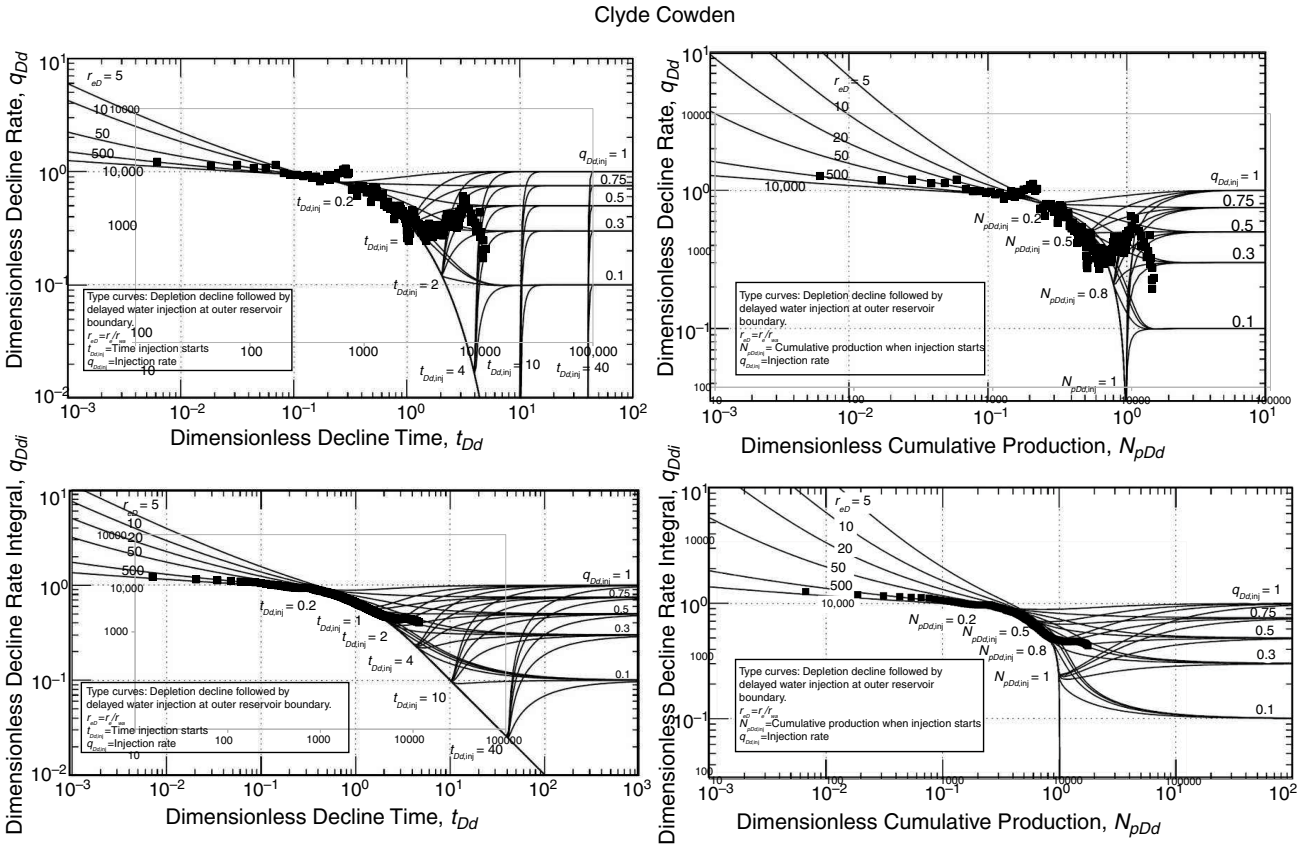

Fig. C-1—Production match for Clyde Cowden lease. Oil rate (in BOPD) is plotted in black points.

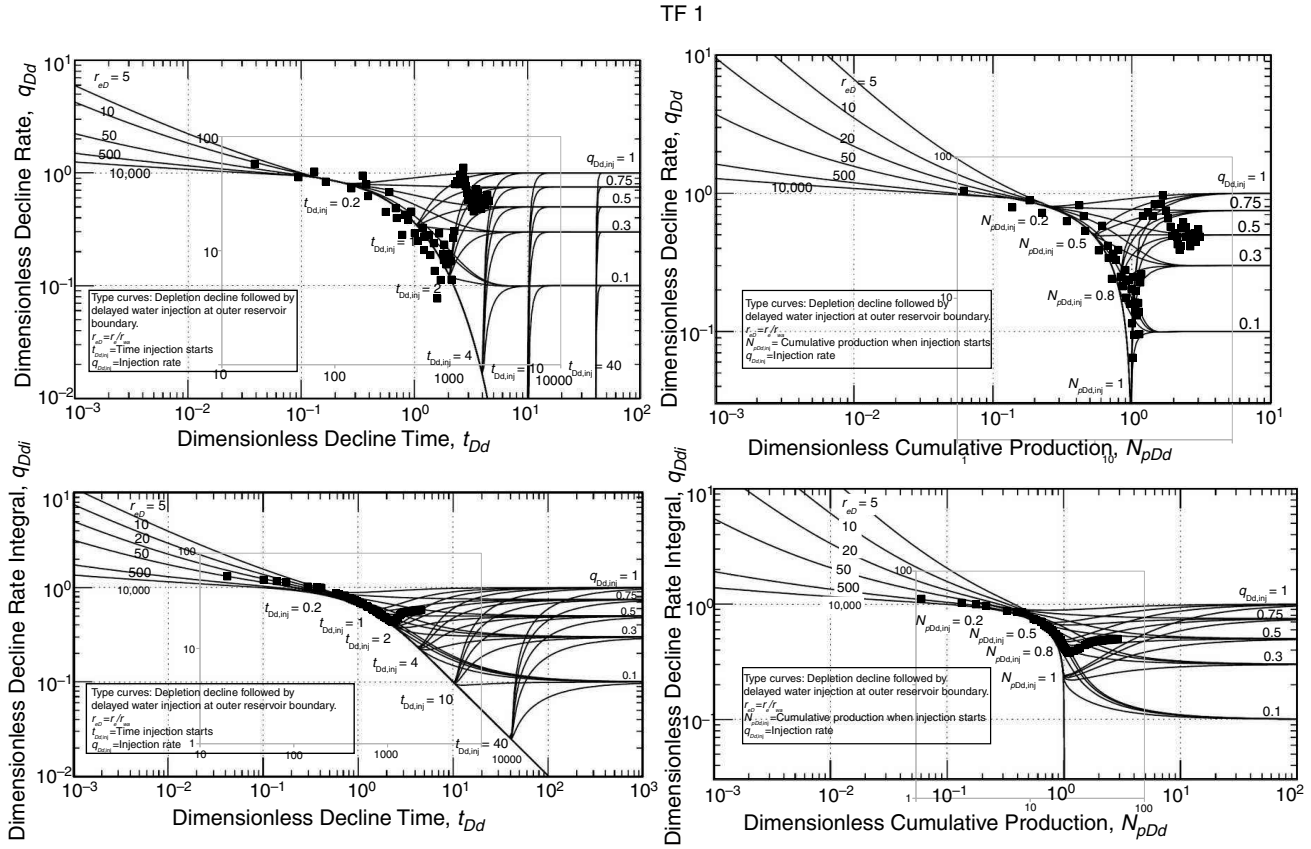

Fig. C-2—Production match for Well TF 1. Oil rate (in BOPD) is plotted in black points.

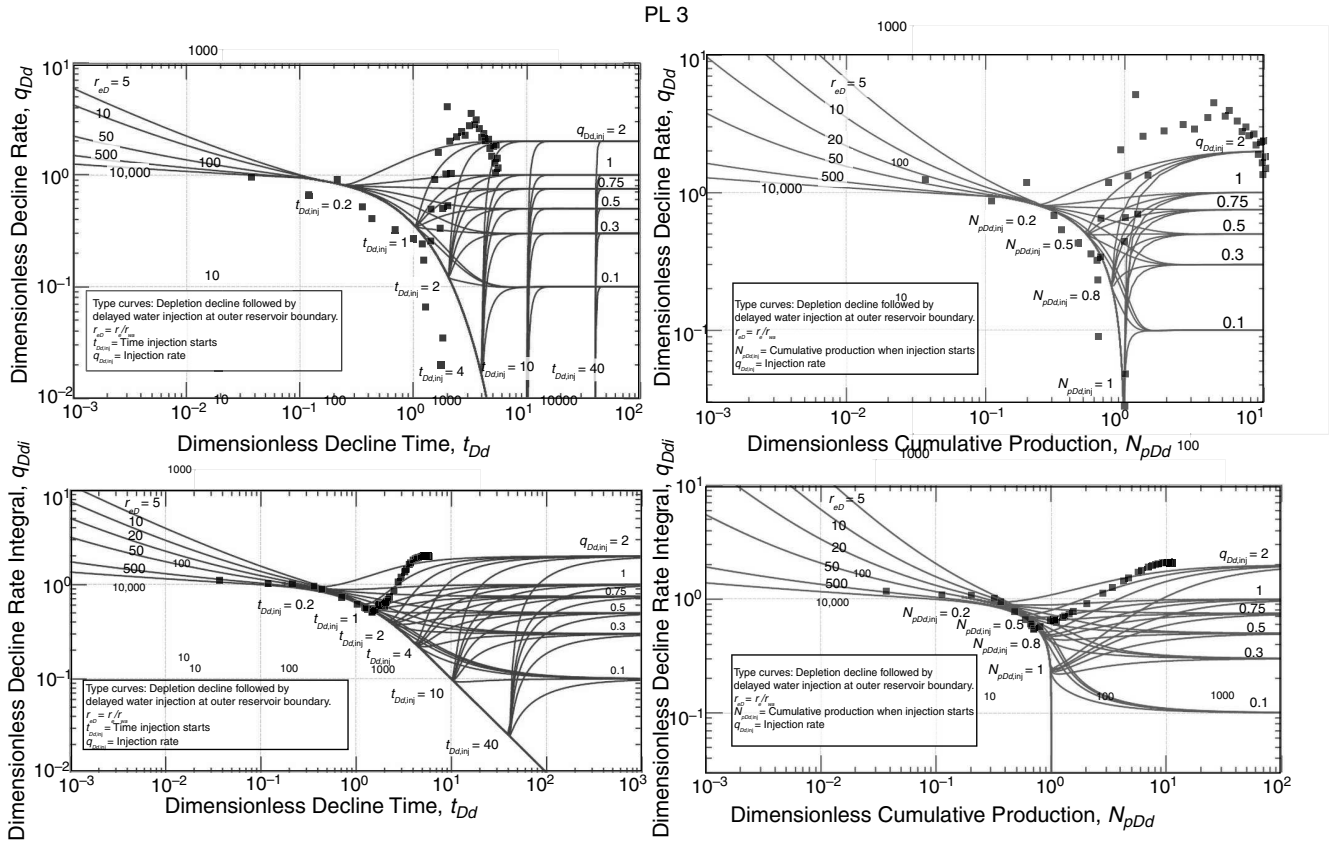

Fig. C-3—Production match for Well PL 3. Oil rate (in BOPD) is plotted in black points.

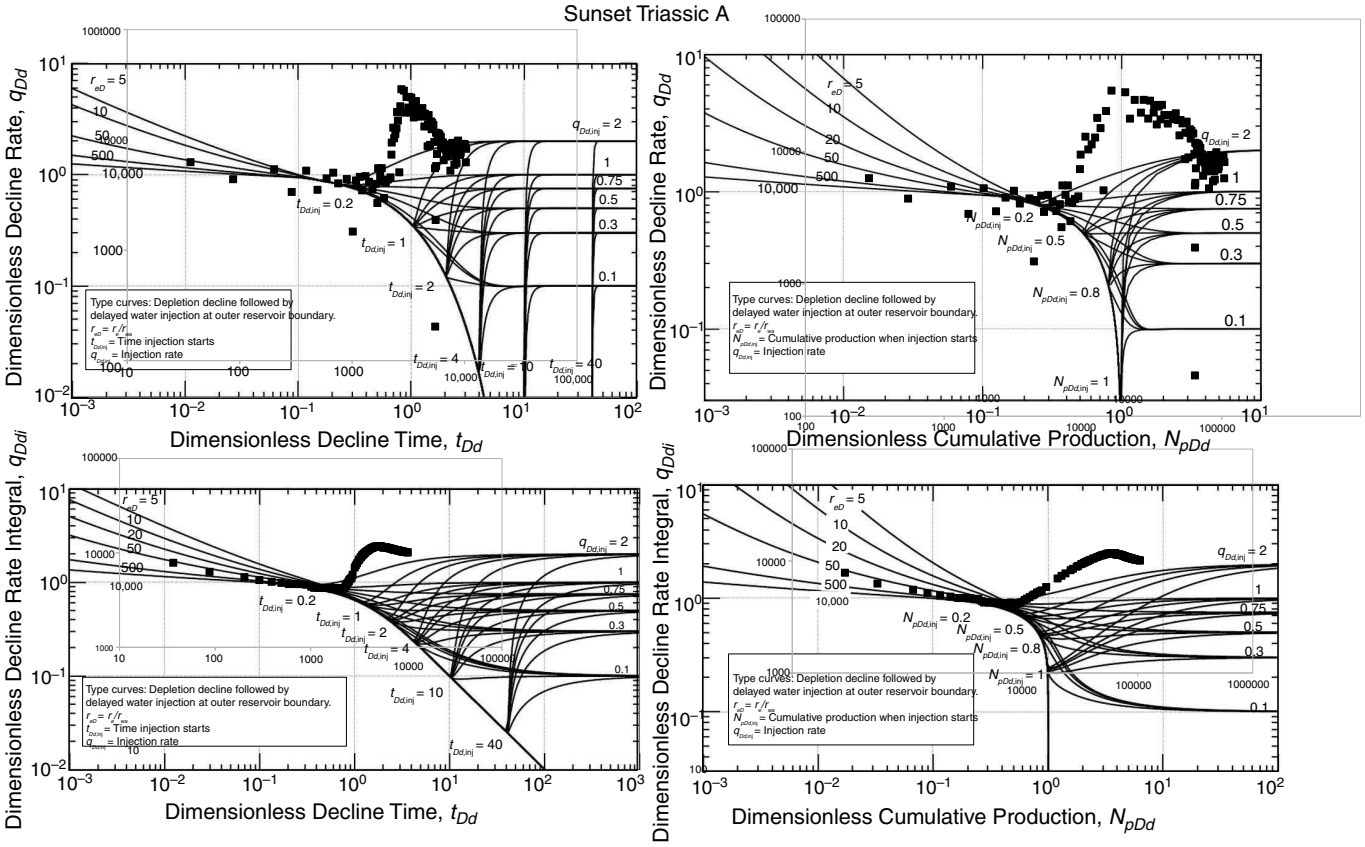

Fig. C-4—Production match for Sunset Triassic A field. Oil rate (in BOPD) is plotted in black points.

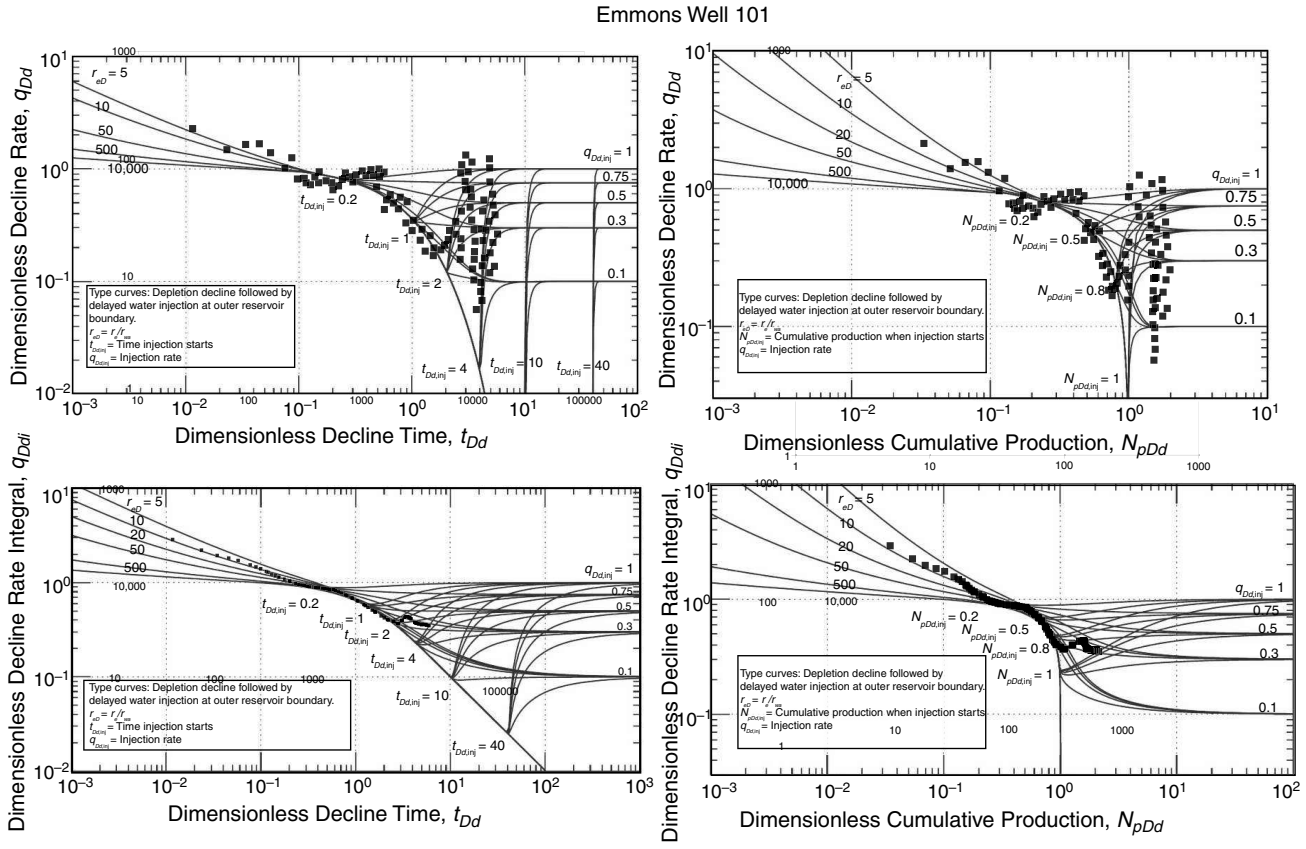

Fig. C-5—Production match for Emmons Well 101. Oil rate (in BOPD) is plotted in black points.

8.1 Selected Computer Code

This reservoir simulation deck corresponds to Case 2 in the journal paper (Table 1). It may be used in the OPM simulator (https://opm-project.org/) or ECLIPSE.

```
RUNSPEC ======================
TITLE
Waterflood
DIMENS
100 100 1 /
TABDIMS
/
OIL
WATER
FIELD
WELLDIMS
10 10 2 2 /
START
1 'JUN' 2020 /
UNIFOUT
UNIFIN

GRID ==========================
INIT
DX
10000*4.667 /
DY
10000*4.667 /
DZ
10000*100 /
PERMX
10000*3 /
PERMY
10000*3 /
PERMZ
10000*3 /
PORO
10000*0.26 /
TOPS
10000*3000 /
RPTGRID
/

PROPS ============================
SWOF
0.3 0 1 0
0.35 0.0168393829 0.8776415154 0
0.4 0.0476289672 0.7607257743 0
0.45 0.0875 0.6495190528 0
0.5 0.1347150628 0.544331054 0
0.55 0.1882700238 0.4455281926 0
0.6 0.2474873734 0.3535533906 0
0.65 0.3118697348 0.2689571768 0
0.7 0.3810317378 0.1924500897 0
0.75 0.454663337 0.125 0
0.8 0.532508042 0.0680413817 0
0.85 0.6143490608 0.0240562612 0
```

```
0.9 0.7 0 0
0.95 0.7 0 0
1 0.7 0 0
/
PVTW
1000 1 3E-6 0.6 0 /
PVCDO
1000 1.2 1E-5 0.65 0 /
ROCK
1000 3E-6 /
DENSITY
40 64 0.05 /
RSCONST
0.004 14.7 /

SOLUTION ============================
PRESSURE
10000*1000 /
SWAT
10000*0.3 /
RPTSOL
'RESTART=2' /

SUMMARY =============================
FWPR
FOPR
FWCT
FWIR
FLPR
FVPR
FOIP
FOE
FPR
WBHP 'INJE'
/

SCHEDULE ============================
RPTRST
'BASIC=1' /
WELSPECS
'INJE' 'G' 100 100 1* 'WATER'/
'OP' 'G' 1 1 1* 'OIL' 1* 1* 1* YES /
/
COMPDAT
'INJE' 100 100 1 1 'OPEN' 2* 0.2 /
'OP' 1 1 1 1 'OPEN' 2* 0.2 /
/
WCONPROD
'OP' 'OPEN' 'BHP' 5* 400 /
/
TSTEP
100*0.01 90*0.1 80*1 /
WCONINJE
'INJE' 'WATER' 'OPEN' 'RATE' 100 3* /
/
TSTEP
100*10 30*100 /
END
```

9 Conclusions and Recommendations

9.1 Conclusive Remarks

In this study, mathematical models have been developed with application to production and injection wells in mature waterflood fields. Field applications of the theory have been shown from the Windalia waterflood or other wells on Barrow Island, Australia, which are currently operated by Chevron Australia. Other case studies appearing in the open literature from international fields have also been applied to the new models. The following conclusions can be drawn from this work:

1. The 2015 rejuvenation of the Windalia waterflood serves as a case study to illustrate the importance of reservoir management and its impact on oil production in mature fields. The chapter documents the reintroduction of reservoir surveillance on the asset, focusing on the execution and interpretation of water injector pressure transient tests. The work follows classical testing methods.
   Overall, this field study shows the physical benefit of reservoir surveillance for readers to consider.

2. Oil wells undergoing artificial lift production are often produced under cyclic flow rate variation. This type of production resembles the pulse test that is studied in pressure transient analysis. It is possible to apply the principles used in pulse testing to derive solutions for short and long-term production of artificial lift wells. Using these equations, it is possible to determine the Productivity Index for cyclic production wells. This allows for the utilisation of more field operating data in future.

3. For oil wells undergoing boundary dominated cyclic production, there are two limiting forms of the developed harmonic equations:

   - For long cycle times, the solution approaches the equivalent pseudo steady or steady state solution (for any proportion of online time %)
   - For short cycle times, the solution approaches the equivalent pseudo steady or steady state solution multiplied by the proportion of online time %. Stated another way, an "average liquid rate" can be used in when determining Productivity Index in this case.

4. The new artificial lift productivity determination methods show accuracy when compared against numerical techniques and actual field cases. In one case, the steady-state method compared closely to a pressure buildup test on the same well. In another case, the transient method was used to identify an under performing oil well that was later selected for reservoir stimulation.
   The new equations should be applied to wells in mature fields where the cost of obtaining full pressure transient surveys is prohibitive.

5. Wells injecting cold water into oil bearing formations must be analysed carefully during the Pressure Fall Off transient period, particularly considering temperature effects inside the well. For injectors lacking a downhole shut-in device, the heating of water in the well during a falloff is substantial and can create a total pressure response that is increasing rather than falling off. A field case study showed agreement with the newly developed analytical model.
   As future work, the combination of the thermal well model with more detailed analytical models should be considered. In this work, a fixed composite model was assumed. The moving flood front model may be considered in future.

6. The temperature heating effect during cold-water injection can lead to the underestimation of mechanical skin if the effect is not properly accounted for. The identification of fluid banks in the pressure response may be difficult if a downhole shut-in is not performed. An important conclusion from this work is that transient tests on high injectivity water injection development wells should be planned carefully with the consideration of specialised downhole equipment where required.

7. The extension of Fetkovich (1980) type curves for the case of delayed water injection at the outer boundary shows that a broader range of production data may be interpreted from waterflooded reservoirs. In addition to the usual derived Fetkovich reservoir properties, the method allows the interpretation of water injection strength and boundary condition (i.e. constant-rate or constant-pressure injection) from oil well production data alone. This is a novel finding, since no injection data are technically required in the analysis chart. Several example field studies validate the physical form of the type curves.

8. Applying the Martin (1959) and Perrine (1956) theory to Rate Transient Analysis provides a simple method to extend the waterflood type curves to the two phase case. Furthermore, during the boundary dominated period, the Buckley-Leverett (1942) displacement theory allows tracking of the displacement front and its eventual breakthrough at the oil production well. Finally, it is shown that waterflood Rate Transient Analysis in stratified reservoir is a simple extension of the analytical model. As a final remark, it is best for analysts to plot total liquid rate on this type of diagnostic type curve.

9.2 Further Work

Further work is possible in several of the areas studied in this thesis. Regarding production wells with oscillating flow rates (Chapters 4, 5 and 6):

1. Wellbore storage (or phase redistribution) modeling can be included in the transient cyclic theory. It was already incorporated into the steady state theory in Chapter 5. It is likely that in many operational wells, wellbore storage effects will be important due to the type of downhole completion.

2. Wellbore hydraulics and pump efficiency should be further incorporated into transient and steady state production theory of oscillating wells.

3. Other flow geometries apart from radial flow should be considered.

4. Development of solutions for unstable reservoir conditions – e.g. for an uneven voidage replacement (non-steady-state case).

5. For many sucker rod pump wells, while the tubing flow may cease flow during shut-in, the annulus may freely flow gas with flow lines still open to separator station. This will happen until such a point that the liquid level rises in the annulus to increase the BHP enough to completely cease inflow. This is an issue that needs further study and is a unique production phenomenon.

On the topics of water injection and general waterflood operations (Chapters 3 and 7):

6. Analytical treatment of the problem of transient water-cut changes in waterflood operating fields following production well shutdown should be studied (Figure 9 of Chapter 3). The behaviour can be shown to occur in reservoir simulation, but an improved understanding of the problem would be obtained after solving analytically. Economically, minimising this problem will assist operating companies when planning shutdowns.

7. Assessment of the uncertainties involved when extrapolating pressure from a gauge (whether at a surface or downhole location) to the reservoir interval of interest. This includes uncertainties present in the temperature gradient and heat transmission properties themselves; these are subject to change over time. In future, practitioners should have a better understanding of this problem to define the confidence intervals for their interpreted reservoir properties.

On topic of rate transient analysis of production wells with water injector support (Chapter 8), the following extension work can be studied:

8. This research studied the displacement of reservoir oil by water. The problem of displacement of a highly compressible phase (e.g. gas) by water in pressure/rate transient analysis is scarcely studied in the literature and should be investigated.

9. The use of pseudogroups in waterflood rate transient analysis should be studied more in future. Some examples are: rate-normalisation, material-balance time and multiphase pseudogroups.

10. Carbon dioxide geosequestration has recently gained popularity in industry and academia and shares some theoretical similarities with waterflooding oil reservoirs. The application of the new rate transient analysis method in this thesis can be considered in CO2 sequestration to derive information about injection efficiency and containment.